# THE LATERAL STABILITY OF TIMBER BEAMS AND ARCHES

A thesis presented for the degree of
Doctor of Philosophy (Engineering)
in the University of London

by

Christian, Kurt, Alexander Stieda, B.Sc., M.Sc.

August, 1968

Imperial College of Science and Technology,
London.

Abstract

The thesis presents an investigation of the lateral stability of beams and arches using the finite element theory of analysis. By means of the force method various matrices which are required for the numerical evaluation of the stability problem, are established. Particular attention is given to the analysis of plywood box-beams. The displacement method is used to establish a finite element solution for the calculation of torsion constants of box-sections. The results of the finite element analysis of the lateral stability of beams are shown to agree with those derived by the classical theory of elastic stability. Using Southwell plots of experimental results from an investigation of the lateral stability of plywood box-beams, it is shown that plywood box beams indeed behave in the manner predicted by theory. Experimental evidence is also given to support the finite element analysis of torsion of box beams. In particular it is shown that the non-uniform shear stress distribution predicted by the finite element analysis for box-beams with deep flanges does indeed exist, contrary to an often made assumption of uniform distribution of shear stresses. Coefficients for the calculation of critical loads for lateral instability of parabolic arches loaded at the crown are given. Experimental corroboration of these coefficients has not yet been obtained and future research in this direction is suggested.

To

Peter,

Daphne, Vivian

Monica, Nicolette

and

Mundi

Acknowledgements

The preparation of this thesis would not have been possible without the help and support of a number of people. The author has great pleasure in thanking all of them.

In particular the author wishes to thank the following individuals, all members, unless stated otherwise, of the Imperial College of Science and Technology, University of London:

Prof. S. R. Sparkes, Head of the Structural Engineering Section, Department of Civil Engineering, for providing the opportunity and the facilities for carrying out the research described in this thesis,

Dr. L. G. Booth, Department of Civil Engineering, who greatly encouraged the author to pursue the work described here, for his general supervision and helpful advice in the preparation of this thesis,

Mr. S. Kelsey, formerly Department of Aeronautics, Imperial College, presently visiting professor, Department of Civil Engineering, University of Notre Dame, Notre Dame, Ind., U.S.A., for his helpful suggestions for the solution of the lateral stability problem and for his guidance and advice towards the solution of the torsion problem,

Mr. A. Bannister, Department of Civil Engineering, Uinversity of Salford, Salford, Lancashire, for making available his experimental findings on the distribution of shear strains in the flanges of box beams subjected to torsion,

Mr. J. Neale, Civil Engineering Structures Laboratories, and his staff, and in particular Mr. D. A. Denness, for their

valuable suggestions and their unfailing support in the construction of equipment and test specimens and the execution of laboratory tests,

Mr. J. F. Levy, Department of Botany and Plant Technology, for identifying the material used for the construction of the plywood box-beams,

Miss J. Gurr, for providing all photographic services,

Miss J. Clarke, for typing the manuscript with great care.

The author also wishes to express his gratitude to Dr. R. E. Foster, Director of the Vancouver Forest Products Laboratory, for providing the opportunity of a two-year educational leave of absence from the Vancouver Forest Products Laboratory and for arranging for the author and his family a grant for travel and living expenses from the Department of Forestry and Rural Development, Government of Canada.

Contents

# Chapter 1

## Introduction

The load carrying capacity of a structure usually is determined by the tensile, compressive and shear strength of its material. In certain cases, however, a structure may fail not due to a lack of strength but due to sudden excessive displacements. Since Euler's analysis in the eighteenth century of the behaviour of axially loaded columns (42)[1] such instability phenomena have been of continuous interest to structural engineers. A failure of this type can occur not only in columns but also in beams and arches. In 1899 Prandtl (35) working in Munich and Michell (32) working independently in Australia both published investigations into the lateral stability of beams. Since that time research into numerous aspects of the lateral stability of beams has been carried out. A historical review of the most important work on the lateral stability of beams has been given by Bleich (6). An extensive review of the literature has also been presented by Kollbrunner and Meister (26).

Under normal conditions loading of a structure will produce a definite and unique deformation pattern. Equilibrium of external and internal forces will be maintained at all times and only one deformed shape will be possible. Under certain circumstances and for loads of a certain magnitude however, equilibrium of forces could be maintained for more than one deformed shape.

---

[1] References are listed following Chapter 6.

Of these the original mode of deformation will be unstable and the structure will therefore, often suddenly, change to a second stable mode of deformation.

If in the course of loading a structure such a load is reached, where more than one deformed shape is possible, a point of bifurcation of the equilibrium deformations is said to have been reached (28). The study of so-called classical buckling problems therefore consists in determining, if more than one deformed shape of the loaded structure is possible. In these investigations usually an idealized member is being assumed with a straight axis and loads are applied either, for columns, concentrically or, for beams, in the principal plane of bending.

It was realized already very early, however, that the idealized conditions assumed for an analysis could not be achieved with an actual structure. Prandtl in his dissertation (35) draws particular attention to this observation that in his experiments with small, rectangular steel beams lateral deflections occured long before the critical load for lateral stability was reached.

Due to initial bow and twist of a beam, as well as accidental eccentricities of the loads, beams are subjected to secondary bending moments and torsional moments in addition to the primary moments usually considered. The stresses in the beam are therefore a combination of the stresses due to the primary moments and those due to the secondary moments. Under these conditions the problem is not one of determining the load at which bifurcation of the equilibrium position will take place, but one of finding the maximum

stress in the beam due to superposition of primary and secondary bending moments. A systematic analysis of this problem was first published by Stüssi (37) in 1935. Analysing a beam subjected to a constant bending moment, $M_x$, Stüssi first derives the critical moment, $M_{cr}$, for which lateral instability of an ideal, straight beam will occur.[1]

$$M_{cr} = \frac{\pi}{L} \sqrt{EI_y \, GJ} \qquad (1.1)$$

where $L$ = span of beam

$EI_y$ = flexural stiffness about the minor principal axis

$GJ$ = torsional rigidity

The maximum stress, $\sigma_{max}$, due to an initial eccentricity, $y_o$, is then derived as

$$\sigma_{max} = \frac{M_x}{S_x} + y_o \frac{1}{(1-\alpha)} \cdot \frac{M_x^2}{GJ \, S_y} \qquad (1.2)$$

where $S_x$ and $S_y$ = section moduli about major and minor axis

$$\alpha = (M_x/M_{cr})^2 \qquad (1.3)$$

For any given critical stress $\sigma_{max}$ Equation (1.2) can be presented in graphical form for various values of $y_o/L$ as a plot

[1] The expression derived by Stüssi, in fact, contains an additional term, accounting for the stresses due to warping of a steel I-section. The effect of warping in timber beams is less pronounced, because of the usually more compact sections that are being used with timber. The effect of warping is therefore not included in the present discussion.

of $\sigma_1$ vs. the ratio $L/L_y$, where the stress $\sigma_1$ is defined by

$$\sigma_1 = M_x/S_x \qquad (1.4)$$

and the span $L_y$ is equal to the span for which the stress due to the buckling load given by Equation (1.1) is equal to the critical stress $\sigma_{max}$.

Stüssi's work is of particular interest, not only because he was the first investigator to consider in detail the effect of initial eccentricities in beams, but also, because he formulated for the first time a finite element solution for the analysis of the lateral stability of beams. The technique employed by Stüssi is very powerful and permitted him to analyse beams (36, 37) as well as arches (38).

In the experimental analysis of stability phenomena it is useful to have a technique which will allow the determination of critical loads from experimental data without loading the structure up to failure. For columns Southwell has shown that a plot of the ratio of deflection/load against deflection will produce an approximately straight line. The slope of this line is equal to the inverse of the critical load (43).

A similar approach can also be used for beams (30, 31). For a beam loaded by a constant bending moment consideration of initial bow, a, and twist, $\Theta$, will result in the following equation for the rotation, $\phi$, of the cross-section at the middle of the beam

$$\phi = \frac{(M^2\Theta/EI_y + M a \pi^2/L^2) \sin(\pi z/L)}{GJ \pi^2/L^2 - M^2/EI_y} \qquad (1.5)$$

With the critical moment for the lateral stability of a beam given by Equation (1.1) this expression for $\phi$ can be rewritten as

$$\frac{\phi}{M} = \frac{(\phi+\theta)}{M_{cr}^2} M + \left(\frac{\pi^2 a\, EI_y}{L^2 M_{cr}^2}\right) \qquad (1.6)$$

If the rotations $\phi$ are large compared to the initial twist $\theta$ of the beam, Equation (1.6) will approach a straight line for $\phi$ /M vs. $\phi$ M. Massey also gives an analogous expression for the critical buckling load ($P_{cr}$) at the mid-point of a beam

$$\frac{\phi}{P^2} = \frac{\phi}{P_{cr}^2} + F_1 \qquad (1.7)$$

where $\phi$ and P are corresponding pairs of rotation and load and $F_1$ is a constant. A plot of $\phi$ /$P^2$ against $\phi$ will again give an approximately straight line whose slope is equal to the inverse of $P_{cr}^2$.

Most investigations on the lateral stability of beams have been concerned with metal structures. As a result beams with I-sections have been studied extensively (6, 26, 43). The torsional stiffening effect resulting from the warping restraint due to a stress gradient along the length of a beam subjected to lateral loads, in particular, has been analysed in detail. Since metal I- and channel sections present relatively wide outstanding flanges the additional torsional resistance produced by non-uniform bending of these flanges can therefore contribute considerably to the calculated buckling load. Composite sections of timber and plywood on the other hand usually do not have these outstanding flanges and consideration of the warping restraint therefore does

not produce the same marked increase in the calculated buckling load as for metal I-sections.

Tests on the lateral stability of narrow rectangular timber sections were performed by Hooley and Madsen (22). The largest difference between theoretical and observed critical stress in these tests was 19 per cent, while half the tests were within 5 per cent. The importance of adequate bracing for beams is stressed in particular by Hooley and Madsen. The possible lateral support that can be expected from a wooden deck system nailed across supporting beams was analysed by Zahn (47).

In the analysis of metal structures it is often necessary to consider the behaviour of the structure after part of it has yielded. The standard results of the theory of elasticity, which assumes linear elastic behaviour, are then not applicable any more and a non-linear analysis is required. Wood, when tested in compression, also shows a marked non-linear behaviour. Tested in tension, however, the resulting load-deformation curve will deviate little from a straight line, even at ultimate loads which for clear wood loaded parallel to the grain can be two to three times its compressive strength in the same direction (27). In practice little use can be made of this high tensile strength of wood.

Natural defects such as knots, grain deviations around knots and spiral grain as well as sloping grain, produced when a straight board is cut from a naturally tapering log, all combine to reduce the effective tensile strength of timber to a level often below that of its compressive strength (14). As a result the load

carrying capacity of timber beams is often determined by the tensile strength of its material. The potentially large plastic deformations that could occur on the compression side therefore frequently will not develop, since under excessive loads the material will rupture on the tension side causing complete collapse of the beam. The effect of plastic deformations on the lateral stability is therefore less important for timber beams and will not be considered here.

In the past the usual approach to the analysis of the lateral stability of beams was to establish a partial differential equation, expressing the equilibrium of the displaced structure in terms of the applied forces, and then to solve this differential equation (43). The only known direct solution of the partial differential equation describing the lateral stability phenomenon is that for the case of a simply supported beam subjected to equal end moments (26). In all other cases approximate methods of analysis have to be used (28).

The rapid development of fast, electronic computers during the last two decades, however, has permitted a completely new approach to the analysis of structural engineering problems. This approach, usually referred to as finite element analysis, can be employed for the solution of stability problems. Finite element solutions for the stability of beam columns, for example, have been published by Gallagher and Padlog (19) as well as by Argyris (3). A finite element solution for the lateral stability of rectangular beams involving non-linear simultaneous equations has been prepared by Bell (5).

The object of the present investigation is to establish a finite element solution for beams as well as arches involving only

linear simultaneous equations. The method being used here was suggested to the author by Kelsey*, who also provided valuable suggestions for the calculation of the torsional rigidity of box-sections.

The finite element approach to the analysis of stability problems, in particular the lateral stability of beams, will be described in detail in Chapter 2. The effect of initial bow and twist of beams will be considered and the application of the finite element to the lateral stability of arches will be discussed. In this analysis extensive use is made of matrices and various standard matrices will be described in detail in Chapter 3. Numerical results obtained by the method ~~obtained~~ outlined in Chapter 2 will be discussed in Chapter 5. The work described below, although general in its application, was undertaken primarily to obtain information on the lateral stability of plywood box-beams. The results of an experimental investigation of such beams will be discussed in Chapter 6. A finite element analysis of the torsional rigidity of plywood box-beams - a section property required for the calculation of buckling loads - is given in Chapter 4.

Coefficients for the calculation of critical loads that will result in lateral instability of parabolic arches are given in Appendix A. Values of the torsional rigidity of box-sections are presented in Appendix B. Appendix C contains the detailed

---

* S. Kelsey, formerly Imperial College, London, now visiting Professor, University of Notre Dame, Notre Dame, Ind., U.S.A.

results of an experimental investigation of the lateral stability of plywood box-beams, as well as those of an experimental determination of the distribution of strains in the flanges of box-sections subjected to a torsional moment. A paper on the shear deflection of box-beams, which also contains a discussion of the flexural properties of composite sections to which reference is made in the main body of this thesis, is attached, finally as Appendix D.

# Chapter 2

## A Finite Element Solution for Lateral Stability

### Introduction

A general expression for the critical loads producing lateral instability of beams or arches will be devloped in this chapter. The effect of the initial bow or initial twist on maximum stresses will be illustrated for beams.

The classical approach to the formulation of stability problems is to establish a differential equation which will relate certain derivatives of the displacement of the deformed structure to the forces acting on it (26, 43). The critical load at which instability occurs is then found from the solution of this differential equation. For beams a direct solution of the differential equation is only possible when the beam is loaded by a constant bending moment (26). For other loading conditions different methods have to be employed (28).

In recent years, aided by the availability of fast, electronic computers a completely new approach for the analysis of structural engineering problems has been developed. Instead of considering the forces on infinitesimally small elements this so-called finite element method analyzes elements of finite dimensions. These elements are assembled subject to certain conditions and instead of solving differential equations, it becomes necessary to solve systems of linear

equations containing either forces or displacements as unknowns. A lucid exposition of this dual nature of the finite element theory, usually referred to as either the force method or the displacement method, has been given by Argyris (2).

The finite element approach to engineering analysis is based on four fundamental concepts. These concepts concern the idealization of the structure or the continuum, the equilibrium conditions, the compatibility conditions and virtual work.

In the first place it is assumed that the body to be analyzed - this may be a linear structure or a continuum - can be represented by a set of elements, which are joined together at discrete points along their boundary. Each element of the idealized body usually will have simple properties. The behaviour of each element will be defined by a number of forces and displacements.

Secondly, the equilibrium conditions concern the relatiohship between the applied loads and the internal forces. From the point of view of equilibrium the body represents a device for transmitting loads. A body or structure in which the equilibrium conditions suffice to find the forces on all components is statically determined. If the internal forces cannot be found by statics alone, the body is said to be statically indeterminate.

The concept of compatibility provides an alternative view of the function of a structure. From this point of view the structure is a means for constraining a system of points in space relative to

each other. If the idealized body, the structure formed by the set of elements, just provides the necessary constraints to prevent the assembly from acting as a mechanism, then the system is kinematically sufficient. In a kinematically redundant system there are additional constraints to the ones provided by the kinematically sufficient system.

Finally, virtual work can be defined as work that would take place by a specified set of forces over a specified set of displacements, if these could take place. The concept of virtual work is the basis of the principle of virtual work. The principle of virtual work can be formulated in terms of either virtual forces or virtual displacements. When used in terms of virtual forces acting on an elastic body the principle of virtual work states that "an elastic body is in an elastically compatible state under a given set of forces if for any virtual increment of forces ($\delta P$) and stresses ($\delta\sigma$) from a position of equilibrium (u) the increase in external complementary work, $\delta W^* = u\,\delta P$, is equal to the increase in complementary strain energy, $\delta U_i^*$ " (2).

$$\delta W^* = \delta U_i^* \tag{2.1}$$

The increase in complementary strain energy is (Fig. 2.1)

$$\delta U_i^* = \int_V \varepsilon\,\delta\sigma\, dV$$

where $\sigma(\varepsilon)$ = stresses (strains) in the body having a volume V.

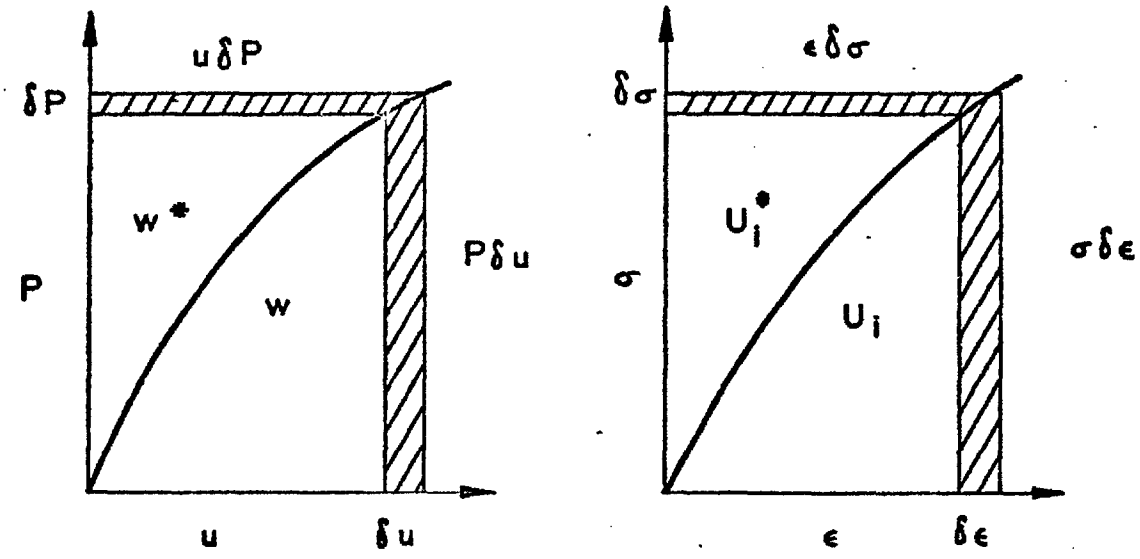


FIG 2.1 - WORK AND COMPLEMENTARY WORK, STRAIN ENERGY AND COMPLEMENTARY STRAIN ENERGY (FROM REF. 2)

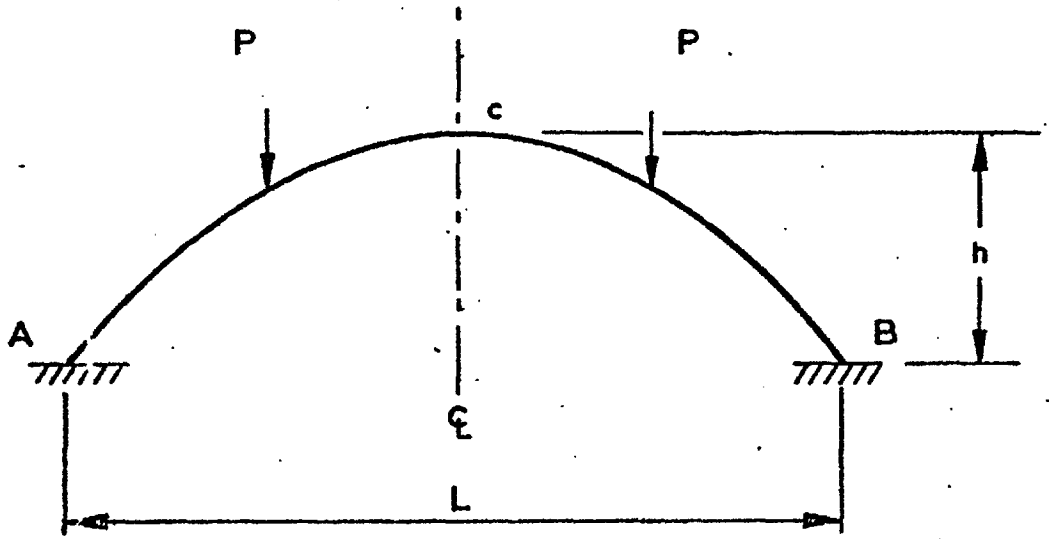


FIG. 2.2 - PARABOLIC ARCH LOADED BY CONCENTRATED FORCES P

For a finite element analysis the body under investigation will be divided into n elements. The virtual internal stresses are then replaced by a column vector* of virtual forces $\bar{S} = \{\bar{S}_1, \bar{S}_2 \ldots \bar{S}_i \ldots \bar{S}_n\}$, where $\bar{S}_i$ is a vector containing all forces acting on an individual element $i$. The virtual external forces are grouped together in the column vector $\bar{R} = \{\bar{R}_1, \bar{R}_2 \ldots \bar{R}_i \ldots \bar{R}_m\}$. Corresponding to the vectors $\bar{R}$ and $\bar{S}$ are displacement vectors $r = \{r_1, r_2 \ldots r_i \ldots r_m\}$ and $v = \{v_1, v_2 \ldots v_i \ldots v_n\}$ which take the place of the external displacements u and the internal strains $\varepsilon$.

The principle of virtual forces applied to finite elements can then be stated as

$$\bar{R}^t r = \bar{S}^t v \qquad (2.2)$$

where $\bar{R}^t$ is a row vector equal to the transpose of the column vector $\bar{R}$.

With correspondence is meant here a displacement which takes place at the same point and in the same direction as a given force. In other words, linear displacements correspond to direct forces and rotations correspond to moments. It is not implied by this definition that a given rotation $\Theta_i$ is the result of a corresponding moment $M_i$.

Redundant Forces in Arches

Consider now an arch fixed at both supports, Fig. 2.2 This

---

* Column vectors will be represented by { }, row vectors by [ ].

arch is three times statically indeterminate. Before analyzing the stability of the arch, it will therefore be necessary to calculate first the redundant reactions. Let the redundant reactions be the moments at the fixed supports and the moment at the crown of the arch. To simplify numerical calculations consider a symmetrical arch under symmetrical loading. The value of the reactions at the left and right support then will be the same and to determine the value of the redundancies, it is sufficient to analyze only one half of the arch, Fig. 2.3. This left half of the arch is to be divided into n elements. The forces acting on a typical element i are axial forces $N_\zeta$ , shear forces $S_\eta$ and moments $M_{\xi\ell}$ and $M_{\xi r}$ at the left and the right end of the element, Fig. 2.4. These forces will be represented by the vector

$$\mathbf{s}_i = \{ S_\eta \; N_\zeta \; M_{\xi\ell} \; M_{\xi r} \} \tag{2.3}$$

Corresponding to these forces are displacements in the $\eta$ - direction, $\Delta\eta$ , displacements in the $\zeta$ -direction, $\Delta\zeta$ and rotations $\Theta_{\xi\ell}$ and $\Theta_{\xi r}$ , represented by the vector

$$\mathbf{v}_i = \{ \Delta\eta \; \Delta\zeta \; \Theta_{\xi\ell} \; \Theta_{\xi r} \}$$

If a sufficient large number of elements is taken the axis of each element can be considered to be straight, and displacements relative to their local coordinates $\xi, \zeta$ can then be expressed in terms of element forces by a flexibility matrix $\mathbf{f}_i$ of size four by four

$$\mathbf{v}_i = \mathbf{f}_i \mathbf{s}_i \tag{2.4}$$

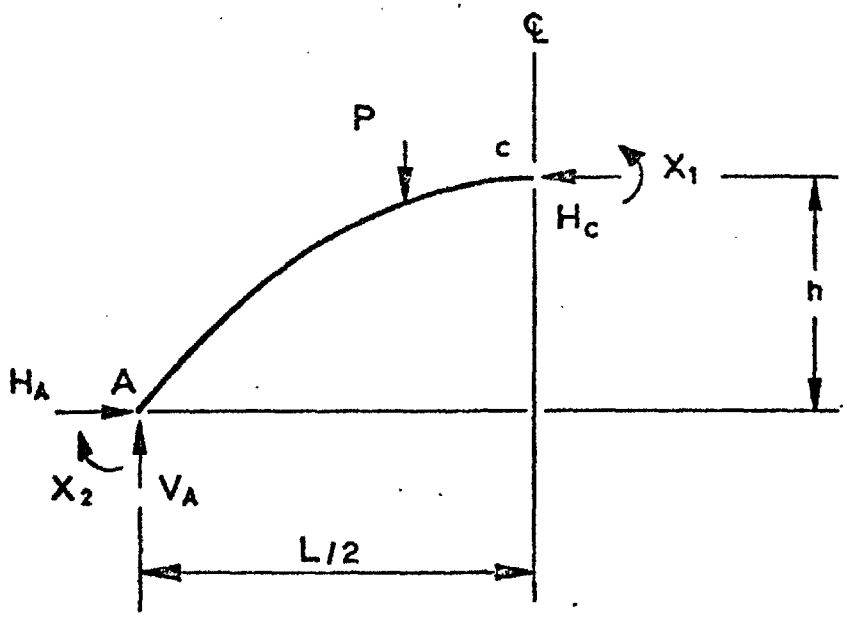


FIG. 2.3 - FORCES, INCLUDING REDUNDANT MOMENTS $X_1$ AND $X_2$ ON LEFT HALF OF SYMMETRICAL ARCH DUE TO SYMMETRICAL LOADING

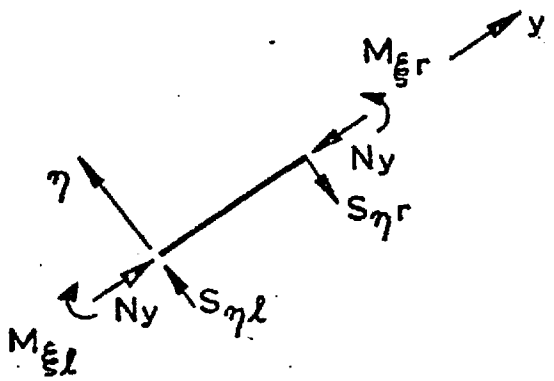


FIG. 2.4 - FORCES ON BEAM ELEMENT

where $\mathbf{f}_i = \frac{\ell}{6EI} \begin{bmatrix} \frac{6EI}{bdGF} & 0 & 0 & 0 \\ 0 & 6I/A & 0 & 0 \\ 0 & 0 & 2 & 1 \\ 0 & 0 & 1 & 2 \end{bmatrix}$ (2.4a)

and where E = modulus of elasticity

G = modulus of rigidity

b = width of cross-section

d = depth of cross-section

I = second moment of area

A = cross-sectional area

The shear stiffness factor F for composite members is discussed in Appendix D.

The displacements of the individual elements are then given by

$$\mathbf{v} = \mathbf{f}\,\mathbf{S} \tag{2.5}$$

where $\mathbf{v} = \{\mathbf{v}_1, \mathbf{v}_2 \cdots \mathbf{v}_i \cdots \mathbf{v}_n\}$ (2.5a)

$\mathbf{S} = \{\mathbf{S}_1, \mathbf{S}_2 \cdots \mathbf{S}_i \cdots \mathbf{S}_n\}$ (2.5b)

The flexibility matrix $\mathbf{f}$ is a diagonal matrix composed of the flexibilities $\mathbf{f}$ of the individual elements.

$$\mathbf{f} = [\mathbf{f}_1, \mathbf{f}_2 \cdots \mathbf{f}_i \cdots \mathbf{f}_n] \tag{2.6}$$

Now let $\mathbf{R}$ be a column vector of m vertical forces

$$\mathbf{R} = \{R_1, R_2 \cdots R_j \cdots R_m\} \tag{2.7}$$

By purely static reasoning it is possible then to find a transformation matrix $\mathbf{b}_o$ which will give the forces on each element in terms of the applied loads $\mathbf{R}$ . The matrix $\mathbf{b}_o$ here is of size $3n$ x m, where n equals the number of elements and m equals the number of external loads.

Similarly let $\mathbf{X}$ be a vector containing the redundant moments at the left support and at the crown of the arch, Fig. 2.3.

$$\mathbf{X} = \{ X_1 \quad X_2 \} \tag{2.8}$$

Again by static reasoning alone, it will be possible to derive a matrix $\mathbf{b}_1$ , which will give the element forces resulting from $\mathbf{X}$ . The total forces on the individual elements can then be obtained by adding the element forces due to the redundant reactions to those due to the external loading

$$\mathbf{S} = \mathbf{b}_1 \mathbf{X} + \mathbf{b}_o \mathbf{R} \tag{2.9}$$

The matrices $\mathbf{b}_o$ and $\mathbf{b}_1$ will be derived in Chapter 3. To find the redundant moments, the unit load method (2) will be used. In place of the redundant forces $X_1$ and $X_2$ , moments of unity are applied, represented by a vector

$$\bar{\mathbf{R}} = \{ 1 \quad 1 \} \tag{2.10}$$

The principle of virtual work, Equation (2.2) can then be used to find the displacements

$$\mathbf{r} = \{ \theta_{1\ell} \quad \theta_{nr} \} \tag{2.11}$$

corresponding to the redundant moments at the left support and the crown. The stresses $\bar{S}$ due to the unit moments at the supports and the crown are

$$\bar{S} = b_1 \bar{R} \tag{2.12}$$

The principle of virtual work therefore yields for the displacements $r$ the expression

$$r = b_1^t v \tag{2.13}$$

In view of Equations(2.5) and (2.9) the displacement vector can also be written

$$\begin{aligned} r &= b_1^t f\, b_0 R + b_1^t f\, b_1 X \\ &= D_0 + D_1 X \end{aligned} \tag{2.14}$$

where $$D_0 = b_1^t f\, b_0 R \tag{2.14a}$$

$$D_1 = b_1^t f\, b_1 \tag{2.14b}$$

The boundary conditions require that the rotations at the supports and at the crown are equal to zero.

$$r = 0 \tag{2.15}$$

Consequently, combining Equations (2.14) and (2.15) the redundant forces can be calculated (2) as

$$X = -D_1^{-1} D_0 \tag{2.16}$$

where $D_1^{-1}$ is equal to the inverse of $D_1$. The size of the matrices $D_0$ and $D_1$ depends on the number of redundancies. If p is

the number of redundancies the size of $\mathbf{D}_0$ will be p x m and that of $\mathbf{D}_1$ will be p x p.

Equation (2.16) is a general expression and by choosing the appropriate matrix $\mathbf{b}_1$ this equation can be used to calculate the single redundant moment $X_1$ at the crown for a single two-hinged arch or the two redundant moments $X_1$ and $X_2$ for an arch fixed against rotations at the supports.

Finite Element Formulation of Lateral Stability

Having calculated the redundant moments $\mathbf{X}$ the forces acting on each element are now completely defined by Equation (2.9). To establish the load which will cause lateral instability, consider now the forces $\mathbf{S}_i$ that will act on each element, if the structure is in a slightly displaced position, Figure 2.5. It will be assumed that at a point i in addition to the displacements due to $N_\zeta$ and $M_\xi$ the cross-section will be displaced in the x-direction by the amount u and will have rotated by a small amount $\Theta_z$. For the structure as a whole the displacements can be represented by a vector

$$\mathbf{r} = \{\mathbf{r}_1\ \mathbf{r}_2 \cdots \mathbf{r}_i \cdots \mathbf{r}_{n+1}\} \qquad (2.17)$$

where $\mathbf{r}_i = \{u\ v\ w\ \Theta_x\ \Theta_y\ \Theta_z\}$ are the displacements of a typical point i.

In terms of the m'th load - all other loads can then be expressed as fractions of the load $P_m$ - the forces on the elements can

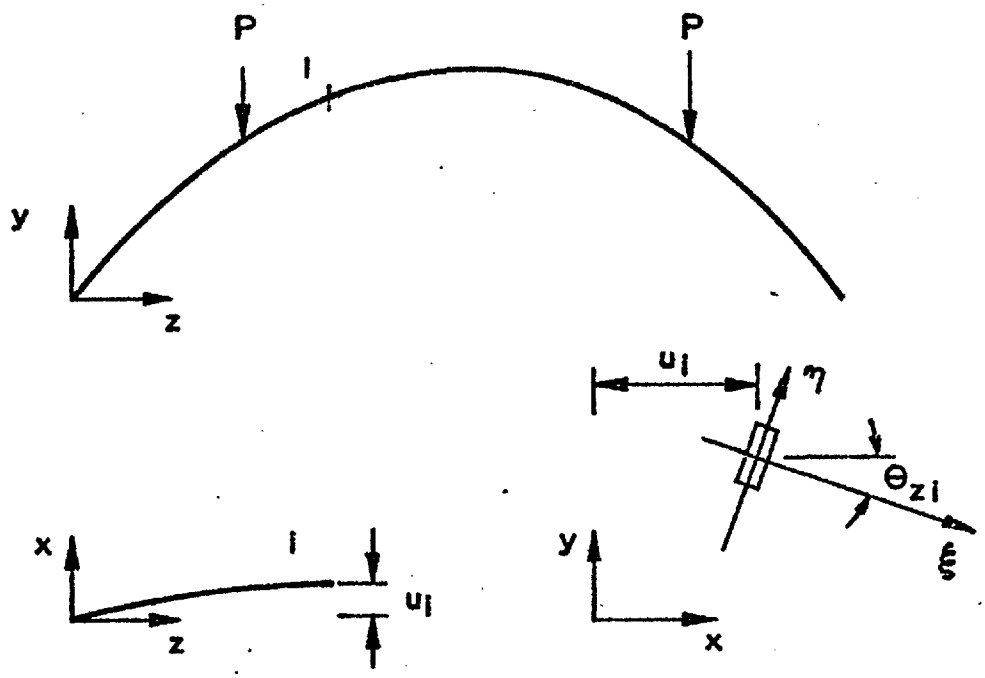


FIG 2.5 - DISPLACED POSITION OF CROSS SECTION AT POINT I

then be written

$$\mathbf{S} = P_m \mathbf{B}\, \mathbf{r} \qquad (2.18)$$

The matrix $\mathbf{B}$ can again be defined purely from statics and will be given in Chapter 3. Since, in the present case, there are n elements and n+1 nodal points, there will be a total of 6n components in the force vector $\mathbf{S}$ and 6(n+1) components in the displacement vector $\mathbf{r}$. Correspondingly the size of $\mathbf{B}$ will be 6n x 6(n+1).

Consider now a typical element $i$ between points i and (i+1). In addition to the axial forces $N_\zeta$ and the moments $M_{\xi\ell}$ and $M_{\xi r}$ about the major axis, this element i will also be subjected to moments $M_{\eta\ell}$ and $M_{\eta r}$ about its minor axis, $\eta$, due to the assumed rotation $\theta_z$, as well as a torsion moment $M_\zeta$ due to the lateral displacements u. These forces are given by the vector $\mathbf{S}_i$.

$$\mathbf{S}_i = \left\{ N_\zeta \;\; M_{\xi\ell} \;\; M_{\xi r} \;\; M_{\eta\ell} \;\; M_{\eta r} \;\; M_\zeta \right\} \qquad (2.19)$$

The local displacements

$$\mathbf{v}_i = \left\{ \Delta\zeta \;\; \theta_{\xi\ell} \; \theta_{\xi r} \; \theta_{\eta\ell} \; \theta_{\eta r} \; \theta_\zeta \right\}$$

of a typical element $i$ of length $\ell$ due to these forces are

$$\mathbf{v}_i = \mathbf{f}_i \mathbf{S}_i \qquad (2.20)$$

where the flexibility matrix $\mathbf{f}_i$ is given by

$$\mathbf{f}_i = \begin{bmatrix} \frac{\ell}{AE} & & & & & & \\ & \frac{\ell}{3EI_\xi} & \frac{\ell}{6EI_\xi} & & & & \\ & \frac{\ell}{6EI_\xi} & \frac{\ell}{3EI_\xi} & & & & \\ & & & \frac{\ell}{3EI_\eta} & \frac{\ell}{6EI_\eta} & & \\ & & & \frac{\ell}{6EI_\eta} & \frac{\ell}{3EI_\eta} & & \\ & & & & & \frac{\ell}{GJ} & \end{bmatrix} \qquad (2.21)$$

where A is equal to the cross-sectional area of the element, E equals the modulus of elasticity, $EI_\xi$ and $EI_\eta$ are equal to the bending stiffness about the major and minor axis of the cross-section and GJ equals the torsional rigidity of the section.

If we let $\mathbf{S} = \{S_1, S_2 \ \dots \ S_i \ \dots \ S_n\}$ be a vector of the forces on each element then, for the displaced structure as a whole, the displacements $\mathbf{v} = \{v_1, v_2 \ \dots \ v_i \ \dots \ v_n\}$ are given by

$$\mathbf{v} = \mathbf{f}\,\mathbf{S} \qquad (2.22)$$

where $\mathbf{f} = [f_1 \ f_2 \ \dots \ f_i \ \dots \ f_n]$ is again a diagonal matrix of the flexibilities $\mathbf{f}_i$.

To establish a relation between the nodal point displacements $\mathbf{r}$ and the element displacements $\mathbf{v}$ again the unit load method can be used. Let $\bar{\mathbf{R}} = \{1 \ 1 \ 1 \ \dots \ 1\}$ be a column vector of size $6(n+1)$, corresponding to the displacements $\mathbf{r}$ of Equation (2.17).

The stresses due to $\bar{\mathbf{R}}$ in the undeformed structure are

$$\bar{\mathbf{S}} = \mathbf{b}\,\bar{\mathbf{R}} \tag{2.23}$$

where $\mathbf{b}$ is a matrix obtained from statics and fully described in Chapter 3. From the principle of virtual work, Equation (2.2), using virtual forces, it follows that

$$\mathbf{r} = \mathbf{b}^{t}\,\mathbf{v} \tag{2.24}$$

Expressing the local displacements in terms of element forces, Equation (2.22), this can be written

$$\mathbf{r} = \mathbf{b}^{t}\,\mathbf{f}\,\mathbf{S} \tag{2.25}$$

Finally substituting Equation (2.18) for the element forces the displacement vector becomes

$$\mathbf{r} = P_{m}\,\mathbf{b}^{t}\,\mathbf{f}\,\mathbf{B}\,\mathbf{r} \tag{2.26}$$

or $$\left[\mathbf{I} - P_{m}\,\mathbf{b}\,\mathbf{f}\,\mathbf{B}\right]\mathbf{r} = \mathbf{0} \tag{2.27}$$

where $\mathbf{I}$ is a unit matrix of size (6n x 6n). This equation defines the eigenvalue problem for the lateral stability of arches and beams and was suggested to the author by Prof. Kelsey.

A solution for this eigenvalue problem can be obtained by an iterative technique, such as given by Collatz (11). The iteration can be initiated by an assumed shape of the displacement function $\mathbf{r} = \mathbf{r}_{0}$. Substituting this value of $\mathbf{r}$ into the right-hand side of Equation (2.26)

a new value $\mathbf{r}_1$ can be calculated. The ratio of the value of the $n^{th}$ element of vector $\mathbf{r}_1$ to the corresponding value of $\mathbf{r}_0$ will give a first estimate of the inverse of the lowest eigenvalue $P_m$. After normalizing the vector $\mathbf{r}_1$, the calculation can then be repeated with the new value of $\mathbf{r}_1$ on the right-hand side of Equation (2.26). The iteration should be repeated until there is no significant difference between two successive estimates of $P_m$. The value of $P_m$ represents the load which will just maintain the displacements without causing collapse, in other words $P_m$ is the critical load for lateral stability.

Reduction of Size of Matrices

The solution, in its present form, requires the complete flexibility matrix $\mathbf{f}$, Equation (2.22), which is of size 6n x 6n, n being the number of elements. A more compact form can be derived in the following manner. Consider the flexibility $\mathbf{f}_i$, Equation (2.21). It is apparent that this matrix can be partitioned into a flexibility for the axial force $N_\zeta$ together with the moments $M_{\zeta\ell}$ and $M_{\zeta r}$ and a flexibility for the remaining three moments $M_{\eta\ell}$, $M_{\eta r}$, and $M_\zeta$.

$$\mathbf{f}_i = \begin{bmatrix} \mathbf{f}_{1i} & \mathbf{0} \\ \mathbf{0} & \mathbf{f}_{2i} \end{bmatrix} \tag{2.28}$$

where

$$\mathbf{f}_{1i} = \frac{\ell}{6EI_\zeta} \begin{bmatrix} I_\zeta/A & 0 & 0 \\ 0 & 2 & 1 \\ 0 & 1 & 2 \end{bmatrix} \tag{2.29}$$

and

$$\mathbf{f}_{2i} = \frac{\ell}{6EI_\eta}\begin{bmatrix} 2 & 1 & 0 \\ 1 & 2 & 0 \\ 0 & 0 & 6EI_\eta/(GJ) \end{bmatrix} \tag{2.30}$$

Correspondingly the displacement vector $\mathbf{v}_i$ for an individual element becomes

$$\mathbf{v} = \begin{bmatrix} \mathbf{v}_{1i} \\ \mathbf{v}_{2i} \end{bmatrix} = \begin{bmatrix} \mathbf{f}_{1i} & \mathbf{0} \\ \mathbf{0} & \mathbf{f}_{2i} \end{bmatrix} \begin{bmatrix} \mathbf{S}_{1i} \\ \mathbf{S}_{2i} \end{bmatrix} \tag{2.31}$$

where $$\mathbf{v}_{1i} = \left\{ \Delta\zeta \quad \Theta_{\xi\ell} \quad \Theta_{\xi r} \right\} \tag{2.32a}$$

$$\mathbf{v}_{2i} = \left\{ \Theta_{\eta\ell} \quad \Theta_{\eta r} \quad \Theta_\zeta \right\} \tag{2.32b}$$

$$\mathbf{S}_{1i} = \left\{ N_\zeta \quad M_{\xi\ell} \quad M_{\xi r} \right\} \tag{2.33a}$$

$$\mathbf{S}_{2i} = \left\{ M_{\eta\ell} \quad M_{\eta r} \quad M_\zeta \right\} \tag{2.33b}$$

The vectors of forces and displacements of all elements can be split in a similar manner

$$\mathbf{v}_1 = \left\{ \mathbf{v}_{11} \quad \mathbf{v}_{12} \quad \cdots \mathbf{v}_{1i} \quad \cdots \mathbf{v}_{1n} \right\} \tag{2.34a}$$

$$\mathbf{v}_2 = \left\{ \mathbf{v}_{21} \quad \mathbf{v}_{22} \quad \cdots \mathbf{v}_{2i} \quad \cdots \mathbf{v}_{2n} \right\} \tag{2.34b}$$

$$\mathbf{S}_1 = \left\{ \mathbf{S}_{11} \quad \mathbf{S}_{12} \quad \cdots \mathbf{S}_{1i} \quad \cdots \mathbf{S}_{1n} \right\} \tag{2.35a}$$

$$\mathbf{S}_2 = \left\{ \mathbf{S}_{21} \quad \mathbf{S}_{22} \quad \cdots \mathbf{S}_{2i} \quad \cdots \mathbf{S}_{2n} \right\} \tag{2.35b}$$

The flexibility matrix $\mathbf{f}$ for the whole structure becomes

$$\mathbf{f} = \begin{bmatrix} \mathbf{f}_1 & \mathbf{0} \\ \mathbf{0} & \mathbf{f}_2 \end{bmatrix} \tag{2.36}$$

where $$\mathbf{f}_1 = \begin{bmatrix} f_{11} & f_{12} & \cdots & f_{1i} & \cdots & f_{1n} \end{bmatrix} \quad (2.36a)$$

$$\mathbf{f}_2 = \begin{bmatrix} f_{21} & f_{22} & \cdots & f_{2i} & \cdots & f_{2n} \end{bmatrix} \quad (2.36b)$$

Assuming small displacements only, the forces $\mathbf{S}_2$ can be calculated from the displacements u and $\Theta_z$ alone, permitting a partitioning of the matrix $\mathbf{B}$

$$\mathbf{S} = \begin{bmatrix} \mathbf{S}_1 \\ \mathbf{S}_2 \end{bmatrix} = P \begin{bmatrix} \mathbf{B}_1 & \mathbf{O} \\ \mathbf{O} & \mathbf{B}_2 \end{bmatrix} \begin{bmatrix} \mathbf{r}_1 \\ \mathbf{r}_2 \end{bmatrix} \quad (2.37)$$

where $$\mathbf{r}_1 = \{ v_1 \quad v_2 \quad \cdots \quad v_i \quad \cdots \quad v_{n+1} \} \quad (2.38a)$$

$$\mathbf{r}_2 = \{ u_1 \quad u_2 \quad \cdots \quad u_i \quad \cdots u_{n+1} \; \Theta_{z1} \Theta_{z2} \cdots \Theta_{zi} \cdots \Theta_{zn+1} \} \quad (2.38b)$$

The sizes of the matrices $\mathbf{B}_1$ and $\mathbf{B}_2$ are $3n \times (n+1)$ and $3n \times 2(n+1)$ respectively

Corresponding to the displacement vectors $\mathbf{r}_1$ and $\mathbf{r}_2$ there are unit loads $\bar{\mathbf{R}}_1$ and $\bar{\mathbf{R}}_2$ .

$$\bar{\mathbf{R}}_1 = \{ 1 \; 1 \; \ldots \quad 1 \} \quad (2.39a)$$

$$\bar{\mathbf{R}}_2 = \{ 1 \; 1 \; \ldots \quad 1 \; 1 \; \ldots \quad 1 \} \quad (2.39b)$$

Since, for the undeformed structure, the vertical forces will only contribute to the stresses $\bar{\mathbf{S}}_1$ , while the horizontal forces and the torques at each point will be responsible for the stresses $\bar{\mathbf{S}}_2$ , the stresses due to the unit loads $\bar{\mathbf{R}}_1$ and $\bar{\mathbf{R}}_2$ can be written as

$$\bar{\mathbf{S}} = \begin{bmatrix} \bar{\mathbf{S}}_1 \\ \bar{\mathbf{S}}_2 \end{bmatrix} = \begin{bmatrix} \mathbf{b}_1 & \mathbf{O} \\ \mathbf{O} & \mathbf{b}_2 \end{bmatrix} \begin{bmatrix} \bar{\mathbf{R}}_1 \\ \bar{\mathbf{R}}_2 \end{bmatrix} \quad (2.40)$$

Applying again the principle of virtual work, the displacements become

$$\mathbf{r} = \begin{bmatrix} \mathbf{r}_1 \\ \mathbf{r}_2 \end{bmatrix} = P_m \begin{bmatrix} \mathbf{b}_1^t \mathbf{f}_1 \mathbf{B}_1 \mathbf{r}_1 \\ \mathbf{b}_2^t \mathbf{f}_2 \mathbf{B}_2 \mathbf{r}_r \end{bmatrix} \tag{2.41}$$

Equation (2.41) indicates that for the assumed small displacements, the lateral displacements and rotations $\mathbf{r}_2$ are independent of the vertical displacements $\mathbf{r}_1$. To find $P_m$ it is therefore sufficient to establish the matrices $\mathbf{b}_2$ and $\mathbf{B}_2$ and to solve the eigenvalue problem

$$\mathbf{r}_2 = P_m \mathbf{b}_2^t \mathbf{f}_2 \mathbf{B}_2 \mathbf{r}_2 \tag{2.42}$$

or

$$\left[\mathbf{I} - P_m \mathbf{b}_2^t \mathbf{f}_2 \mathbf{B}_2\right] \mathbf{r}_2 = \mathbf{0} \tag{2.43}$$

The unit matrix $\mathbf{I}$ here is only of size $3n \times 3n$. When evaluating the critical load $P_m$ with an electronic computer this formulation therefore will require only $\frac{1}{4}$ of the storage space required for the previous formulation, Equation (2.27), with a corresponding reduction in computing time. Equation (2.43) is sufficient for the calculation of critical loads for the lateral stability of arches or beams. The subscript 2 therefore will be omitted in the future, when referring to any of the matrices $\mathbf{b}_2$, $\mathbf{B}_2$ or $\mathbf{f}_2$.

## Nondimensional Matrix Formulation for Arches

It is also convenient to use a non-dimensional representation

for the displacements. Linear displacements can be divided by the span length L, so that

$$\mathbf{r} = \left\{ u_1/L \quad u_2/L \quad u_3/L \ \ldots \ u_i/L \ldots \ u_{n+1}/L \quad \Theta_1 \ldots \Theta_{n+1} \right\} \qquad (2.44)$$

Further to obtain non-dimensional expressions for the matrices $\mathbf{b}$, $\mathbf{B}$ and $\mathbf{f}$, it is also convenient to divide all moments by the span to give

$$\mathbf{S}_i = \left\{ M_{\eta\ell}/L \quad M_{\eta r}/L \quad M_\zeta/L \right\} \qquad (2.45)$$

Finally, instead of using the definition for the element load vector $\mathbf{S}$ given by Equation (2.35b) it is more convenient to choose a different order, i.e. to collect all $M_\eta$ into one sub-vector and all $M_\zeta$ into a second sub-vector

$$\mathbf{S} = \left\{ \mathbf{S}_b \ \mathbf{S}_t \right\} \qquad (2.46)$$

where $$\mathbf{S}_b = \frac{1}{L} \left\{ M_{\eta\ell 1} \quad M_{\eta r 1} \ \ldots \ M_{\eta\ell n} \quad M_{\eta r n} \right\} \qquad (2.46a)$$

$$\mathbf{S}_t = \frac{1}{L} \left\{ M_{\zeta 1} \quad M_{\zeta 2} \ \ldots \ M_{\zeta i} \ \ldots \ M_{\zeta n} \right\} \qquad (2.46b)$$

In Chapter 3 it will be shown that with these definitions the matrices $\mathbf{b}$ and $\mathbf{B}$ become dimensionless and the flexibility matrix will be given by the following expression

$$\mathbf{f} = \frac{L^2}{6EI} \begin{bmatrix} \mathbf{f}_b & \mathbf{0} \\ \mathbf{0} & \mathbf{f}_t \end{bmatrix} \qquad (2.47)$$

where

$$\mathbf{f}_b = \left[ f_{b1} \quad f_{b2} \quad \cdots f_{bi} \cdots \quad f_{bn} \right] \tag{2.48a}$$

$$\mathbf{f} = \left[ f_{t1} \quad f_{t2} \quad \cdots f_{ti} \cdots \quad f_{tn} \right] \tag{2.48b}$$

and

$$\mathbf{f}_{bi} = \begin{bmatrix} 2\,\ell/L & \ell/L \\ \ell/L & 2\,\ell/L \end{bmatrix} \tag{2.49}$$

$$f_{ti} = \frac{6\ell\, EI_\eta}{LGJ} \tag{2.50}$$

The constants $EI_\eta$ and GJ are the bending stiffness about the minor axis and the torsional rigidity respectively of the beam element. If the structure has a variable cross-section along the length of the arch or the span the same formulation can still be used. In that case $EI_\eta$ can be taken as the stiffness of an element at the centre, for example, and the flexibilities $\mathbf{f}_i$ of all other elements can be expressed in terms of the ratio of the centre stiffness to their own stiffness. To evaluate the non-dimensional part of the stiffness matrix, it is sufficient to know the ratio of bending stiffness, $EI_\eta$ , to torsional rigidity, GJ.

With the above, non-dimensional definition of the flexibility matrix the eigenvalue problem becomes

$$\mathbf{r} = P_m \frac{L^2}{6EI_\eta}\, \mathbf{b}^t\, \mathbf{f}\, \mathbf{B}\, \mathbf{r} \tag{2.51}$$

If we call the first eigenvalue of Equation (2.51) c and let $c_2 = 6c$, then the critical load for lateral stability of the arch will be

$$P_{cr} = \frac{c_2 EI_\eta}{L^2} \tag{2.52}$$

Since the flexibility matrix, Equation (2.47) includes the non-dimensional parameters $f_{ti}$ it is apparent that $c_2$ is a function of the ratio $EI_\eta / GJ$.

Nondimensional Matrix Formulation for Beams

In the case of straight beams a still more ~~general~~ specific formulation is possible. In Chapter 3 it will be shown that for beams the matrices **B** and **b** can be partitioned in the following manner

$$\mathbf{B} = \begin{bmatrix} \mathbf{0} & L\mathbf{B}_b \\ \mathbf{B}_t & \mathbf{0} \end{bmatrix} \tag{2.53}$$

$$\mathbf{b} = \begin{bmatrix} L\mathbf{b}_b & \mathbf{0} \\ \mathbf{0} & \mathbf{b}_t \end{bmatrix} \tag{2.54}$$

As previously, the flexibility of the structure can be partitioned into two parts, one derived from the lateral bending stiffness and the other from the torsional rigidity.

In this case, however, constants will be attached to the two individual flexibilities rather than to the overall flexibility

$$\mathbf{f}_b = \frac{L}{6EI_\eta}\left[\mathbf{f}_{b1}\ \mathbf{f}_{b2}\ldots\mathbf{f}_{bi}\ldots\mathbf{f}_{bn}\right] \tag{2.55a}$$

$$\mathbf{f}_t = \frac{L}{GJ}\left[f_{t1}\ f_{t2}\ldots f_{ti}\ldots f_{tn}\right] \tag{2.55b}$$

where $\mathbf{f}_{bi}$ is given by Equation (2.49) and $f_{ti} = \ell/L$.

Substitution of Equations (2.53), (2.54) and (2.55) into Equation (2.42) results in the following expression for the displacements

$$\mathbf{r} = \left\{\mathbf{r}_b\ \mathbf{r}_t\right\} \tag{2.56}$$

where

$$\mathbf{r}_b = \frac{P_m L^3}{6EI_\eta}\,\mathbf{b}_b^t\,\mathbf{f}_b\,\mathbf{B}_b\,\mathbf{r}_t \tag{2.56a}$$

$$\mathbf{r}_t = \frac{P_m L}{GJ}\,\mathbf{b}_t^t\,\mathbf{f}_t\,\mathbf{B}_t\,\mathbf{r}_b \tag{2.56b}$$

Combining Equations (2.56a) and (2.56b) the eigenvalue problem for the straight beam can finally be written as

$$\mathbf{r}_t = \frac{P_m^2 L^4}{6EI_\eta GJ}\,\mathbf{b}_t^t\,\mathbf{f}_t\,\mathbf{B}_t\,\mathbf{b}_b^t\,\mathbf{f}_b\,\mathbf{B}_b\,\mathbf{r}_t \tag{2.57}$$

Designating the lowest eigenvalue of Equation (2.57) by c, and using the notation $c_t = 6c$, the critical load at which a straight beam becomes unstable in the lateral direction becomes

$$P_{cr} = c_t\sqrt{EI_\eta\,GJ}\,/L^2 \tag{2.58}$$

Values of $c_t$ can be calculated for different loading conditions from Equation (2.57).

Stresses due to Initial Eccentricities

Finally the effect of initial bow, $u_i$ , or twist, $\theta_i$ , on the lateral stability of a beam will be discussed. If initially the beam axis is not straight or if the load has some lateral eccentricity then torsional moments $M_z$ and consequently bending moments $M_\eta = \theta_z M_x$ about the minor axis of the cross-section will be present from the very beginning of loading. In this case the problem is not one of bifurcation but rather one of excessive stresses. Added to the stresses $\sigma_\xi$ due to bending about the major axis are stresses $\sigma_\eta$ due to bending about the minor axis. The maximum stress on any particular cross-section therefore is

$$\sigma_{max} = \sigma_\xi + \sigma_\eta$$

$$= \frac{M_x}{S_\xi} \left(1 + \theta \, S_\xi / S_\eta \right) \qquad (2.59)$$

where $S_\xi$ and $S_\eta$ are section moduli about $\xi$ and $\eta$ -axis respectively.

To find the maximum stress for some initial displacement $\mathbf{r}_o$ , due to a given load vector $P_m \mathbf{R}$ , it is therefore necessary to find the corresponding rotations $\theta$ . Let the actual displacements due to $P_m \mathbf{R}$ be designated by the vector $\mathbf{r}^*$. Then at each point the total displacement will be $u_i/L = u_i^*/L + u_{oi}/L$. Similarly, the total rotations will be $\theta_i = \theta_i^* + \theta_{oi}$ .

For the structure as a whole the vector

$\mathbf{r} = \{ u_1/L \;\; u_2/L \cdots u_i/L \cdots u_{n+1}/L \;\; \theta_1 \cdots \theta_{n+1} \}$ will be

$$\mathbf{r} = \mathbf{r}^* + \mathbf{r}_o \qquad (2.60)$$

Analogous to Equation (2.25) by applying the principle of virtual work, the actual displacements $\mathbf{r}^*$ can be expressed in terms of the element forces $\mathbf{S}$

$$\mathbf{r}^* = \mathbf{b}^t \mathbf{f} \mathbf{S} \tag{2.61}$$

The element forces, in this case, are the result of initial displacements as well as subsequent actual displacements

$$\mathbf{S} = P_m [\mathbf{B} \ \mathbf{B}] \begin{bmatrix} \mathbf{r}^* \\ \mathbf{r}_o \end{bmatrix} \tag{2.62}$$

The additional displacements therefore become

$$\mathbf{r}^* = P_m \mathbf{b}^t \mathbf{f} [\mathbf{B} \ \mathbf{B}] \begin{bmatrix} \mathbf{r}^* \\ \mathbf{r}_o \end{bmatrix} \tag{2.63}$$

As previously, Equation (2.56), this can be written in terms of the partitioned matrices as

$$\mathbf{r}_b^* = P_m \mathbf{b}_b^t \mathbf{f}_b \mathbf{B}_b [\mathbf{r}_t^* + \mathbf{r}_{to}] \tag{2.64}$$

$$\mathbf{r}_t^* = P_m \mathbf{b}_t^t \mathbf{f}_t \mathbf{B}_t [\mathbf{r}_b^* + \mathbf{r}_{bo}] \tag{2.65}$$

Substituting Equation (2.64) into (2.65) the vector of additional rotations due to torsion becomes

$$\mathbf{r}_t^* = P_m^2 \mathbf{b}_t^t \mathbf{f}_t \mathbf{B}_t \mathbf{b}_b^t \mathbf{f}_b \mathbf{B}_b [\mathbf{r}_t^* + \mathbf{r}_{to}] + P_m \mathbf{b}_t^t \mathbf{f}_t \mathbf{B}_t \mathbf{r}_{bo} \tag{2.66}$$

This equation can be solved for $\mathbf{r}_t^*$ by an iterative process,

similar to the one used for the solution of the eigenvalue problem, Equation (2.26). Contrary to the eigenvalue problem, however, Equation (2.66) does not yield directly a critical value of $P_m$. It is necessary to solve Equation (2.66) for a number of values of $P_m$. For a given value of $P_m$ the solution for the vector $r_t^*$ then also contains the rotation $\theta_i^*$ for the particular section i for which the stresses are to be calculated.

The total rotation $\theta_i$ at this point then will be

$$\theta_i = \theta_{oi} + \theta_i^* \qquad (2.67)$$

With this value of $\theta_i$ the maximum stress $\sigma_{max}$ for the section i can then be calculated with Equation (2.59). To determine the critical load $P_{cr}$, which will produce a critical stress $\sigma_{cr}$, the calculations have to be repeated for a number of values of $P_m$ until $\sigma_{max}$ equals $\sigma_{cr}$.

# Chapter 3

## Matrices for the Solution of the Lateral Stability Problem

### Introduction

Having established a general procedure for calculating the critical loads for the lateral stability of arches and beams, it will be necessary to derive the various transformation matrices required for these calculations. First the transformations $\mathbf{b}_o$ and $\mathbf{b}_1$ required for the calculation of the redundant forces in the ~~two-hinged~~ arch will be considered. This will be followed by the derivation of the matrices $\mathbf{B}$ and $\mathbf{b}$ required for the lateral stability of arches loaded in a vertical direction. Matrices will also be derived for beams subjected to constant end moments or concentrated forces.

### Matrix $\mathbf{b}_o$

The forces chosen as redundancies are the moments at the supports A and B and at the crown C. The basic system therefore is a three-hinged arch. For a symmetrical arch under symmetrical loading the forces for the left half of the arch are shown in Fig. 3.1. The vertical and horizontal reactions for a load at a point j are

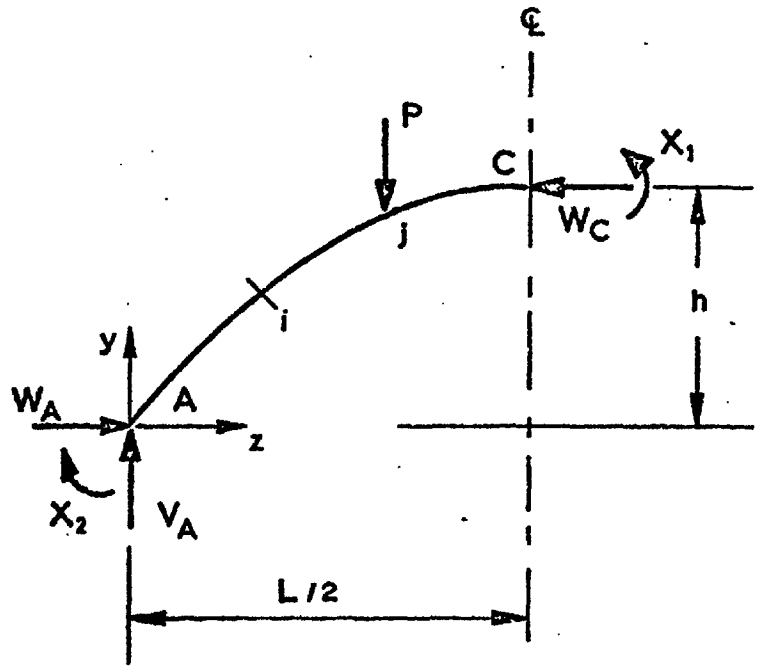


FIG. 3.1 - FORCES ON LEFT HALF OF ARCH DUE TO SYMMETRICAL LOADING

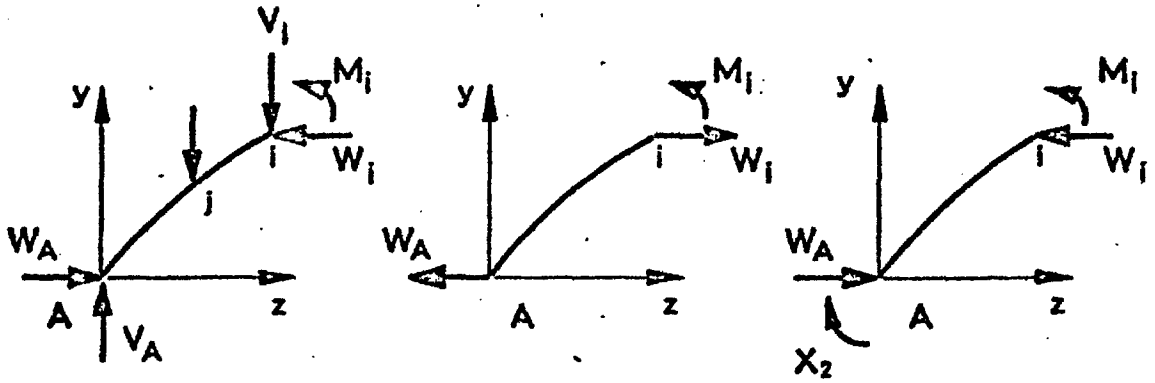


FIG. 3.2 - FORCES AT POINT I OF ARCH DUE TO VERTICAL LOADS $P_j$

$$V_C = 0 \qquad W_C = (z_j / h)\, P_j$$

$$V_A = P_j \qquad W_A = H_C \tag{3.1}$$

For a point i less than j the forces are

$$V_i = P_j$$

$$W_i = P_j\, z_j / h$$

$$M_i = (z_i - z_j\, y_i / h)\, P_j \tag{3.2}$$

For a point i equal to or larger than j, Fig. 3.2(a), the forces are

$$V_i = 0$$

$$W_i = P_j\, z_j / h$$

$$M_i = (1 - y_i / h)\, z_j\, P_j \tag{3.3}$$

To allow non-dimensional representation of transformation matrices, it is convenient to express moments in terms of the overall span L, i.e. moments will be given as $M_i / L$.

In matrix form the forces $\mathbf{F} = \{ V_i \; W_i \; M_i / L \}$ at a point i can therefore be written

$$\mathbf{F}_i = \mathbf{t}_{oi}\, \mathbf{R} \tag{3.4}$$

where the external vertical forces $P_1$, $P_2$ etc. are represented by the vector

$$\mathbf{R} = \{ P_1 \; P_2 \; \ldots \; P_j \; \ldots \; P_m \} \tag{3.5}$$

and the transformation matrix $\mathbf{t}_{oi}$ is given by

$$\mathbf{t}_{oi} = \left[\begin{array}{cccc:ccc} 1 & 1 & \cdots & 1 & 0 & \cdots & 0 \\ z_1/h & \cdots & & & z_j/h & \cdots & z_m/h \\ \cdots & \left(\frac{z_i}{L} - \frac{z_j}{L}\frac{y_i}{h}\right) & \cdots & & \cdots & \frac{z_i}{L}\left(1 - \frac{y_i}{h}\right) & \cdots \end{array}\right] \qquad (3.6)$$

Next consider an element i. This element lies between points i and (i + 1). The direction cosines of the element axis are $n_i$ and $m_i$. The forces $\mathbf{F}_i$ and $\mathbf{F}_{i+1}$ acting on this element at either end have to be transformed into forces parallel to the local coordinate axes $\xi$, $\eta$, $\zeta$. The effect of shear on the deformation of beams will not be considered at present and the ~~relative~~ relevant terms in $\mathbf{S}_i$, Equation 2.3, therefore will be suppressed. Furthermore, since the axial forces $W_\zeta$ at points i and i+1 are equal in magnitude, only one of these forces will be included in the vector $\mathbf{S}_i$. The element forces are then given by

$$\mathbf{S}_i = \mathbf{C}_i \begin{bmatrix} \mathbf{F}_i \\ \mathbf{F}_{i+1} \end{bmatrix} \qquad (3.7)$$

where $$\mathbf{S}_i = \left\{ N_i \quad M_{i\ell}/L \quad M_{ir}/L \right\} \qquad (3.8)$$

and $$\mathbf{C}_i = \begin{bmatrix} m_i & n_i & 0 & 0 & 0 & 0 \\ 0 & 0 & 1 & 0 & 0 & 0 \\ 0 & 0 & 0 & 0 & 0 & 1 \end{bmatrix} \qquad (3.9)$$

Combining Equations 3.4 and 3.7 the forces on the element i

are therefore

$$\mathbf{S}_i = \mathbf{C}_i \begin{bmatrix} \mathbf{t}_{oi} \\ \mathbf{t}_{oi+1} \end{bmatrix} \mathbf{R} \qquad (3.10)$$

Equation (3.10) can also be written as

$$\mathbf{S}_i = \mathbf{b}_{oi}\, \mathbf{R} \qquad (3.11)$$

where $$\mathbf{b}_{oi} = \mathbf{C}_i \begin{bmatrix} \mathbf{t}_{oi} \\ \mathbf{t}_{oi+1} \end{bmatrix} \qquad (3.12)$$

This, however, is the required relationship between the external forces and the element forces. If the forces $\mathbf{S}_i$ on all elements are combined into a single vector $\mathbf{S}_o = \{\mathbf{S}_1\ \mathbf{S}_2 \cdots\ \mathbf{S}_i \cdots\ \mathbf{S}_n\}$, the relation between element forces and external loads can then be written

$$\mathbf{S}_o = \mathbf{b}_o\, \mathbf{R} \qquad (3.13)$$

where $$\mathbf{b}_o = \{\mathbf{b}_{o1}\ \mathbf{b}_{o2}\ \mathbf{b}_{o3} \cdots\ \mathbf{b}_{oi} \cdots\ \mathbf{b}_{on}\} \qquad (3.14)$$

A single transformation matrix $\mathbf{b}_o$ for the basic system can therefore be established by evaluating Equations (3.6) and (3.9) for each element. The individual components of the transformation matrix $\mathbf{b}_o$, Equation (3.14), are then obtained from Equation (3.10).

Matrix $\mathbf{b}_1$

The transformation matrix $\mathbf{b}_1$ gives the additional element forces due to the redundant moments $\mathbf{X} = \{X_1/L \qquad X_2/L\}$.

A consideration of the equilibrium of forces and moments, due to the moments $X_1$ and $X_2$ shown in Fig. 3.1 gives the following reactions

due to $X_1$ : $V_A = V_C = 0$, $W_A = -X_1/h$, $W_C = W_A$

due to $X_2$ : $V_A = V_C = 0$, $W_A = X_2/h$, $W_C = W_A$

(3.15)

For a point i the forces are, Fig. 3.2,

due to $X_1$ : $V_i = 0$, $W_i = -X_1/h$, $M_i = X_1 y/h$

due to $X_2$ : $V_i = 0$, $W_i = X_2/h$, $M_i = X_2(1 - y/h)$

(3.16)

In matrix form the forces $\mathbf{F}_i = \{ V_i \; W_i \; M_i/L \}$ at point i become

$$\mathbf{F}_i = \mathbf{t}_{1,i} \, \mathbf{X} \qquad (3.17)$$

where

$$\mathbf{t}_{1,i} = \begin{bmatrix} 0 & 0 \\ -L/h & L/h \\ \frac{y_i}{L}/\frac{h}{L} & 1 - \frac{y_i}{L}/\frac{h}{L} \end{bmatrix} \qquad (3.18)$$

As for the basic system the forces at point i and (i+1) at either end of an element i have to be combined and premultiplied by

the appropriate direction cosines to obtain the element forces

$$\mathbf{S}_{1i} = \mathbf{C}_i \begin{bmatrix} \mathbf{t}_{1i} \\ \mathbf{t}_{1i+1} \end{bmatrix} \mathbf{X} = \mathbf{b}_{1i} \mathbf{X} \qquad (3.19)$$

The combined vector $\mathbf{S}_1 = \{ \mathbf{S}_{11} \ \mathbf{S}_{12} \cdots \ \mathbf{S}_{1i} \cdots \ \mathbf{S}_{1n} \}$ of all element forces due to $\mathbf{X}$ then will be

$$\mathbf{S}_1 = \mathbf{b}_1 \mathbf{X} \qquad (3.20)$$

where $\mathbf{b}_1 = \{ \mathbf{b}_{11} \ \mathbf{b}_{12} \cdots \ \mathbf{b}_{1i} \cdots \ \mathbf{b}_{1n} \}$ (3.21)

Similar to $\mathbf{b}_0$ the matrix $\mathbf{b}_1$ also is dimensionless.

Matrix **b**

The transformation matrix $\mathbf{b}$ will give the element forces $\bar{\mathbf{S}} = \{ \mathbf{S}_b \ \mathbf{S}_t \}$ in the undeformed structure due to external (virtual) forces $\bar{\mathbf{U}} = \mathrm{U} \quad \mathrm{U} \ \cdots \ \mathrm{U} \ \cdots \ \mathrm{U}$ and $\bar{\mathbf{M}}_z = \{ \bar{\mathrm{M}}_{z1} \ \bar{\mathrm{M}}_{z2} \cdots \ \bar{\mathrm{M}}_{zi} \cdots \bar{\mathrm{M}}_{z\,n+1} \}$ where U and $\mathrm{M}_z$ are unit forces corresponding to displacements u and rotations $\Theta_z$. The undeformed structure under the action of these unit forces $\bar{\mathbf{R}} = \{ \bar{\mathbf{U}} \ \bar{\mathbf{M}}_z \}$ is shown in Fig. 3.3. The element forces consist of bending moments about the $\eta$ -axis of each element, $\mathbf{S}_b = \{ \mathrm{M}_{\eta 1 \ell} \ \mathrm{M}_{\eta 1 r} \ \mathrm{M}_{\eta 2 \ell} \ \mathrm{M}_{\eta 2 r} \cdots \mathrm{M}_{\eta n \ell} \ \mathrm{M}_{\eta n r} \}$ and torsion moments about the $\zeta$ -axis, $\mathbf{S}_t = \{ \mathrm{M}_{\zeta 1} \cdots \mathrm{M}_{\zeta i} \cdots \mathrm{M}_{\zeta n} \}$. These element forces for the undeformed structure are to be given by

$$\bar{\mathbf{S}} = \mathbf{b} \bar{\mathbf{R}} \qquad (3.22)$$

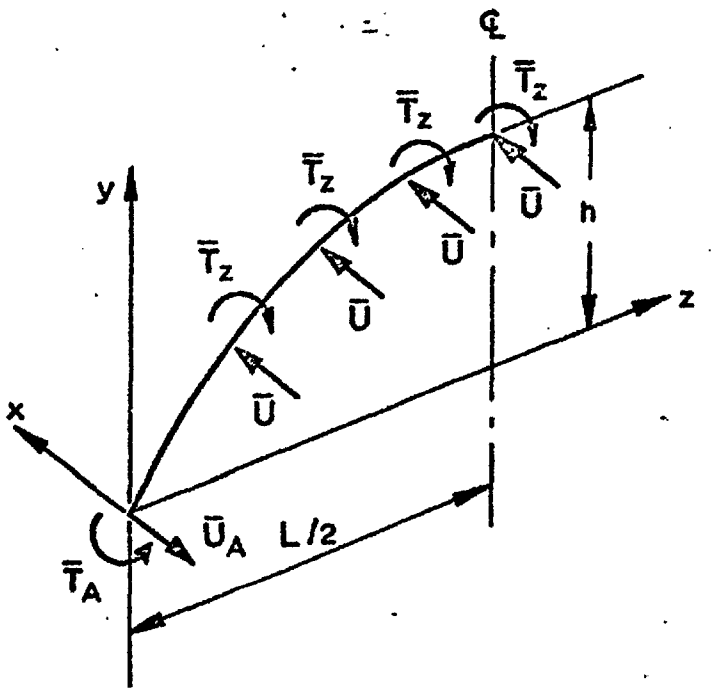


NB all T should read M

FIG. 3.3 - FORCES $\bar{U}$ AND MOMENTS $\bar{T}_z$ OF UNITY ON SYMMETRICAL ARCH

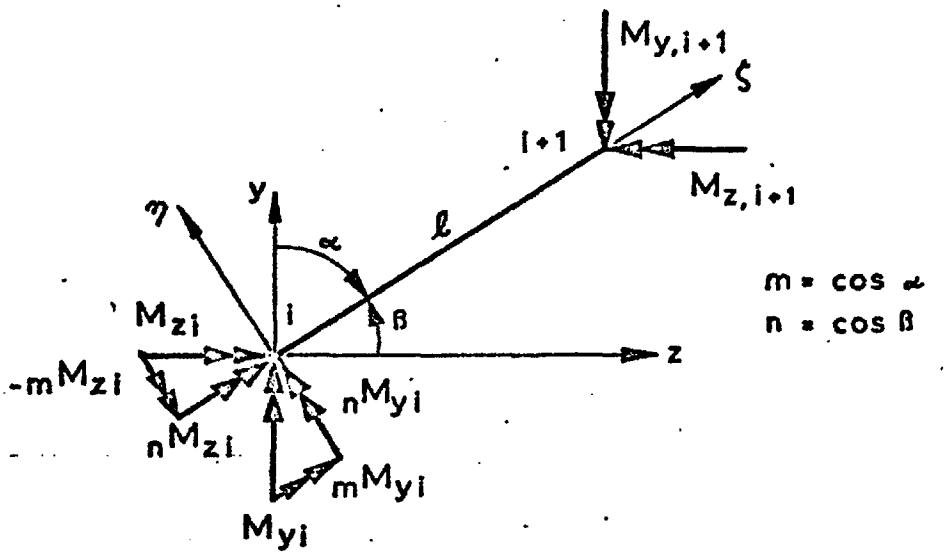


FIG. 3.4 - MOMENTS ON ELEMENT i

Two cases have to be considered. In the first case the structure is free to rotate about the $y$ -axis at points A and B. In the second case, the supports are restrained from rotation.

Consider first the simply supported case. At a point i the bending moment about the $y$ -axis due to the $\bar{U}$ -forces is

$$M_{yi} = -\sum_{j=1}^{i}(U_j\ z_j) - \left(\sum_{j=i+1}^{n+1} U_j\right) z_i \qquad (3.23)$$

The torsional moment at the same point due to the unit torsion $\bar{M}_z$ is

$$M_{zi} = -\sum_{j=i}^{n+1} \bar{M}_{zj} \qquad (3.24)$$

If $\mathbf{M}_y = \left\{ M_{y1} \quad M_{y2} \ldots M_{yi} \ldots \quad M_{yn+1} \right\}$ and

$\mathbf{M}_z = \left\{ M_{z1} \quad M_{z2} \ldots M_{zi} \ldots \quad M_{zn+1} \right\}$ are vectors containing the moments $M_y$ and $M_z$ then a vector $\bar{\mathbf{M}} = \left\{ \mathbf{M}_y \ \mathbf{M}_z \right\}$ can be calculated from

$$\bar{\mathbf{M}} = \mathbf{S}_x\, \bar{\mathbf{R}} \qquad (3.25)$$

where, the matrix $\mathbf{S}_x$ of size 2(n+1) x 2(n+1) is given by

$$\mathbf{S}_x = \left[\begin{array}{cc} \begin{array}{cccc} 0 & \ldots & & 0 \\ 0 & -z_2 & \ldots & -z_2 \\ 0 & -z_2 & -z_3 \ldots & -z_3 \\ 0 & -z_2 & -z_3 \ldots z_i \ldots & -z_i \\ 0 & -z_2 & -z_3 \ldots & -z_{n+1} \end{array} & \mathbf{O}_{(n+1)\times(n+1)} \\ \mathbf{O}_{(n+1)\times(n+1)} & \begin{array}{ccc} -1 & -1 \ldots & -1 \\ 0 & -1 \ldots & -1 \\ 0 & \ldots & -1 \end{array} \end{array}\right] \qquad (3.26)$$

So far moments have been related to the x-, y- and z-system of coordinates. The final step is to select from the force vectors $\mathbf{M}_z$ and $\mathbf{M}_y$ the forces for each element i and to present these forces relative to each local coordinate system $\xi$ , $\eta$ and $\zeta$ , Fig. 3.4. For a typical element i the moments $M_\eta$ and $M_\zeta$ are therefore

$$M_{\eta i} = n_i M_{z i} - m_i M_{y i}$$

$$M_{\zeta i} = m_i M_{y i} + n_i M_{z i} \qquad (3.27)$$

For the whole structure the forces will be

$$\mathbf{S} = \mathbf{C}\, \mathbf{S}_x\, \bar{\mathbf{R}} \qquad (3.28)$$

where $$\mathbf{C} = \begin{bmatrix} \mathbf{C}_1 & \mathbf{C}_2 \\ \mathbf{C}_3 & \mathbf{C}_4 \end{bmatrix} \qquad (3.29)$$

and $$\mathbf{C}_1 = \begin{bmatrix} n_1 & & & & \\ & n_1 & & & \\ & n_2 & n_2 & & \\ & & & \ddots & \\ & & & & n_n \; n_n \end{bmatrix} \qquad (3.29a)$$

$$\mathbf{C}_2 = \begin{bmatrix} -m_1 & & & & \\ & -m_1 & & & \\ & -m_2 & -m_2 & & \\ & & & \ddots & \\ & & & & -m_n \\ & & & & & -m_n \end{bmatrix} \qquad (3.29b)$$

$$\mathbf{C}_3 = \begin{bmatrix} 0 & m_1 & & & \\ & m_2 & \ddots & & \\ & & & m_{n-1} & \\ & & & & m_n \end{bmatrix} \qquad (3.29c)$$

$$\mathbf{C}_4 = \begin{bmatrix} 0 & n_1 & & & \\ & n_2 & \ddots & & \\ & & & n_{n-1} & \\ & & & & n_n \end{bmatrix} \qquad (3.29d)$$

In view of Equation (3.22) the transformation matrix $\mathbf{b}$ for the arch able to rotate about the y-axis at points A and B can therefore be calculated as

$$\mathbf{b} = \mathbf{C}\,\mathbf{S}_x \qquad (3.30)$$

If the arch is built in at points A and B it will not be able to rotate about the y-axis at these locations. As far as loading due to the unit forces $\bar{\mathbf{U}}$ and $\bar{\mathbf{M}}_z$ is concerned, the arch is indeterminate to the second degree. Because of symmetry, the number of redundancies can be reduced to one. To determine the redundant reaction the method outlined in Chapter 2 can be used again. Here the moment chosen as redundancy will be the moment $X_3$ about the y-axis at point A. The basic system then will be the structure already analyzed above resulting in the matrix $\mathbf{b}_0$, Equation (3.30).

A second matrix, $\mathbf{b}_1$, has now to be established, relating the moment $X_3$ to the element forces $\mathbf{S} = \{\mathbf{S}_b\ \mathbf{S}_t\}$. Since the moment $M_{yi}$ due to $X_3$ will be constant along the length of the arch, the

resulting moments $M_{\eta\ell}$ , $M_{\eta r}$ and $M_{\zeta}$ for an element i will be

$$\mathbf{S}_i = \left\{ n_i \;\; n_i \;\; m_i \right\} X_3 \tag{3.31}$$

For the whole structure the element forces due to $X_3$ will be

$$\left\{ \mathbf{S}_{b1} \; \mathbf{S}_{t1} \right\} = \mathbf{b}_1 \;\; X_3 \tag{3.32}$$

where

$$\mathbf{b}_1 = \left\{ n_1 \; n_1 \; n_2 \; n_2 \; \cdots \; n_i \; n_i \; \cdots \; n_n \; n_n \; m_1 \; \cdots \; m_n \right\} \tag{3.33}$$

Equations (3.30) and (3.33) can now be used to evaluate the redundant moment $X_3$ , using Equation (2.16 ).

$$X_3 = -\left[\mathbf{b}_1^t \, \mathbf{f} \, \mathbf{b}_1\right]^{-1} \mathbf{b}_1^t \, \mathbf{f} \, \mathbf{b}_o \bar{\mathbf{R}} \tag{3.34}$$

where the flexibility matrix $\mathbf{f}$ is given by Equation (2.47 ).

The total forces on each element will be given by

$$\bar{\mathbf{S}} = \mathbf{b}_o \bar{\mathbf{R}} + \mathbf{b}_1 X_3 \tag{3.35}$$

Substituting finally Equation (3.34) into Equation (3.35) will result in the required relation between element forces and unit forces

$$\mathbf{S} = \mathbf{b} \, \bar{\mathbf{R}} \tag{3.36}$$

where

$$\mathbf{b} = \mathbf{b}_o - \mathbf{b}_1 \left[\mathbf{b}_1^t \mathbf{f} \; \mathbf{b}_1\right]^{-1} \mathbf{b}_1^t \mathbf{f} \; \mathbf{b}_o \tag{3.37}$$

Matrix **b** for Beams

(a) Beams free to rotate about y-axis at supports. For beams with a straight axis, all direction cosines n are equal to one, and all m are reduced to zero. For a beam free to rotate about the y-axis at the supports the transformation matrix **b** therefore will be reduced to

$$\mathbf{b} = \begin{bmatrix} \mathbf{b}_b & \mathbf{O} \\ \mathbf{O} & \mathbf{b}_t \end{bmatrix} \tag{3.38}$$

where

$$\mathbf{b}_b = \mathbf{C}_1 \, \mathbf{S}_1 \tag{3.38a}$$

$$\mathbf{b}_t = \mathbf{C}_4 \, \mathbf{S}_4 \tag{3.38b}$$

The submatrices $\mathbf{C}_1$ and $\mathbf{C}_4$, $\mathbf{S}_{x1}$ and $\mathbf{S}_{x4}$ are given by the non-zero elements of the matrices $\mathbf{C}$ and $\mathbf{S}_x$, Equations (3.26) and (3.29). If the beam is divided into 2n elements of equal length, the transformation matrices become

$$\mathbf{b}_b = \frac{1}{2n} \begin{bmatrix} 0 & 0 & 0 & \cdots & 0 \\ 0 & 1 & 1 & \cdots & 1 \\ 0 & 1 & 1 & \cdots & 1 \\ 0 & 1 & 2 & \cdots & 2 \\ \vdots & & & & \vdots \\ 0 & 1 & 2 & 3 \cdots & (n-1) \\ 0 & 1 & 2 & 3 \cdots & (n-1) \\ 0 & 1 & 2 & 3 \cdots & n \end{bmatrix} \tag{3.39a}$$

$$\mathbf{b}_t = \begin{bmatrix} 0 & 1 & 1 & \cdots & & 1 \\ 0 & 0 & 1 & \cdots & & 1 \\ \vdots & & & & & \vdots \\ 0 & \cdots & & & 1 & 1 \\ 0 & \cdots & & & 0 & 1 \end{bmatrix} \qquad (3.39b)$$

(b) Beams restrained from rotation about y-axis at supports. If the beam is restrained from rotations about the y-axis at the two supports, the forces on the elements due to unit forces have to be modified. While the reactions due to unit torsions about the z-axis will not be affected by additional restraints at the supports, such restraints certainly will result in bending moments about the y-axis. Instead of using Equation (3.34) to calculate these moments, $X_3$ can be obtained directly by differentiating once the second order differential equation for the deflection of beams, Equation (3.40), (43), substituting the appropriate boundary conditions and solving for the moments at the supports.

$$\frac{d^2u}{dz^2} = \frac{M(y)}{EI_\eta} \qquad (3.40)$$

For a beam fixed at the supports and loaded by two symmetrically placed concentrated forces $P_j$ , Fig. 3.5, the moments will be

$$\text{for} \quad i < j \qquad M_i = P_j \, z_i - M_A$$

$$\text{for} \quad j < i < L/2 \qquad M_i = P_j \, c - M_A \qquad (3.41)$$

Observing that for a symmetrically loaded beam the slope $dw/dz$ at the supports and at the centre have to be equal to zero, the moment

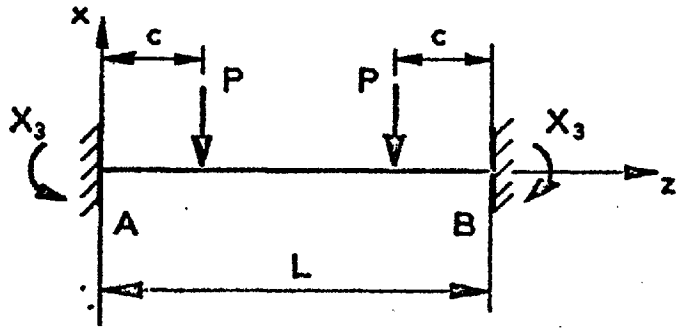


FIG. 3.5 BEAM FIXED AGAINST ROTATION ABOUT Y-AXIS

at the supports can be calculated as

$$X_3 = P_j \; c_j \; (1 - c_j/L) \tag{3.42}$$

In matrix notation the moment $X_3$ resulting from a number of lateral forces $\bar{U}$ can be written

$$X_3/L = \mathbf{b}_1' \, \bar{U} \tag{3.43}$$

where $$\mathbf{b}_1' = \left[ c_1/L \; (1 - c_1/L) \ldots \; c_j/L \; (1 - c_j/L) \ldots \right] \tag{3.44}$$

The moment $X_3$ has to be added to the moments of the simply supported beam. The row vector $\mathbf{b}_1'$ therefore has to be added to each row of the matrix $\mathbf{b}_b$ calculated with Equation (3.39a). For a beam divided into 2n elements of equal length the new transformation matrix $\mathbf{b}_b$ therefore becomes

$$\mathbf{b}_b = \frac{1}{2n} \begin{bmatrix} 0 & 0 & \ldots & 0 \\ 0 & 1 & 1 \ldots & 1 \\ 0 & 1 & 1 \ldots & 1 \\ 0 & 1 & 2 \ldots & 2 \\ \vdots & & & \vdots \\ 0 & 1 & 2 \; 3 \ldots & n \end{bmatrix} + \frac{1}{(2n)^2} \begin{bmatrix} 0 & (2n-1) & 2(2n-2) \ldots & n^2 \\ 0 & (2n-1) & 2(2n-2) \ldots & n^2 \\ 0 & & & \\ \vdots & & & \\ 0 & (2n-1) & 2(2n-2) \ldots & n^2 \end{bmatrix} \tag{3.45}$$

The transformation matrix $\mathbf{b}_t$ remains the same for a beam fixed at the ends as that for a simply supported beam, Equation (3.39b).

Matrix **B**

It is required to find the element forces $\mathbf{S} = \{\mathbf{S}_b \; \mathbf{S}_t\}$ due to vertical forces $\mathbf{R} = P_m \{ P_1/P_m \;\; P_2/P_m \;\ldots\; P_i/P_m \;\ldots\; 1 \}$ when displacements $\mathbf{r} = \{\mathbf{r}_b \; \mathbf{r}_t\}$ take place. The lateral displacements $\mathbf{r}_b = \{ u_1 \; u_2 \; u_3 \;\ldots\; u_i \;\ldots\; u_{n+1} \}$ and rotations $\mathbf{r}_t = \{ \theta_1 \; \theta_2 \;\ldots\; \theta_i \;\ldots\; \theta_{n+1} \}$ are defined relative to the global system of coordinates x, y and z, Fig. 2.5 and 3.6. The vectors $\mathbf{S}_b = \{ M_{\eta l}/L \;\; M_{\eta r}/L \;\ldots\; M_{\eta i l}/L \;\; M_{\eta i r}/L \;\ldots \}$ and $\mathbf{S}_t = \{ M_{\zeta 1}/L \;\; M_{\zeta 2}/L \;\ldots\; M_{\zeta i}/L \;\ldots\; M_{\zeta n}/L \}$ will contain the moments about the $\eta$ - and the $\zeta$ -axis respectively of each element.

Before displacements $\mathbf{r}$ take place the only forces at a point i are the vertical and horizontal components $V_i$ and $W_i$ of the internal forces and the moment $M_{xi}$, Fig. 3.2. When displacements $\mathbf{r}_b$ and $\mathbf{r}_t$ occur additional forces will be required to keep the left end of the arch in equilibrium. Before deriving these forces consider once more the forces at a point i.

In the present analysis, where only vertical forces P are being considered, it is convenient to calculate the W forces directly and to use the moment $M_x$, given by Equation (2.9). To find the horizontal force $W_i$ acting at a point i, the horizontal reaction at the left support of the arch, Fig. 3.2, has to be calculated first. Equilibrium of moments requires that

$$W_A = W_C = \frac{P_m}{h/L} \left[ \Sigma R \;\; - X_1/L + X_2/L \right] \qquad (3.46)$$

where $$\mathbf{Z} = \left[ z_1/L \quad z_2/L \ \ldots \ z_j/L \ \ldots \ z_m/L \right] \qquad (3.47)$$

is a row vector containing the z-coordinates for the location of each of the forces in vector $\mathbf{R}$ . The moments $X_1$ and $X_2$ here are calculated on the basis of the vector $\mathbf{R}$ defined in terms of the load $P_m$ . In the absence of any external horizontal loads the horizontal thrust at any point i therefore is

$$W_i = W_A \qquad (3.48)$$

These horizontal forces can be placed into a diagonal matrix $\mathbf{W}$ , which can be obtained by multiplying a unit matrix of size (n+1) x (n+1) with a constant equal to the horizontal reaction at A.

$$\mathbf{W} = W_A \mathbf{I} \qquad (3.49)$$

As will be seen later it is convenient to place the moments $M_{xi}$ into a diagonal matrix

$$\mathbf{M_x} = P_m \left[ M_{x1} \quad M_{x2} \quad \ldots \quad M_{xi} \quad \ldots \quad M_{xn+1} \right] \qquad (3.50)$$

The moments $M_{xi}$ can be selected from the force vector $\mathbf{S}$ , Equation (2.9). The resulting forces on the left end of the arch, as yet undisplaced, are shown in Fig. 3.2(a)-(c). The vertical force V is not required for the calculation of elastic stability and no matrix expression for this force is therefore given.

Having obtained a matrix representation of the forces at each point of the undeflected structure, the additional forces resulting from lateral displacements $\mathbf{r}_b$ and rotations $\mathbf{r}_t$ can now be

considered. Consider first the effect of lateral displacements $\mathbf{r}_b$ . In Fig. 3.6 the arch is shown in a slightly deflected position. A vertical force $P_j$ at a point j will therefore produce a torsion moment about the z-axis equal to $P_j u_j$ . At a point i less than j the resulting torque is

$$M_{zi} = P_j (u_j - u_i) \tag{3.51}$$

The components of $M_{zi}$ in the $\eta$ - and $\zeta$ -directions, Fig. 3.4, are

$$\begin{aligned} M_\eta &= -m P_j (u_j - u_i) \\ M_\zeta &= n P_j (u_j - u_i) \end{aligned} \tag{3.52}$$

In a symmetrical structure for a point i greater than j the torsional moment about the z-axis due to the symmetrically positioned loads $P_j$ is zero.

The moment $M_{zi}$ about the z-axis at a point i due to vertical loads $\mathbf{R}$ can therefore be written

$$M_{zi} = P_m \mathbf{R}^t \mathbf{S}_{1i} \mathbf{r}_b \tag{3.53}$$

where

$$\mathbf{S}_{1i} = \begin{bmatrix} \mathbf{0} & \mathbf{0} \\ \cdots -1 \cdots & \cdots 1 \cdots \\ -1 & 1 \\ -1 & \ddots \\ -1 & 1 \end{bmatrix} \begin{matrix} \\ i^{th}\text{ row} \\ \\ \\ \end{matrix} \tag{3.54}$$

$i^{th}$ column $\quad$ $j^{th}$ column

Correspondingly the torsional moment $\mathbf{M}_z = \{ M_{z1} \quad M_{z2} \quad \dots \quad M_{zi} \quad \dots \quad M_{z\,n+1} \}$ will be

$$\mathbf{M}_z = P_m \mathbf{R}^t \mathbf{S}_1 \mathbf{r}_b \tag{3.55}$$

where $$\mathbf{S}_1 = \{ S_{11} \; S_{12} \; S_{13} \dots \; S_{1i} \dots \; S_{1\,n+1} \} \tag{3.56}$$

The deflections $\mathbf{r}_b$ in Equation (3.54) are changing continuously along the length of the span. As a result also the torsional moments $M_z$ are varying continuously. Instead of assigning the torsional moment $M_z$ at a point (i+1) to the element i, it will be more appropriate to use the average torsion from points i and (i+1) for the element i. This can be done by premultiplying the vector $\mathbf{M}_z$ with a matrix $\mathbf{S}_2$ . Placing the average torsion $\bar{M}_{z(i+1)} = 0.5(M_{zi} + M_{z\,i+1})$ in a vector $\bar{\mathbf{M}}_z = \{ 0 \; \bar{M}_{z2} \dots M_{z\,n+1} \}$ it is therefore possible to calculate the average torsion for each element from

$$\bar{\mathbf{M}}_z = P_m \mathbf{S}_2 \mathbf{R}^t \mathbf{S}_1 \mathbf{r}_b \tag{3.57}$$

where $$\mathbf{S}_2 = 0.5 \begin{bmatrix} 0 & 0 & \dots & & & 0 \\ 1 & 1 & & & & \\ 0 & 1 & 1 & & & \\ \cdot & & 1 & 1 & & \\ \cdot & & & \cdot & \cdot & \\ \cdot & & & & \cdot & \cdot \\ & & & & \cdot & 0 \\ 0 & \cdot & \cdot & \cdot & 0 \; 1 & 1 \end{bmatrix} \tag{3.58}$$

Next consider the effect of lateral displacements on the moments $M_x$ . Let the displacement of the left end of an element of length $\ell$ be equal to $u_i$ and that of the right end be equal to $u_{i+1}$ , Fig. 3.7. The projection $\ell'$ of the element axis on the

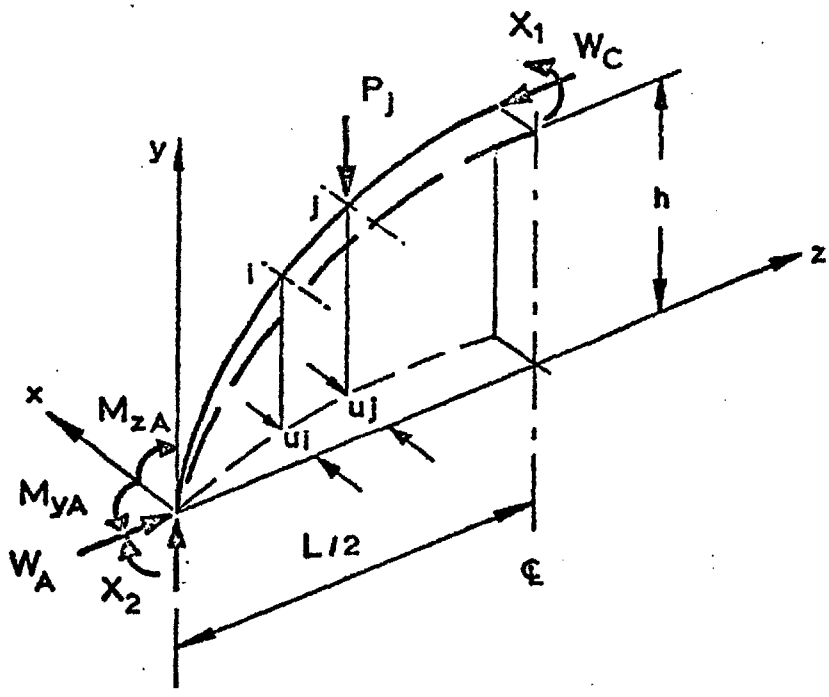


FIG. 3.6 - LATERAL DISPLACEMENT OF ARCH

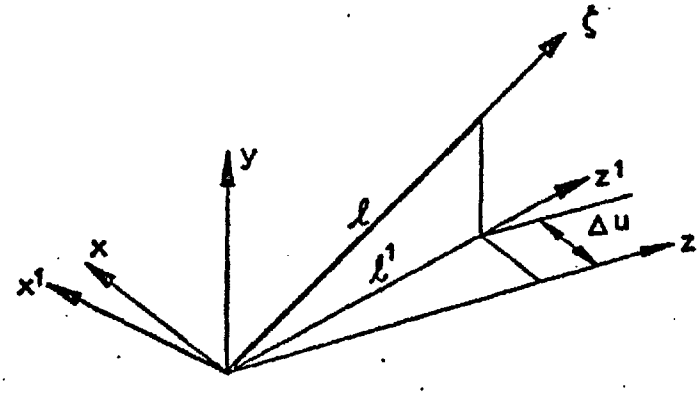


FIG. 3.7 - ELEMENT AXIS IN DISPLACED POSITION

horizontal plane x-z will have the same lateral displacements in the x-direction, Fig. 3.7. The projected element axis $\ell'$ therefore will be inclined to the z-direction by an angle approximately equal to $(u_{i+1} - u_i)/\ell'$. The length of the projected element is $\ell' = n\,\ell$. As a result a moment $M_x$ at a point i can be resolved into components parallel and perpendicular to the projected element axis, Fig. 3.8a. Of these two components the torsional moment $M_z$ about the z -axis has to be retained for the calculation of the matrix $\mathbf{B}$ .

The moments $M_{z'}$ at points i and (i+1) due to lateral deflections of an element i, i.e. the components of $M_{xi}$ and $M_{x\,i+1}$ will be

$$M_{z'\ell} = M_{xi}\,(u_{i+1} - u_i)/\ell'$$
$$M_{z'r} = M_{x\,i+1}\,(u_{i+1} - u_i)/\ell' \qquad (3.59)$$

Again only the average torsion $\bar{M}_{z'(i+1)} = 0.5(M_{z'\ell} + M_{z'r})$ is required for each element. Equation (3.59) can therefore be condensed into

$$M_{z'} = 0.5(M_{xi} + M_{x(i+1)})\,(u_{i+1} - u_i)/\ell_i' \qquad (3.60)$$

The average of the moments $M_{xi}$ can be placed into a diagonal matrix

$$\mathbf{M}_x' = 0.5\,\mathrm{diag}\,(0\;(M_{x1} + M_{x2})\quad (M_{x2} + M_{x3})\;\ldots(M_{xn} + M_{x\,n+1})\;).$$

For the whole structure the average torsional moments therefore will be given by the vector $\mathbf{M}_{z'} = \{0\quad M_{z'2}\quad \ldots\ M_{z'i}\quad \ldots\ M_{z'\,n+1}\}$, which can be calculated from

$$\mathbf{M}_{z'} = \mathbf{M}_x'\,\mathbf{S}_3\,\mathbf{r}_b \qquad (3.61)$$

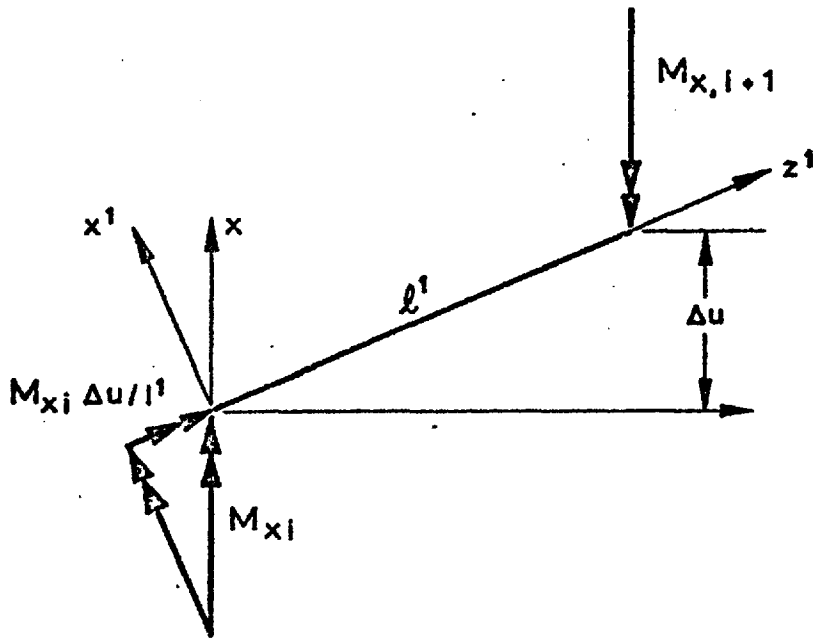


(a) LATERAL DISPLACEMENT

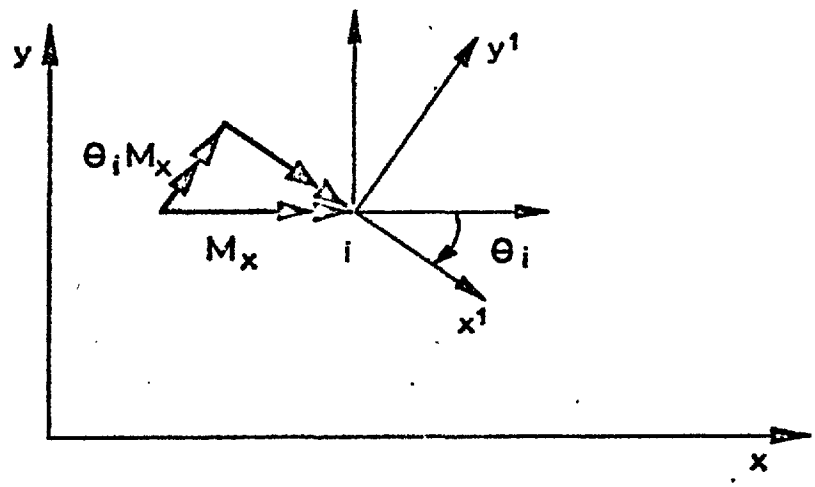


(b) ROTATION

FIG. 3.8 - MOMENTS DUE TO LATERAL DISPLACEMENTS AND ROTATIONS

The (n+1) x (n+1) matrix $\mathbf{S}_3$ defines the differences between the lateral deflections of points i and (i+1) and is given by Equation (3.62).

$$\mathbf{S}_3 = \begin{bmatrix} 0 & 0 & & & & 0 \\ & -L/\ell_1' & L/\ell_1' & & & \\ & & -L/\ell_2' & L/\ell_2' & & \\ & & & \cdot & \cdot & \\ & & & & \cdot & 0 \\ 0 & & & & -L/\ell_n' & L/\ell_n' \end{bmatrix} \quad (3.62)$$

In addition to the torsional moments $\mathbf{M}_z$ and $\mathbf{M}_{z'}$ lateral bending moments will also be created as a result of lateral deflections and rotations. Considering the horizontal forces W, Fig. 3.2 and Fig. 3.6, it will be seen that as a result of lateral displacements $u_i$ moments $M_y$ are required to keep the displaced structure in equilibrium.

$$M_y = u_i \; W_i \quad (3.63)$$

A vector $\mathbf{M}_y = \{M_{y1} \; M_{y2} \; \ldots M_{yi} \; \ldots M_{y\,n+1}\}$ can therefore be calculated, which will contain the moments due to the lateral displacements.

$$\mathbf{M}_y = W_A \; \mathbf{I} \; \mathbf{r}_b \quad (3.64)$$

Finally the effect of rotations $\theta$ on the moments $M_x$ has to be considered. At each point i the moment $M_x$ can be replaced by its components $M_z$ and $M_{y'}$, Fig. 3.8b. Assuming small rotations, the bending moments about the x-axis will remain practically

unchanged, $M_{z'} \simeq M_x$ . The bending moment about the $y'$ axis will be $\Theta M_x$ . For the whole structure the components due to rotations will be

$$M_{y'} = P_m M_x r_t \tag{3.65}$$

Neglecting terms involving products of u and $\Theta$ , no additional forces will arise as a result of displacing and rotating a cross-section subjected to forces $W_i$ and $V_i$ and moments $M_i$ . The moments $M_y$ , $M_{y'}$ , $M_z$ and $M_{z'}$ resulting from the lateral displacement and the rotation of the cross-section of the arch at every nodal point now have to be translated into element forces $S = \{ S_b \; S_t \}$ . It will be noted that the angle between the axes z and $z'$, as well as that between y and $y'$ is small, Fig. 3.8. No appreciable error will therefore be introduced by simply adding the vectors $M_z$ and $M_{z'}$ , Equation (3.57) and Equation (3.61). The combined vectors can then be premultiplied by the transformation matrix $C$ , Equation (3.29), to give the element forces $S$ .

$$S = \begin{bmatrix} S_b \\ S_t \end{bmatrix} = P_m \left[\begin{array}{c|c} C_1 & C_2 \\ \hline C_3 & C_4 \end{array}\right] \left[\begin{array}{c|c} W_A/P_m \; I & M \\ \hline S_2 R^t S_1 + M_x' S_3 & O \end{array}\right] \begin{bmatrix} r_b \\ r_t \end{bmatrix} \tag{3.66}$$

Equation (3.66) defines the required transformation matrix $B$ for an arch subjected to vertical loads. The transformation matrix $B$ can therefore be written

$$B = \left[\begin{array}{c|c} C_1 & C_2 \\ \hline C_3 & C_4 \end{array}\right] \left[\begin{array}{c|c} W_A/P_m \; I & M \\ \hline S_2 R^t S_1 + M_x' S_3 & O \end{array}\right] \tag{3.67}$$

Matrices $\mathbf{B}_b$ and $\mathbf{B}_t$ for Beams Subjected to Forces in the Major Plane of Bending

For a beam the thrust $W_A$ and all direction cosines m are zero. The direction cosines in matrices $\mathbf{C}_1$ and $\mathbf{C}_4$ will all be equal to one. For a straight beam the matrix $\mathbf{B}$ therefore reduces to

$$\mathbf{B} = \begin{bmatrix} \mathbf{O} & \mathbf{B}_b \\ \mathbf{B}_t & \mathbf{O} \end{bmatrix} \tag{3.68}$$

where $$\mathbf{B}_b = \mathbf{C}_1 \mathbf{M}_x \tag{3.69}$$

and $$\mathbf{B}_t = \mathbf{C}_4 \left[ \mathbf{S}_2 \mathbf{R}^t \mathbf{S}_1 + \mathbf{M}'_x \mathbf{S}_3 \right] \tag{3.70}$$

For a concentrated force at the centre of a beam divided into 2n equal elements the transformation matrices, utilizing symmetry, will be

$$\mathbf{B}_b = \frac{1}{2n} \begin{bmatrix} \begin{bmatrix} 0 & 0 \\ 0 & 1 \end{bmatrix} & 0 & \cdots & & 0 \\ 0 & \begin{bmatrix} 1 & 0 \\ 0 & 2 \end{bmatrix} & & & \\ \cdot & & \begin{bmatrix} 2 & 0 \\ 0 & 3 \end{bmatrix} & & \\ \cdot & & & \ddots & 0 \\ & & & & \begin{bmatrix} n-1 & 0 \\ 0 & n \end{bmatrix} \\ 0 & & & 0 & \end{bmatrix} \tag{3.71}$$

$$\mathbf{B}_t = 0.25 \begin{bmatrix} -1 & -1 & 0 & \cdots & & 0 & 2 \\ 0 & -1 & -1 & & & & 2 \\ \cdot & & -1 & -1 & & & 2 \\ \cdot & & & \cdot & \cdot & & \cdot \\ \cdot & & & & \cdot & \cdot & \cdot \\ & & & & & -1 & 2 \\ 0 & & & & & 0 & 1 \end{bmatrix} + \tag{3.72}$$

$$+ 0.25 \begin{bmatrix} -1 & 1 & 0 & 0 & \cdots & & 0 \\ 0 & -3 & 3 & 0 & & & \\ 0 & 0 & -5 & 5 & & & \\ \vdots & & & \ddots & \ddots & & \\ \vdots & & & & \ddots & \ddots & 0 \\ 0 & & & & 0 & -(2n-1) & (2n-1) \end{bmatrix} \qquad (3.72)$$

Matrices $B_b$ and $B_t$ for Beams Subjected to Equal End Moments

Finally for a beam subjected to constant end moments $M_x$ the transformation matrices $B_b$ and $B_t$ can be obtained from Equation (3.69) and Equation (3.70) by considering only the diagonal matrices $M_x$ and $M_x'$ . For a beam divided into 2n elements of equal length the transformation matrices therefore will be

$$B_b = \begin{bmatrix} \begin{bmatrix} 1 & 0 \\ 0 & 1 \end{bmatrix} & 0 & \cdots & & 0 \\ 0 & \begin{bmatrix} 1 & 0 \\ 0 & 1 \end{bmatrix} & & & \vdots \\ \vdots & & \ddots & & \vdots \\ & & & \ddots & 0 \\ 0 & \cdots & 0 & \begin{bmatrix} 1 & 0 \\ 0 & 1 \end{bmatrix} \end{bmatrix} \qquad (3.73)$$

$$B_t = 2n \begin{bmatrix} -1 & 1 & 0 & \cdots & & 0 \\ 0 & -1 & 1 & & & \vdots \\ \vdots & & -1 & 1 & & \vdots \\ \vdots & & & \ddots & \ddots & \vdots \\ \vdots & & & & \ddots & 0 \\ 0 & \cdots & & 0 & -1 & 1 \end{bmatrix} \qquad (3.74)$$

# Chapter 4

## The Torsional Rigidity of Box Sections

### Introduction

Beam properties required for the calculation of critical loads for lateral stability are the bending stiffness about the minor axis of the cross-section, $EI_\eta$ , and the torsional stiffness GJ. Calculation of the bending stiffness, the product of the second moment of area, $I_\eta$, and the modulus of elasticity, E, has been discussed by the author in an unpublished paper on the shear deflection of composite beams (Appendix D). For composite structures it is merely necessary to recall that the bending stiffness of the total section is calculated from the individual stiffnesses of the various elements which compose the structure. For composite plywood structures, usually consisting of lumber flanges and plywood webs, the total bending stiffness, $EI_\eta$ , about the $\eta$ -axis of the cross-section is

$$(EI)_\eta = E_1 \; I_{1\eta} + E_2 \; I_{2\eta} \qquad (4.1)$$

where $E_1$ , $E_2$ = modulus of elasticity of flange, web

$I_{1\eta}$ , $I_{2\eta}$ = second moment of area of flange, web

The torsional stiffness GJ is a measure of the torque required to produce in a shaft over a distance of unit length, Fig. 4.1, an angle of twist $\Theta$ equal to unity (18).

$$M_z = G \; J \; \Theta \qquad (4.2)$$

The torsional stiffness is the product of the modulus of rigidity, G, of the material and the torsion constant, J, of the cross-section. It is assumed that cross-sections are free to warp, when the torsion $M_z$ is being applied. This type of torsion is often referred to as Saint Venant torsion, after the eighteenth century mathematician Saint Venant (42), who first investigated torsion in detail and calculated tables of torsion constants for solid rectangular sections.

The torsional rigidity of thin-walled, closed sections can be calculated with the following equation (18)

$$J = 4 A^2 / \int_s \frac{ds}{t(s)} \qquad (4.3)$$

where A is the area enclosed by the middle curve s and t is the thickness of the wall, which may be variable, Fig. 4.2.

For a box section with webs of thickness t and flanges of depth $d_1$ and $d_2$, Fig. 4.3, evaluation of the integral in Equation (4.3) results in (21)

$$J = \frac{t \left[ (2h - d_1 - d_2)(b_1 - t) \right]^2}{\left[ 2h - d_1 - d_2 + (b_1 - t)\, t/d_1 + (b_1 - t)\, t/d_2 \right]} \qquad (4.4)$$

This equation, in slightly different form, for beams with equal flanges, was first proposed by Trayer and March (45). For box sections with uniform wall thickness t on all four sides Equation (4.4) reduces to

$$J = 2 t (b_1 - t)(h - t)^2/(b_1 - h - 2t) \qquad (4.5)$$

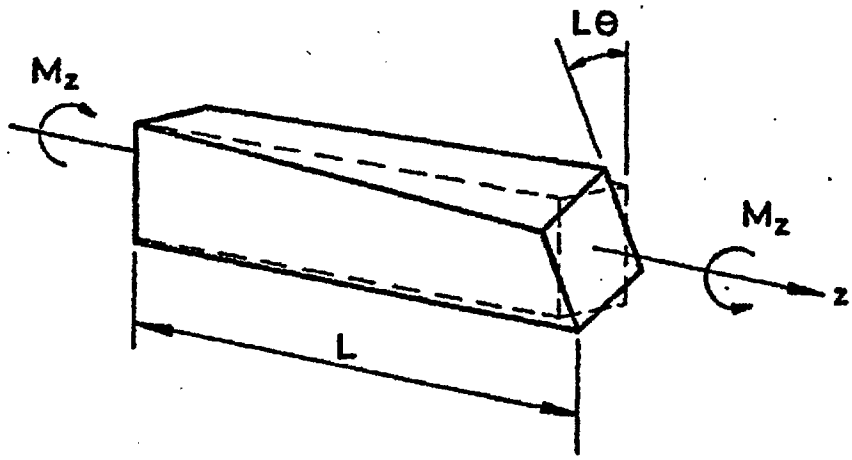


FIG. 4.1 - BAR IN TORSION

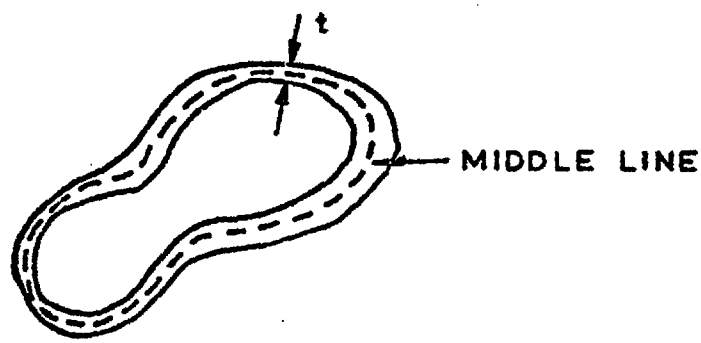


FIG. 4.2 - HOLLOW SECTION

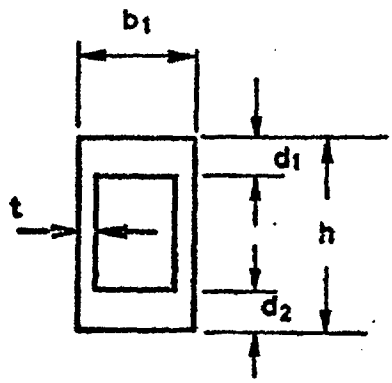


FIG. 4.3 - BOX SECTION

Experimental work with thin-walled box-sections by Wilson in 1923 indicated the validity of this equation, and Wilson (46) therefore suggested that the torsion constant of box-sections be calculated with Equation (4.5). The later extension of this approach to cross-sections with deep flanges, however, as expressed by Equation (4.4), violates the initial assumptions of uniform shear stresses throughout all wall thicknesses and can lead to erroneous results.

If, for example, a section with a given height h, width $b_1$ and wall thickness t is considered, then it will be found that, as a result of the second power in the numerator in Equation (4.4), an increase in $d_1$ and $d_2$ will result in a decrease in the magnitude of the torsion constant J. This, of course, appears to be unreasonable, since an increase in the amount of material in the flanges of a given box-section of given overall dimensions presumably will result in an increase in its torsional rigidity. Likewise, for t approaching $b_1/2$ and for $(d_1 + d_2)$ approaching h, the torsion constant implied by Equation (4.4) does not approach the corresponding value for a solid section. This again appears to be the result of exceeding the limitations set by the original assumptions of uniform shear stresses throughout the wall thickness.

The torsion constant J usually is evaluated by solving a second order partial differential equation for Prandtl's stress function (18). Results of a numerical evaluation of Prandtl's stress function for certain box-sections by means of finite differences were presented by Byrne (8). However Byrne's results still apply only to relatively shallow flange depth and were not suitable for the present investigation.

Here a different technique for the calculation of torsion constants will be employed. To allow the effect of non-uniform shear stress distributions to be taken into account, Kelsey* suggested to the author a finite element solution for the calculation of the torsional rigidity of box-sections. This finite element solution is developed fully below.

Torsion Constant in Terms of Stiffness Matrix **K**

To evaluate the torsion constant for a box-section, the finite element method using displacements as unknowns, will be used. Consider a component divided into a number of elements connected at their nodal points. Let the displacements of the n nodal points relative to a global system of cartesian coordinates be equal to $\mathbf{r}$, where $\mathbf{r}$ is a vector containing all displacements $\mathbf{r}_1$, $\mathbf{r}_2$, ... $\mathbf{r}_n$. Let $\mathbf{R}$ be a vector of forces acting at the n nodal points corresponding to the displacements $\mathbf{r}$. These forces can then be expressed by the corresponding displacements by means of a stiffness matrix (2).

$$\mathbf{R} = \mathbf{K}\,\mathbf{r} \qquad (4.6)$$

In a bar subjected to a torque, shear stresses will be set up on sections perpendicular to the axis of the bar. If the torque is constant along the length of the bar the stress distribution on any section along its length will be the same. For the analysis of the torsion problem it is therefore only necessary to consider a slice of unit thickness. This slice can be divided into a number

* S. Kelsey, formerly Imperial College, London, now visiting Professor, University of Notre Dame, Notre Dame, Ind., U.S.A.

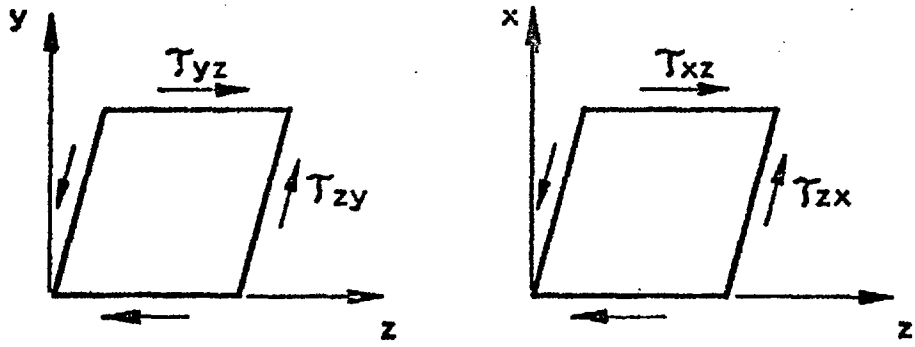


FIG. 4.4 - SHEAR STRESS ON X-, Y- AND Z PLANES

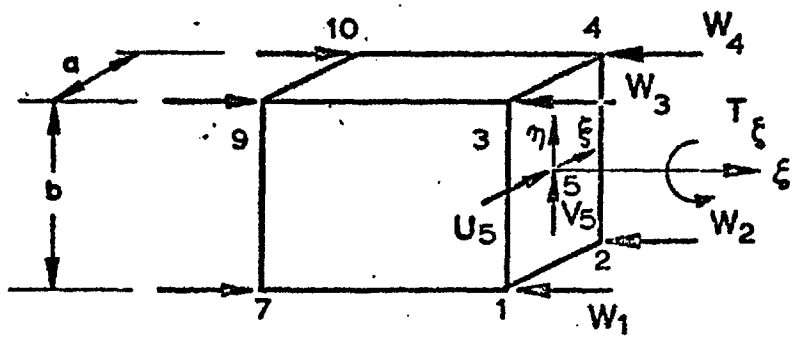


FIG. 4.5 - FORCE SYSTEM ON FINITE TORSION ELEMENT.

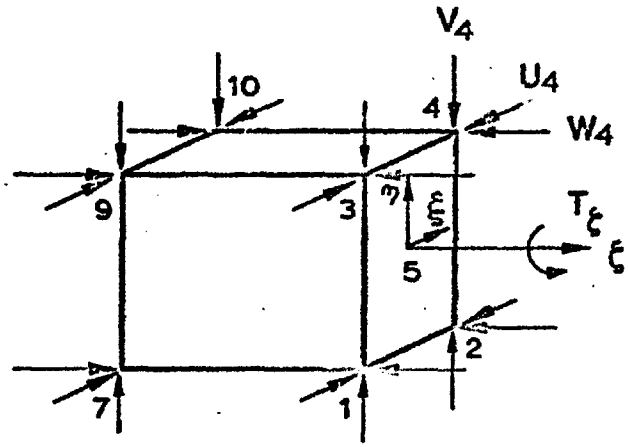


FIG. 4.6 - ALTERNATE FORCE SYSTEM FOR TORSION ELEMENT.

of elements. The basic element chosen in the present analysis is a prism with a length of unity and a rectangular cross-section of width a and height b, Fig. 4.5.

The shear stresses on the face of each element can be resolved into stresses in the $\xi$ - and $\eta$ -directions. Corresponding to these shear stresses $\tau_{\zeta\xi}$ and $\tau_{\eta\zeta}$ on the $\zeta$ -surface, there will also be shear stresses $\tau_{\xi\zeta}$ on the $\xi$ -surface and $\tau_{\eta\zeta}$ on the $\eta$ -surface in the $\zeta$ -direction, Fig. 4.4. In the present analysis it will be assumed that the shear stresses $\tau_{\zeta\xi}$ and $\tau_{\zeta\eta}$ are distributed uniformly over the $\zeta$ -face of individual elements. These shear stresses will be replaced in the analysis by the effective forces U and V acting at the centre of the $\zeta$ -surfaces, Fig. 4.5. Alternatively, the shear stresses can also be represented by effective forces U and V at the corners of each element, Fig. 4.6.

The other effective forces acting on each element are W-forces in the $\zeta$ -direction at each corner and a torque $T_\zeta$ about the local $\zeta$ -axis, Fig. 4.5.

Corresponding to these forces there will be displacements w at each corner in the $\zeta$ -direction and displacements u and v of the centre of each $\zeta$ -face in the $\xi$ - and $\eta$ -directions respectively. Since it is assumed that the section will retain its shape, while a torsion is being applied, the twist $\theta$ of each element will be the same and has to be equal to the overall twist of the component, i.e. $\theta$ is a constant.

Equation (4.6) can now be written in expanded form

$$\mathbf{R} = \begin{bmatrix} \mathbf{W} \\ \mathbf{U} \\ \mathbf{T} \end{bmatrix} = \begin{bmatrix} \mathbf{K}_{11} & \mathbf{K}_{12} & \mathbf{K}_{13} \\ \mathbf{K}_{21} & \mathbf{K}_{22} & \mathbf{K}_{23} \\ \mathbf{K}_{31} & \mathbf{K}_{32} & \mathbf{K}_{33} \end{bmatrix} \begin{bmatrix} \mathbf{w} \\ \mathbf{u} \\ \Theta \end{bmatrix} \qquad (4.7)$$

where $\mathbf{W}$, $\mathbf{U}$ and $\mathbf{T}$ are vectors containing the effective forces $W_i$, $U_i$, $V_i$ and $T_i$ respectively acting on the component.

$$\mathbf{W} = \{ W_1 \; W_2 \; W_3 \ldots W_i \ldots W_n \} \qquad (4.8)$$

$$\mathbf{U} = \{ U_1 \; V_1 \; U_2 \; V_2 \ldots U_i \; V_i \ldots U_n \; V_n \} \qquad (4.9)$$

$$\mathbf{T} = \{ T_1 \; T_2 \ldots \quad T_i \quad \ldots T_n \} \qquad (4.10)$$

The vector $\mathbf{W}_i$ for each element contains the W-components at the four corners of an element i, $\mathbf{W}_i = \{ W_1 \; W_2 \; W_3 \; W_4 \}$. The corresponding displacement vectors are

$$\mathbf{w} = \{ w_1 \; w_2 \; w_3 \ldots w_i \ldots w_n \} \qquad (4.11)$$

$$\mathbf{v} = \{ u_1 \; v_1 \; u_2 \; v_2 \ldots u_i \; v_i \ldots u_n \; v_n \} \qquad (4.12)$$

$$\Theta = \Theta \qquad (4.13)$$

The w-displacements of an element i are $\mathbf{W}_i = \{ w_1 \; w_2 \; w_3 \; w_4 \}$. $\mathbf{K}_{11}$ etc. are submatrices of the stiffness matrix $\mathbf{K}$.

Since a torque about a longitudinal axis will not result in any direct stresses in that direction the effective forces $\mathbf{W}_i$ have all to be equal to zero.

$$\mathbf{W} = \mathbf{K}_{11}\mathbf{w} + \mathbf{K}_{12}\mathbf{u} + \mathbf{K}_{13}\Theta = \mathbf{0} \qquad (4.14)$$

Premultiplying this equation with the inverse of $\mathbf{K}_{11}$ , the displacements in the $z$ -direction become

$$\mathbf{w} = -\mathbf{K}_{11}^{-1}\left[\mathbf{K}_{12}\,\mathbf{u} + \mathbf{K}_{13}\Theta\right] \tag{4.15}$$

However the displacements u and v of the centre of the element faces at $z = 0$ and $z = 1$ are also functions of the twist $\Theta$ . If the coordinates of the centre of each element are x and y, then the displacements due to the twist are $u = -y\,\Theta$ and $v = x\,\Theta$ . In matrix notation this becomes

$$\mathbf{u} = \begin{bmatrix} -\mathbf{y} \\ \mathbf{x} \end{bmatrix} \Theta = \mathbf{M}_c\,\Theta \tag{4.16}$$

where $$\mathbf{y} = \{y_1\ y_2\ y_3\ \cdots\ y_i\ \cdots\ y_n\} \tag{4.16a}$$

$$\mathbf{x} = \{x_1\ x_2\ x_3\ \cdots\ x_i\ \cdots\ x_n\} \tag{4.16b}$$

Equation (4.15) can therefore be written

$$\mathbf{w} = -\mathbf{K}_{11}^{-1}\left[\mathbf{K}_{12}\mathbf{M}_c + \mathbf{K}_{13}\right]\Theta \tag{4.17}$$

With this expression for the displacements $\mathbf{w}$ in the longitudinal direction the total torsional resistance of the section can now be written

$$M_z = \mathbf{M}_c^t\,\mathbf{U} + \sum_{1}^{n} T_i \tag{4.18}$$

where $\mathbf{M}_c^t$ is the transpose of the matrix $\mathbf{M}_c$ , $\mathbf{U}$ , as defined previously, is a column vector of all forces $U_i$ and $V_i$ and $T_i$ is the $i$ th component of vector $\mathbf{T}$ .

Writing the forces in Equation (4.18) in terms of their stiffness matrices from Equation (4.7), introducing for the w-displacements the vector given in Equation (4.17) and noting, as will be shown later, that the submatrices $\mathbf{K}_{23}$ and $\mathbf{K}_{32}$ are both equal to zero, the torsional resistance of a slice of unit thickness can be written

$$M_z = \Big[ \mathbf{M}_c^t \Big\{ -\mathbf{K}_{21} \mathbf{K}_{11}^{-1} (\mathbf{K}_{12} \mathbf{M}_c + \mathbf{K}_{13}) + \mathbf{K}_{22} \mathbf{M}_c \Big\} + \sum \Big\{ -\mathbf{K}_{31} \mathbf{K}_{11}^{-1} (\mathbf{K}_{12} \mathbf{M}_c + \mathbf{K}_{13}) + \mathbf{K}_{33} \Big\} \Big] \Theta \qquad (4.19)$$

The torsion constant J for any section can therefore be evaluated provided the stiffness matrix $\mathbf{K}$ can be determined.

Comparing Equation (4.19) with Equation (4.2) it is evident that the matrix expression in Equation (4.19) defines the torsional rigidity GJ of the section.

The Stiffness Matrix $\mathbf{K}$

Consider again the element chosen for the analysis of the torsion problem, Fig. 4.5. Effective forces W are acting at the eight corners of the element in the $\zeta$ -direction. At the centre of the two $\zeta$ -faces U- and V-forces are being applied and a torque T is twisting the element about its $\zeta$ -axis. The displacements $\mathbf{v}_g$ of an individual element relative to a global system of cartesian

coordinates are related to the corresponding forces by a stiffness matrix $\mathbf{k}_g$ , called the element stiffness matrix (3).

$$\mathbf{P}_g = \mathbf{k}_g \mathbf{v}_g \tag{4.20}$$

where

$$\mathbf{P}_g = \{W_1 \ldots\ldots W_8 , U_5, U_6, V_5, V_6, T_5, T_6\} \tag{4.20a}$$

$$\mathbf{v}_g = \{w_1 \ldots\ldots w_8, u_5 \ldots\ldots \Theta_6\} \tag{4.20b}$$

This force vector $\mathbf{P}_g$ contains all forces acting on the element. Since the component investigated is of unit thickness, one half of the forces in $\mathbf{P}_g$ will be reactions and need not be considered in the derivation of the stiffness matrix. The vectors $\mathbf{P}_g$ and $\mathbf{v}_g$ therefore reduce to seven forces and displacements respectively and the corresponding stiffness matrix $\mathbf{k}_g$ will be of size 7 x 7.

The displacement system $\mathbf{v}_g$ in Equation (4.20) is specified relative to a global system of coordinates. Displacements of the corners of an individual element can also be specified relative to a local system of coordinates. Such displacements then will not include any rigid body movements. Corresponding to such local displacements $\mathbf{v}_N$ a force system $\mathbf{P}_N$ can be defined

$$\mathbf{P}_N = \mathbf{k}_N \mathbf{v}_N \tag{4.21}$$

This stiffness $\mathbf{k}_N$ is frequently called the natural stiffness of an element (3). It gives the elastic response of the element and involves a kinematic idealisation, i.e. a certain shape of the deformed element is assumed. In the present case, for example, it

is assumed that only shear deformations of planes parallel to the x- and y-planes take place and that these shear deformations are constant throughout one plane. No normal strains in any of the three principle directions will be allowed.

Let the displacement systems $\mathbf{v}_N$ and $\mathbf{v}_g$ be connected by a transformation matrix $\mathbf{a}_N$ (3)

$$\mathbf{v}_N = \mathbf{a}_N \mathbf{v}_g \tag{4.22}$$

Using these displacements now as virtual displacements and applying the principle of virtual work, Equation (2.2) it is seen from

$$\mathbf{v}_N^t \mathbf{P}_N = \mathbf{v}_g^t \mathbf{P}_g \tag{4.23}$$

that the force systems corresponding to displacements $\mathbf{v}_g$ and $\mathbf{v}_N$ are related by

$$\mathbf{P}_g = \mathbf{a}_N^t \mathbf{P}_N \tag{4.24}$$

In view of Equations (4.20), (4.21) and (4.22), the element stiffness $\mathbf{k}_g$ can therefore be calculated from

$$\mathbf{k}_g = \mathbf{a}_N^t \mathbf{k}_N \mathbf{a}_N \tag{4.25}$$

The transformation matrix $\mathbf{a}_N$ depends on the natural or independent modes of deformation, which will be considered next. In the most general case the displacements of each of the eight corners of a prismatic body of rectangular cross-section relative

to a global system of cartesian coordinates can be described by displacement components in three mutually perpendicular directions, i.e. the element has 24 degrees of freedom as far as its displacements are concerned. By assuming that no direct strains will take place, i.e. no deformations of any of the twelve edges of the prism, the number of degrees of freedom is reduced to twelve. The further assumption of no shear strain in the two faces parallel to the $\zeta$ -plane reduce the number of degrees of freedom to ten. Displacements of the corners of the element will therefore only be caused by rigid body displacements of the element as a whole and by shear deformations of the four sides parallel to the $\xi$ - and $\eta$ -planes. Since there are six independent rigid body movements, translations in the $\xi$-, $\eta$- and $\zeta$ -directions and rotations about the corresponding axes, the number of independent modes of deformation is therefore finally reduced to four.

As shown by Argyris (3) the force systems corresponding to these so-called natural modes of deformation have to be (a) self-equilibrating and (b) independent in the sense that a force system $\mathbf{P}_{Nj}$ only does work if the corresponding $\mathbf{v}_{Nj}$ deformation takes place. A force vector $\mathbf{P}$ is said to correspond to a displacement vector $\mathbf{v}$ if both have the same origin and the same direction.

In the present case it is therefore necessary to define four independent modes of deformation of the chosen element, such that each of the force systems, causing one of these deformation vectors $\mathbf{v}_N$ is in equilibrium. To be independent, the force system

causing a given mode of deformation should not produce any work, while any of the other modes of deformation takes place.

The four independent modes of deformation are shown in Fig. 4.7. They consist of shear deformations constant throughout the thickness of the element in the $\xi$ - or the $\eta$ -direction respectively, a warping of the $\zeta$ -surfaces and a rotation of the $\zeta$ -surfaces. None of these deformations will produce any normal strains, neither are any of the $\zeta$ -surfaces subjected to shear deformations. The forces shown in Fig. 4.7 for each mode of deformation are calculated for $\mathbf{v}_N$ displacements of unity and are obtained by setting to unity the work done by a force system $\mathbf{P}_N$. Inspection of Fig. 4.7 also will show that the force system shown for mode N = 1 will not do any work, while any of the other three modes of deformation take place, as was required. Likewise all other force systems will only do work, if their own mode of deformation takes place.

In terms of the displacement vector $\mathbf{v}_N$, the displacements u, v and w in the $\xi$, $\eta$ and $\zeta$ -directions are

$$\begin{bmatrix} u \\ v \\ w \end{bmatrix} = \begin{bmatrix} 0 & \zeta/2 & 0 & -\zeta\eta \\ \zeta/2 & 0 & 0 & \zeta\xi \\ \eta/2 & \xi/2 & \xi\eta/ab & 0 \end{bmatrix} \begin{bmatrix} \mathbf{v}_{N1} \\ \mathbf{v}_{N2} \\ \mathbf{v}_{N3} \\ \mathbf{v}_{N4} \end{bmatrix} \tag{4.26}$$

Partial differentiation of the deformations with respect to $\eta$ and $\zeta$ for shear strains $\varepsilon_{\eta\zeta}$ in the $\xi$ -plane and with

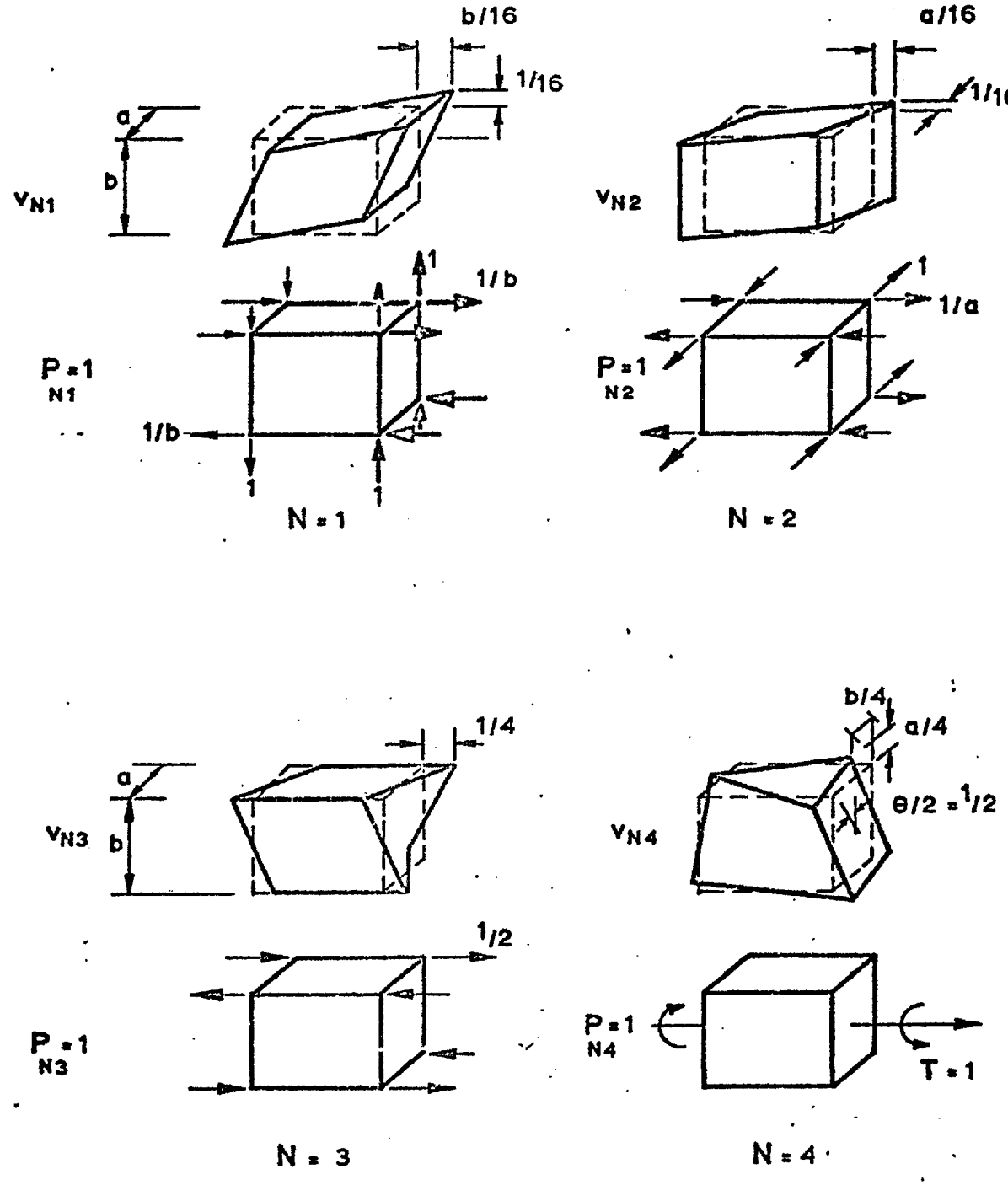


FIG. 4.7 MODES OF DEFORMATION - TORSION ELEMENT

respect to $\xi$ and $\zeta$ for shear strains $\varepsilon_{\zeta\xi}$ in the $\eta$ -plane results in

$$\begin{bmatrix} \varepsilon_{\eta\zeta} \\ \varepsilon_{\zeta\xi} \end{bmatrix} = \begin{bmatrix} 1 & 0 & \xi/ab & \xi \\ 0 & 1 & \eta/ab & -\eta \end{bmatrix} \begin{bmatrix} \mathbf{v}_{N1} \\ \mathbf{v}_{N2} \\ \mathbf{v}_{N3} \\ \mathbf{v}_{N4} \end{bmatrix} \qquad (4.27)$$

This can be written in condensed form as

$$\boldsymbol{\varepsilon} = \mathbf{n}\, \mathbf{v}_N \qquad (4.28)$$

where $\boldsymbol{\varepsilon}$ , $\mathbf{n}$ and $\mathbf{v}_N$ are matrices corresponding to the expressions given in Equation (4.27).

To find the natural stiffness $\mathbf{k}_N$ the principle of virtual work will be applied, i.e. the work done by the shear stresses is to be equivalent to the work done by the effective forces.

$$\mathbf{v}_N^t \mathbf{p}_N = \int_V \boldsymbol{\varepsilon}^t \tau \, dV \qquad (4.29)$$

or

$$\mathbf{k}_N = \int_V \mathbf{n}^t \mathbf{k}_G \mathbf{n} \, dV \qquad (4.30)$$

where for an orthotrpoic material with moduli of rigidity $G_{\eta\zeta}$ and $G_{\zeta\xi}$ the unit stiffness $\mathbf{k}_G$ is given by

$$\mathbf{k}_G = \begin{bmatrix} G_{\eta\zeta} & 0 \\ 0 & G_{\zeta\xi} \end{bmatrix}$$

$$= G_{\eta\zeta} \begin{bmatrix} 1 & 0 \\ 0 & \beta \end{bmatrix} \qquad (4.30a)$$

with

$$\beta = G_{\zeta\xi} / G_{\eta\zeta} \qquad (4.30b)$$

Substitution of the expression for $\mathbf{n}$ in Equation (4.30) and integration results in the following matrix expression for the natural stiffness $\mathbf{k}_N$ of the element

$$\mathbf{k}_N = G_{\eta\zeta}\, a\, b \begin{bmatrix} 1 & 0 & 0 & 0 \\ 0 & \beta & 0 & 0 \\ 0 & 0 & c_1 & c_2 \\ 0 & 0 & c_2 & c_3 \end{bmatrix} \tag{4.31}$$

where $c_1 = (1 + \beta\, b^2/a^2)/(12\, b^2)$ (4.31a)

$c_2 = (1 - \beta b^2/a^2)\, a/(12\, b)$ (4.31b)

$c_3 = (1 + \beta b^2/a^2)\, a^2/12$ (4.31c)

Before calculating the element stiffness $\mathbf{k}_q$ the transformation matrix $\mathbf{a}_N$ has to be determined. According to Equation (4.24) this transformation matrix can be found by expressing the elastic forces on the element, corresponding to the displacements within the global system of coordinates, in terms of the forces corresponding to the displacements relative to the local system of coordinates. Inspection of the forces shown in Fig. 4.7 gives immediately

$$\begin{bmatrix} W_1 \\ W_2 \\ W_3 \\ W_4 \\ U_5 \\ V_5 \\ T_5 \end{bmatrix} = \begin{bmatrix} 1/2b & -1/2a & -1 & 0 \\ 1/2b & 1/2a & +1 & 0 \\ -1/2b & -1/2z & +1 & 0 \\ -1/2b & 1/2a & -1 & 0 \\ 0 & 1 & 0 & 0 \\ 1 & 0 & 0 & 0 \\ 0 & 0 & 0 & 1 \end{bmatrix} \begin{bmatrix} P_{N1} \\ P_{N2} \\ P_{N3} \\ P_{N4} \end{bmatrix} \tag{4.32}$$

Transposition of this matrix gives the matrix $\mathbf{a}_N$. Evaluation of Equation (4.25) is now possible and the element stiffness $\mathbf{k}_g$ becomes

$$\mathbf{k}_g = G_{\eta\zeta} \begin{bmatrix} \mathbf{k}_{11} & \mathbf{k}_{12} & \mathbf{k}_{13} \\ \mathbf{k}_{21} & \mathbf{k}_{22} & \mathbf{o} \\ \mathbf{k}_{31} & \mathbf{o} & \mathbf{k}_{33} \end{bmatrix} \qquad (4.33)$$

where the submatrices $\mathbf{k}_{11}$ etc. are given by the following expressions

$$\mathbf{k}_{11} = \frac{a}{6b} \begin{bmatrix} \alpha_1 & \alpha_2 & \alpha_3 & \alpha_4 \\ \alpha_2 & \alpha_1 & \alpha_4 & \alpha_3 \\ \alpha_3 & \alpha_4 & \alpha_1 & \alpha_2 \\ \alpha_4 & \alpha_3 & \alpha_2 & \alpha_1 \end{bmatrix} = \mathbf{n}_{11} \frac{a}{6b} \qquad (4.34)$$

where
$$\alpha_1 = 2\,(1 + \beta\, b^2/a^2)$$
$$\alpha_2 = (1 - 2\beta\, b^2/a^2)$$
$$\alpha_3 = -\,(2 - \beta\, b^2/a^2)$$
$$\alpha_4 = -\,(1 + \beta\, b^2/a^2)$$

$$\mathbf{k}_{12} = \frac{a}{2} \begin{bmatrix} -\alpha_5 & 1 \\ \alpha_5 & 1 \\ -\alpha_5 & -1 \\ \alpha_5 & -1 \end{bmatrix} = \frac{a}{2}\, \mathbf{n}_{12} \qquad (4.35)$$

where $\alpha_5 = \beta\, b/a$

$$\mathbf{k}_{13} = a^2/12 \left\{ -\alpha_6 \quad \alpha_6 \quad \alpha_6 \quad -\alpha_6 \right\} = \mathbf{n}_{13}\, a^2/12 \qquad (4.36)$$

$$\alpha_6 = 1 - \beta\,(b/a)^2$$

$$\mathbf{k}_{21} = \mathbf{k}_{12}^t = \frac{a}{2}\begin{bmatrix} -\alpha_5 & \alpha_5 & -\alpha_5 & \alpha_5 \\ 1 & 1 & 1 & 1 \end{bmatrix} = \mathbf{n}_{21}\frac{a}{2} \qquad (4.37)$$

$$\mathbf{k}_{22} = ab\begin{bmatrix} \beta & 0 \\ 0 & 1 \end{bmatrix} \qquad (4.38)$$

$$\mathbf{k}_{31} = \mathbf{k}_{13}^t = a^2/12\left[ -\alpha_6 \quad \alpha_6 \quad \alpha_6 \quad -\alpha_6 \right] = \mathbf{n}_{31}\, a^2/12 \qquad (4.39)$$

$$\mathbf{k}_{33} = (a^3 b/12)(1 + \beta\, b^2/a^2) = \mathbf{n}_{33}\frac{a^3 b}{12} \qquad (4.40)$$

Finally the matrices $\mathbf{k}_q$ of all the individual elements have to be assembled to give the required stiffness matrix $\mathbf{K}$ for the component. Formally this can be effected by introducing a boolean matrix which selects the elements of any particular displacement vector $\mathbf{v}_q$ from the vector $\mathbf{r}$ .

$$\mathbf{v}_q = \mathbf{a}_q\, \mathbf{r} \qquad (4.41)$$

By applying the principle of virtual work the stiffness matrix then becomes

$$\mathbf{K} = \sum_q \mathbf{a}_q^t\, \mathbf{k}_q\, \mathbf{a}_q \qquad (4.42)$$

For the torsional constant the assembly operation was simply written directly into the computer programme.

In the present analysis the submatrices $\mathbf{K}_{11}$ etc. are required individually to allow the calculation of the torsion constant J,

Equation (4.19), and the computer program was therefore written to make these submatrices available when required.

Torsion Constant J for Box Sections

Consider again the torsional rigidity as expressed by Equation (4.19). The individual submatrices are now available. Combining Equation (4.19) with Equation (4.2) the torsion constant can be written

$$J = 1/G\left[\mathbf{M}_c^t\left\{-\mathbf{K}_{21}\mathbf{K}_{11}^{-1}(\mathbf{K}_{12}\mathbf{M}_c+\mathbf{K}_{13})+\mathbf{K}_{22}\mathbf{M}_c\right\} + \sum_1^n\left\{-\mathbf{K}_{31}\mathbf{K}_{11}^{-1}(\mathbf{K}_{12}\mathbf{M}_c+\mathbf{K}_{13})+\mathbf{K}_{33}\right\}\right] \qquad (4.43)$$

Substituting the expressions found for the submatrices and expressing the dimensions of the element as well as the coordinates of the element locations in terms of the overall dimensions of the section, $b_1$ and h, the torsion constant finally becomes

$$J = k_1\, b_1^3\, h \qquad (4.44)$$

$$\text{where } k_1 = \frac{4\,(a/b_1)(b/b_1)}{h/b_1}\left(T_1+T_2+T_3+T_4\right) \qquad (4.45)$$

$$\text{and } T_1 = -0.25\,(a/b_1)\sum \mathbf{K}_{31}\mathbf{K}_{11}^{-1}\left\{\mathbf{K}_{12}\mathbf{M}_c+\mathbf{K}_{13}\frac{a}{6b_1}\right\} \qquad (4.45a)$$

$$T_2 = -1.5\,\mathbf{M}_c^t\,\mathbf{K}_{21}\mathbf{K}_{11}^{-1}\left\{\mathbf{K}_{12}\mathbf{M}_c+\mathbf{K}_{13}\frac{a}{6b_1}\right\} \qquad (4.45b)$$

$$T_3 = \mathbf{M}_c^t\,\mathbf{K}_{22}\mathbf{M}_c \qquad (4.45c)$$

$$T_4 = \mathbf{K}_{33}\frac{(a/b_1)^2}{12} \qquad (4.45d)$$

In Equation (4.45) $\mathbf{K}_{II}$ etc. are the assembled submatrices of the stiffness matrix $\mathbf{K}$ in their dimensionless form without their coefficients, e.g. $\mathbf{K}_{II} = \sum \mathbf{a}_g^t \mathbf{n}_{II} \mathbf{a}_g$

The inversion of $\mathbf{K}_{II}$, shown in Equation (4.45), need not be formally executed. Since $\mathbf{W}$ is a vector, the content of the square bracket in Equation (4.17) and the corresponding expressions in Equations (4.43) and (4.45) also have to be vectors. It is therefore possible to solve for $\mathbf{W}$ directly by using any convenient method for the solution of simultaneous linear equations. In the present work a Gauss-Jordan solution (15) modified for banded matrices has been used.

The above expression for the torsion constant assumes that all elements are of the same size and that each element has the same two moduli of rigidity $G_{\eta\zeta}$ and $G_{\zeta\xi}$. A slight modification of the matrices $\mathbf{n}_{ij}$ for the individual elements makes it possible, however, to vary the size of the elements as well as the elastic properties in various parts of the component. This has been done in the computer program developed for the calculation of torsion constants for box beams and several of the results obtained with this program will be discussed in Chapter 5.

Shear Stress Distribution due to Torsion

The average shear stresses $\tau_{zx}$ and $\tau_{yz}$ for each element can be calculated from Equation (4.7). In view of Equations (4.15) and

(4.16) all forces $U_i$ and $V_i$ are given by

$$\mathbf{U} = -\mathbf{K}_{21}\mathbf{K}_{11}^{-1}\left[\mathbf{K}_{12}\mathbf{u} + \mathbf{K}_{13}\,\Theta\right] + \mathbf{K}_{22}\mathbf{u}$$

$$= \left(-\mathbf{K}_{21}\mathbf{K}_{11}^{-1}\left[\mathbf{K}_{12}\mathbf{M}_c + \mathbf{K}_{13}\right] + \mathbf{K}_{22}\mathbf{M}_c\right)\Theta G \qquad (4.46)$$

Expressing $\Theta$ in terms of the applied torsion T, Equation (4.2), the forces $U_i$ and $V_i$ become

$$\mathbf{U} = \left(-\mathbf{K}_{21}\mathbf{K}_{11}^{-1}\left[\mathbf{K}_{12}\mathbf{M}_c + \mathbf{K}_{13}\right] + \mathbf{K}_{22}\mathbf{M}_c\right)T/J \qquad (4.47)$$

The average shear stresses for an element i, having a cross-sectional area of a × b, due to a torsional moment T are therefore

$$\tau_{xz} = U_i/(ab) \qquad (4.48)$$

$$\tau_{yz} = V_i/(ab) \qquad (4.49)$$

where $U_i = k_{zxi}\,T/J$ and $V_i = k_{zyi}\,T/J$ are the forces on the faces of the element i in the $x$ - and $y$ -direction. The coefficients $k_{zxi}$ and $k_{zyi}$ are obtained from Equation (4.47). Substituting the expression for J, Equation (4.44), into Equation (4.47) the shear stresses finally can be written in terms of the applied torsion T as

$$\tau = \frac{k_{zi}}{K_1 b_1^2 h} = K_{2i}\,\frac{T}{b_1^2 h} \qquad (4.50)$$

where the coefficient $k_{2i} = k_{zi}/k_1$ depends on the direction of the shear stress and the location of the element.

# Chapter 5

## Theoretical Results

### Introduction

Coefficients for the lateral stability of beams and arches were calculated using the method outlined in Chapter 2. These, as well as torsion factors for box beams, calculated by the method developed in Chapter 4 will be discussed in this Chapter.

The equations developed in the preceeding Chapters were programmed in the Fortran IV language. The calculations were done on an IBM-7094 computer at the Computing Centre of the Imperial College of Science and Technology, University of London. For the solution of simultaneous equations, Gauss's method of successive elimination of unknowns (15) was used. This method was modified to the extent, that only the banded part of the coefficient matrix was used in the calculations.

A description of the various computer programs developed in connection with the work outlined here falls outside the scope of this thesis and only the results of the calculations will be given.

### The Lateral Stability of Beams

Coefficients for the lateral stability of a number of

straight beams were calculated. With these coefficients the critical load for lateral stability can be calculated directly with Equation (2.58), reproduced below

$$P_{cr} = C_1 \sqrt{EI_y GJ} / L^2 \qquad (5.1)$$

where $C_1$ = lateral stability coefficient

$L$ = span length

$E$ = modulus of elasticity

$G$ = modulus of rigidity

$I_y$ = second moment of area about minor axis

$J$ = torsion constant

It will be recalled that Equations(3.39a) and (3.39b) in Chapter 3 apply to all beams which are free to rotate at the supports about the minor axis of their cross-section, regardless of the type of loading applied to the beams. The coefficients discussed below were therefore calculated on the basis of these equations. All loading conditions discussed below are symmetrical and it was sufficient therefore to consider only half the span of the beam. Likewise the number of elements referred to will be the number of elements in one half of the span.

The element force matrix for a simply supported beam subjected to equal end moments is given by Equations(3.72) and (3.73). For three elements the resulting lateral stability coefficient is $C_1 = 3.178$, about one per cent larger than the lateral stability coefficient of 3.1416 by Timoshenko (43). Equation (5.1) in this case gives the critical moment, $M_{cr}$, in terms of the span L, since

here $P_{cr} = M_{cr}/L$. If the number of elements is increased to fifteen, the lateral stability coefficient reduces to $C_1 = 3.143$ or 0.04 per cent larger than that of Timoshenko. The error here is calculated from

$$\text{error (per cent)} = \frac{C_1 - C_1^*}{C_1^*} \qquad (5.2)$$

where $C_1^*$ is the lateral stability coefficient obtained by the classical methods of the theory of elasticity. In Fig. 5.1 the change in the error of the lateral stability coefficient is plotted as a function of the number of elements. It is apparent that an increase in the number of elements produces a very rapid convergence to the usually accepted value.

For a simply supported beam with a concentrated force at the centre, the convergence to the value of 16.94, first calculated by Prandtl (35), is equally rapid as the number of elements increases, Fig. 5.1. Here three elements give a coefficient $C_1 = 16.771$, which increases to 16.932 for fifteen elements. It is interesting that for the case of equal end moments the finite element theory should give an upper bound solution, while for a concentrated force a lower bound solution is being produced. While it is apparent that the estimate of the lateral stability coefficient must depend on the various matrices appearing in Equation (2.57), it is not clear why a change in the loading condition should cause a change in the direction from which the true solution is approached. Since the solution for each loading case. converges quite rapidly, however, to the known value, the method appears to be acceptable.

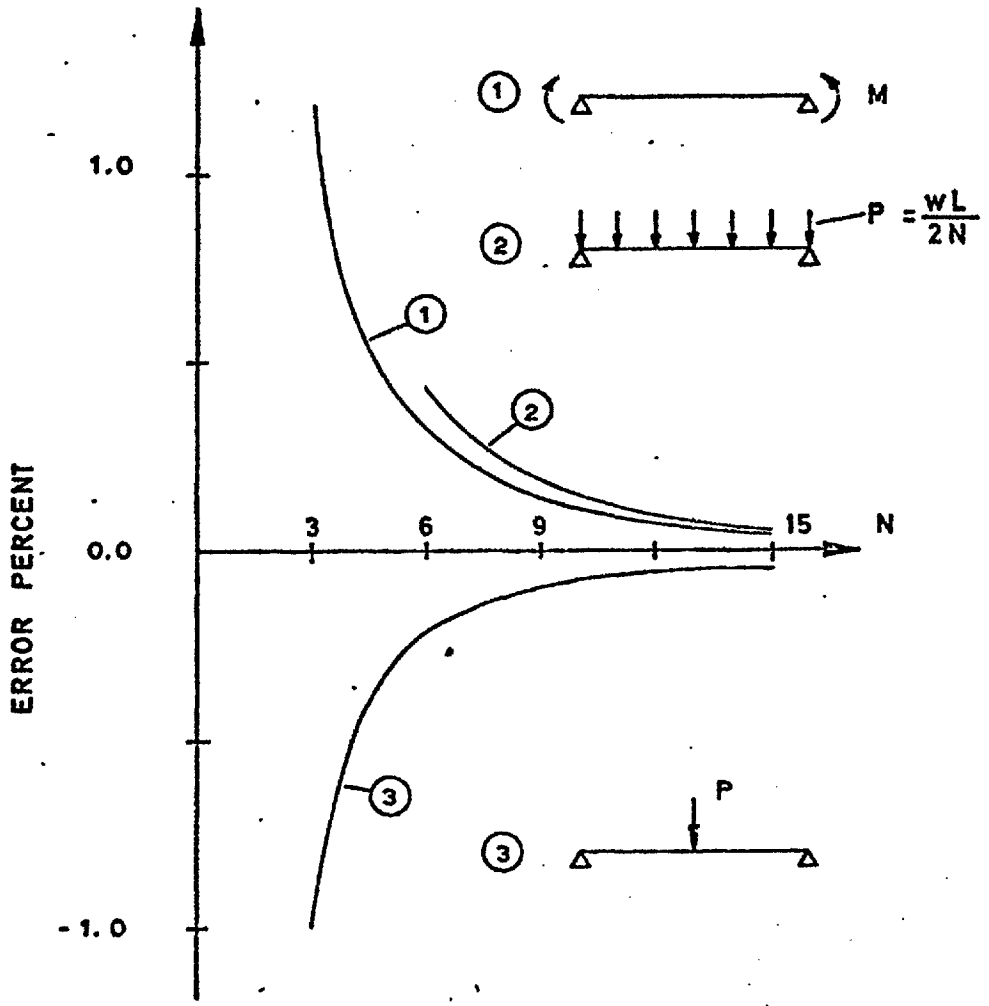


FIG. 5.1 ERROR IN BUCKLING COEFFICIENT AS FUNCTION OF NUMBER OF ELEMENTS, N.

## The Lateral Stability of Parabolic Arches

In Chapter 2 it was shown that the critical load for the lateral stability of arches can be written as

$$P_{cr} = C_2 \, EI_y/L^2 \qquad (5.3)$$

where $C_2$ = lateral stability coefficient for arches

In Chapter 3 the matrices required for the calculation of the coefficient $C_2$ have been developed for two-hinged arches as well as for fixed arches. At present calculations have been done only for two-hinged parabolic arches of constant cross-section loaded at the crown by a single concentrated force. Some of the results obtained so far are given in Appendix A. A summary of these results is given in Table 5.1 below.

Table 5.1

Lateral Stability Coefficients $C_2$ for Symmetrical Two-Hinged Arches

Concentrated Force P at Crown

| h/L | Coefficients $C_2$ $EI_y/GJ$ | | |
|---|---|---|---|
| | 0.715 | 4.0 | 6.0 |
| 0.1 | 2.0 | 1.7 | 1.6 |
| 0.2 | 4.0 | 2.5 | 2.0 |
| 0.3 | 5.7 | 2.7 | 2.0 |
| 0.4 | 7.0 | 2.7 | 2.0 |
| 0.5 | 7.7 | | |

Table 5.1 shows stability coefficients for several ratios of lateral bending stiffness to torsional rigidity, $EI_y/GJ$. For isotropic material, the ratio of modulus of elasticity to modulus of rigidity is E/G = 2.58. For timber this ratio varies considerably. Values ranging from 13.5 for Douglas fir to 27 for birch have been reported (1). The ratio of the second moment of area to the torsion constant for a narrow rectangular section is approximately $I_y J = 0.278$. The resulting ratios of lateral bending stiffness to torsional rigidity are, for isotropic materials, 0.715 and for timber 3.75 to 7.5. The coefficients given in Table 5.1 are therefore representative of isotropic materials as well as of orthotropic materials such as wood.

Table 5.1 shows that a decrease in the magnitude of the torsional rigidity relative to the lateral bending stiffness will result in a decrease in the critical load for lateral stability. Increasing the rise, h, of an arch relative to its span, L, will increase the lateral stability coefficient only for small ratios of $EI_y/GJ$. As the relative magnitude of the torsional rigidity decreases, the increase in the stability coefficients due to an increase in the rise h becomes less and less, until finally, for $EI_y/GJ = 6.0$, the increase in h will actually result in a small decrease in the magnitude of the stability coefficients for h/L = 0.4 (Appendix A).

The coefficients in Table 5.1 may also be compared with corresponding values for a straight beam. A comparison of Equations (5.1) and (5.3) will show that for a straight beam the critical load can be calculated with Equation (5.3), if we set

$$C_2 = C_1 \sqrt{GJ/EI_y} \qquad (5.4)$$

For a straight beam of narrow rectangular section loaded at midspan the lateral stability coefficient $C_2$ therefore becomes $C_2 = 20.1$, for a timber beam of similar dimensions but with $EI_y/GJ = 4.0$, the stability coefficient will only be $C_2 = 8.47$. These values are considerably larger than the stability coefficients for a shallow arch with a rise to span ratio of, say, 0.1. While this appears to throw some doubt on the validity of the coefficients shown in Table 5.1, it should be borne in mind that a shallow arch is subjected to a considerable thrust, which will contribute to the potential instability of the arch. Comparing on the other hand, the critical thrust $W_{cr}$ for a shallow arch of isotropic material, $W_{cr} = 2.4 \times 2.0 = 4.8\ EI_y/L^2$ for $h/L = 0.1$, with the critical load of a straight column hinged at both ends, it is found that the critical thrust for the arch is somewhat less than half of the critical Euler load of $\pi^2 EI_y/L^2$ for the column. In view of the additional torsion produced by the force at the crown of the arch, if small lateral deflections were to take place, it is not unreasonable, that the critical load for the arch should be less than that for the straight column.

To provide an unequivocal answer to the question of the validity of the coefficients in Table 5.1, it will be necessary therefore to conduct a series of tests on the lateral stability of arches, similar to the ones conducted with beams and described in the next Chapter.

## Torsion Constants for Solid Rectangular Sections

Using the method outlined in Chapter 4, torsion constants were calculated for various cross-sections. To test the accuracy of the method, calculations were done for solid rectangular sections with a height-to-width ratio $h/b_1 = 2.0$ for various numbers of elements. With eight square elements for one-quarter of the section, the torsion factor F equals 0.2339, decreasing to 0.2296 for fifty elements. The error in the calculated torsion constant as a percentage of the corresponding value given by Goodier (18) is shown in Fig. 5.2. It is apparent that an increase in the number of elements results in a rapid convergence to the usually accepted value of the torsion constant for isotropic materials. Table 5.2 gives a comparison of the torsion constants for rectangular sections calculated by the finite element theory with those obtained by means of a series solution (18).

Table 5.2

Torsion Factor F for Solid Rectangular Sections

| | Height-to-Width Ratio, $h/b_1$ | | | | |
|---|---|---|---|---|---|
| Method of Calculation | 1.0 | 1.2 | 2.0 | 4.0 | 10.0 |
| Series solution | 0.141 | 0.166 | 0.229 | 0.281 | 0.312 |
| Finite element solution | 0.142 | 0.167 | 0.230 | 0.283 | 0.318 |

The torsion constants J in Table 5.2 are given in terms of the quantity $b_1^3 h$

$$J = F\, b_1^3\, h \qquad (5.5)$$

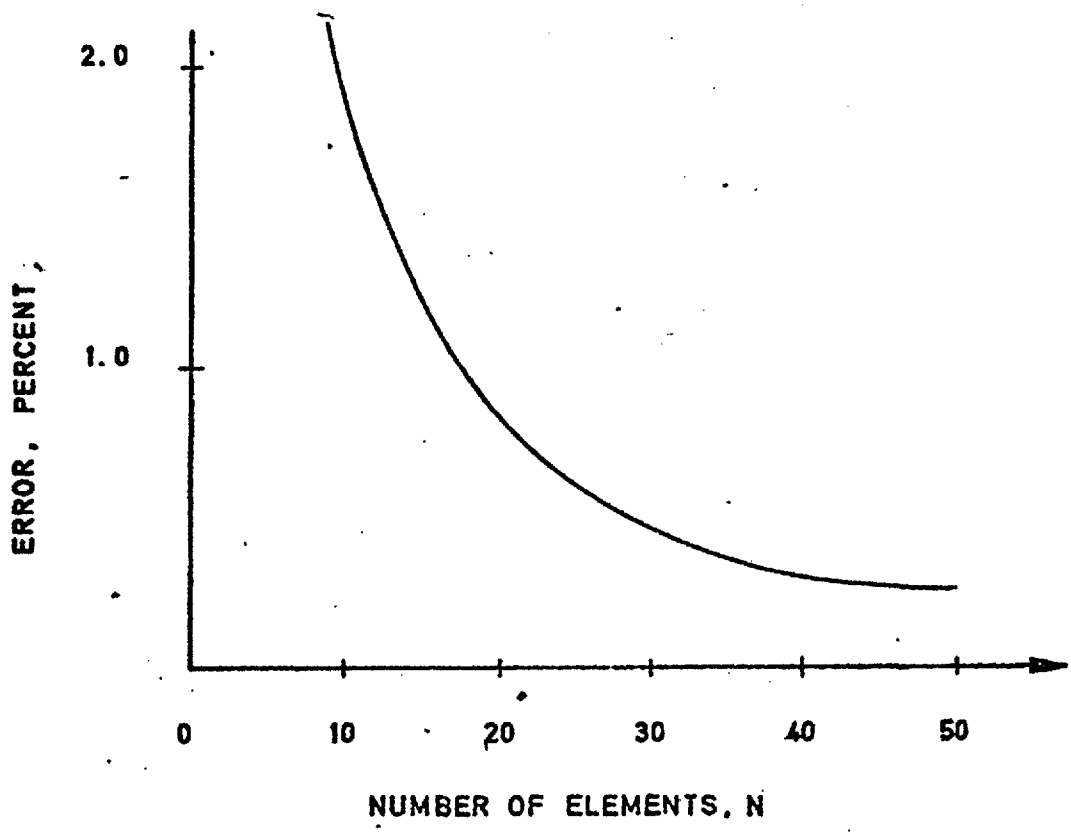


FIG. 5.2 ERROR IN TORSION FACTOR FOR RECTANGULAR SECTION, $h/b_1 = 2.0$

i.e. the tabulated quantity is the torsion factor F, which is given for various height, h, to width, $b_1$, ratios. As is evident from Table 5.2 the torsion constant obtained by means of the displacement method slightly overestimates the stiffness of the section and therefore represents an upper bound solution for the torsion constant.

A further test of the accuracy of the solution can be obtained by considering the torsional rigidity of orthotropic sections. A detailed study of the torsional rigidity of such sections has been published by ~~Taylor~~ Trayer and March (45). These authors consider solid cross-sections in which the axes of the orthotropic system are oriented at an arbitrary angle to the axes of symmetry of the cross-section. If these two axes coincide the expression for the torsion constant of a rectangular section reduces to

$$J = J_o \sqrt{G_{zx}/G_{yz}} \qquad (5.5)$$

where $J_o$ = torsion constant for corresponding section of isotropic material

$G_{zx}$ ($G_{yz}$) = modulus of rigidity for angular deformation of zx-plane (yz-plane)

Torsion factors for a solid square section calculated with Equation (5.5) and corresponding values obtained by means of the finite element theory are given in Table 5.3.

The largest difference in Table 5.3 between torsion constants obtained by the two different methods is about 2 per cent. This difference could be reduced further by increasing the number of elements used for the finite element solution.

Table 5.3

Torsion Factors F for Square Section of Orthotropic Material

| $G_{zx}/G_{yz}$ | Equation 5.5 | Finite Element Solution, N = 25 |
|---|---|---|
| 0.6 | 0.1089 | 0.1067 |
| 0.8 | 0.1258 | 0.1261 |
| 1.0 | 0.1406 | 0.1418 |
| 1.2 | 0.1540 | 0.1548 |

Torsion Constants for Box Sections

(a) Flange and web constructed from same material

Isotropic Case: Torsion factors F for a number of box- and I-sections were calculated. All cross-sections considered here are double-symmetrical, i.e. the flange depth d at the top and the bottom of the section are the same. Likewise the web thickness t on either side of the section is also the same. The results of these calculations are given in Appendix B. The torsion factor F is given for a number of height-to-width ratios, flange depth-to-width ratios and web thickness-to-width ratios. For isotropic materials the torsion factor F for a web thickness-to-width ratio of $t/b_1 = 0.05$ is plotted in Fig. 5.4. Curves for a number of depth-to-width ratios of $d/b_1$ are shown. Where the depth of the flange reaches one half the height, $d/b_1 = 0.5\ h/b_1$, the torsion factor for a box-section approaches that of a solid section of corresponding dimensions. For thin flanges, $d/b_1 = 0.20$ the torsion factors calculated with Equation (4.4) are nearly identical to those

calculated by means of the finite element theory. For large values of $d/b_1$, however, for example $d/b_1 = 2.0$, the approximate equation gives quite erroneous results. Fig. 5.3 gives the torsion factors for box-sections of isotropic materials having a web thickness-to-width ratio of $t/b_1 = 0.1$. Torsion factors for web thickness-to-width ratios of 0.01 and 0.15 will be found in Tables B-1 and B-4 in Appendix B.

Orthotropic Case: The treatment of orthotropic material is restricted to the case where the elastic axes of the material coincide with the axes of symmetry of the cross-section. In that case the orthotropic material, as far as torsion is concerned, is characterized by the presence of two different moduli of rigidity, one for the zx-plane and one for the yz-plane. Tables B-5 and B-6 give torsion factors for various ratios of $G_{zx}/G_{yz}$ for sections with $t/b_1 = 0.1$ and $d/b_1 = 0.5$ and 2.0. In all cases the material in the flanges and the webs is the same. The torsion factors for $d/b_1 = 0.5$ have been plotted in Fig. 5.5. It is apparent that the effect on torsion of differences between $G_{zx}$ and $G_{yz}$ is most pronounced for shallow sections, e.g. $h/b_1 = 1.0$. For deep sections, $h/b_1 = 10.0$, an increase in the ratio $G_{zx}/G_{yz}$ results only in a relatively small change in the torsion factor.

(b) Different Values of G in Web and Flange

Isotropic Case: In timber construction it frequently happens that the material used for the webs of a box-beam is not the same as that used for the flanges. As a result the modulus of rigidity for the flanges may not be the same as that for the web.

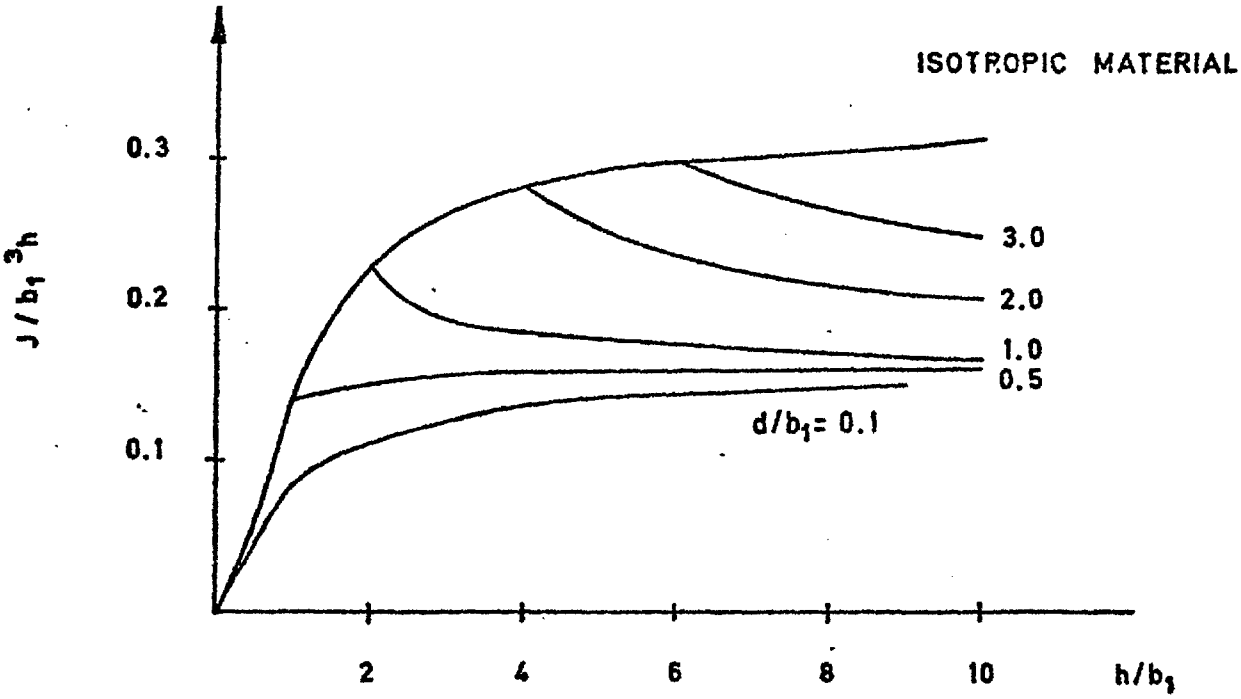


FIG. 5.3 TORSION CONSTANTS FOR BOX SECTIONS, $t/b_1 = 0.10$

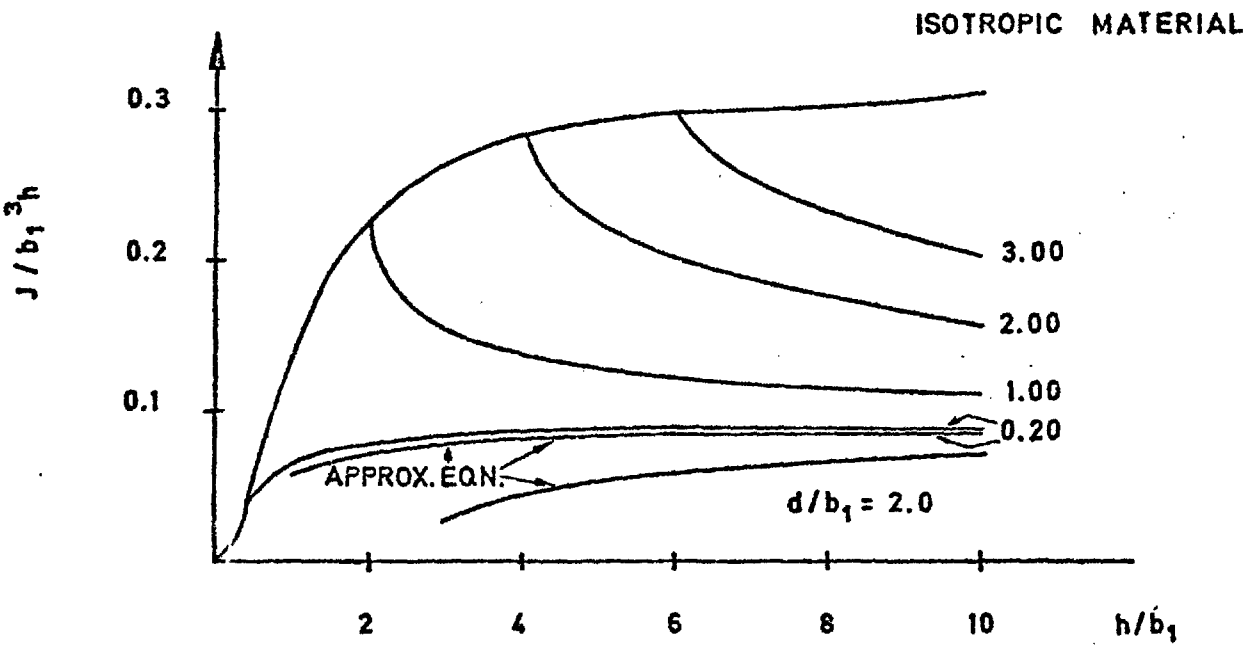


FIG. 5.4 TORSION CONSTANTS FOR BOX SECTIONS, $t/b_1 = 0.05$

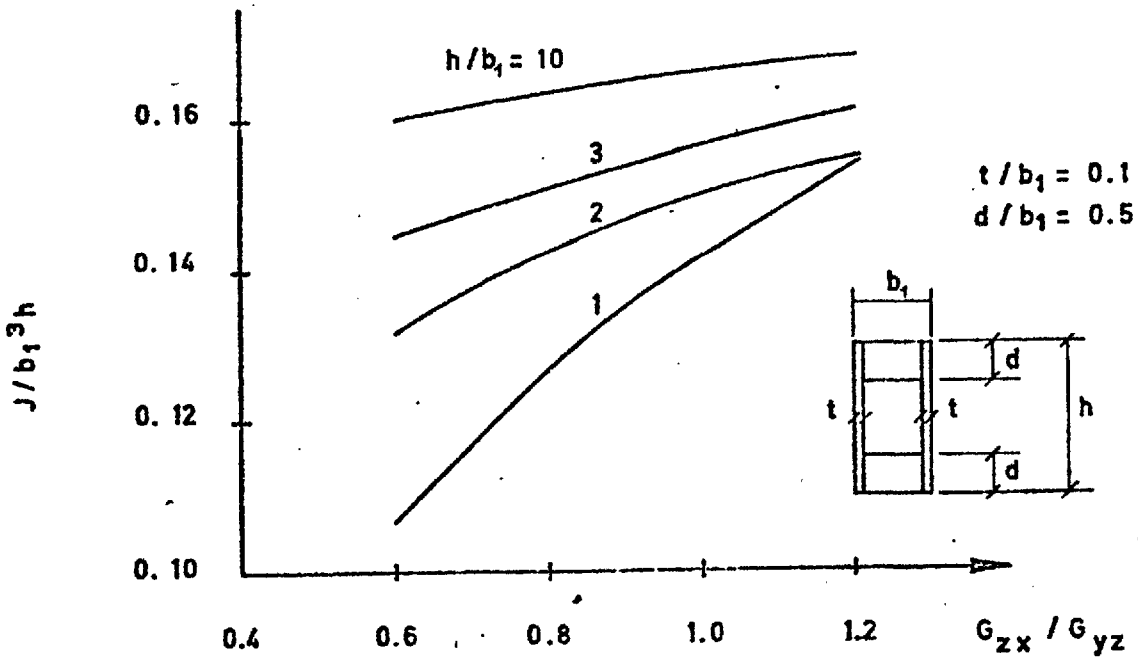


FIG. 5.5 TORSION CONSTANTS FOR BOX SECTIONS. ORTHOTROPIC MATERIAL.

As an example of the effect of such differences in the modulus of rigidity in web and flange torsion factors for box-beams with flange depth-to-width ratios of $d/b_1 = 0.5$ and $d/b_1 = 2.0$ and a web thickness-to- width ratio of $t/b_1 = 0.1$ were calculated for isotropic materials. The results are shown in **Tables B-7** and B-8 and are plotted in Fig. 5.6. It appears from Fig. 5.6 that the variation of the torsion factor due to changes in the $G_{web}/G_{flange}$ ratio is practically linear. The question arises therefore, if it would be possible to calculate torsion factors for this type of cross-section from a relation

$$J = J_o + b\ (R_G - 1.0) \qquad (5.6)$$

where $R_G = G_{web}/G_{flange}$

$J_o$ = torsion constant for $R_G = 1.0$

$b$ = slope of straight line for given values of $h/b_1$ $d/b_1$ and $t/b_1$

If it could be established that such a linear correlation between the torsion factor and the G-ratio exists, the calculation of torsion factors for box-sections with different moduli of rigidity for their web and flanges would be much simplified. At the present, not sufficient calculations have been done to confirm the trend which suggests itself in Fig. 5.6. A complete verification of Equation (5.6) will require a series of tests for a number of $R_G$ values and was outside the scope of the present investigation.

Different Values of G in Web and Flange

Orthotropic Case: Finally, it will be realized, it is also possible to have sections of orthotropic materials with moduli of rigidity for the flanges different from those for the web. Such a combination again will affect the torsion factor. As an example Table B-9 gives torsion factors for box-sections with $t/b_1 = 0.1$ and $d/b_1 = 0.5$. The three ratios of the two moduli of rigidity for the flanges are $G_{zx}/G_{yz} = 0.8$, 1.0 and 1.2. For the web the same three ratios were considered. Calculations for the resulting nine combinations were then repeated for moduli of rigidity $G_{yz}$ in the webs equal to 0.8, 1.0 and 1.2 times the modulus of rigidity $G_{yz}$ in the flanges.

A perusal of Table B-9 will show that the linear relation of torsion factors for variations in the ratio $G_{yz}$ for flange and web, already observed for isotropic materials, also appears to exist for orthotropic materials. For any given value of $G_{zx}/G_{yz}$ and $G_{wzx}/G_{wyz}$, changes in the $G_{wyz}/G_{yz}$ ratio seem to result in a corresponding linear change in F. The approach proposed for isotropic materials may therefore also be applicable here.

For the example given, changes in the moduli of rigidity ratio of the web, $G_{wzx}/G_{wyz}$, do not affect the torsion factor F. No doubt, this reflects the observation that in a thin web shear stresses in the direction of the web are many times larger than those oriented across the width of the web, a point to be discussed in greater detail in Chapter 6.

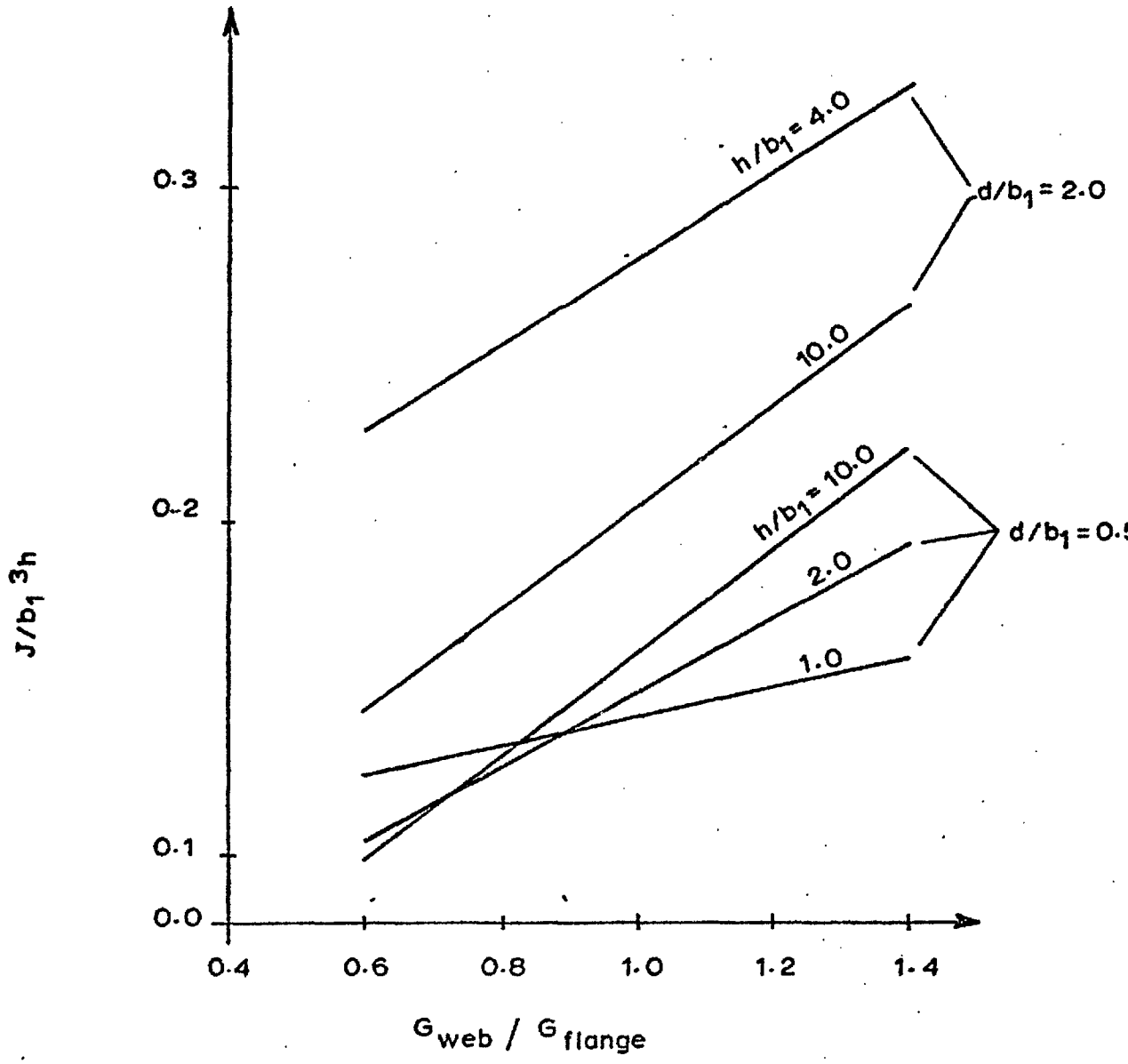


FIG. 5.6 TORSION CONSTANTS FOR BOX SECTIONS, $t/b_1 = 0.1$

A variation of the G-ratio for the flanges affects shallow sections more than deep sections. This appears to be the case for all three ratios $G_{wyz}/G_{yz}$ considered in Table B-9. On the other hand, for given values of $G_{zx}/G_{yz}$ and $G_{wzx}/G_{wyz}$, the effect of changes in the ratio of G for web and flanges is always larger for deep sections than for shallow ones.

Finally the data in Table B-9 suggest that on the whole differences between the material in the web and the flange will have a greater effect on the torsion factor than orthotropicity, as measured by the $G_{zx}/G_{yz}$ ratio. For example a twenty per cent change in the $G_{wyz}/G_{yz}$ ratio for flanges and web both with $G_{zx}/G_{yz} = 0.8$ for a height-to-width ratio of 2.0 will change F by about fifteen per cent. But keeping $G_{wyz}/G_{yz}$ constant at 0.8 and changing the ratio of $G_{zx}/G_{yz}$ for both web and flange from 0.8 to 1.0 will change F only by five per cent.

## Torsion Constants for I-Sections

The methods developed in Chapter 4 can also be used for the calculation of torsion constants of I-sections. For I-sections of isotropic materials, with a web thickness-to-width ratio of 0.1, torsion factors F are given in Table B-10. These results are plotted in Fig. 5.7. Here an increase in the flange depth to one-half the beam height will not result in the same torsion constant as that for a solid rectangular section with the same overall dimensions. In an I-beam with d = h/2 the top and bottom

flange are able to move relative to each other along the middle surface of the beam, except, of course, where the two flanges are joined together by the web. As a result the torsional rigidity of such a section will only be equal to the sum of the torsional rigidities of the top and the bottom flange. The corresponding torsion factor is equal to the F-value for an $h/b_1$ ratio of only one-half of that for the corresponding solid section. The resulting curve is shown in Fig. 5.7 as "sum of two half sections".

The torsional rigidities for the cross-sections of Fig. 5.7 can also be obtained by simply adding the individual torsional rigidities of flanges and web. This approach is usually chosen in the calculation of the torsional rigidity of steel I-sections (43). If this approach is used, care should be taken, however, to ensure that the actual torsional rigidity of the flange is being used. For steel I-sections, which usually consist of relatively thin webs and flanges, it is sufficient to estimate the torsional rigidity of the individual components from

$$J = wt^3/3 \qquad (5.7)$$

where $w$ = width of flange or height of web

$t$ = thickness of flange or web

For timber elements on the other hand, where for the flange the ratio of w/t is not large, the torsion factor cannot be approximated by the value one-third. For timber I-sections, therefore, the actual values of F corresponding to the dimensions of the solid flanges and the web should be used for the calculation of the individual torsional rigidities, which can then be added to give the torsional rigidity of the I-section.

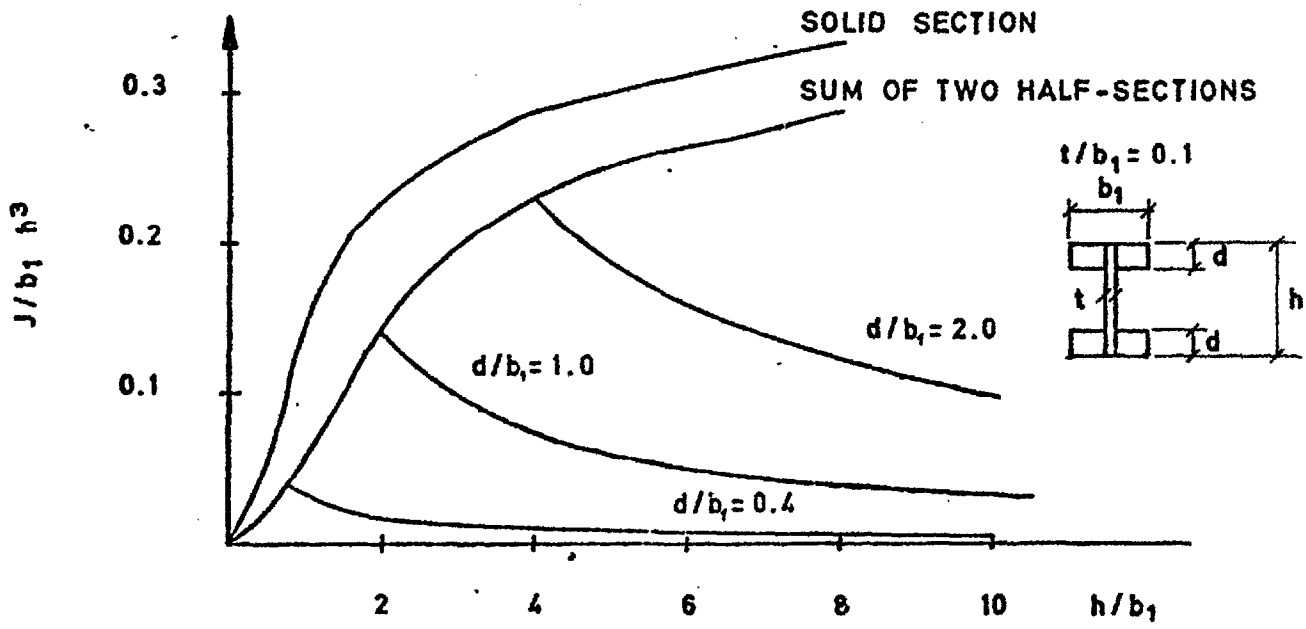


FIG. 5.7 TORSION CONSTANTS FOR I-SECTIONS, $t/b_1 = 0.1$

# Chapter 6

## Experimental Results

### Introduction

Results from two groups of tests will be given in this Chapter. The first group of experiments dealt with the lateral stability of plywood box beams loaded at midspan. Four different cross-sections were investigated. Each of these four beam types was represented by three beams and the tests were repeated for three different spans. Beams were loaded in the principal plane of bending as well as eccentrically. The effect of initial rotations of the beam ends, which were held in a fixed position, was also investigated.

The second group of experiments concerned the distribution of shear strains in the flanges of a box beam subjected to torsion. Only one beam was investigated. But the results agreed so well with the theoretical analysis that no further tests were deemed necessary.

### Lateral Stability of Box Beams

#### Box Beams for the Investigation of Lateral Stability.

Four different types of beams were constructed. These four beam types, their cross-sections are shown in Fig. 6.1,

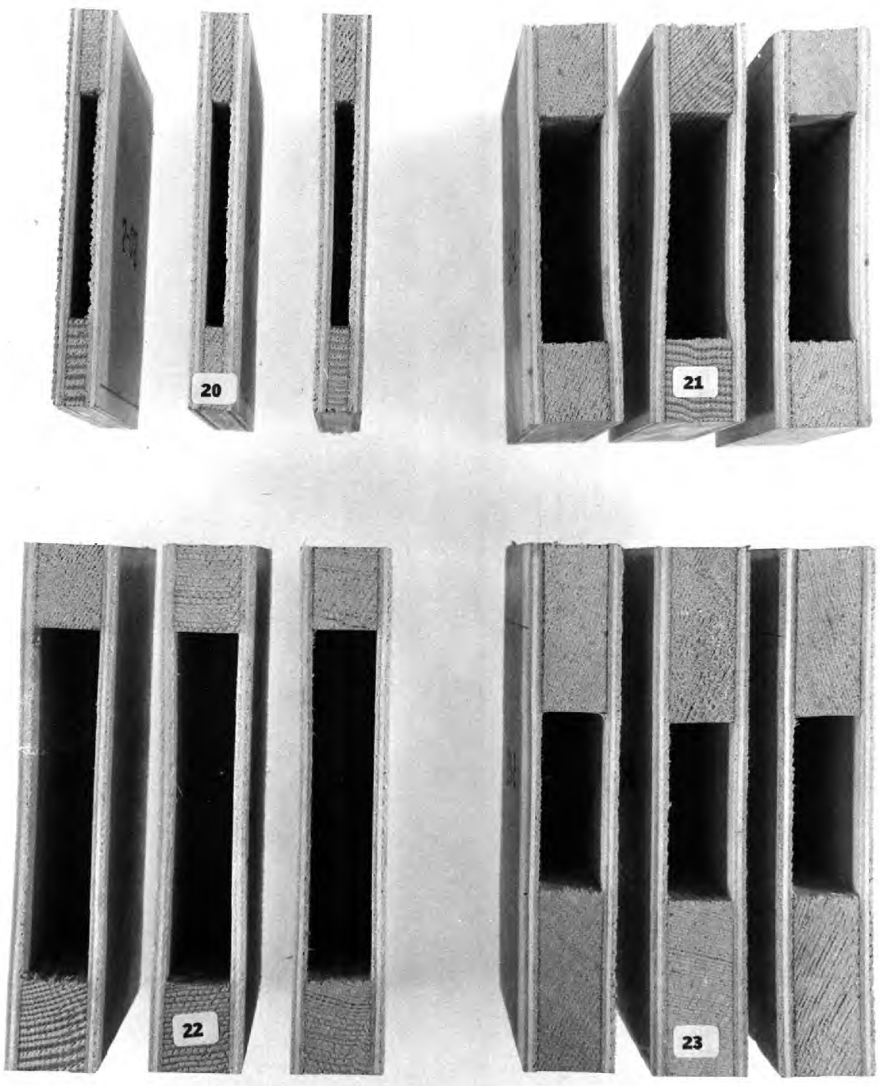


Fig. 6.1 Beam Cross Sections

will be referred to as beam types 20, 21, 22 and 23. The dimensions of these cross-sections are shown in Table 6.1. These cross-sections were chosen to give a range of height-to-width ratios of 9, 6 and 4.5, as well as flange-depth-to-width ratios of 1.0 and 2.0. The thickness of the plywood web was kept constant for all four beam types. The beams therefore are representative of web-thickness-to-width ratios of approximately 0.3, beam type 20, and 0.15, beam types 21, 22 and 23. The actual sizes of these cross-sections were determined by the equipment available for loading the beams. Of each beam type three specimens were built and tested.

The initial length of each beam was twelve feet. After completing all tests for a span of eleven feet, beams were reduced in length by 33 inch. and tested again on a 99.5 inch. span. Finally beams were reduced by another 33 inch. It was found, however, that for the corresponding span of 67.25 inch. lateral instability could only be enforced for beams of type 20.

Physical Properties of Flanges and Webs. The beams were built from material of unidentified origin, that had been stored in the carpenter's shop at Imperial College for some years. The flanges of the beams consisted of solid lumber, while for the webs birch plywood (Betula verrucosa) was used. Before assembling the composite sections, the flanges were cut to size and planed. Webs and flanges were then glued together with a resin-type adhesive (Cascamite Resin Glue) and clamped until the glue had set and hardened.

Table 6.1

Dimensions of Cross Sections

Test Beams

| Beam Type | Height h, in. | Width b, in. | Flange Depth d, in. | Web Thickness t, in. |
|---|---|---|---|---|
| 20 | 4.5 | 0.56 | 1.00 | 0.156 |
| 21 | 4.5 | 1.07 | 0.99 | 0.156 |
| 22 | 6.0 | 1.06 | 0.99 | 0.156 |
| 23 | 6.0 | 1.06 | 2.00 | 0.156 |

The material for the flanges was straight-grained and free from visible defects. The material was superficially identified as Douglas fir. A more detailed inspection, after testing of the beams had been completed, confirmed that the flanges, indeed, were Douglas fir (Pseudotsuga menziesii). Some of the material, however, had an exceptionally low specific gravity, and as a consequence, an unusually low modulus of elasticity, Table 6.2. Growth rates ranged from a low of 8 rings per inch to a high of 36 rings per inch. These, however, did not appear to be correlated to the specific gravity or the elastic properties.

After testing had been completed three samples, approximately 1 inch x $\frac{3}{4}$ inch x 14 inch., were cut from each of the two flanges of every beam. These samples were used to determine the modulus of elasticity, the specific gravity and the moisture content of the flanges. A detailed analysis of these three sets of data is given in Appendix C.

To determine the modulus of elasticity of the flanges the six 14 inch long samples taken from each beam were tested in bending. These minor specimens were supported on a 11 inch span and loaded at the centre by a concentrated force. Load was increased at a uniform rate up to a maximum load of 100 kg in about two minutes. Deflections at midspan, relative to the frame supporting the specimens, were measured with a dial-micrometer graduated into 0.0001 inch. The load-deflection curve for each bending test was a straight line. The slope of these load-deflection curves was used to calculate the modulus of elasticity of each minor specimen. A statistical evaluation of the test data is given in Appendix C, Table C-2. Each average modulus of elasticity given in Table C-2 is the average for six sample beams taken from the flanges of every beam. With one exception, beam 21-3, all moduli of elasticity are smaller than the average value of 1 970 000 psi reported for air-dry Douglas fir by Kennedy (24). About half the E-values in Table C-2 are within a range of one standard deviation, 414 000 psi, from the average, using the coefficient of variation (CV = 21.4 %) given by Kennedy. Of the remaining six averages two, beams 20-3 and 21-2, fall slightly outside the range given by twice the standard deviation. Low values of E, such as those for beams 20-3 and 21-2 are unusual, but still within the range of possible moduli of elasticity for Douglas fir.

Table 6.2

Moduli of Elasticity of Flanges and Beams

Specific Gravity of Flanges

| Beam Type | Beam No | Box Beams: Apparent Modulus of Elasticity, $E_a$, $10^6$ psi | Flanges: Average Modulus of Elasticity, E, $10^6$ psi | Flanges: Specific Gravity |
|---|---|---|---|---|
| 20 | -1 | 1.19 | 1.68 | 0.52 |
| | -2 | 1.31 | 1.59 | 0.53 |
| | -3 | 1.09 | 1.10 | 0.43 |
| 21 | -1 | 0.99 | 1.28 | 0.44 |
| | -2 | 0.99 | 1.11 | 0.43 |
| | -3 | 1.20 | 1.94 | 0.60 |
| 22 | -1 | 1.21 | 1.59 | 0.51 |
| | -2 | 1.20 | 1.34 | 0.47 |
| | -3 | 1.26 | 1.55 | 0.48 |
| 23 | -1 | 1.04 | 1.19 | 0.41 |
| | -2 | 1.26 | 1.59 | 0.52 |
| | -3 | 1.04 | 1.29 | 0.44 |

It is instructive to compare these average moduli of elasticity with the corresponding specific gravities of the beams. This comparison has been made in Table 6.2, which also shows the apparent modulus of elasticity of each of the 24 large composite beams. It is quite apparent that high specific gravities correspond to high moduli of elasticity of the flanges.

The apparent modulus of elasticity, $E_a$, shown in Table 6.2 was calculated with Equation (6.1)

$$E_a = \frac{(P/y)\, L^3}{48\, I_x}\left[1 - 3\, c/L + 6\, (c/L)^2 - 8\, (c/L)^3\right] \qquad (6.1)$$

where $P/y$ = slope of initial, straight part of load-deflection curve, deflection measured at centre

$I_x$ = second moment of area, Table C-1

$L$ = span

$c$ = distance from support to nearest load point

The load-deflection curves, on which these calculations are based, were obtained during a final test, when each beam was loaded to failure, as shown in Fig. 6.5.

These apparent moduli of elasticity cannot be compared directly with the average moduli of elasticity of the flanges, since they are also affected by the modulus of elasticity of the plywood in the web and by the shear deflection of the beams. Nevertheless the same trend of high moduli of elasticity being correlated with high specific gravities is also evident for the apparent modulus of elasticity. The only exceptions are beams 20-1 and 20-2, which can probably be explained by the relatively small ratio of flange area to total cross-sectional area in these particular beams. Such strong correlation between specific gravity and modulus of elasticity in timber is well known and has been documented, for example, by Kollmann (27).

Specific gravity was determined as the ratio of oven-dry weight of a sample to its volume measured immediately after removing the specimens from the drying oven. Specimens taken from the flanges measured approximately 1 inch x $\frac{3}{4}$ inch x 7 inch and were dried at a temperature of 102 degrees centigrade for about two days until reaching constant weight. The volume of the specimens was calculated from the measured dimensions of the prismatic samples.

Moisture content of a sample is the difference in weight between the original and the completely dry state of a sample, expressed as a percentage of its dry weight.

A statistical analysis of these data is given in Tables C-4 and C-5.

Two distinct groups of specific gravities were evident, the average of one group being 0.52 and that of the other group being 0.43. The average moisture content of the flanges was 10 per cent. Of all the specimens tested only those cut from beams 21-1 and 21-2 showed a moisture content significantly different from that of the remainder of the beams.

Because of the relatively small size of the experimental beams in this investigation, very thin plywood had to be chosen for the webs. The material selected for the webs was birch plywood, 5/32 inch thick, consisting of three layers of veneer. No samples for the determination of the modulus of elasticity were cut from the webs and only the specific gravity and the

moisture content of the plywood were determined. The details of the statistical analysis of these data are also given in Tables C-4 and C-5. The average specific gravity of the birch plywood was 0.66, with significantly lower values observed for beams 20-3, 21-1 to 3 and 22-1. The average value of 0.66 is somewhat higher than the species average for birch plywood given by Kollmann (27) as 0.61. Average moisture content of the plywood was 7.9 per cent, excluding the somewhat higher moisture contents of 8.3, 8.2 and 8.4 per cent found for beams 22-2, 23-2 and 23-3.

For the modulus of elasticity of European birch plywood of three-ply construction with the outer veneer oriented parallel to the span, Keylwerth gives a value of 1 820 000 psi at a moisture content of 7 per cent; for the same type of plywood Keylwerth also gives a modulus of rigidity of 104 000 psi. For the modulus of rigidity of the flanges a value of 100 000 psi has been used. This value was determined during the study of the strain distribution in the flanges of a box beam.

Bending Stiffness and Torsional Rigidity of Box Sections.

The moduli of elasticity and rigidity of web and flanges were used to calculate the bending stiffness and the torsional rigidity of the beam sections. Details of the calculation of the bending stiffness of orthotropic sections are given in Appendix D. The torsional rigidity was determined by the method outlined in Chapter 4. The second moments of area, $I_y$, and the torsion constant, J, used in these calculations are given

Table 6.3

Average Bending Stiffness and Torsional Rigidity

| Beam Type | Bending $EI_y$, 1000 lb-in$^2$ | Torsion $GJ$, 1000 lb-in$^2$ | |
|---|---|---|---|
| | Calculated | Observed | Calculated |
| 20 | 134 | 22.9 | 24.2 |
| 21 | 725 | 124.0 | 124.0 |
| 22 | 927 | 165.0 | 164.0 |
| 23 | 1012 | 207.0 | 193.0 |

in Appendix C, Table C-1. The resulting average bending stiffness and torsional rigidity of each beam type are given in Table 6.3.

To check the calculated torsional rigidity the torsional rigidity was also determined experimentally. A 33 inch long section of each beam was twisted about its central axis and the relative rotation of two sections 18 inches apart was measured. In order to apply a torque, the beam was clamped at one end to a rigid steel frame in a manner similar to that shown in Fig. 6.2. At the opposite end a lever arm was attached to the beam from which weights could be suspended. To prevent bending, a pin was fixed to the centre of rotation of the box section. This pin was supported in the vertical direction. This arrangement allowed the beam to twist freely without being subjected to any bending moments.

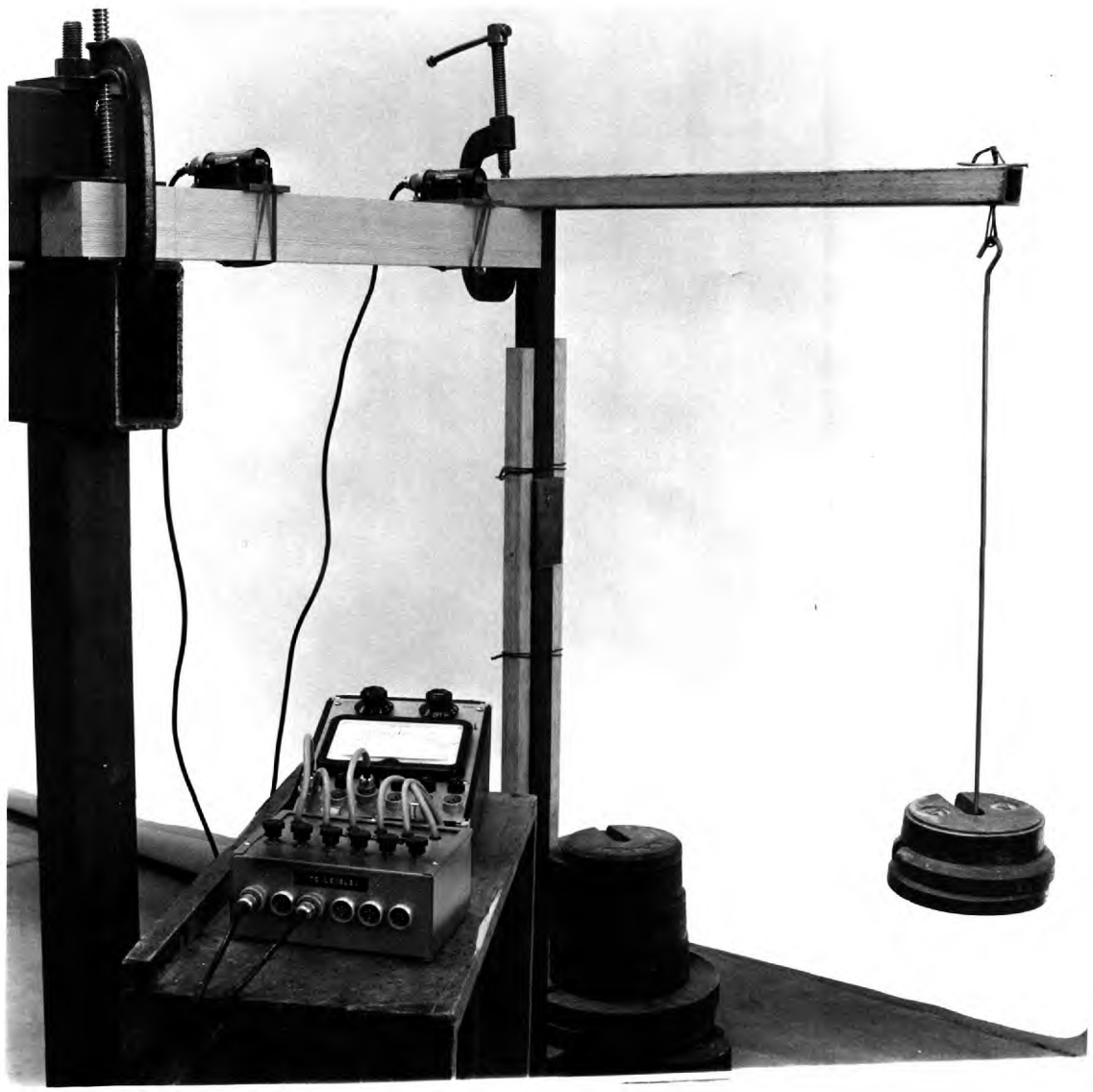

Fig. 6.2 Torsion Test

Torsion was applied in eight to twelve increments by suspending weights at the end of the lever arm. The rotation resulting from this torsion was measured at two sections approximately 6 inches from either end of the beam. The resulting load-rotation curve for each beam was a straight line. The corresponding regression lines for rotation on loads are given in Table C-6. The slope of these regression lines was then used to calculate the torsional rigidity, GJ, of each beam from the relation

$$GJ = L_1 L_2/b \qquad (6.2)$$

where $L_1$ and $L_2$ are lever arm and gauge length respectively and where b equals the slope of the regression line, Table C-6, converted to radians. The resulting average torsional rigidity obtained from the experimental data is shown in Table 6.3. The differences between the observed torsional rigidity and the values calculated on the basis of the torsion constant J and a value of G equal to 100 000 psi can be attributed to the variability of the modulus of rigidity. For the calculation of the critical loads for the lateral stability the observed values for the torsional rigidity have been used.

Description of Test Equipment. In the experimental investigation of the lateral stability of beams it is essential that the boundary conditions assumed in the theoretical analysis are also provided in the experiment. In the present case it was assumed that only vertical loads were being applied

and that the beam cross-section was free to rotate as well as deflect laterally everywhere along the length of the beam except at the ends. It was also assumed that the beam was simply supported at the ends, both in the vertical as well as the horizontal plane.

The simple support at the ends allowing rotations in the vertical plane of the beam was provided by a single steel roller of $\frac{1}{2}$ inch diameter at either end of the beam. A $\frac{1}{2}$ inch thick steel plate between the roller and the beam prevented the roller from being pressed into the lower face of the plywood box-beam and assured that movement in the direction of the beam axis could take place. To prevent lateral rotation of the ends about the beam axis, beams were fitted into slots at the supports. The beam ends could thus freely rotate about the supporting roller without any possibility of the beam tipping sideways. At the same time the ends of the beam could also freely rotate in the horizontal plane. The whole arrangement was supported by a rigid steel frame at an elevation approximately three feet above the ground. A general view of the test set-up is shown in Fig. 6.3.

Each beam was loaded by a single, concentrated force at midspan. To prevent any possibility of lateral restraints it was necessary to load the beam by means of weights suspended at the centre of the span. To allow unrestricted rotation of the beam cross-section at midspan a special loading rig was constructed. This rig consisted of a plywood yoke, a free-floating spreader beam and some cable and is shown in Fig. 6.4. With it loads could be

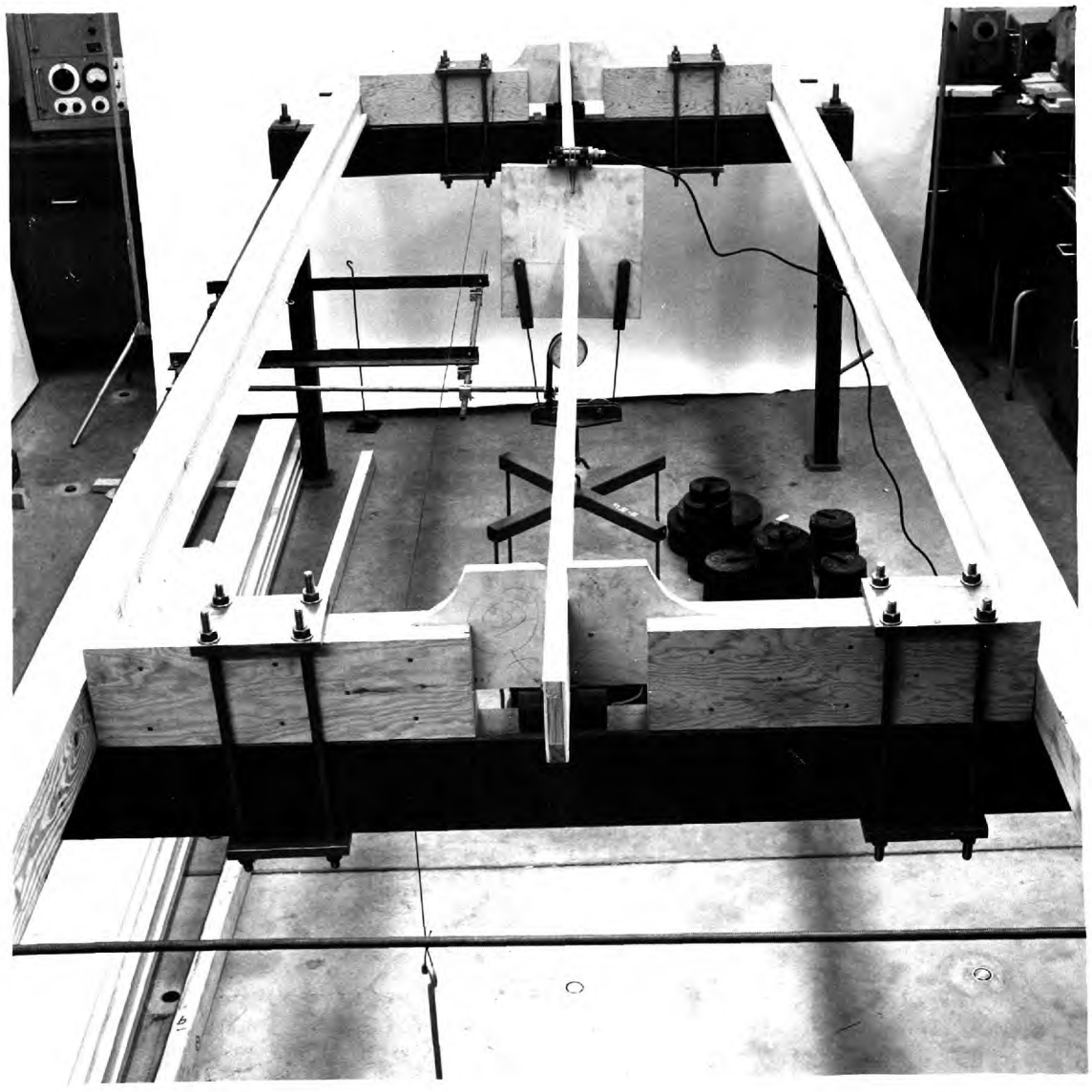

Fig. 6.3 Test for Lateral Stability of Box Beams

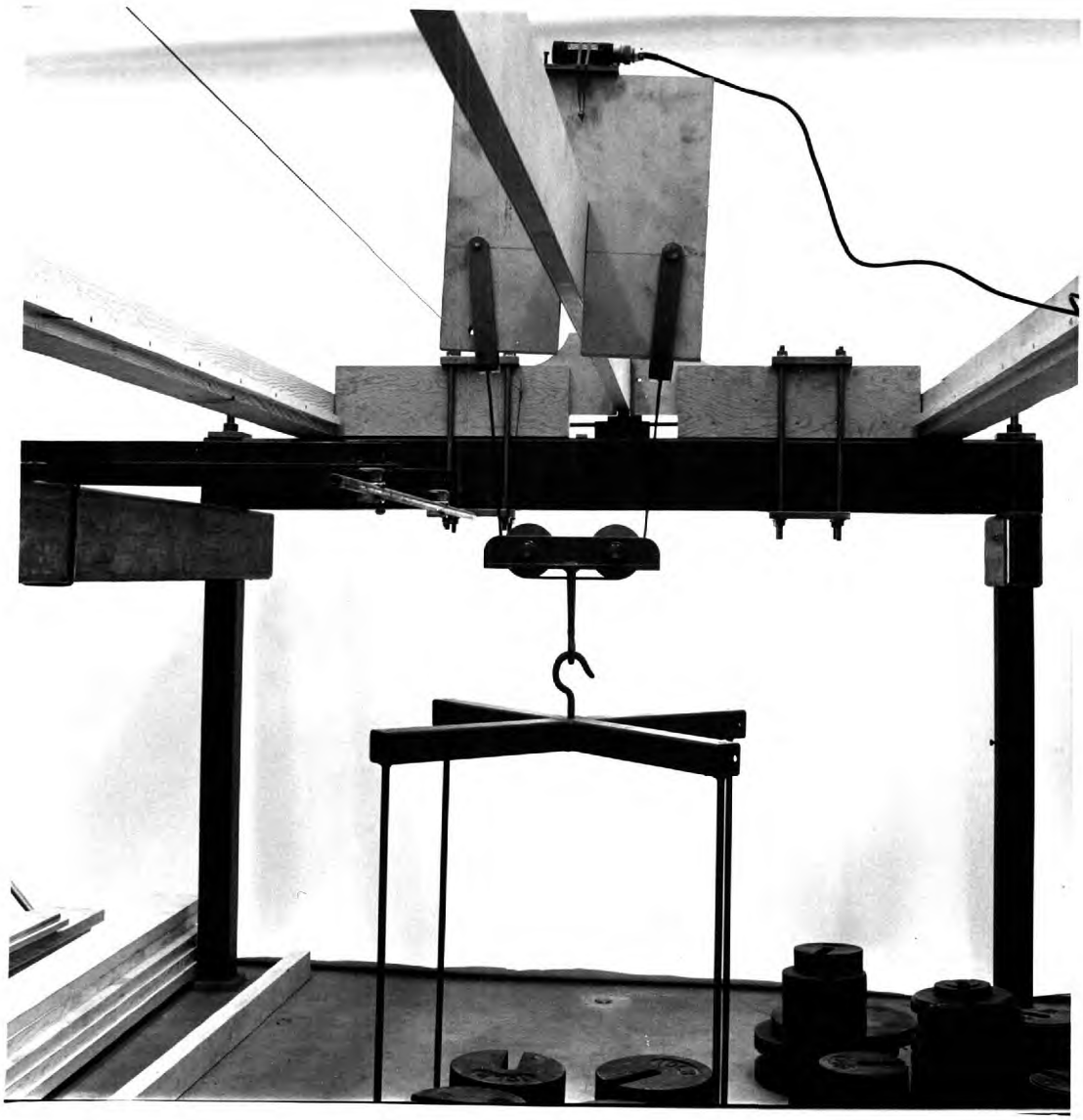

Fig. 6.4 Yoke for Loading of Box Beams

positioned in such a way that during rotation of the beam cross-section at the centre, the resultant of the applied load would act either at midheight of the beam or at any other desired position above or below the centroid of the cross-section.

Testing of Plywood Box Beams. After some preliminary tests, which indicated the test equipment to be adequate, the box beams of Type 20, 21, 22 and 23 were constructed. Three beams were made of each type giving a total of twelve beams. A number of studies were then conducted with these beams. All beams were tested at spans of 132 inch. and 99.5 inch. Beam types 20 and 21 were also tested for a span of 67.25 inch. For these tests the load was applied at the centroid of the beam cross-section and the tests were labelled Series 1, 2 and 3 corresponding to the three different spans, Table 6.4.

All other tests were conducted with the three beams of Type 22. In these tests the effect of locating the load at the top or the bottom edge of the box beam was investigated (Test Series 4). Tests involving the initial rotation of the ends of box beams were labelled Series 5. The effect of lateral eccentricities on the lateral stability of plywood box beams, finally was studied with tests in Series 6. Details of the loading conditions for Series 4 to 6 are given in Table 6.5. The span length for all tests of Series 4 to 6 was 132 inch.

Beams were loaded in equal increments for approximately the first ten to fifteen increments. The size of any further

Table 6.4

Lateral Stability of Plywood

Box Beams

Load at Centroid of Cross-Section

| Test Series | Beam Types | Span, in. |
|---|---|---|
| 1 | 20, 21, 22 and 23 | 132.0 |
| 2 | 20, 21, 22 and 23 | 99.5 |
| 3 | 20 and 21 | 67.25 |

Table 6.5

Lateral Stability of Plywood

Box Beams

Eccentricities and Initial End Rotations

Beam Type 22
Span length 132.0 in.

| Test Series | Load Position x, in. | y, in. | Initial End Rotation degrees |
|---|---|---|---|
| 4 - 1 | 0 | +3 | 0 |
| 4 - 2 | 0 | 0 | 0 |
| 4 - 3 | 0 | -3 | 0 |
| 5 - 1 | 0 | 0 | 1 |
| 5 - 2 | 0 | 0 | 2 |
| 5 - 3 | 0 | 0 | 3 |
| 6 - 1 | 0.5 | 0 | 0 |
| 6 - 2 | 1.0 | 0 | 0 |

load increments was governed by the amount of rotation produced up to this stage of loading. For each increment the vertical deflection and the rotation of the cross-section at the centre were measured. Deflections were measured with a dial-gauge giving increments of 0.001 inch. Rotations were observed with an electrolevel, having ranges of $\pm$ 5 degrees, $\pm$ 1 degree and $\pm$ 0.25 degrees. Only the 5 and 1 degree ranges were being used in this investigation. The scale of this electrolevel was divided into 20 equal parts, giving for the coarsest range increments of 0.5 degrees per division.

Since the same beams were used for a number of investigations, it was essential not to damage the beams during loading. On the other hand, loading had to be carried sufficiently far to produce rotations large enough to allow an estimate of the buckling load to be made.

Finally, after completion of Test Series 1 to 6, the beams were loaded to failure to determine their maximum load carrying capacity in bending. These tests were carried out with a hand-operated testing machine. Beams of Type 20 and 21 were tested on a 72 inch span, those of Type 22 and 23 on a 96 inch span. The beams were loaded by two point loads located 14 inches to either side of the middle of the beam. For these tests lateral buckling had to be prevented in order to develop the full bending strength of the box beams. The beams were therefore guided in slots at the points of load application. An overall view of the loading arrangement for these final beam tests is shown in Fig. 6.5.

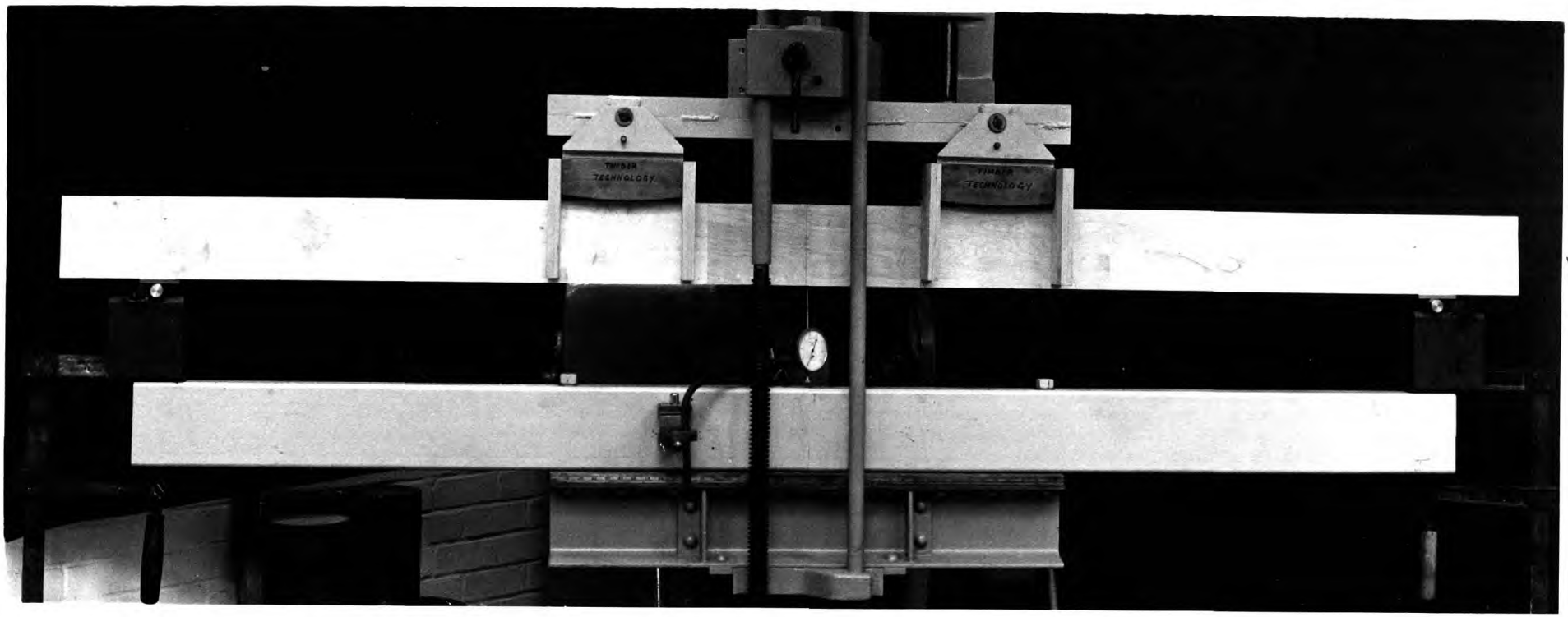


Fig. 6.5 Bending Test of Plywood Box Beam

Results of Beam Tests. Using the observed load-rotation curves a Southwell plot, $\theta/P^2$ against $\theta$, was constructed for each beam. These Southwell plots are shown in Appendix C, Fig. C-1(a) to (f). The majority of these graphs show the characteristic straight line, which is obtained, if the rotations are large enough and the load sufficiently close to the critical load. In a few cases, beams of Type 21 in Series 2 for example, the loading had not been carried far enough to result in the desired straight line. In general it was found that the loading had to be increased far enough to produce at least three rotations larger than one degree before the $\theta/P^2$ vs. $\theta$ plot resulted in a straight line. Since it was imperative that the beams would not be damaged and because of the uncertainty of the actual load carrying capacity of the beams this requirement could not always be fulfilled.

To obtain an estimate of the critical load for each beam, the slope of the straight line, passing through the experimental points of the Southwell plot, was calculated. For this purpose it was assumed that, for a given value of $\theta$, the quantity $\theta/P^2$ was subject to experimental error. The slope B of the straight line $\theta/P^2 = A + B\theta$ can then be calculated by minimizing the sum of squares of the vertical deviations of the experimental points from the straight line (12). The slope B for each test, together with the maximum load and the maximum rotation are given in Table C-7 in Appendix C. To calculate these slopes only rotations larger than 0.65 degrees were used for Series 1 and 3. For all other test series only rotations larger than one degree were utilized.

The slope of the straight line was used to calculate the critical load by means of Equation(1-7). The results of these calculations are given in Table C-8 as critical experimental loads. Table C-8 also gives the maximum load placed on each beam for each particular test as well as the theoretical load calculated with Equation (2.58).

The critical experimental loads for Series 1 to 3 obtained by means of the Southwell plot are also given in Fig. 6.6, which shows the critical load P for a simply supported beam as a function of the span length L. Fig. 6.6 shows curves for critical loads for beams of Type 20, 21 and 23. The corresponding curve for beam Type 22 does not differ greatly from that of Type 23 and is not shown. These curves were calculated for a modulus of elasticity equal to 1 600 000 psi and a modulus of rigidity equal to 100 000 psi. In addition Fig. 6.6 also shows the increase or the decrease in the calculated critical loads for beam Type 23 if the modulus of elasticity changes by plus or minus one standard deviation. In a test series involving a large number of plywood box beams with an average value of E = 1 600 000 psi, one would expect that about two-thirds of all critical loads would fall in this region.

The experimental results for beam Type 20 appear to fit the theoretical curve reasonably well. In general, however, the observed critical loads are higher than would be expected from Equation (2.58). In view of the low moduli of elasticity of some of the beams, it is surprising that the experimental

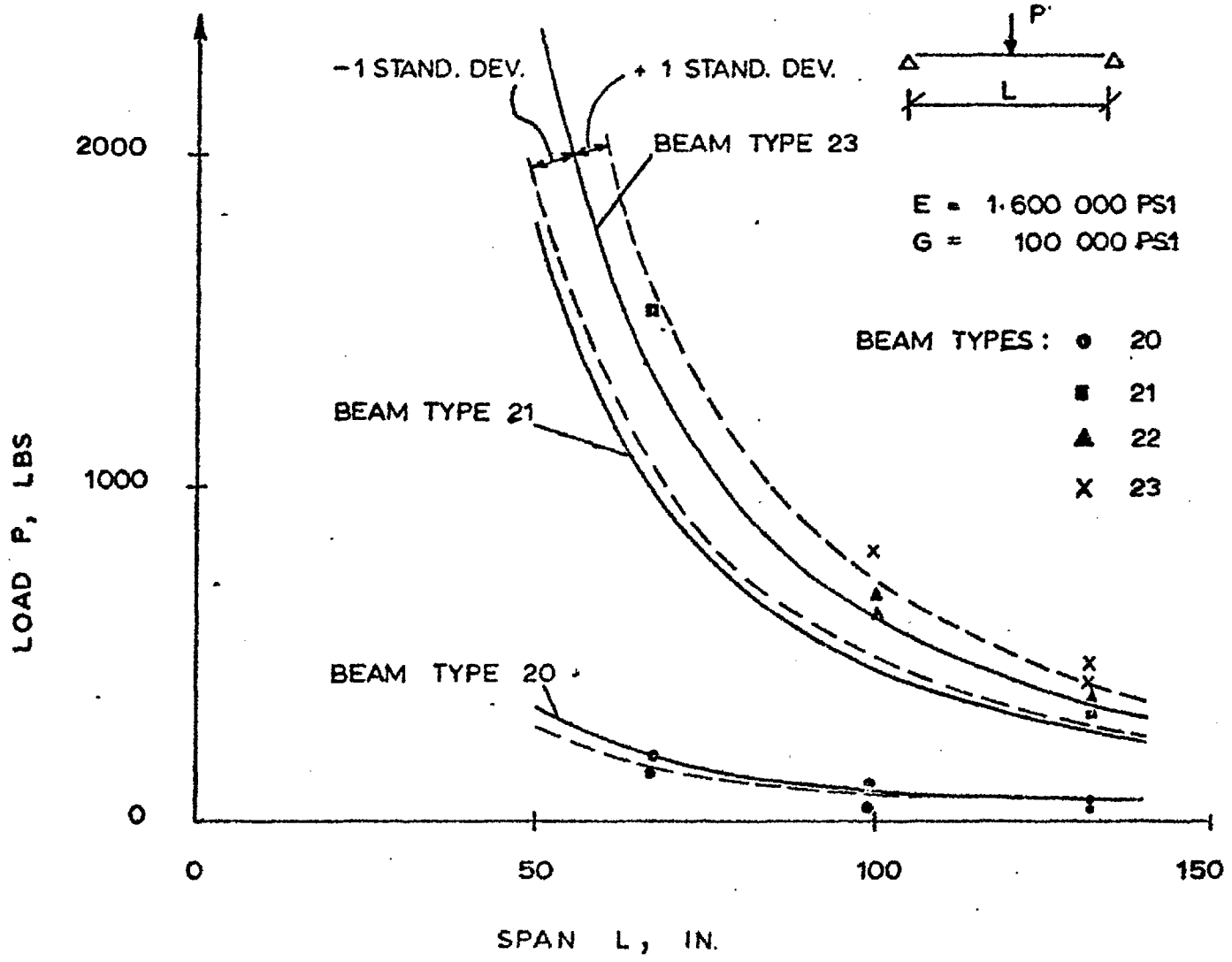


FIG. 6.6 CRITICAL EXPERIMENTAL LOADS FOR LATERAL STABILITY

loads should be as high as shown in Fig. 6.6. Since the specific gravity of the birch plywood was higher than the species average given by Kollmann (27), it is possible, however, that the modulus of elasticity for the birch plywood was higher than the value assumed. Since the relative contribution of the web to the second moment of area about the minor axis is larger than its relative contribution to that about the major axis, the effect of any differences in the modulus of elasticity of the birch plywood from the value quoted by Keylwerth would be less pronounced for the bending stiffness in the vertical plane than for that in the horizontal plane. Since only the deflections in the vertical plane were measured, it is possible that such differences in the modulus of elasticity of the birch plywood went undetected. While the actual value of the observed critical loads was higher than expected, the loads do follow the general trend indicated by the theoretical solution.

In Fig. 6.7 the critical loads have been plotted as a function of the torsion constant J and the second moment of area $I_y$. Again the experimental loads are somewhat higher than the theoretical loads. But here, too, the pattern given by the theoretical solution is followed by the experimental values. Loads do appear to increase linearly for a given span as the value of $\sqrt{JI_y}$ increases and likewise a decrease in the span length does result in an increase in the slope of the line P vs. $\sqrt{JI_y}$.

The effect of a change in the vertical location of the concentrated force on the critical loads was investigated by

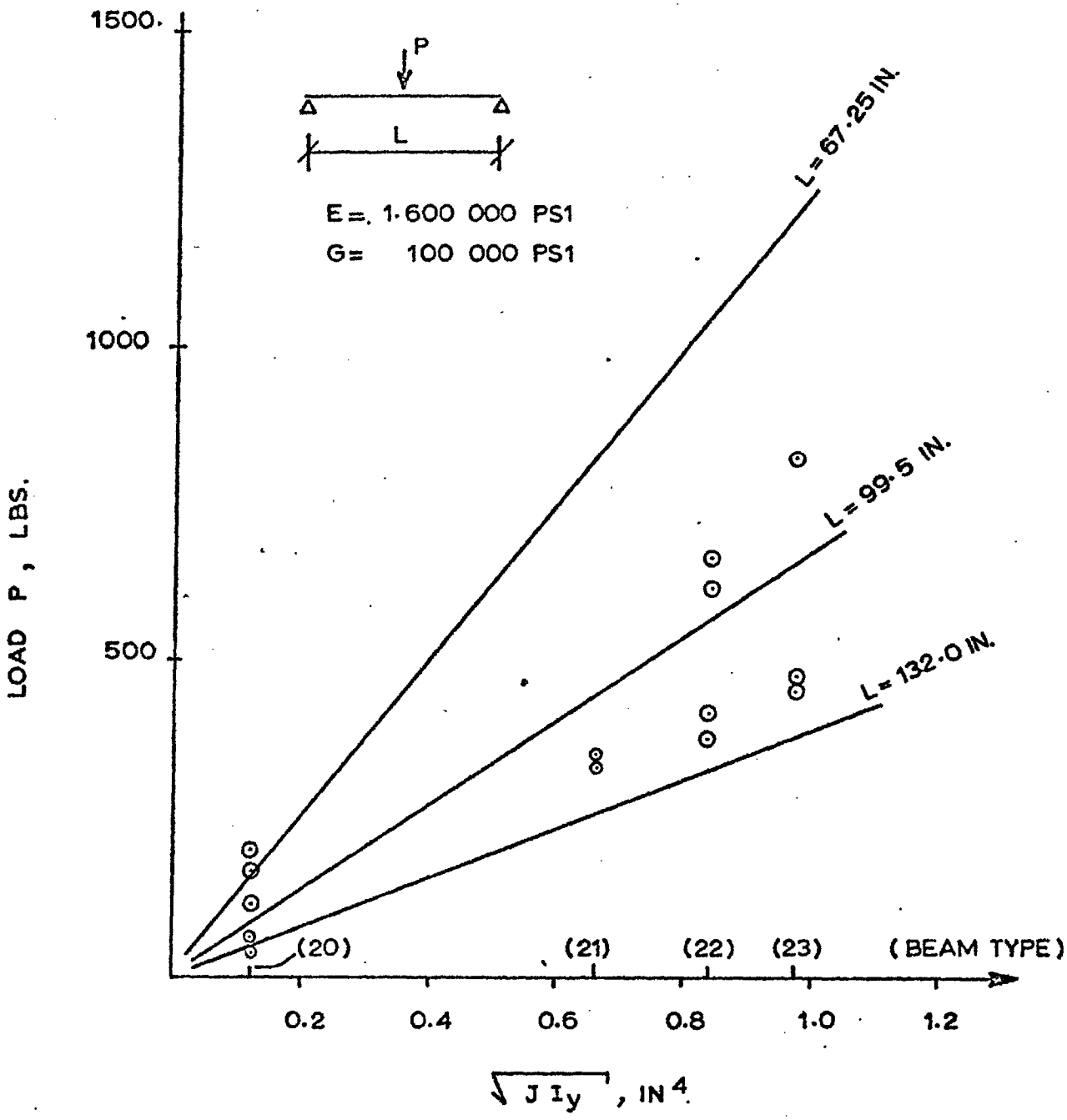


FIG. 6·7 CRITICAL LOADS AS FUNCTION OF SECTION PROPERTIES J AND $I_y$.

nine tests in Series 4. According to Kollbrunner (26) the critical load, $P_e$, for lateral stability in the case of a vertical eccentricity of $\pm$ h/2 can be calculated from

$$P_e = P\left[\sqrt{(1 + 3.24\,(EI_y/GJ)(h/2L)^2} \mp 1.8(h/2L)\sqrt{EI_y/GJ}\right] \qquad (6.3)$$

where P = critical load, load applied at centroid of cross-section

h = beam height.

For the beams of Type 22 and a 132 inch span Equation (6.3) gives an increase in the critical load of about nine per cent, when the load is applied at the lower edge of the beam. Similarly, when the load is placed on the upper edge, the critical load will be decreased by nine per cent. The corresponding experimental results are given in Table 6.6.

Table 6.6

Effect of Vertical Eccentricities on Critical Experimental Loads

Test Series 4

| Location of Load | Critical Experimental Loads, lbs. Beam Number 1 | 2 | 3 |
|---|---|---|---|
| Top edge | - | 344 | 426 |
| Centroid | 375 | - | 447 |
| Bottom edge | 439 | - | 481 |

Only tests with beams No. 1 and 3 resulted in usable information. However these results do confirm, generally speaking, the theoretical prediction. Locating the load on the top edge resulted in a five per cent decrease in the critical load of beam No. 3. When the load was placed a distance h/2 below the centroid of the cross-section the critical load of beam No.1 increased by sixteen per cent and that of beam No. 3 by eight per cent.

The results from the last two test series, given in Table C-8, show quite an erratic behaviour. An inclination of the ~~major~~ minor axis of the beam of 1, 2 or 3 degrees to the vertical, Series 5, does not give rise to a discernible pattern in the critical experimental loads. For the tests on the effects of lateral eccentricities only beam No. 3 gave a usable Southwell plot for both eccentricities. But the critical experimental loads obtained from the Southwell plot appear to be meaningless.

Great care had been taken in the loading of these beams and an attempt had been made to carry the loading as close as possible to a state of instability. Indeed, in a few cases, the loads placed on a beam were so large that the centre section continued to rotate and deflect sideways without any further increase in loads. When this happened, the beam had to be physically restrained from collapsing and loads had to be taken off quickly to obtain again a state of stability.

The loads shown in the column labelled P-Max in Table C-8,

which are the actual maximum loads placed on the beam, are therefore much more representative of the actual critical loads for instability than the loads obtained by means of the Southwell plot. The only conclusion that can be stated therefore is, that the Southwell plot, as used in this investigation, cannot be used for the calculation of critical loads in the case of large initial lateral eccentricities or initial rotations.

The modulus of rupture of each beam, obtained from a final bending test after completion of test Series 1 to 6, is given in Table 6.7. The modulus of rupture, $\sigma_r$, was calculated from

$$\sigma_r = M_r/S_x \qquad (6.4)$$

where $M_r$ = moment causing failure of beam

$S_x$ = section modulus of gross-section of beam

The gross-section of the beam here is equal to the actual beam cross-section given by the dimensions in Table 6.1. No allowance is made for any possible change in the cross-sectional properties at a joint in the plywood web. The failure of most of these beams occurred in a manner similar to that observed by the author in an earlier study of the strength of plywood box-beams (41). Most of the beams displayed a linear load-deflection behaviour almost up to their maximum load carrying capacity. Except for those of Type 22, beams usually failed suddenly and ruptured completely on the tension side. Failure usually occurred in the tension flange near a butt-joint in the plywood. It is

Table 6.7

Modulus of Rupture

of Plywood Box Beams

| Beam No. | Modulus of Rupture, psi | | | |
|---|---|---|---|---|
| | Beam Type | | | |
| | 20 | 21 | 22 | 23 |
| 1 | 2350 | 6040 | 5070 | 5470 |
| 2 | 4920 | 7900 | 7490 | 8810 |
| 3 | 5430 | 9910 | 7110 | 6880 |

self-evident that such butt-joints represent a point of stress concentration, since stresses cannot be transferred continuously from one web to the next at such a location. Beams of Type 22 yielded considerably on the compression side, before finally failing in tension. Average modulus of rupture of beams of Type 21, 22 and 23 was 7 190 psi.

Beams of Type 20 failed by lateral buckling, even though they were restrained from moving laterally at the points of load application. Failure usually occurred in the glue line between the web and the flange after large lateral deformations had taken place. The low load carrying capacity of beam No. 20-1 may have been the result of earlier damage sustained during the last test in Series 3.

The strength of all box-beams was well above the stresses induced by the loads required to produce lateral instability. It

may be concluded therefore that for plywood box beams, just as for any other beams, consideration of the resistance to lateral instability should form an important part in the analysis of their load carrying capacity.

Shear Stress Distribution in Plywood Box Sections. A theoretical expression for the shear stresses in box sections subjected to torsion has been derived in Chapter 4, Equation (4.50). The resulting shear stress distribution for a typical box section (h = 6.75 inch., $b_1$ = 2.187 inch., d= 1.687 inch., t = 0.25 inch.) has been evaluated and is shown in Figs. 6.8 and 6.9. It is apparent that the shear stress distribution in the flanges is far from being uniform. From a negative value at the outside of the flange, the shear stresses along the centre line of the cross-section diminish almost linearly until they become zero. Shear stresses in the opposite direction are then being built up until a second maximum stress is reached at the inside of the flange. It appears, that in addition to the shear flow around the outside of the box section, a secondary shear flow, producing an additional couple resisting torsion, is being set up in a deep flange.

The presence of these secondary shear flows was first pointed out to the author by Bannister*(private communication), who recently found a reversal of shear stresses such as shown in Fig. 6.8, while measuring shear strain distributions in plywood box-beams. To confirm the caluclated stress pattern and the findings of Bannister, strains were investigated on

---

*A. Bannister, Department of Civil Engineering, University of Salford, Salford 5, Lancashire.

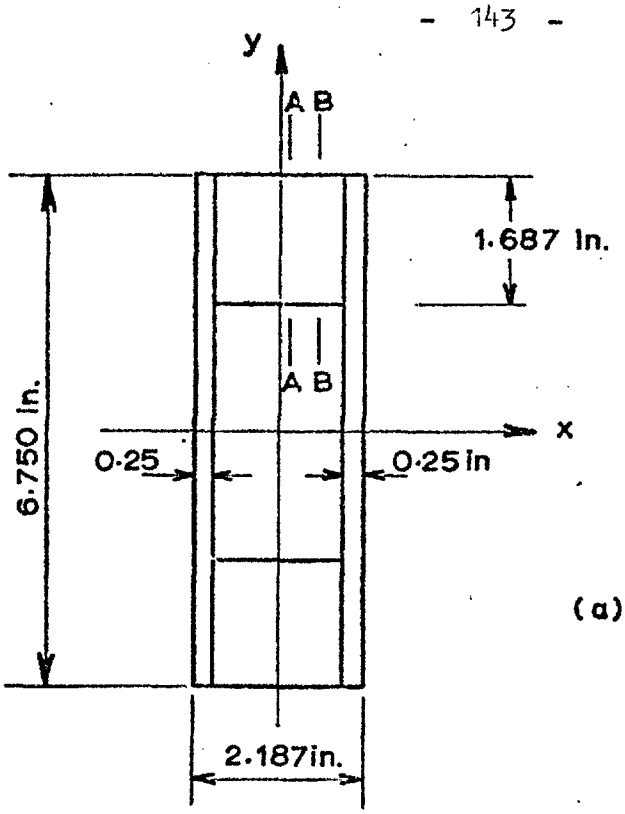


(a) CROSS SECTION OF PLYWOOD BOX BEAM

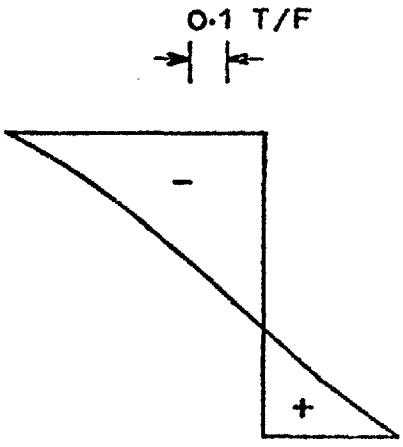


(b) SHEAR STRESSES AT A – A.

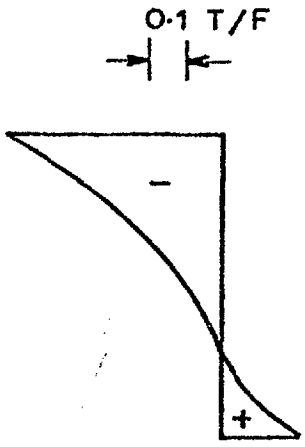


(c) SHEAR STRESSES AT B – B.

T = APPLIED TORSION

F = TORSION FACTOR

FIG. 6.8 DISTRIBUTION OF $\tau_{zx}$ SHEAR STRESSES IN FLANGE OF BOX BEAM.

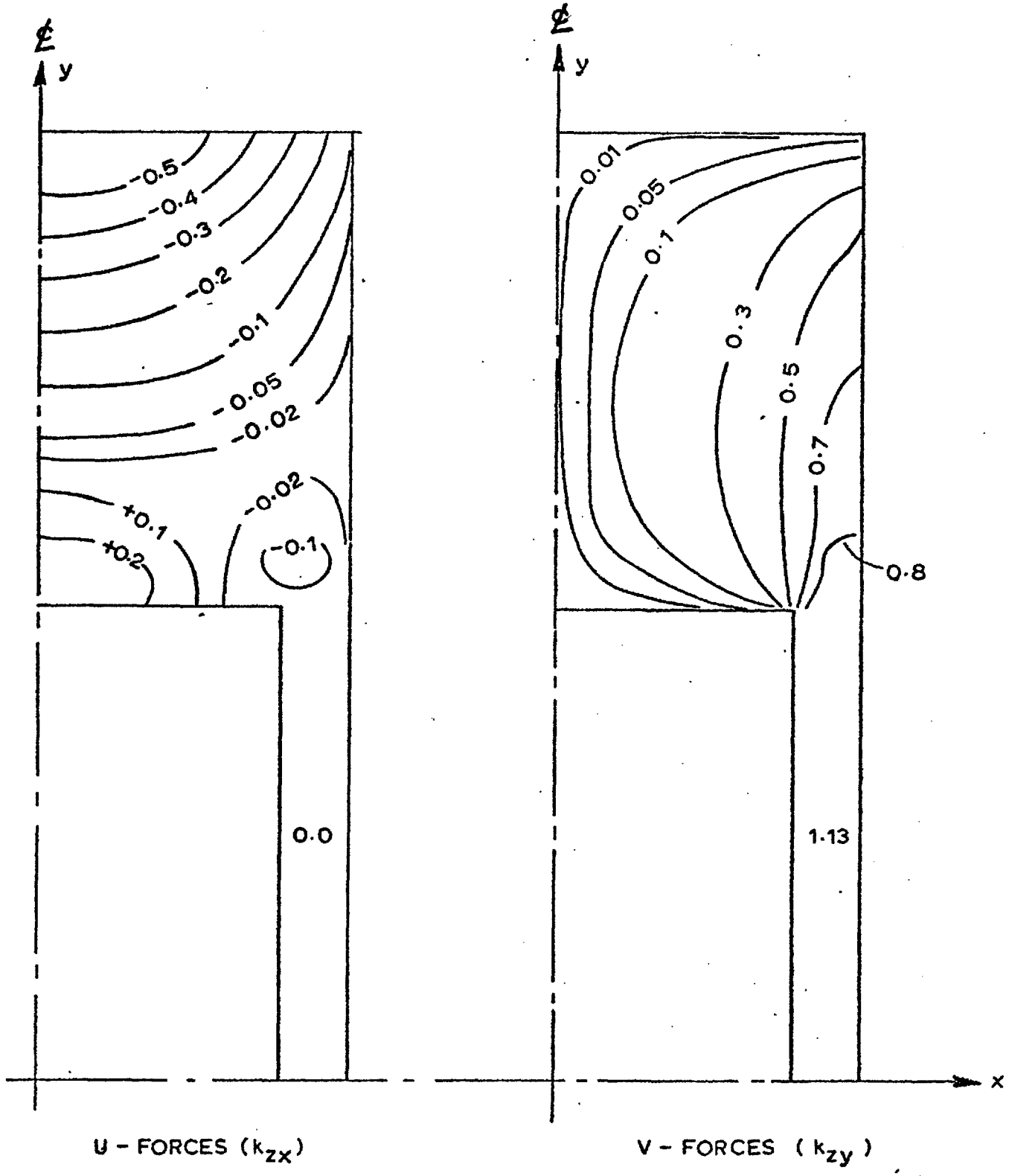


FIG. 6.9 LINES OF EQUAL INTENSITY FOR SHEAR STRESS COEFFICIENTS $k_{zx}$ & $k_{zy}$

the inside and the outside of the flanges of a 2-3/16 inch. by 6-3/4 inch. plywood box-beam. The flanges of this box-beam were Douglas fir, 1.69 inch. deep and the web consisted of 0.25 inch. birch plywood of five-ply construction, Fig. 6.8(a). The outer grain of the plywood was oriented perpendicular to the span. Flange and web were glued together with a resin type glue.

Prior to assembling web and flanges, electric resistance wire strain gauge rosettes were placed on two opposite sides of the two pieces of Douglas fir, which later were to form the flanges. Each rosette consisted of three gauges. Of these, one was oriented in the longitudinal direction of the wood, and two crossed the grain direction at +45 and -45 degrees respectively. Strain gauge rosettes were placed at two locations along the length of the beam a distance of twelve inch. apart. All gauges at one location were 5 mm, at the second location 10 mm long. Total number of strain gauge rosettes was eight.

Before assembling the box-beam the two flanges were tested individually in torsion. The 1.69 x 1.69 inch. flanges were clamped at one end and freely supported at the other end where a moment arm was attached. Distance between the clamped and the freely supported end was 48 inch. The strain gauges were located approximately 18 inches from the nearest support. At the end where the moment arm was attached, the flange was simply supported but free to rotate about its own axis, so that it could rotate without being subjected to bending. Torsion was applied

by placing weights at the end of the 12 inch moment arm attached to the flange. Load was increased in steps of two pounds from zero to a maximum of 14 lbs.

Each test was repeated once. A regression analysis of the resulting load-strain distribution for each gauge is given in Table C-9(a). The rotation of the two strain-gauged sections, a distance of 12 inch. apart, was also measured.

After testing the flanges individually, flanges and web were glued together to form the box-section, Test Series 2, with a moment arm of 24 inch. Load increments of five pounds were used up to a maximum load of 35 lbs. For the complete box-beam, distance between lateral supports was increased to six feet to avoid possible interference of support conditions with the strain distribution. Regression analyses of the resulting load-strain distributions are given in Table C-9(b). Again two tests were performed.

The regression analysis represents a plot of strains, e, against loads, P, where the strains are treated as the dependent variable. The slope, B, of the regression line $e = A + B P$ is equal to the strain, in micro-inches per inch, per pound of load for each gauge. This regression line is a least squares estimate of the unknown true line, i.e. the sum of squares of vertical deviations of observed points from the regression line is minimised (12). The regression lines are given in Table C-9 in Appendix C. The correlation coefficient R for all load

strain curves is 1.0 or nearly 1.0, indicating a good fit of the observed strains with the calculated straight line.

Gauge No. 2 for each location measured the strain in the longitudinal direction. While, theoretically, the strain in this direction should be zero, possible misalignment of gauges as well as grain deviations actually resulted in some strain in this direction. However these strains are small and the assumption of zero forces in the longitudinal direction, which is being made in the derivation of the torsion constant, is therefore justified.

Gauges 1 and 3 were placed symmetrically on either side of the centre line of the beam. It would be expected, therefore, that the strains for these directions, apart from a sign, are equal. The results again confirm the assumption, the small differences being attributable to experimental error. Locations 1 and 2 on each flange were opposite each other and were instrumented with 5 mm long gauges. Similarly locations 3 and 4 formed a pair, but were equipped with 10 mm long gauges. The results for these two different gauge lengths do not appear to differ greatly.

The strain readings for Test Series 2 follow a similar pattern. The correlation between load and strain for the individual gauges is good and the strain readings follow the pattern that is expected from the condition of symmetry.

Table 6.8

Flange Shear Strain Distribution

Torsion Specimens

| | | Shear Strains, microinches/inch | |
|---|---|---|---|
| | | Individual Flanges | Box Section |
| | Applied Torsion: | 24 in-lb | 840 in-lb |
| Flange | Face | | |
| 1 | 1 | -210 | -805 |
| | 2 | +112 | +385 |
| 2 | 1 | -204 | -350 |
| | 2 | +238 | +805 |

Shear strains, v, at each location were then calculated as the difference between the measured strains $e_1$ and $e_3$ in the 1 and 3 directions.

$$v = e_1 - e_3 \qquad (6.5)$$

The shear strain v here is defined as the angular change between the longitudinal and the perpendicular direction across the width of the beam. The results of these calculations are given in Tables C-10(a) and C-10(b) and are summarized in Table 6.8. for an applied load of 24 in-lb.

To obtain the corresponding shear stress distribution a modulus of rigidity, G, can be calculated from the observed relative rotation $\theta$ between two sections. For the two individual flanges

Test Series 1, the relative rotations of two sections 12 inches apart due to a load of 14 lbs. was 0.95 degrees and 1.05 degrees respectively. For a square section of size a x a the torsion constant J equals $0.1406\ a^4$ (18). The modulus of rigidity can therefore be estimated from

$$G = \frac{T\,L}{J\,\theta} \qquad (6.6)$$

The resulting moduli of rigidity for the two individual Douglas fir flanges are G = 105 000 psi and G = 95 000 psi. It should be noted that this modulus of rigidity represents only a mean of the two moduli for the longitudinal-tangential and the longitudinal-radial directions of the wood. However for softwoods these two values usually do not differ greatly (1, 25) and it is sufficient therefore to use this mean modulus of rigidity for the calculation of shear stresses. Keylwerth (25) quotes a value of $G_{LR}$ for Douglas fir at approximately 12 per cent moisture content of 9 000 $kg/cm^2$ (128 000 psi), which is reasonably close to the value found above.

Using an average value of G = 100 000 psi, the average shear stress at the middle of one side of an individual flange, calculated from the observed strains, will therefore be equal to 21.0 psi. This shear stress can be compared with a theoretical value due to an applied torque T

$$v = \frac{T}{k_2\ a^3} \qquad (6.7)$$

where for a square section $k_2$ is given by Goodier (18) as 0.208.

The resulting shear stress for a torque of 24.0 in.-lb is $v = 23.8$ psi, indicating close agreement between the theoretical and the observed shear stresses.

The mean modulus of rigidity found from the relative rotation of the individual flanges can now be used to calculate the expected relative rotation of the box section. To calculate the torsion factor F and the shear stress coefficient $k_2$ half the top flange was divided into eight rows and five columns, giving a total of forty elements in one half of the flange. Using Equation (4.43) the torsion factor for an isotropic section was calculated as $F = 0.18$. The relative twist for a torque of 840 in.-lb will therefore be

$$\Theta = \frac{840 \times 57.30 \times 12}{100\,000 \times 0.18 \times 2.19^3 \times 6.75} = 0.45 \text{ degrees}$$

The difference between the observed rotations at sections 1 and 2 of the box-beam is $\Theta = 2.05 - 1.6 = 0.45$ degrees, identical to the calculated twist. If, on the other hand, Equation (4.4) is used for the determination of the torsion constant, the resulting value of J is 9.1 $in^4$ and consequently the relative twist would be overestimated by about 40 per cent.

The average shear stresses at the outside and the inside of the flanges of the box-section can be calculated from the shear strains given in Table 6.7. Using again the average modulus of rigidity obtained from the tests of the individual flanges, the experimental shear stresses become $v = -81$ psi at the outside

and v = +37 psi at the inside of the flange. Using Equation (4.48) the shear stress coefficient $k_2$ for the centre element of the outside row of the flange was calculated as 0.593/0.18 = 3.29 and the expected shear stress for a torque of 840 in.-lb therefore is

$$v = \frac{3.29 \times 840}{2.19^2 \times 6.75} = 85 \text{ psi}$$

Similarly, for the inside of the flange, $k_2$ = 1.61 and the expected shear stress is 42 psi. Both locations, the inside as well as the outside of the flange in the box beam investigated therefore show good agreement between the experimental and the theoretical shear strain distribution. These shear stresses may also be compared with Bredt's first formula (18)

$$v = \frac{T}{2 A t} \qquad (6.8)$$

where A = area enclosed by the middle curve of the cross-section(Fig.4.2).

t = wall thickness

Admittedly Equation (6.8) should only be used for box-sections with thin walls and it is therefore not surprising that Bredt's formula, when used for the above cross-section, does give a completely erroneous result of v = 12.6 psi.

While this experimental investigation of the torsional shear stress distribution and rigidity for box sections only formed a minor part of the current investigation, the results suggest that the torsion constants calculated by means of the finite

element theory outlined in Chapter 4 do give a good estimate of the torsional rigidity of such sections. Similarly, from the limited experimental evidence available, it appears that the shear stress coefficients derived in Chapter 4 will give a good estimate of the shear stresses in box-sections having deep flanges.

Summary

An application of the finite element method of analysis to the investigation of the lateral stability of beams and arches is presented in this thesis. Particular attention was given to the analysis of plywood box-beams, a form of composite construction particularly suitable for the combination of plywood and lumber. An experimental investigation of the lateral stability of plywood box-beams is also described. As a result of this investigation the following points can be summarized.

1. Using the finite element method of analysis a general expression for the lateral stability of beams and arches, Equation (2.52), has been developed.

2. The expression for the lateral stability of beams, Equation (2.58), is a special case of the more general expression derived for arches. The finite element analysis, when applied to beams, will result in the same critical loads as those calculated by the classical theory of elastic stability.

3. A general expression for the calculation of the torsion constant J for box-sections, Equation (4.44), also has been derived by means of a finite element approach. Torsion factors for a number of cross-sections have been calculated and are given in Appendix B.

4. The analysis of the torsional rigidity of box-sections, given in Chapter 4, indicates that in box-sections with deep flanges shear stresses due to torsion are not distributed uniformly across the depth of the flange. On the contrary, shear stresses on the outside of the flange will be oriented in a direction opposite to that on the inside of the same flange. An assumption of uniform shear stress for box-beams with deep flanges will result in an erroneous value of the torsional rigidity of such a section.

5. The non-uniform distribution of shear stresses in box-beams with deep flanges indicated by the finite element analysis was confirmed by an experimental investigation.

6. An experimental investigation of the lateral stability of plywood box-beams confirmed the validity of the classical analysis and the finite element analysis. These tests indicated in particular the importance of an accurate knowledge of the lateral bending stiffness and torsional rigidity of plywood box-beams for the calculation of critical loads. The tests confirmed the changes in the critical load predicted by the classical theory, which will result if the point of load application is moved in a vertical direction.

7. When a single concentrated force was applied eccentrically relative to the major plane of bending or when the ends of the beams were rotated relative to a vertical plane, a Southwell plot of the corresponding experimental test

results did not give a reasonable estimate of the critical loads. The effect of initial eccentricities should therefore receive some further attention.

8. Coefficients for the lateral stability of two-hinged parabolic arches have been calculated and are given in Appendix A. Experimental verification of these constants has not yet been sought. An experimental study of the lateral stability of arches in the immediate future will therefore be of considerable interest.

## References


1. Anonymous. Wood Handbook. U. S. Forest Products Laboratory, Handbook 72. Washington, 1955.

2. Argyris, J. H. and S. Kelsey. Energy theorems and structural analysis. Butterworths, London, 1960.

3. Argyris, J. H., S. Kelsey and H. Kamel. Matrix methods of structural analysis. AGARograph 72, Edited by B. F. de Veubeke. Pergamon Press, London, 1964.

4. Argyris, J. H. Continua and Discontinua. Paper presented at Conference on Matrix Structural Analysis, Wright-Patterson Air Force Base, Ohio. 1965.

5. Bell, L. A. Lateral stability of rectangular beams. M.Sc. Thesis. University of British Columbia, Vancouver. 1966.

6. Bleich, F. Buckling strength of metal structures. McGraw Hill, New York. 1952.

7. Booth, L. G. and P. O. Reece. The structural use of timber. A commentary on the British Standard Code of Practice CP.112. E. and F. N. Spon, London. 1967.

8. Byrne, J. G. Torsion of hollow beams. Ph. D. Thesis, University of Dublin, Trinity College. 1960.

9. British Standards Institution. The structural use of timber, CP.112. London. 1967.

10. Canadian Standards Association. Engineering design in timber, CSA-C86. Ottawa. 1959.

11. Collatz, L. Eigenvalue problems. Chapter 18 in reference 17.

12. Crow, E. L. et al. Statistics Manual. Dover Publications, New York. 1960.

13. Deutscher Normenausschuss. Holzbauwerke, DIN 1952. Beuth Vertrieb, Berlin. 1965.

14. Doyle, D. V. and L. J. Markwardt. Tension parallel-to-grain properties of Southern pine dimension lumber. U.S. Forest Service, Research Paper No. FPL 84. Madison. 1967.

15. Faddeeva, V. N. Computational methods of linear algebra. Dover Publication, New York. 1959.

16. Flint, A. R. The lateral stability of unrestrained beams. Engineering No. 173, 25th Jan. 1952.

17. Flügge, W. Editor. Handbook of Engineering Mechanics. McGraw-Hill, London, 1962.

18. Goodier, J. N. Torsion. Chapter 36 in reference 17.

19. Gallagher, R. H. and J. Padlog. Discrete element approach to structural instability analysis. American Inst. Aeronautics and Astronautics, J. v. 1, No. 6. p. 1437 - 39.

20. Graf, U. and H.-J. Henning. Formeln und Tabellen der mathematischen Statistik. Springer Verlag, Berlin. 1958.

21. Halasz, R. V. and E. Cziesielski. Berechnung und Konstruktion geleimter Träger mit Stegen aus Furnierplatten. In "Berichte aus der Holzforschung", No. 47. Ernst und Sohn, Berlin. 1966.

22. Hooley, R. F. and B. Madsen. Lateral stability of glued laminated beams. ASCE, Proc. V. 90, No. ST3 (J. Struct. Div.), p. 201 - 218. June, 1964.

23. Karman, Th. v. and M. A. Biot. Mathematical methods in engineering. McGraw-Hill, London. 1940.

24. Kennedy, E. I. Strength and related properties of woods grown in Canada. Dept. of Forestry (Canada). Publication No. 1104. Ottawa. 1965.

25. Keylwerth, R. Die anisotrope Elastizität des Holzes und der Lagenhölzer. VDI - Forschungsheft 430. Deutscher Ingenieur Verlag, Düsseldorf. 1951.

26. Kollbrunner, C. F. and M. Meister. Knicken, Biegedrillknicken, Kippen. Springer Verlag. Berlin. 1961.

27. Kollmann, F. Technologie des Holzes und der Holzwerkstoffe. 2nd Ed. Vol. 1. Springer Verlag, Berlin. 1951.

28. Libove, C. Elastic stability. Chapter 44 in reference 17.

29. Littleford, T. W. Mechanical stress-rating of Western Canadian species. Proc. Second Symposium on the Nondestructive Testing of Wood. Spokane, Washington, 1965.

30. Massey, C. Elastic and inelastic lateral instability of I-beams. The Engineer, vol. 216, p. 672 - 674, Oct. 1963.

31. Massey, C. Southwell plot applied to lateral instability of beams. The Engineer, vol. 218, p. 320. 28th August, 1964.

32. Michell, A. G. M. Elastic stability of long beams under transverse forces. Phil. Mag. vol. 48. p. 298. 1899.

33. Nemeth, L. J. Correlation between tensile strength and modulus of elasticity for dimension lumber. Proc. Second Symposium on the Nondestructive Testing of Wood. Spokane, Washington. 1965.

34. Niskanen, E. On the strength and elasticity characteristics of Finnish structural birch plywood. State Inst. for Technical Research, Finland. Publication No. 81. Helsinki. 1963.

35. Prandtl, L. Kipperscheinungen. Ein Fall von instabilem elastischem Gleichgewicht. München. 1899.

36. Stüssi, F. Die Stabilität des auf Biegung beanspruchten Trägers. Int. Assoc. Bridge and Struct. Engineering. Vol. 3, p. 401. Zürich. 1935.

37. Stüssi, F. Exzentrisches Kippen. Schweizerische Bauzeitung. Vol. 105, No. 11, p. 123 - 125. March, 1935.

38. Stüssi, F. Kippen und Querschwingungen von Bogenträgern. Int. Assoc. Bridge and Struct. Engineering. Vol. 7, p. 237. Zürich. 1943/44.

39. Stieda, C. K. A. A shear stiffness factor for plywood box beams. Information Report No. VP-X-31. Forest Products Laboratory, Vancouver. 1967.

40. Stieda, C. K. A. Stress concentrations around holes and notches and their effect on the strength of wood beams. J. of Materials, Vol. 1, No. 3. American Soc. for Testing and Materials. Sept. 1966.

41. Stieda, C. K. A. Strength of plywood box beams. CWPI/Wood Industries. July, 1967.

42. Timoshenko, S. History of strength of materials. McGraw-Hill, London. 1953.

43. Timoshenko, S. and J. M. Gere. Theory of elastic stability. 2nd Ed. McGraw-Hill, London, 1961.

44. Timoshenko, S. and J. N. Goodier. Theory of elasticity. 2nd Ed. McGraw-Hill, London. 1951.

45. Trayer, G. W. and H. W. March. The torsion of members having section in common in aircraft construction. Technical Report No. 334 in 15. Annual Report of (U.S.A.) Nat. Advis. Com. Aeronautics. 1929.

46. Wilson, T. R. C. Torsion tests of box beams. (U.S.A.) Forest Prod. Lab. Report. Madison. 1923.

47. Zahn, J. J. Lateral stability of deep beams with shear beam support. U. S. Forest Service, Research Paper No. FPL 43. 1965.

## Basic Notation

Symbols are defined in the text, where they first appear. A list of basic symbols and their meaning is given below.

| | | |
|---|---|---|
| a | = | initial bow, also width of torsion element |
| A | = | area |
| b | = | subscript indicating bending, also height of torsion element |
| $b_1$ | = | width of cross-section |
| **b** , $\mathbf{b}_0$ | = | transformation matrices |
| **B** | = | force-displacement transformation matrix |
| d | = | depth of flange of I- or box-section |
| e, $\varepsilon$ | = | strain |
| E | = | modulus of elasticity |
| **f** | = | flexibility matrix |
| G | = | modulus of rigidity |
| h | = | rise of arch, also height of cross-section |
| I | = | second moment of area |
| J | = | torsion constant |
| **I** | = | unit matrix |
| **k** | = | element stiffness matrix |
| **K** | = | stiffness of total structure or component |
| $\ell$ | = | length of beam element |
| l, m, n | = | direction cosines |
| L | = | span |
| M | = | bending moment |
| n | = | number of elements |
| N | = | axial force |

| | | |
|---|---|---|
| $\mathbf{0}$ | = | zero matrix |
| $P$ | = | single concentrated force |
| $\mathbf{P}$ | = | vector of element forces |
| $\mathbf{r}$ | = | vector of nodal point displacements relative to global system of co-ordinates |
| $\mathbf{R}$ | = | vector of external forces |
| $S$ | = | section modulus |
| $\mathbf{S}$ | = | vector of element forces |
| $t$ | = | subscript indicating torsion, also web-thickness |
| $\mathbf{T}$ | = | vector of torsion moments |
| $u, v, w$ | = | displacements in x-, y- or z-direction |
| $U, V, W$ | = | forces in x-, y- or z-direction |
| $\mathbf{U}, \mathbf{V}, \mathbf{W}$ | = | vectors of forces in x-, y- or z-direction |
| $\mathbf{v}$ | = | vector of element displacements, i.e. nodal point displacements relative to local system of co-ordinates |
| $\mathbf{X}$ | = | vector of redundancies |
| $x, y, z$ | = | orthogonal system of co-ordinates (global system) |
| $\phi$ | = | rotation |
| $\Theta$ | = | twist |
| $\xi, \eta, \zeta$ | = | local orthogonal system of axes |

# Appendix A

## Lateral Stability Coefficients $C_2$ for Two-Hinged Parabolic Arches Loaded at the Crown by a Single Concentrated Force

LATERAL STABILITY OF TWO-HINGED ARCH

RECTANGULAR SECTIONS

CONCENTRATED FORCE AT CENTRE OF SPAN

CRITICAL LOAD, P-CR=C2*EI(ETA)/L**2

| H/L | D/L | REACTIONS MOMENTS M(A)/P | REACTIONS MOMENTS M(C)/P | HOR. THRUST W(A)/P | BUCKLING COEFFICIENTS, C2 EI(ETA)/GJ 0.715 | 4.000 | 6.000 |
|---|---|---|---|---|---|---|---|
| 0.10 | 1/10 | 0. | 0.008 | 2.419 | 2.026 | 1.734 | 1.594 |
| | 1/20 | 0. | 0.006 | 2.438 | 2.010 | 1.721 | 1.582 |
| 0.20 | 1/10 | 0. | 0.013 | 1.187 | 3.988 | 2.503 | 2.042 |
| | 1/20 | 0. | 0.011 | 1.193 | 3.969 | 2.493 | 2.033 |
| 0.30 | 1/10 | 0. | 0.018 | 0.773 | 5.722 | 2.708 | 2.050 |
| | 1/20 | 0. | 0.017 | 0.776 | 5.703 | 2.700 | 2.045 |
| 0.40 | 1/10 | 0. | 0.024 | 0.565 | 7.024 | 2.721 | 1.980 |
| | 1/20 | 0. | 0.023 | 0.566 | 7.007 | 2.715 | 1.976 |

# Appendix B

## Torsion Constants

## for

## Box and I- Sections

The torsion factor F is given as a function of the ratios $d/b_1$, $t/b_1$ and $h/b_1$, where

d = depth of flanges

t = thickness of one web

$b_1$ = width of section

h = height of section

Torsion constant: $J = F\, b_1^3\, h$

Table B-1

Torsion Factor F for Box Sections

Isotropic Material

$t/b_1 = 0.01$

| $d/b_1$ | Height - to - Width Ratio, $h/b_1$ | | | | | | | |
|---|---|---|---|---|---|---|---|---|
| | 0.4 | 1.0 | 2.0 | 3.0 | 4.0 | 6.0 | 8.0 | 10.0 |
| 0.2 | 0.041 | | 0.023 | 0.022 | 0.021 | 0.021 | 0.021 | 0.020 |
| 0.5 | | 0.142 | 0.047 | 0.038 | 0.033 | 0.029 | 0.026 | 0.025 |
| 1.0 | | | 0.229 | 0.109 | 0.087 | 0.064 | 0.053 | 0.047 |
| 1.5 | | | | 0.263 | 0.159 | 0.113 | 0.090 | 0.076 |
| 2.0 | | | | | 0.279 | 0.165 | 0.129 | 0.108 |
| 3.0 | | | | | | 0.295 | 0.205 | 0.169 |
| 4.0 | | | | | | | 0.306 | 0.232 |

Table B-2

Torsion Factor F for Box Sections

Isotropic Material

$t/b_1 = 0.05$

| $d/b_1$ | Height - to - Width Ratio, $h/b_1$ | | | | | | | |
|---|---|---|---|---|---|---|---|---|
| | 0.4 | 1.0 | 2.0 | 3.0 | 4.0 | 6.0 | 8.0 | 10.0 |
| 0.2 | 0.0402 | 0.066 | 0.078 | | 0.088 | 0.089 | 0.089 | 0.090 |
| 0.5 | | 0.142 | 0.102 | 0.098 | 0.096 | 0.095 | 0.094 | 0.093 |
| 1.0 | | | 0.229 | 0.155 | 0.138 | 0.121 | 0.118 | 0.113 |
| 1.5 | | | | 0.263 | 0.196 | 0.160 | 0.142 | |
| 2.0 | | | | | 0.279 | 0.202 | 0.175 | 0.158 |
| 3.0 | | | | | | 0.295 | 0.232 | 0.205 |

Table B-3

Torsion Factor F for Box Sections

Isotropic Material

$t/b_1 = 0.10$

| $d/b_1$ | Height - to - Width Ratio, $h/b_1$ | | | | | | | |
|---|---|---|---|---|---|---|---|---|
| | 0.4 | 1.0 | 2.0 | 3.0 | 4.0 | 6.0 | 8.0 | 10.0 |
| 0.2 | 0.0402 | 0.096 | 0.127 | 0.138 | 0.145 | 0.151 | 0.154 | |
| 0.5 | | 0.142 | 0.150 | 0.154 | 0.157 | 0.159 | 0.161 | 0.161 |
| 1.0 | | | 0.229 | 0.194 | 0.186 | 0.179 | 0.175 | 0.173 |
| 1.5 | | | | 0.263 | 0.228 | 0.206 | 0.195 | 0.189 |
| 2.0 | | | | | 0.279 | 0.237 | 0.219 | 0.208 |
| 3.0 | | | | | | 0.295 | 0.259 | 0.241 |
| 4.0 | | | | | | | 0.306 | 0.291 |

Table B-4

Torsion Factor F for Box Sections

Isotropic Material

$t/b_1 = 0.15$

| $d/b_1$ | Height - to - Width Ratio, $h/b_1$ | | | | | | | |
|---|---|---|---|---|---|---|---|---|
| | 0.4 | 1.0 | 2.0 | 3.0 | 4.0 | 6.0 | 8.0 | 10.0 |
| 0.2 | 0.0413 | 0.112 | 0.159 | 0.177 | 0.187 | 0.198 | 0.203 | |
| 0.5 | | 0.142 | 0.183 | 0.195 | 0.202 | 0.208 | 0.211 | 0.213 |
| 1.0 | | | 0.229 | 0.221 | 0.221 | 0.221 | 0.221 | 0.221 |
| 1.5 | | | | 0.263 | 0.248 | 0.238 | 0.234 | |
| 2.0 | | | | | 0.279 | 0.257 | 0.248 | 0.243 |
| 3.0 | | | | | | 0.295 | 0.277 | 0.265 |

Table B-5

Torsion Factor F for Box Sections

of Orthotropic Material

$t/b_1 = 0.1$

$d/b_1 = 0.5$

| $G_{zx}/G_{yz}$ | Height - to - Width Ratio, $h/b_1$ | | | |
|---|---|---|---|---|
| | 1.0 | 2.0 | 5.0 | 10.0 |
| 0.6 | 0.107 | 0.133 | 0.153 | 0.160 |
| 0.8 | 0.126 | 0.142 | 0.158 | 0.164 |
| 1.0 | 0.142 | 0.150 | 0.162 | 0.166 |
| 1.2 | 0.155 | 0.156 | 0.166 | 0.169 |

Table B-6

Torsion Factor F for Box Sections

of Orthotropic Material

$t/b_1 = 0.1$

$d/b_1 = 2.0$

| $G_{zx}/G_{yz}$ | Height - to - Width Ratio, $h/b_1$ | | |
|---|---|---|---|
| | 4.0 | 6.0 | 10.0 |
| 0.6 | 0.264 | 0.219 | 0.198 |
| 0.8 | 0.273 | 0.226 | 0.201 |
| 1.0 | 0.280 | 0.232 | 0.205 |
| 1.2 | 0.285 | 0.236 | 0.208 |

Table B-7

Torsion Factor F for Box Sections with Different Moduli of Rigidity for Web and Flanges

Isotropic Material

$d/b_1 = 0.5$

$t/b_1 = 0.1$

| G(web)/G(flange) | Height - to - Width Ratio, $h/b_1$ | | | | | |
|---|---|---|---|---|---|---|
| | 1.0 | 2.0 | 3.0 | 4.0 | 6.0 | 10.0 |
| 0.6 | 0.124 | 0.102 | | 0.100 | 0.099 | 0.099 |
| 0.8 | 0.133 | 0.127 | 0.128 | 0.129 | 0.130 | 0.130 |
| 0.9 | 0.138 | 0.138 | 0.141 | 0.143 | 0.145 | 0.146 |
| 1.0 | 0.142 | 0.150 | 0.154 | 0.157 | 0.159 | 0.161 |
| 1.1 | 0.146 | 0.161 | 0.167 | 0.171 | 0.174 | 0.177 |
| 1.2 | 0.150 | 0.172 | | 0.184 | 0.188 | 0.191 |
| 1.4 | 0.157 | 0.193 | | 0.211 | 0.217 | 0.222 |

Table B-8

Torsion Factor F for Box Sections with Different Moduli of Rigidity for Web and Flanges

Isotropic Material

$d/b_1 = 2.0$

$t/b_1 = 0.1$

| G(web)/G(flange) | Height - to - Width Ratio, $h/b_1$ | | |
|---|---|---|---|
| | 4.0 | 6.0 | 10.0 |
| 0.6 | 0.227 | 0.174 | 0.144 |
| 0.8 | 0.254 | 0.203 | 0.174 |
| 1.0 | 0.280 | 0.232 | 0.205 |
| 1.2 | 0.305 | 0.261 | 0.235 |
| 1.4 | 0.330 | 0.289 | 0.265 |

Table B-9

## Torsion Factor F for Box Sections with Different Moduli of Rigidity for Web and Flanges

### Orthotropic Material

$d/b_1 = 0.5$

$t/b_1 = 0.1$

| Flange | Web | | Height - to - Width Ratio, $h/b_1$ | | | |
|---|---|---|---|---|---|---|
| $G_{zx}/G_{yz}$ | $G_{wzx}/G_{wyz}$ | $G_{wyz}/G_{yz}$ | 1.0 | 2.0 | 4.0 | 10.0 |
| 0.8 | 0.8 | 0.8 | 0.119 | 0.121 | 0.128 | 0.132 |
| | | 1.0 | 0.126 | 0.142 | 0.156 | 0.164 |
| | | 1.2 | 0.133 | 0.163 | 0.183 | 0.195 |
| 0.8 | 1.0 | 0.8 | 0.119 | 0.121 | 0.129 | 0.133 |
| | | 1.0 | 0.126 | 0.143 | 0.157 | 0.165 |
| | | 1.2 | 0.133 | 0.164 | 0.185 | 0.197 |
| 0.8 | 1.2 | 0.8 | 0.119 | 0.122 | 0.130 | 0.135 |
| | | 1.0 | 0.127 | 0.144 | 0.158 | 0.167 |
| | | 1.2 | 0.133 | 0.166 | 0.186 | 0.199 |
| 1.0 | 0.8 | 0.8 | 0.133 | 0.126 | 0.130 | 0.133 |
| | | 1.0 | 0.142 | 0.149 | 0.159 | 0.165 |
| | | 1.2 | 0.150 | 0.171 | 0.187 | 0.196 |
| 1.0 | 1.0 | 0.8 | 0.133 | 0.127 | 0.131 | 0.134 |
| | | 1.0 | 0.142 | 0.150 | 0.160 | 0.166 |
| | | 1.2 | 0.150 | 0.172 | 0.188 | 0.198 |
| 1.0 | 1.2 | 0.8 | 0.133 | 0.127 | 0.132 | 0.136 |
| | | 1.0 | 0.142 | 0.151 | 0.161 | 0.168 |
| | | 1.2 | 0.150 | 0.173 | 0.190 | 0.200 |
| 1.2 | 0.8 | 0.8 | 0.144 | 0.130 | 0.132 | 0.134 |
| | | 1.0 | 0.154 | 0.154 | 0.161 | 0.166 |
| | | 1.2 | 0.163 | 0.177 | 0.190 | 0.198 |
| 1.2 | 1.0 | 0.8 | 0.145 | 0.131 | 0.134 | 0.135 |
| | | 1.0 | 0.155 | 0.155 | 0.163 | 0.167 |
| | | 1.2 | 0.164 | 0.178 | 0.191 | 0.199 |
| 1.2 | 1.2 | 0.8 | 0.145 | 0.132 | 0.135 | 0.137 |
| | | 1.0 | 0.155 | 0.156 | 0.164 | 0.169 |
| | | 1.2 | 0.164 | 0.179 | 0.193 | 0.201 |

Table B-10

Torsion Factor F for I-Sections

Isotropic Material

$t/b_1 = 0.10$

| $d/b_1$ | Height - to - Width Ratio, $h/b_1$ | | | | | | |
|---|---|---|---|---|---|---|---|
| | 0.4 | 1.0 | 2.0 | 4.0 | 6.0 | 8.0 | 10.0 |
| 0.2 | 0.122 | 0.0055 | 0.0030 | 0.0026 | 0.0022 | 0.0020 | |
| 0.5 | | 0.0578 | 0.041 | 0.026 | 0.021 | 0.018 | 0.017 |
| 1.0 | | | 0.144 | 0.075 | 0.051 | 0.040 | 0.033 |
| 2.0 | | | | 0.229 | 0.162 | 0.12[illegible] | 0.099 |
| 3.0 | | | | | 0.264 | 0.200 | 0.161 |

## Appendix C

## Experimental Results

For the interpretation of some of the test results a number of statistical quantities have been calculated (12, 20). A definition of statistical terms used is given below:

Observed quantities: $x, y$

Number of observations: $N$

Mean: $\bar{x} = \frac{1}{N} \sum_{1}^{N} x$

Variance: $s^2 = \frac{1}{N-1} \left[ \sum_{1}^{N} x^2 - \frac{1}{N} \left( \sum_{1}^{N} x \right)^2 \right]$

Standard deviation: $s$

Coefficient of variation: $V = \frac{s}{\bar{x}} \times 100\ \%$

### t-Test

Pooled variance for two populations $(N_1, \bar{x}_1, s_1^2)$ and $(N_2, \bar{x}_2, s_2^2)$

$$s_d^2 = \frac{s_1^2 (N_1 - 1) + s_2^2 (N_2 - 1)}{N_1 + N_2 - 2}$$

The t-test for difference between two populations

$$t = \frac{|\bar{x}_1 - \bar{x}_2|}{s_d} \sqrt{\frac{N_1 N_2}{N_1 + N_2}}$$

Degrees of freedom $n = N_1 + N_2 - 2$

Interpretation of t-test:

$t \geq t_{99}$ difference $\bar{x}_1 - \bar{x}_2$ is highly significant (**)

$t_{99} \geq t \geq t_{95}$ difference $\bar{x}_1 - \bar{x}_2$ is significant (*) but may require further tests.

$t < t_{95}$ difference is not significant, observations $x_1$ and $x_2$ are drawn from the same population.

The values $t_{95}$ and $t_{99}$ are the limits of an integral, defining the probability of an event to occur. The limit $\pm t_{95}$ defines a 95 per cent, $\pm t_{99}$ a 99 per cent probability.

Regression Analysis

The quantities x, y are pairs of observations.

Variances: $$s_x^2 = \frac{1}{N-1} \sum_1^N (x - \bar{x})^2$$

$$s_{yx}^2 = \frac{1}{N-2} \sum_1^N (y - y^1)^2$$

where $y^1$ = value calculated from regression line

Regression line: $y^1 = a + bx$

Regression coefficient: $$b = \frac{\sum (x - \bar{x})(y - \bar{y})}{\sum (x - \bar{x})^2}$$

Sample correlation coefficient

$$r = \frac{(x - \bar{x})(y - \bar{y})}{(n-1)\, s_x\, s_y}$$

Confidence interval for slope b

$$s_b = \frac{s_{yx}}{s_x \sqrt{n-1}}$$

# TABLE C-1

## SECTION PROPERTIES

| BEAM TYPE | BEAM NO. | DIMENSIONS, IN. H | B | D | T | SECOND MOMENTS OF AREA, IN**4 XI - AXIS I1 | I2 | I | ETA - AXIS I1 | I2 | I | TORSION IN**4 J |
|---|---|---|---|---|---|---|---|---|---|---|---|---|
| 20 | 1 | 4.5 | 0.56 | 1.00 | 0.156 | 1.57 | 2.37 | 3.95 | 0.0026 | 0.0609 | 0.0635 | 0.2367 |
| 20 | 2 | 4.5 | 0.56 | 1.00 | 0.156 | 1.57 | 2.37 | 3.95 | 0.0026 | 0.0609 | 0.0635 | 0.2367 |
| 20 | 3 | 4.5 | 0.56 | 1.00 | 0.156 | 1.57 | 2.37 | 3.95 | 0.0026 | 0.0609 | 0.0635 | 0.2367 |
| 21 | 1 | 4.5 | 1.07 | 0.99 | 0.156 | 4.77 | 2.39 | 7.16 | 0.0717 | 0.2970 | 0.3687 | 1.1768 |
| 21 | 2 | 4.5 | 1.07 | 0.98 | 0.156 | 4.77 | 2.40 | 7.17 | 0.0710 | 0.2976 | 0.3687 | 1.1794 |
| 21 | 3 | 4.5 | 1.05 | 1.00 | 0.156 | 4.69 | 2.40 | 7.10 | 0.0669 | 0.2849 | 0.3518 | 1.1145 |
| 22 | 1 | 6.0 | 1.06 | 1.00 | 0.156 | 9.47 | 5.62 | 15.09 | 0.0696 | 0.3866 | 0.4562 | 1.5393 |
| 22 | 2 | 6.0 | 1.06 | 1.00 | 0.156 | 9.47 | 5.62 | 15.09 | 0.0696 | 0.3866 | 0.4562 | 1.5393 |
| 22 | 3 | 6.0 | 1.06 | 0.98 | 0.156 | 9.35 | 5.62 | 14.97 | 0.0682 | 0.3866 | 0.4548 | 1.5393 |
| 23 | 1 | 6.0 | 1.06 | 2.00 | 0.156 | 12.96 | 5.62 | 18.58 | 0.1393 | 0.3866 | 0.5259 | 1.8058 |
| 23 | 2 | 6.0 | 1.06 | 2.00 | 0.156 | 12.96 | 5.62 | 18.58 | 0.1393 | 0.3866 | 0.5259 | 1.8058 |
| 23 | 3 | 6.0 | 1.06 | 2.00 | 0.156 | 12.96 | 5.62 | 18.58 | 0.1393 | 0.3866 | 0.5259 | 1.8058 |

# TABLE C-2

## MODULUS OF ELASTICITY

### FLANGES OF BOX BEAMS

| BEAM TYPE | BEAM NO. | N | S PSI | CV PERCENT | CONFIDENCE LIMITS 95 PC | 99 PC | EI PSI |
|---|---|---|---|---|---|---|---|
| 20 | 1 | 6 | 0.410E 03 | 0.383E 02 | 0.430E 03 | 0.674E 03 | 0.168E 07 |
| 20 | 2 | 6 | 0.132E 03 | 0.121E 02 | 0.138E 03 | 0.216E 03 | 0.159E 07 |
| 20 | 3 | 6 | 0.197E 03 | 0.263E 02 | 0.207E 03 | 0.325E 03 | 0.110E 07 |
| 21 | 1 | 6 | 0.355E 03 | 0.136E 02 | 0.373E 03 | 0.585E 03 | 0.128E 07 |
| 21 | 2 | 6 | 0.234E 03 | 0.946E 01 | 0.245E 03 | 0.385E 03 | 0.111E 07 |
| 21 | 3 | 6 | 0.320E 03 | 0.821E 01 | 0.336E 03 | 0.526E 03 | 0.194E 07 |
| 22 | 1 | 6 | 0.113E 04 | 0.319E 02 | 0.119E 04 | 0.187E 04 | 0.159E 07 |
| 22 | 2 | 6 | 0.130E 03 | 0.419E 01 | 0.136E 03 | 0.213E 03 | 0.134E 07 |
| 22 | 3 | 6 | 0.354E 03 | 0.110E 02 | 0.371E 03 | 0.582E 03 | 0.155E 07 |
| 23 | 1 | 6 | 0.526E 03 | 0.198E 02 | 0.552E 03 | 0.866E 03 | 0.119E 07 |
| 23 | 2 | 6 | 0.804E 03 | 0.234E 02 | 0.843E 03 | 0.132E 04 | 0.159E 07 |
| 23 | 3 | 6 | 0.218E 03 | 0.800E 01 | 0.228E 03 | 0.358E 03 | 0.129E 07 |

Table C-3

Apparent Modulus of Elasticity and

Modulus of Rupture of Box Beams.

Two-Point Loading

(Fig. 6.5)

L = span

a = position of load from nearest support

P = total load on beam

| Beam Type | Beam No | L | a | Initial Slope P/y | P, Max. | Modulus of Elasticity | Modulus of Rupture |
|---|---|---|---|---|---|---|---|
| | | in. | in. | tons*/in. | lbs. | psi | psi |
| 20 | 1 | 72.0 | 22.0 | 0.422 | 230 | $1.11^{\times 10^6}$ | 2 350 |
| | 2 | | | 0.465 | 770 | 1.22 | 4 920 |
| | 3 | | | 0.385 | 830 | 1.01 | 5 430 |
| 21 | 1 | 72.0 | 22.0 | 0.700 | 1750 | 0.99 | 6 040 |
| | 2 | | | 0.700 | 2280 | 0.99 | 7 900 |
| | 3 | | | 0.894 | 2860 | 1.27 | 9 910 |
| 22 | 1 | 96.0 | 34.0 | 0.666 | 1500 | 1.19 | 5 070 |
| | 2 | | | 0.663 | 2220 | 1.20 | 7 490 |
| | 3 | | | 0.695 | 2000 | 1.27 | 7 110 |
| 23 | 1 | 96.0 | 34.0 | 0.705 | 1990 | 1.04 | 5 470 |
| | 2 | | | 0.246 | 3210 | 1.25 | 8 800 |
| | 3 | | | 0.705 | 2510 | 1.04 | 6 880 |

* 1 ton = 2240 lbs.

# TABLE C-4 (a)

## SPECIFIC GRAVITY

### FLANGES

| BEAM TYPE | BEAM NO. | N | SP.GR. | S**2 | S | T | SIGNIFICANCE LEVEL |
|---|---|---|---|---|---|---|---|
| 20 | 1 | 6 | 0.517 | 0.012 | 0.111 | 0. | NS |
| | | 6 | 0.517 | 0.012 | 0.111 | | |
| 20 | 2 | 6 | 0.528 | 0.003 | 0.057 | 0.233 | NS |
| | | 12 | 0.522 | 0.007 | 0.084 | | |
| 20 | 3 | 6 | 0.434 | 0.001 | 0.037 | 2.432 | * |
| 21 | 1 | 6 | 0.436 | 0.000 | 0.018 | 2.464 | * |
| 21 | 2 | 6 | 0.426 | 0.000 | 0.021 | 2.712 | * |
| 21 | 3 | 6 | 0.597 | 0.001 | 0.026 | 2.106 | NS |
| | | 18 | 0.547 | 0.006 | 0.078 | | |
| 22 | 1 | 6 | 0.513 | 0.014 | 0.119 | 0.826 | NS |
| | | 24 | 0.539 | 0.008 | 0.088 | | |
| 22 | 2 | 6 | 0.468 | 0.001 | 0.033 | 1.911 | NS |
| | | 30 | 0.525 | 0.007 | 0.085 | | |
| 22 | 3 | 6 | 0.479 | 0.001 | 0.024 | 1.284 | NS |
| | | 36 | 0.517 | 0.006 | 0.080 | | |
| 23 | 1 | 6 | 0.412 | 0.001 | 0.034 | 3.159 | ** |
| 23 | 2 | 6 | 0.524 | 0.010 | 0.102 | 0.188 | NS |
| | | 42 | 0.518 | 0.007 | 0.082 | | |
| 23 | 3 | 6 | 0.444 | 0.000 | 0.022 | 2.198 | * |

TABLE C-4 (b)

SPECIFIC GRAVITY

WEB

| BEAM TYPE | BEAM NO. | N | SP.GR. | S**2 | S | T | SIGNIFICANCE LEVEL |
|---|---|---|---|---|---|---|---|
| 20 | 1 | 6 | 0.657 | 0.000 | 0.014 | 0. | NS |
| | | 6 | 0.657 | 0.000 | 0.014 | | |
| 20 | 2 | 6 | 0.659 | 0.000 | 0.013 | 0.224 | NS |
| | | 12 | 0.658 | 0.000 | 0.013 | | |
| 20 | 3 | 6 | 0.616 | 0.000 | 0.009 | 7.197 | ** |
| 21 | 1 | 6 | 0.638 | 0.000 | 0.017 | 2.868 | * |
| 21 | 2 | 6 | 0.622 | 0.000 | 0.013 | 5.530 | ** |
| 21 | 3 | 6 | 0.634 | 0.000 | 0.011 | 4.066 | ** |
| 22 | 1 | 6 | 0.675 | 0.000 | 0.019 | 2.172 | * |
| 22 | 2 | 6 | 0.654 | 0.000 | 0.010 | 0.794 | NS |
| | | 18 | 0.657 | 0.000 | 0.012 | | |
| 22 | 3 | 6 | 0.662 | 0.000 | 0.010 | 1.048 | NS |
| | | 24 | 0.658 | 0.000 | 0.012 | | |
| 23 | 1 | 6 | 0.650 | 0.000 | 0.014 | 1.440 | NS |
| | | 30 | 0.657 | 0.000 | 0.012 | | |
| 23 | 2 | 6 | 0.655 | 0.000 | 0.011 | 0.227 | NS |
| | | 36 | 0.656 | 0.000 | 0.012 | | |
| 23 | 3 | 6 | 0.655 | 0.000 | 0.019 | 0.254 | NS |
| | | 42 | 0.656 | 0.000 | 0.013 | | |

# TABLE C-5 (a)

## MOISTURE CONTENT

## FLANGES

| BEAM TYPE | BEAM NO. | N | M.C. PERCENT | S**2 | S | T | SIGNIFICANCE LEVEL |
|---|---|---|---|---|---|---|---|
| 20 | 1 | 6 | 10.1 | 0.565 | 0.752 | 0. | NS |
| | | 6 | 10.1 | 0.565 | 0.752 | | |
| 20 | 2 | 6 | 10.2 | 0.251 | 0.501 | 0.297 | NS |
| | | 12 | 10.1 | 0.374 | 0.612 | | |
| 20 | 3 | 6 | 10.1 | 0.228 | 0.477 | 0.240 | NS |
| | | 18 | 10.1 | 0.310 | 0.557 | | |
| 21 | 1 | 6 | 9.4 | 0.002 | 0.049 | 2.986 | ** |
| 21 | 2 | 6 | 9.6 | 0.034 | 0.185 | 2.225 | * |
| 21 | 3 | 6 | 9.9 | 0.107 | 0.327 | 0.802 | NS |
| | | 24 | 10.1 | 0.260 | 0.510 | | |
| 22 | 1 | 6 | 9.9 | 0.209 | 0.457 | 0.475 | NS |
| | | 30 | 10.0 | 0.244 | 0.494 | | |
| 22 | 2 | 6 | 10.2 | 0.182 | 0.427 | 0.799 | NS |
| | | 36 | 10.1 | 0.233 | 0.482 | | |
| 22 | 3 | 6 | 10.1 | 0.142 | 0.377 | 0.306 | NS |
| | | 42 | 10.1 | 0.216 | 0.465 | | |
| 23 | 1 | 6 | 10.0 | 0.097 | 0.311 | 0.435 | NS |
| | | 48 | 10.1 | 0.200 | 0.447 | | |
| 23 | 2 | 6 | 10.1 | 0.124 | 0.352 | 0.025 | NS |
| | | 54 | 10.1 | 0.189 | 0.435 | | |
| 23 | 3 | 6 | 9.8 | 0.016 | 0.128 | 1.328 | NS |
| | | 60 | 10.0 | 0.176 | 0.420 | | |

# TABLE C-5 (b)

## MOISTURE CONTENT

## WEB

| BEAM TYPE | BEAM NO. | N | M.C. PERCENT | S**2 | S | T | SIGNIFICANCE LEVEL |
|---|---|---|---|---|---|---|---|
| 20 | 1 | 6 | 7.8 | 0.078 | 0.279 | 0. | NS |
| | | 6 | 7.8 | 0.078 | 0.279 | | |
| 20 | 2 | 6 | 7.9 | 0.088 | 0.297 | 0.926 | NS |
| | | 12 | 7.8 | 0.082 | 0.286 | | |
| 20 | 3 | 6 | 8.0 | 0.061 | 0.246 | 0.977 | NS |
| | | 18 | 7.9 | 0.075 | 0.274 | | |
| 21 | 1 | 6 | 7.9 | 0.054 | 0.232 | 0.197 | NS |
| | | 24 | 7.9 | 0.067 | 0.259 | | |
| 21 | 2 | 6 | 7.8 | 0.071 | 0.267 | 0.900 | NS |
| | | 30 | 7.9 | 0.068 | 0.260 | | |
| 21 | 3 | 6 | 7.9 | 0.039 | 0.197 | 0.064 | NS |
| | | 36 | 7.9 | 0.062 | 0.248 | | |
| 22 | 1 | 6 | 7.9 | 0.030 | 0.172 | 0.621 | NS |
| | | 42 | 7.9 | 0.057 | 0.238 | | |
| 22 | 2 | 6 | 8.3 | 0.109 | 0.330 | 3.789 | ** |
| 22 | 3 | 6 | 7.9 | 0.027 | 0.165 | 0.415 | NS |
| | | 48 | 7.9 | 0.053 | 0.229 | | |
| 23 | 1 | 6 | 7.8 | 0.635 | 0.797 | 0.457 | NS |
| | | 54 | 7.9 | 0.107 | 0.327 | | |
| 23 | 2 | 6 | 8.2 | 0.181 | 0.425 | 2.460 | * |
| 23 | 3 | 6 | 8.4 | 0.136 | 0.369 | 3.937 | ** |

TABLE C-6

TORSIONAL RIGIDITY

EXPERIMENTAL BOX BEAMS

REGRESSION ANALYSIS

| BEAM TYPE | BEAM NO. | NO. OF READINGS | A DEG | B DEG/LB | SY | SB | R | P-MAX LBS | GJ LB-IN**2 |
|---|---|---|---|---|---|---|---|---|---|
| 20 | 1 | 8 | -0.039 | 1.159 | 0.568 | 0.016 | 1.00 | 1.6 | 0.218E 05 |
| 20 | 2 | 8 | -0.007 | 1.023 | 0.501 | 0.005 | 1.00 | 1.6 | 0.246E 05 |
| 20 | 3 | 8 | -0.043 | 1.137 | 0.557 | 0.019 | 1.00 | 1.6 | 0.222E 05 |
| 21 | 1 | 8 | -0.018 | 0.200 | 0.489 | 0.001 | 1.00 | 8.0 | 0.126E 06 |
| 21 | 2 | 8 | -0.021 | 0.199 | 0.486 | 0.001 | 1.00 | 8.0 | 0.127E 06 |
| 21 | 3 | 8 | -0.029 | 0.210 | 0.514 | 0.001 | 1.00 | 8.0 | 0.120E 06 |
| 22 | 1 | 12 | -0.012 | 0.131 | 0.472 | 0.001 | 1.00 | 12.0 | 0.173E 06 |
| 22 | 2 | 12 | -0.023 | 0.143 | 0.515 | 0.001 | 1.00 | 12.0 | 0.159E 06 |
| 22 | 3 | 12 | -0.006 | 0.140 | 0.503 | 0.001 | 1.00 | 12.0 | 0.163E 06 |
| 23 | 1 | 15 | -0.006 | 0.108 | 0.483 | 0.000 | 1.00 | 15.0 | 0.210E 06 |
| 23 | 2 | 15 | -0.001 | 0.115 | 0.513 | 0.001 | 1.00 | 15.0 | 0.198E 06 |
| 23 | 3 | 15 | -0.003 | 0.106 | 0.476 | 0.000 | 1.00 | 15.0 | 0.213E 06 |

Table C-7

Southwell Plot for Centre-Loaded Beams

Theta Vs. Theta/$P^2$

Y1 = A + BP

| Test Series | Beam Type | Beam No | A | B | Maximum Values Observed: Theta | Maximum Values Observed: Theta/$P^2$ |
|---|---|---|---|---|---|---|
| 1 | 20 | 1 | 0.408E-02 | 0.330E-03 | 6.30 | 0.615E-02 |
| | 20 | 2 | 0.111E-02 | 0.853E-03 | 4.25 | 0.472E-02 |
| | | | N = 1 too small for calculations | | | |
| | 21 | 1 | 0.420E-04 | 0.801E-05 | 2.50 | 0.625E-04 |
| | 21 | 2 | 0.231E-04 | -0.299E-05 | 1.00 | 0.209E-04 |
| | 21 | 3 | 0.104E-04 | 0.887E-05 | 1.85 | 0.276E-04 |
| | 22 | 1 | 0.237E-05 | 0.718E-05 | 4.50 | 0.347E-04 |
| | | | N = 1 too small for calculations | | | |
| | 22 | 3 | 0.111E-04 | 0.585E-05 | 3.50 | 0.321E-04 |
| | 23 | 1 | 0.203E-05 | 0.487E-05 | 2.05 | 0.122E-04 |
| | | | N = 1 too small for calculations | | | |
| | 23 | 3 | 0.351E-05 | 0.441-05 | 4.00 | 0.216E-04 |
| 2 | 20 | 1 | 0.942E-03 | 0.678E-03 | 2.75 | 0.269E-02 |
| | 20 | 2 | 0.786E-03 | 0.477E-04 | 2.90 | 0.959E-03 |
| | 20 | 3 | 0.129E-02 | -0.776E-04 | 3.75 | 0.104E-02 |
| | | | N = 2 too small for calculations | | | |
| | 21 | 2 | 0.667E-05 | 0.105E-05 | 1.50 | 0.850E-05 |
| | | | N = 1 too small for calculations | | | |
| | 22 | 1 | 0.331E-05 | 0.207E-05 | 2.40 | 0.845E-05 |
| | 22 | 2 | 0.535E-05 | 0.331E-06 | 1.40 | 0.588E-05 |
| | 22 | 3 | 0.115E-05 | 0.256E-05 | 3.20 | 0.938E-05 |
| | | | N = 0 too small for calculations | | | |
| | | | N = 1 too small for calculations | | | |
| | 23 | 3 | 0.283E-05 | 0.115E-05 | 3.10 | 0.670E-05 |
| 3 | | | N = 1 too small for calculations | | | |
| | 20 | 2 | 0.123E-04 | 0.257E-04 | 1.50 | 0.507E-04 |
| | 20 | 3 | 0.401E-04 | 0.429E-04 | 3.50 | 0.189E-03 |
| | 21 | 1 | 0.706E-06 | 0.424E-06 | 0.86 | 0.107E-05 |
| | | | N = 0 too small for calculations | | | |
| | | | N = 0 too small for calculations | | | |

Table C-7 (Continued)

Southwell Plot for Centre-Loaded Beams

Theta Vs. $Theta/P^2$

$Y1 = A + BP$

| Test Series | Beam Type | Beam No | Initial Conditions | A | B | Maximum Values Observed: Theta | Maximum Values Observed: $Theta/P^2$ |
|---|---|---|---|---|---|---|---|
| 4 | | | $e_y$= +3.0in. | N = 0 too small for calculations | | | |
| | 22 | 2 | | 0.221E-05 | 0.845E-05 | 3.20 | 0.294E-04 |
| | 22 | 3 | | 0.181E-04 | 0.550E-05 | 4.20 | 0.437E-04 |
| | 22 | 1 | $e_y$= 0.0 | 0.231E-05 | 0.519E-05 | 3.90 | 0.226E-04 |
| | | | | N = 2 too small for calculations | | | |
| | 22 | 3 | | 0.105E-04 | 0.433E-05 | 3.95 | 0.289E-04 |
| | 22 | 1 | $e_y$= -3.0in. | 0.361E-05 | 0.711E-05 | 4.15 | 0.329E-04 |
| | | | | N = 1 too small for calculations | | | |
| | 22 | 3 | | 0.128E-04 | 0.501E-05 | 3.75 | 0.324E-04 |
| 5 | 22 | 1 | $\theta$ = 1.0° | 0.121E-04 | 0.698E-05 | 3.35 | 0.349E-04 |
| | 22 | 2 | | 0.105E-04 | 0.728E-05 | 3.45 | 0.359E-04 |
| | 22 | 3 | | 0.352E-05 | 0.726E-05 | 2.35 | 0.203E-04 |
| | 22 | 1 | $\theta$ = 2.0° | 0.161E-04 | 0.794E-05 | 3.00 | 0.383E-04 |
| | 22 | 2 | | 0.158E-04 | 0.673E-05 | 2.60 | 0.332E-04 |
| | 22 | 3 | | 0.914E-05 | 0.666E-05 | 3.40 | 0.322E-04 |
| | 22 | 1 | $\theta$ = 3.0° | 0.311E-04 | 0.377E-05 | 4.40 | 0.489E-04 |
| | 22 | 2 | | 0.219E-04 | 0.686E-05 | 3.75 | 0.478E-04 |
| | 22 | 3 | | 0.140E-04 | 0.650E-05 | 3.90 | 0.393E-04 |
| 6 | 22 | 1 | $e_x$= 0.5in. | 0.222E-04 | 0.202E-05 | 3.15 | 0.308E-04 |
| | 22 | 2 | | 0.357E-04 | 0.266E-05 | 4.60 | 0.511E-04 |
| | 22 | 3 | | 0.170E-04 | 0.495E-05 | 4.65 | 0.414E-04 |
| | 22 | 1 | $e_x$= 1.0in. | 0.107E-03 | -0.120E-04 | 4.65 | 0.638E-04 |
| | 22 | 2 | | 0.591E-04 | -0.186E-05 | 5.05 | 0.543E-04 |
| | 22 | 3 | | 0.355E-04 | 0.156E-05 | 4.80 | 0.469E-04 |

Table C-8

Lateral Stability - Plywood Box Beams

Experimental and Theoretical Loads

| Test Series | Beam Type | Beam No | P Max Lbs | Critical Loads, Lbs Exper. | Theor. |
|---|---|---|---|---|---|
| 1 | 20 | 1 | 32.0 | 55.1 | 50.7 |
| | 20 | 2 | 30.0 | 34.2 | 50.7 |
| | 20. | 3 | 30.0 | -0.0 | 50.4 |
| | 21 | 1 | 200.0 | 353.4 | 264.8 |
| | 21 | 2 | 239.0 | -0.0 | 262.7 |
| | 21 | 3 | 259.0 | 335.8 | 261.0 |
| | 22 | 1 | 360.0 | 373.2 | 343.8 |
| | 22 | 2 | 390.0 | -0.0 | 340.1 |
| | 22 | 3 | 330.0 | 413.5 | 342.8 |
| | 23 | 1 | 410.0 | 454.0 | 384.8 |
| | 23 | 2 | 460.0 | - | 397.0 |
| | 23 | 3 | 430.0 | 476.0 | 387.7 |
| 2 | 20 | 1 | 32.0 | 38.4 | 89.2 |
| | 20 | 2 | 55.0 | 144.8 | 89.1 |
| | 20 | 3 | 60.0 | -0.0 | 88.7 |
| | 21 | 1 | 440.0 | -0.0 | 466.1 |
| | 21 | 2 | 420.0 | 975.7 | 462.2 |
| | 21 | 3 | 500.0 | -0.0 | 459.3 |
| | 22 | 1 | 533.0 | 695.0 | 605.1 |
| | 22 | 2 | 516.0 | 1737.7 | 598.5 |
| | 22 | 3 | 584.0 | 625.5 | 603.2 |
| | 23 | 1 | 540.0 | - | 677.2 |
| | 23 | 2 | 612.0 | - | 698.6 |
| | 23 | 3 | 680.0 | 934.0 | 682.3 |
| 3 | 20 | 1 | 110.0 | -0.0 | 195.4 |
| | 20 | 2 | 172.0 | 197.3 | 195.2 |
| | 20 | 3 | 136.0 | 152.7 | 194.1 |

Table C-8 (Continued)

Lateral Stability - Plywood Box Beams

Experimental and Theoretical Loads

Beam Type 22

Theoretical loads in Test Series 5 and 6 are for beams without initial lateral eccentricity, $e_x$, or initial rotation, $\phi$.

| Test Series | Beam No | Initial Condition | P Max Lbs | Critical Loads, Lbs Exper. | Theor. |
|---|---|---|---|---|---|
| 4 | 1 | $e_y$ = +3.0 in. | 370.0 | - | 313.9 |
| | 2 | | 340.0 | 343.9 | 311.9 |
| | 3 | | 310.0 | 426.3 | 312.6 |
| | 1 | $e_y$ = 0.0 | 355.0 | 375.1 | 343.8 |
| | 2 | | 410.0 | - | 340.1 |
| | 3 | | 340.0 | 446.7 | 342.8 |
| | 1 | $e_y$ = -3.0 in. | 415.0 | 438.9 | 373.7 |
| | 2 | | 400.0 | - | 368.3 |
| | 3 | | 370.0 | 480.8 | 373.0 |
| 5 | 1 | $\phi$ = 1.0° | 310.0 | 378.5 | 343.8 |
| | 2 | | 310.0 | 370.7 | 340.1 |
| | 3 | | 345.0 | 371.2 | 342.8 |
| | 1 | $\phi$ = 2.0° | 280.0 | 354.8 | 343.8 |
| | 2 | | 280.0 | 385.4 | 340.1 |
| | 3 | | 325.0 | 387.4 | 342.8 |
| | 1 | $\phi$ = 3.0° | 300.0 | 514.8 | 343.8 |
| | 2 | | 280.0 | 381.9 | 340.1 |
| | 3 | | 315.0 | 392.1 | 342.8 |
| 6 | 1 | $e_x$ = 0.5 in. | 320.0 | 704.0 | 343.8 |
| | 2 | | 300.0 | 613.7 | 340.1 |
| | 3 | | 335.0 | 449.6 | 342.8 |
| | 1 | $e_x$ = 1.0 in. | 270.0 | - | 343.8 |
| | 2 | | 305.0 | - | 340.1 |
| | 3 | | 320.0 | 801.3 | 342.8 |

# TABLE C-9 (a)

## STRAIN DISTRIBUTION DUE TO TORSION IN FLANGES OF BOX BEAMS

## REGRESSION ANALYSIS

## TORSION TEST

## TEST SERIES 1

## LOAD VS. STRAIN

Y1 = A + B*P (REGRESSION LINE)
SYX= STANDARD ERROR OF ESTIMATE
SB = STANDARD ERROR OF REGRESSION COEFFICIENT B
R = CORRELATION COEFFICIENT

STRAINS IN MICROINCHES (M.IN.)/ IN.

FLANGE NO. 1
TEST RUN NO. 1

| LOCATION NO. | GAUGE NO. | A M.IN. | B M.IN./LB | SYX M.IN. | SB M.IN./LB | MAXIMUM OBSERVED R | MAXIMUM OBSERVED P LBS | MAXIMUM OBSERVED Y M.IN. | VALUES CALCULATED Y1 M.IN. |
|---|---|---|---|---|---|---|---|---|---|
| 1 | 1 | 17.2 | -58.6 | 9.88 | 0.76 | 1.00 | 14.0 | -813.7 | -802.7 |
| 1 | 2 | -1.2 | -1.7 | 1.47 | 0.11 | 0.99 | 14.0 | -24.6 | -24.6 |
| 1 | 3 | -6.5 | 45.1 | 3.95 | 0.31 | 1.00 | 14.0 | 627.5 | 624.2 |
| 2 | 1 | -10.3 | 47.5 | 6.27 | 0.48 | 1.00 | 14.0 | 660.1 | 654.4 |
| 2 | 2 | -2.0 | 1.8 | 1.71 | 0.13 | 0.98 | 14.0 | 24.5 | 22.9 |
| 2 | 3 | 8.6 | -40.1 | 4.96 | 0.38 | 1.00 | 14.0 | -556.7 | -553.0 |
| 3 | 1 | 15.7 | -51.8 | 8.77 | 0.68 | 1.00 | 14.0 | -715.0 | -708.9 |
| 3 | 2 | -2.0 | 5.9 | 1.68 | 0.13 | 1.00 | 14.0 | 82.1 | 80.5 |
| 3 | 3 | -14.2 | 54.3 | 8.44 | 0.65 | 1.00 | 14.0 | 752.4 | 746.0 |
| 4 | 1 | -15.8 | 52.4 | 9.59 | 0.74 | 1.00 | 14.0 | 728.2 | 718.4 |
| 4 | 2 | -2.0 | -1.4 | 1.68 | 0.13 | 0.97 | 14.0 | -19.3 | -20.9 |
| 4 | 3 | 13.7 | -51.2 | 8.17 | 0.63 | 1.00 | 14.0 | -710.1 | -703.3 |

TABLE C-9 (a) (Continued)

REGRESSION ANALYSIS

TORSION TEST

TEST SERIES 1

LOAD VS. STRAIN

Y1 = A + B*P (REGRESSION LINE)
SYX= STANDARD ERROR OF ESTIMATE
SB = STANDARD ERROR OF REGRESSION COEFFICIENT B
R = CORRELATION COEFFICIENT

STRAINS IN MICROINCHES (M.IN.) / IN.

FLANGE NO. 1
TEST RUN NO. 2

| LOCATION NO. | GAUGE NO. | A M.IN. | B M.IN./LB | SYX M.IN. | SB M.IN./LB | MAXIMUM OBSERVED VALUES R | P LBS | Y M.IN. | CALCULATED Y1 M.IN. |
|---|---|---|---|---|---|---|---|---|---|
| 1 | 1 | 14.3 | -58.6 | 8.28 | 0.64 | 1.00 | 14.0 | -813.7 | -806.0 |
| 1 | 2 | 0.4 | -1.6 | 1.84 | 0.14 | 0.98 | 14.0 | -24.6 | -22.6 |
| 1 | 3 | -11.8 | 44.9 | 6.59 | 0.51 | 1.00 | 14.0 | 622.5 | 617.2 |
| 2 | 1 | -9.9 | 47.6 | 5.88 | 0.45 | 1.00 | 14.0 | 660.1 | 656.4 |
| 2 | 2 | 1.2 | 1.7 | 1.46 | 0.11 | 0.99 | 14.0 | 24.5 | 24.5 |
| 2 | 3 | 8.2 | -40.1 | 4.99 | 0.38 | 1.00 | 14.0 | -556.7 | -553.8 |
| 3 | 1 | 15.3 | -51.8 | 8.30 | 0.64 | 1.00 | 14.0 | -715.0 | -709.7 |
| 3 | 2 | -0.8 | 6.1 | 1.84 | 0.14 | 1.00 | 14.0 | 82.1 | 84.1 |
| 3 | 3 | -12.1 | 54.7 | 7.88 | 0.61 | 1.00 | 14.0 | 762.1 | 753.6 |
| 4 | 1 | -13.3 | 52.7 | 7.95 | 0.61 | 1.00 | 14.0 | 733.0 | 724.5 |
| 4 | 2 | -0.0 | -1.2 | 1.97 | 0.15 | 0.96 | 14.0 | -14.5 | -16.9 |
| 4 | 3 | 11.7 | -50.8 | 6.79 | 0.52 | 1.00 | 14.0 | -705.3 | -698.9 |

TABLE C-9 (a) (Continued)

REGRESSION ANALYSIS

TORSION TEST

TEST SERIES 1

LOAD VS. STRAIN

Y1 = A + B*P (REGRESSION LINE)
SYX= STANDARD ERROR OF ESTIMATE
SB = STANDARD ERROR OF REGRESSION COEFFICIENT B
R = CORRELATION COEFFICIENT

STRAINS IN MICROINCHES (M.IN.)/ IN.

FLANGE NO. 2
TEST RUN NO. 1

| LOCATION NO. | GAUGE NO. | A M.IN. | B M.IN./LB | SYX M.IN. | SB M.IN./LB | R | MAXIMUM OBSERVED P LBS | MAXIMUM OBSERVED Y M.IN. | VALUES CALCULATED Y1 M.IN. |
|---|---|---|---|---|---|---|---|---|---|
| 1 | 1 | 25.0 | -39.5 | 14.22 | 1.10 | 1.00 | 14.0 | -536.9 | -527.5 |
| 1 | 2 | 0. | 0. | -0. | -0. | 0. | 14.0 | 0. | 0. |
| 1 | 3 | -43.5 | 61.7 | 25.58 | 1.97 | 1.00 | 14.0 | 847.3 | 820.6 |
| 2 | 1 | -24.5 | 40.4 | 14.57 | 1.12 | 1.00 | 14.0 | 558.8 | 541.7 |
| 2 | 2 | 0.8 | -3.8 | 1.91 | 0.15 | 1.00 | 14.0 | -54.2 | -52.5 |
| 2 | 3 | 55.6 | -77.7 | 30.49 | 2.35 | 1.00 | 14.0 | -1049.0 | -1032.3 |
| 3 | 1 | 37.0 | -50.9 | 20.07 | 1.55 | 1.00 | 14.0 | -690.8 | -675.9 |
| 3 | 2 | -2.8 | 3.4 | 2.48 | 0.19 | 0.99 | 14.0 | 48.3 | 45.1 |
| 3 | 3 | -32.0 | 52.0 | 17.46 | 1.35 | 1.00 | 14.0 | 708.7 | 695.8 |
| 4 | 1 | -28.3 | 44.9 | 15.71 | 1.21 | 1.00 | 14.0 | 611.7 | 599.9 |
| 4 | 2 | 0.0 | -2.0 | 1.44 | 0.11 | 0.99 | 14.0 | -29.0 | -27.8 |
| 4 | 3 | 45.3 | -75.4 | 24.69 | 1.91 | 1.00 | 14.0 | -1024.5 | -1009.8 |

TABLE C-9 (a) (Continued)

REGRESSION ANALYSIS

TORSION TEST

TEST SERIES 1

LOAD VS. STRAIN

Y1 = A + B*P (REGRESSION LINE)
SYX= STANDARD ERROR OF ESTIMATE
SB = STANDARD ERROR OF REGRESSION COEFFICIENT B
R = CORRELATION COEFFICIENT

STRAINS IN MICROINCHES (M.IN.) / IN.

FLANGE NO. 2
TEST RUN NO. 2

| LOCATION NO. | GAUGE NO. | A M.IN. | B M.IN./LB | SYX M.IN. | SB M.IN./LB | MAXIMUM OBSERVED R | MAXIMUM OBSERVED P LBS | MAXIMUM OBSERVED Y M.IN. | VALUES CALCULATED Y1 M.IN. |
|---|---|---|---|---|---|---|---|---|---|
| 1 | 1 | 23.8 | -38.3 | 14.18 | 1.09 | 1.00 | 14.0 | -517.2 | -512.7 |
| 1 | 2 | 0. | 0. | -0. | -0. | 0. | 14.0 | 0. | 0. |
| 1 | 3 | -34.5 | 62.4 | 19.55 | 1.51 | 1.00 | 14.0 | 847.3 | 838.7 |
| 2 | 1 | -24.1 | 39.2 | 14.15 | 1.09 | 1.00 | 14.0 | 539.2 | 524.1 |
| 2 | 2 | 2.9 | -4.0 | 2.16 | 0.17 | 0.99 | 14.0 | -54.2 | -53.4 |
| 2 | 3 | 55.1 | -79.0 | 35.31 | 2.72 | 1.00 | 14.0 | -1073.5 | -1051.5 |
| 3 | 1 | 32.6 | -50.5 | 19.76 | 1.52 | 1.00 | 14.0 | -676.3 | -673.9 |
| 3 | 2 | -2.0 | 3.5 | 1.68 | 0.13 | 1.00 | 14.0 | 48.3 | 46.7 |
| 3 | 3 | -27.5 | 51.7 | 15.62 | 1.21 | 1.00 | 14.0 | 708.7 | 696.2 |
| 4 | 1 | -35.6 | 45.4 | 19.63 | 1.51 | 1.00 | 14.0 | 606.8 | 599.9 |
| 4 | 2 | 1.6 | -1.8 | 1.55 | 0.12 | 0.99 | 14.0 | -24.2 | -23.3 |
| 4 | 3 | 48.6 | -76.4 | 26.55 | 2.05 | 1.00 | 14.0 | -1039.2 | -1021.7 |

TABLE C-9 (b)

REGRESSION ANALYSIS

TORSION TEST

TEST SERIES 2

LOAD VS. STRAIN

Y1 = A + B*P (REGRESSION LINE)
SYX= STANDARD ERROR OF ESTIMATE
SB = STANDARD ERROR OF REGRESSION COEFFICIENT B
R = CORRELATION COEFFICIENT

STRAINS IN MICROINCHES (M.IN.) / IN.

FLANGE NO. 1
TEST RUN NO. 1

| LOCATION NO. | GAUGE NO. | A M.IN. | B M.IN./LB | SYX M.IN. | SB M.IN./LB | MAXIMUM OBSERVED R | MAXIMUM OBSERVED P LBS | MAXIMUM OBSERVED Y M.IN. | VALUES CALCULATED Y1 M.IN. |
|---|---|---|---|---|---|---|---|---|---|
| 1 | 1 | 8.2 | -11.5 | 6.21 | 0.19 | 1.00 | 35.0 | -402.0 | -395.4 |
| 1 | 2 | 0. | 0. | -0. | -0. | 0. | 35.0 | 0. | 0. |
| 1 | 3 | -7.8 | 10.6 | 4.79 | 0.15 | 1.00 | 35.0 | 367.6 | 361.9 |
| 2 | 1 | -3.7 | 4.8 | 3.11 | 0.10 | 1.00 | 35.0 | 167.5 | 165.0 |
| 2 | 2 | 3.3 | 0.3 | 2.43 | 0.08 | 0.86 | 35.0 | 14.7 | 13.9 |
| 2 | 3 | 5.3 | -5.7 | 4.55 | 0.14 | 1.00 | 35.0 | -197.0 | -192.5 |
| 3 | 1 | 7.2 | -10.7 | 4.53 | 0.14 | 1.00 | 35.0 | -372.0 | -367.1 |
| 3 | 2 | -2.8 | 1.9 | 1.51 | 0.05 | 1.00 | 35.0 | 62.8 | 62.0 |
| 3 | 3 | -10.9 | 13.1 | 6.52 | 0.20 | 1.00 | 35.0 | 451.5 | 446.6 |
| 4 | 1 | -2.0 | 4.2 | 2.13 | 0.07 | 1.00 | 35.0 | 145.6 | 146.4 |
| 4 | 2 | -2.0 | 0.3 | 2.09 | 0.06 | 0.85 | 35.0 | 9.7 | 6.8 |
| 4 | 3 | 8.5 | -8.0 | 4.06 | 0.15 | 1.00 | 35.0 | -275.4 | -271.7 |

TABLE C-9 (b) (Continued)

REGRESSION ANALYSIS

TORSION TEST

TEST SERIES 2

LOAD VS. STRAIN

Y1 = A + B*P (REGRESSION LINE)
SYX= STANDARD ERROR OF ESTIMATE
SB = STANDARD ERROR OF REGRESSION COEFFICIENT B
R = CORRELATION COEFFICIENT

STRAINS IN MICROINCHES (M.IN.) / IN.

FLANGE NO. 1
TEST RUN NO. 2

| LOCATION NO. | GAUGE NO. | A M.IN. | B M.IN./LB | SYX M.IN. | SB M.IN./LB | MAXIMUM OBSERVED R | MAXIMUM OBSERVED P LBS | MAXIMUM OBSERVED Y M.IN. | VALUES CALCULATED Y1 M.IN. |
|---|---|---|---|---|---|---|---|---|---|
| 1 | 1 | 6.5 | -11.7 | 3.79 | 0.12 | 1.00 | 35.0 | -406.9 | -402.4 |
| 1 | 2 | -2.9 | -0.1 | 1.54 | 0.05 | 0.58 | 35.0 | -4.9 | -5.7 |
| 1 | 3 | -6.5 | 10.6 | 3.94 | 0.12 | 1.00 | 35.0 | 367.6 | 365.6 |
| 2 | 1 | -5.7 | 4.8 | 3.07 | 0.09 | 1.00 | 35.0 | 162.6 | 160.9 |
| 2 | 2 | -2.0 | 0.3 | 1.83 | 0.06 | 0.92 | 35.0 | 9.8 | 9.4 |
| 2 | 3 | 7.0 | -5.7 | 4.42 | 0.14 | 1.00 | 35.0 | -197.0 | -194.2 |
| 3 | 1 | 6.0 | -10.7 | 4.33 | 0.13 | 1.00 | 35.0 | -372.0 | -367.1 |
| 3 | 2 | -2.4 | 2.0 | 2.66 | 0.08 | 0.99 | 35.0 | 67.6 | 66.4 |
| 3 | 3 | -11.3 | 13.4 | 7.07 | 0.22 | 1.00 | 35.0 | 466.0 | 456.7 |
| 4 | 1 | -1.2 | 4.3 | 2.65 | 0.08 | 1.00 | 35.0 | 150.5 | 149.3 |
| 4 | 2 | -0.8 | 0.4 | 1.55 | 0.05 | 0.96 | 35.0 | 14.5 | 12.9 |
| 4 | 3 | 6.0 | -8.0 | 4.86 | 0.15 | 1.00 | 35.0 | -280.2 | -274.2 |

TABLE C-9 (b) (Continued)

REGRESSION ANALYSIS

TORSION TEST

TEST SERIES 2

LOAD VS. STRAIN

Y1 = A + B*P (REGRESSION LINE)
SYX= STANDARD ERROR OF ESTIMATE
SB = STANDARD ERROR OF REGRESSION COEFFICIENT B
R = CORRELATION COEFFICIENT

STRAINS IN MICROINCHES (M.IN.) / IN.

FLANGE NO. 2
TEST RUN NO. 1

| LOCATION NO. | GAUGE NO. | A M.IN. | B M.IN./LB | SYX M.IN. | SB M.IN./LB | MAXIMUM OBSERVED R | MAXIMUM OBSERVED P LBS | MAXIMUM OBSERVED Y M.IN. | VALUES CALCULATED Y1 M.IN. |
|---|---|---|---|---|---|---|---|---|---|
| 1 | 1 | 2.5 | -3.4 | 2.01 | 0.06 | 1.00 | 35.0 | -118.2 | -118.2 |
| 1 | 2 | 0. | -0. | -0. | -0. | 0. | 35.0 | -0. | -0. |
| 1 | 3 | -8.6 | 6.3 | 9.39 | 0.29 | 0.99 | 35.0 | 216.7 | 213.1 |
| 2 | 1 | -6.1 | 10.4 | 3.89 | 0.12 | 1.00 | 35.0 | 357.8 | 356.6 |
| 2 | 2 | 2.1 | -0.3 | 1.84 | 0.06 | 0.92 | 35.0 | -9.9 | -9.4 |
| 2 | 3 | 9.0 | -13.2 | 6.51 | 0.20 | 1.00 | 35.0 | -446.1 | -451.4 |
| 3 | 1 | 2.8 | -5.4 | 2.09 | 0.06 | 1.00 | 35.0 | -188.4 | -186.4 |
| 3 | 2 | 0.0 | 0.3 | 1.44 | 0.04 | 0.94 | 35.0 | 9.7 | 10.9 |
| 3 | 3 | -5.3 | 4.5 | 3.34 | 0.10 | 1.00 | 35.0 | 155.3 | 153.3 |
| 4 | 1 | -8.1 | 10.2 | 4.80 | 0.15 | 1.00 | 35.0 | 354.4 | 349.1 |
| 4 | 2 | 1.2 | -0.1 | 1.58 | 0.05 | 0.76 | 35.0 | -4.8 | -3.6 |
| 4 | 3 | 10.6 | -14.2 | 6.60 | 0.20 | 1.00 | 35.0 | -495.1 | -487.3 |

TABLE C-9 (b) (Continued)

REGRESSION ANALYSIS

TORSION TEST

TEST SERIES 2

LOAD VS. STRAIN

Y1 = A + B*P (REGRESSION LINE)
SYX= STANDARD ERROR OF ESTIMATE
SB = STANDARD ERROR OF REGRESSION COEFFICIENT B
R = CORRELATION COEFFICIENT

STRAINS IN MICROINCHES (M.IN.)/ IN.

FLANGE NO. 2
TEST RUN NO. 2

| LOCATION NO. | GAUGE NO. | A M.IN. | B M.IN./LB | SYX M.IN. | SB M.IN./LB | MAXIMUM OBSERVED VALUES R | P LBS | Y M.IN. | CALCULATED Y1 M.IN. |
|---|---|---|---|---|---|---|---|---|---|
| 1 | 1 | 2.1 | -3.4 | 1.71 | 0.05 | 1.00 | 35.0 | -118.2 | -116.6 |
| 1 | 2 | 0. | -0. | -0. | -0. | 0. | 35.0 | -0. | -0. |
| 1 | 3 | -5.3 | 6.5 | 3.88 | 0.12 | 1.00 | 35.0 | 226.6 | 220.9 |
| 2 | 1 | -7.8 | 10.5 | 4.96 | 0.15 | 1.00 | 35.0 | 362.7 | 359.5 |
| 2 | 2 | 2.1 | -0.3 | 1.84 | 0.06 | 0.92 | 35.0 | -9.9 | -9.4 |
| 2 | 3 | 4.9 | -12.9 | 4.26 | 0.13 | 1.00 | 35.0 | -446.1 | -447.3 |
| 3 | 1 | 3.6 | -5.3 | 2.42 | 0.07 | 1.00 | 35.0 | -183.6 | -182.4 |
| 3 | 2 | -1.2 | 0.3 | 1.58 | 0.05 | 0.94 | 35.0 | 9.7 | 10.9 |
| 3 | 3 | -4.9 | 4.6 | 3.18 | 0.10 | 1.00 | 35.0 | 155.3 | 155.3 |
| 4 | 1 | -5.3 | 10.2 | 3.90 | 0.12 | 1.00 | 35.0 | 349.5 | 351.1 |
| 4 | 2 | 0. | 0. | -0. | -0. | 0. | 35.0 | 0. | 0. |
| 4 | 3 | 8.6 | -14.0 | 5.00 | 0.15 | 1.00 | 35.0 | -485.3 | -480.4 |

TABLE C - 10 (a)

TORSION TEST

SHEAR STRAIN DISTRIBUTION

FLANGES, 1.69*1.69 IN**2 DOUGLAS FIR

APPLIED TORSION = 12.0 IN-LB

SHEAR STRAINS, MICROINCHES/INCH

| LOCATION | SECTION1 | SECTION 2 |
|---|---|---|
| 1 | -104. | -106. |
| 2 | 88. | 104. |
| 3 | -101. | -103. |
| 4 | 118. | 121. |

TABLE C - 10 (b)

TORSION TEST

SHEAR STRAIN DISTRIBUTION

BOX SECTION, 2.19*6.75 IN**2
WEB, 0.25 IN. BIRCH PLYWOOD
FLANGES, 1.69*1.69 IN**2 DOUGLAS FIR

APPLIED TORSION = 24.0 IN-LB

SHEAR STRAINS, MICROINCHES/INCH

| LOCATION | SECTION1 | SECTION 2 |
|---|---|---|
| 1 | -22. | -24. |
| 2 | 10. | 12. |
| 3 | -10. | -10. |
| 4 | 23. | 24. |

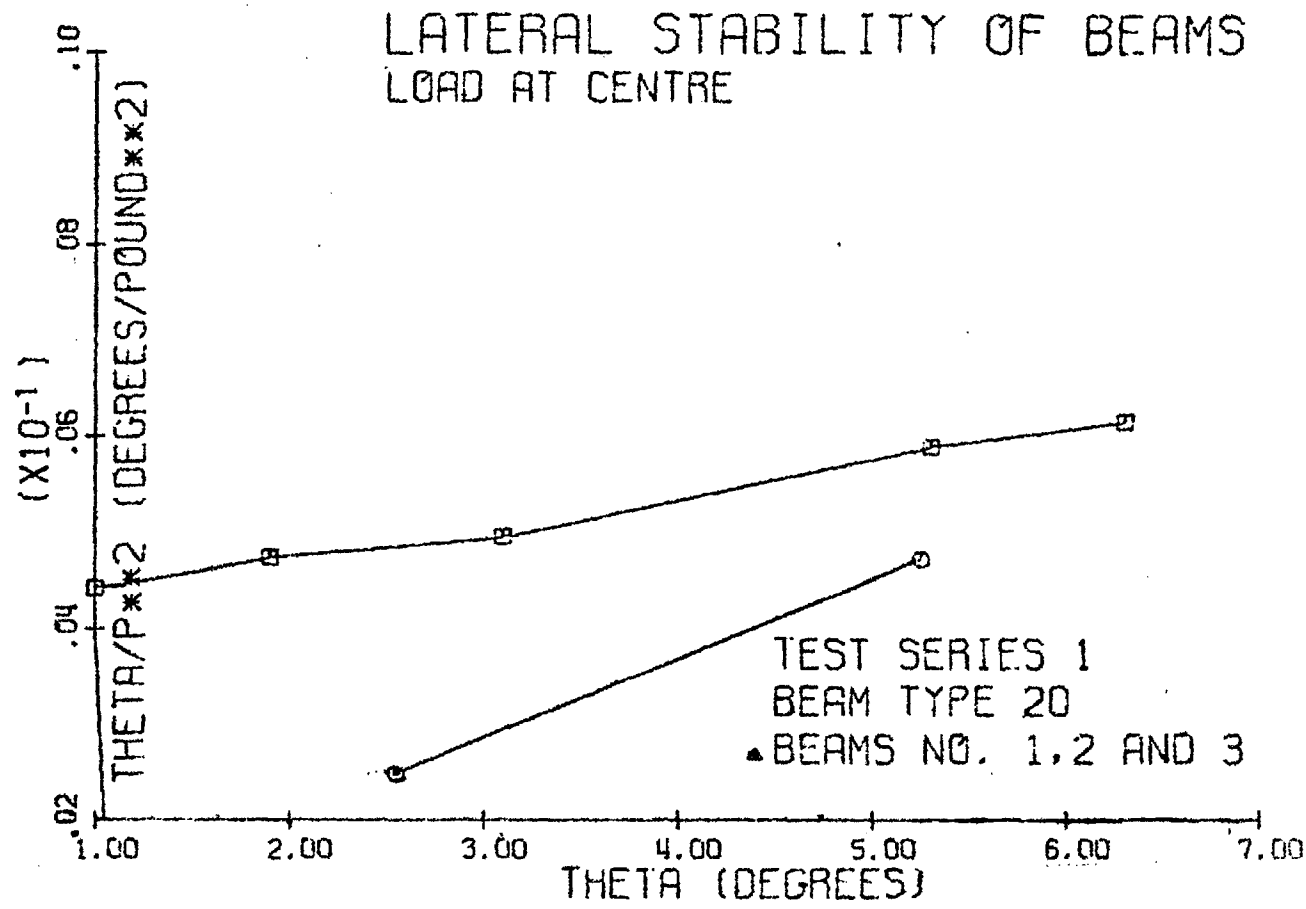


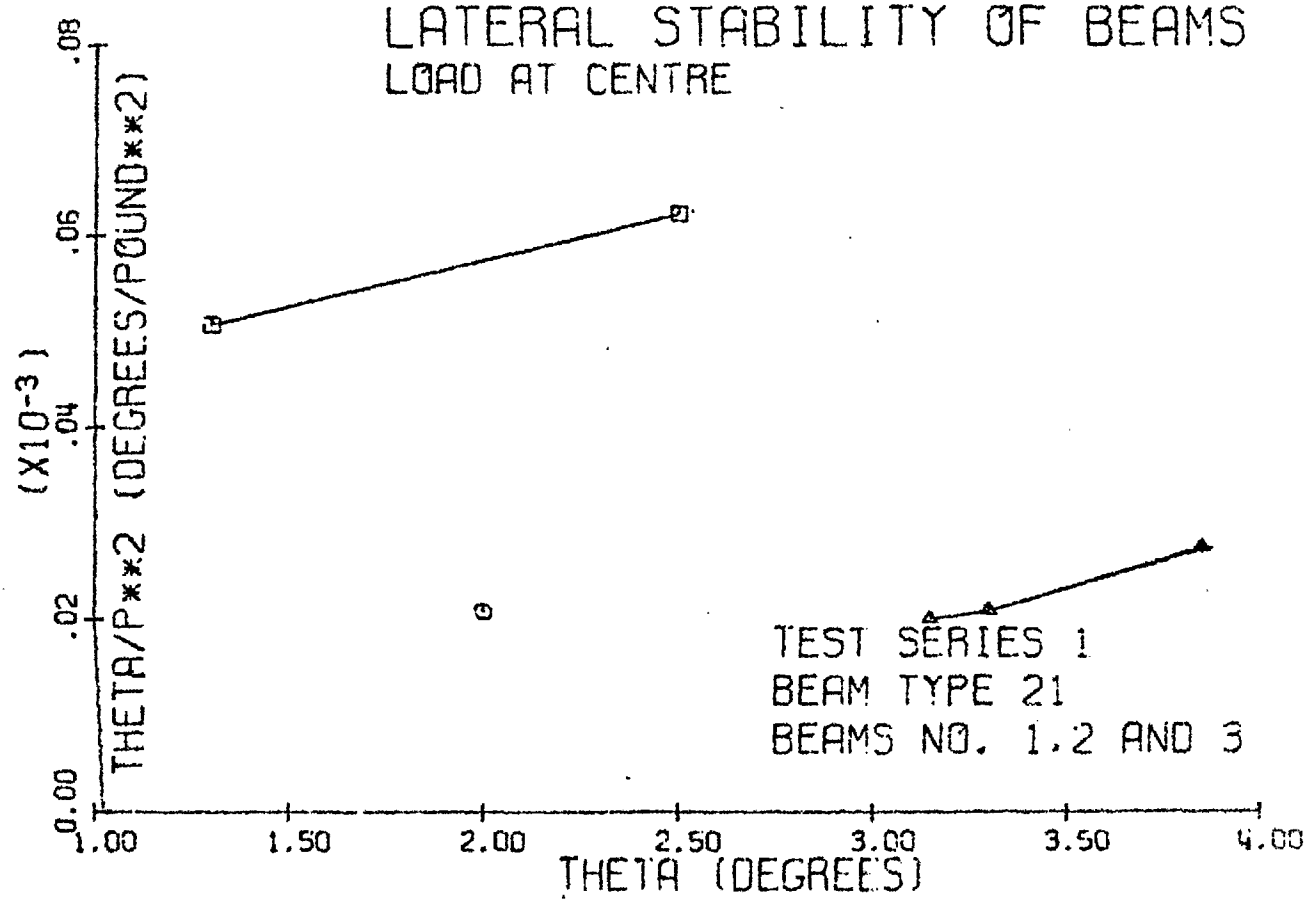


Figure C-1(a) Southwell plot, Test Series 1.

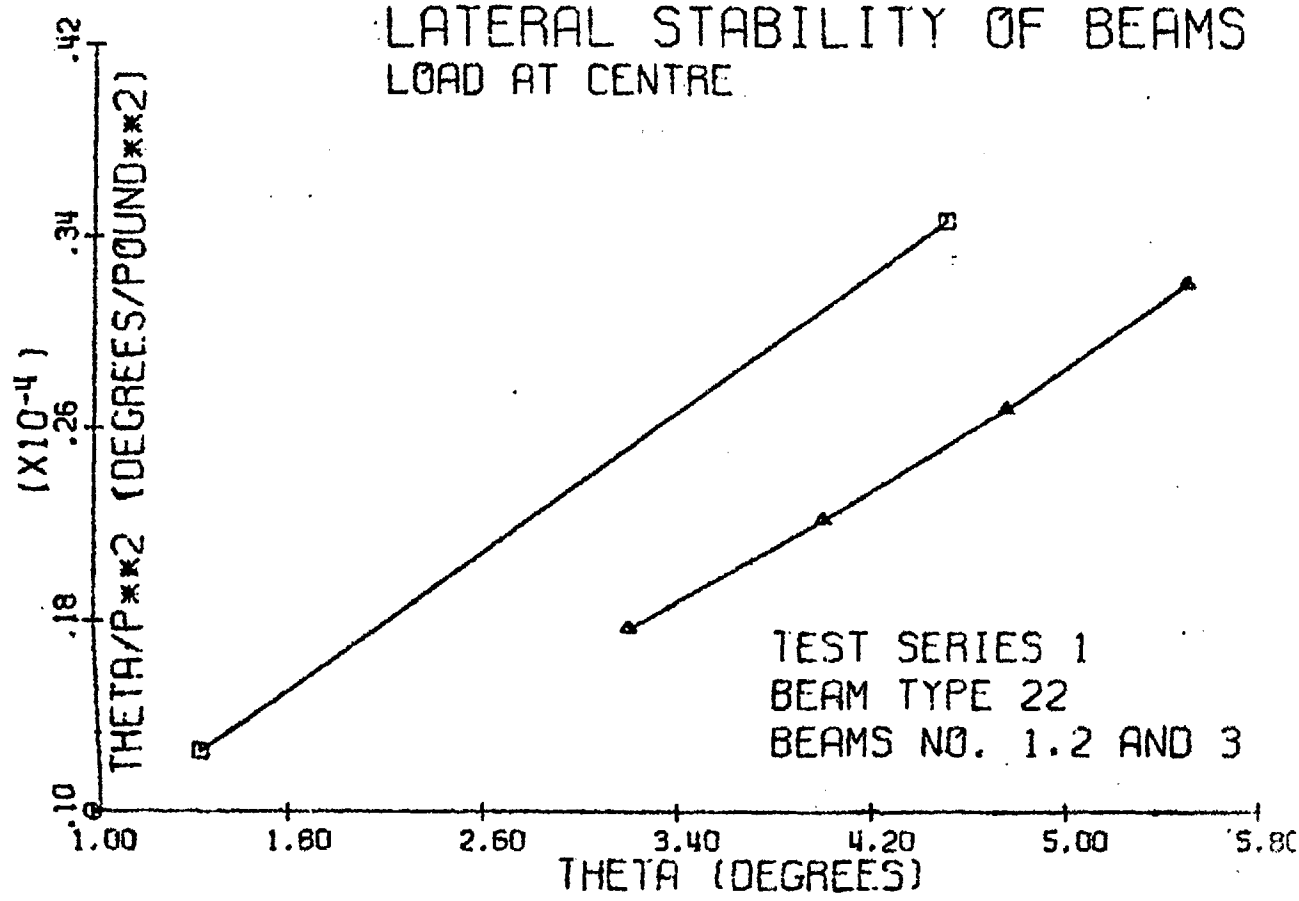


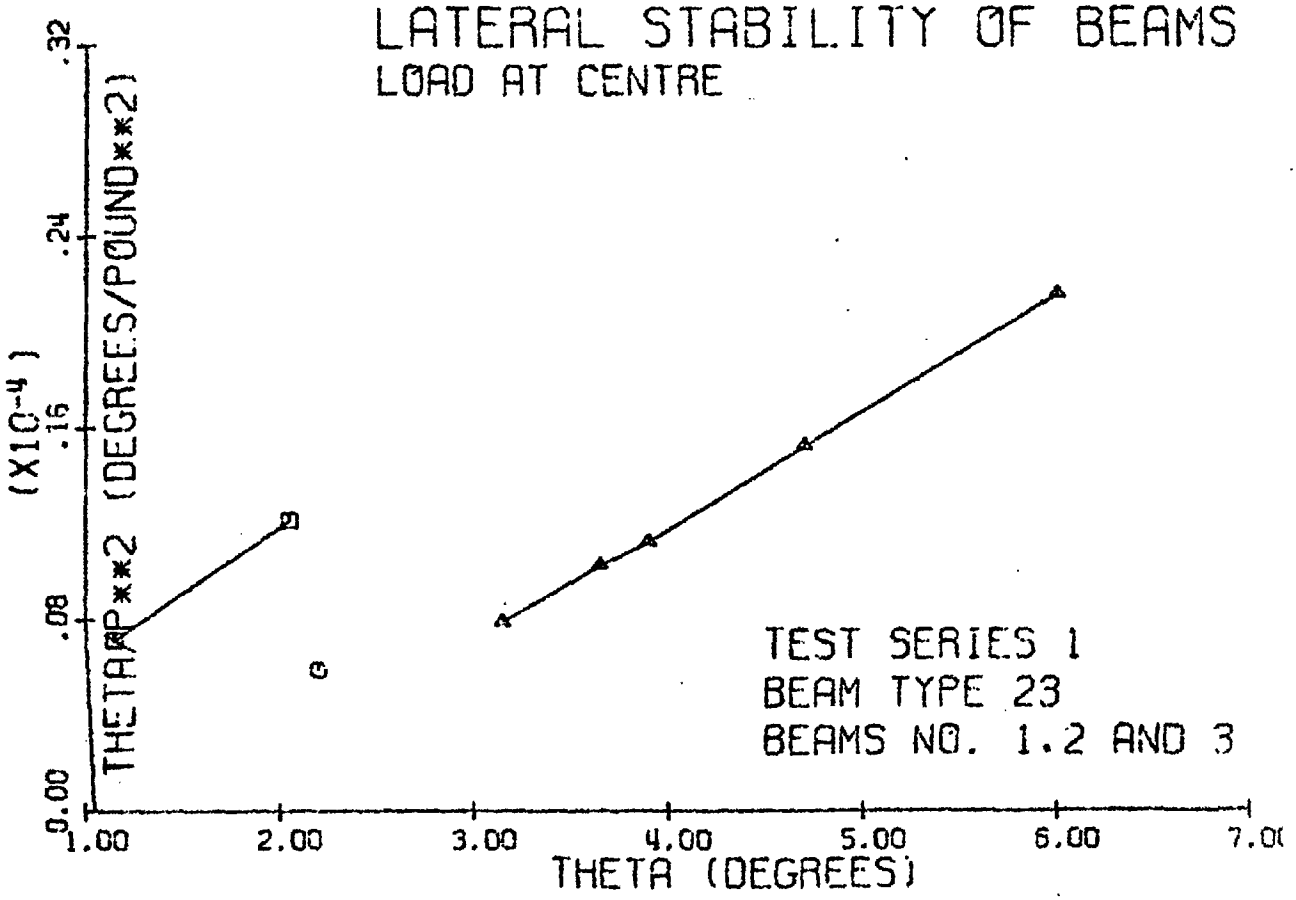


Figure C-1(a) (Continued) Southwell plot, Test Series 1

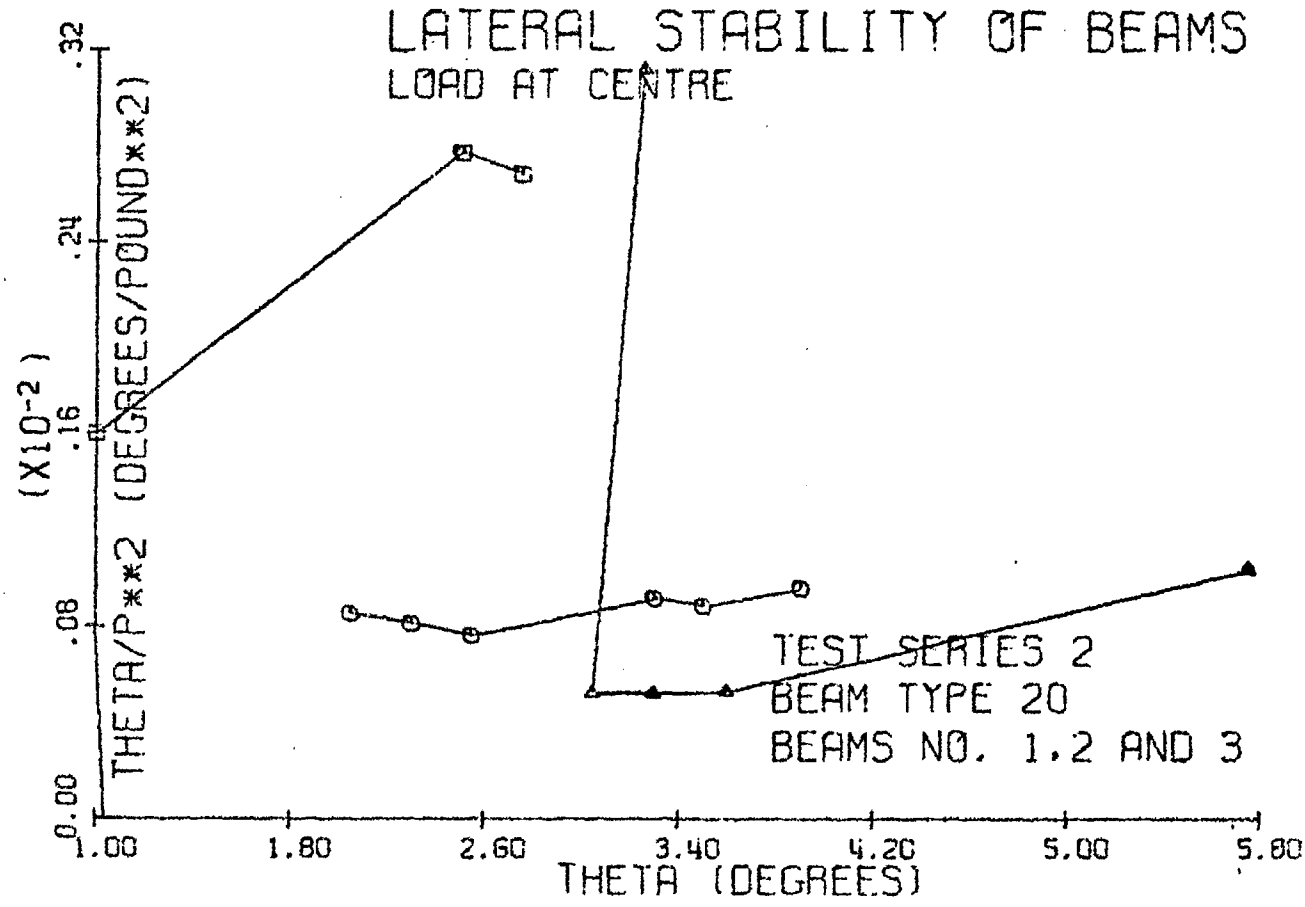


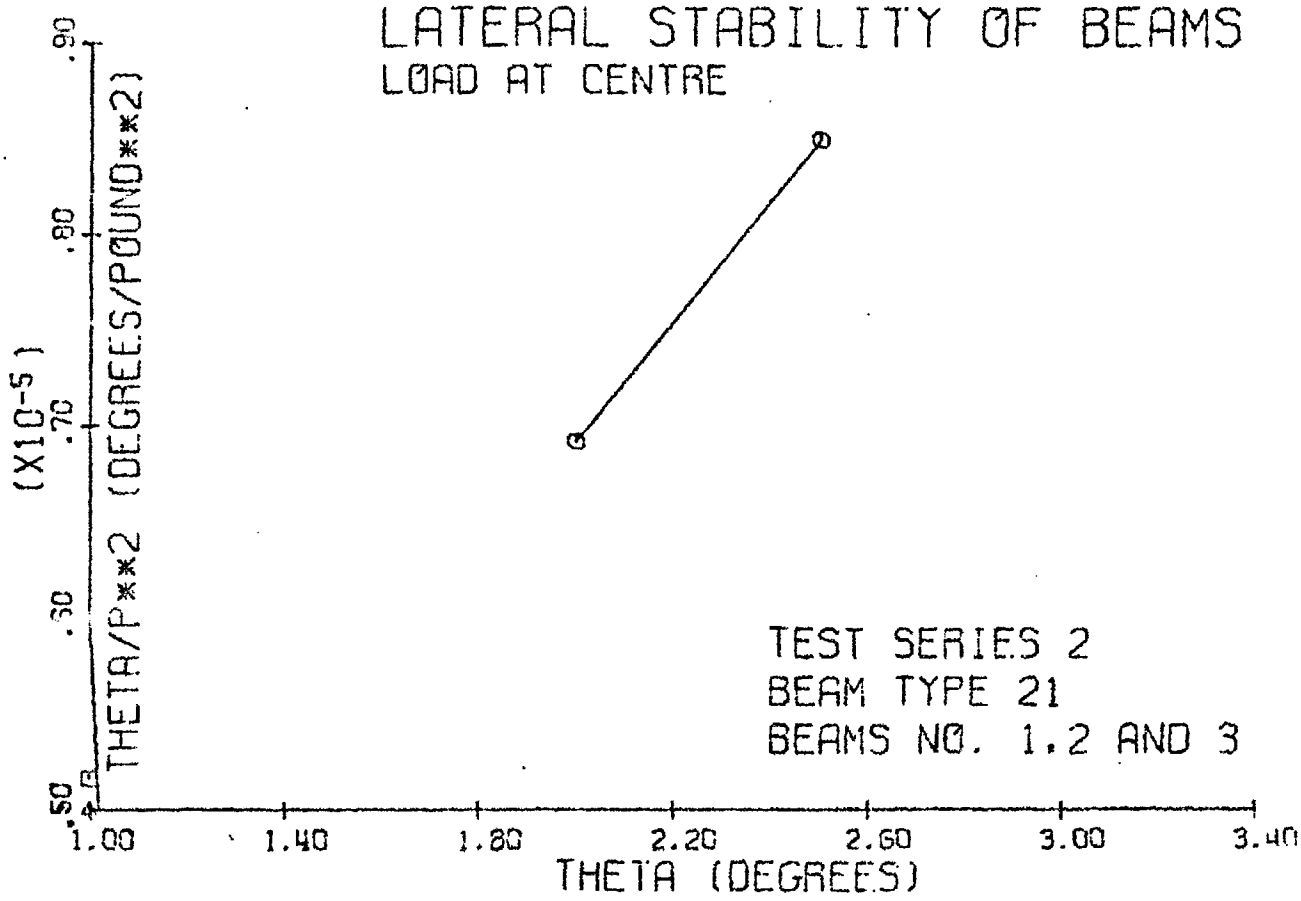


Figure C-1(b) Southwell plot, Test Series 2

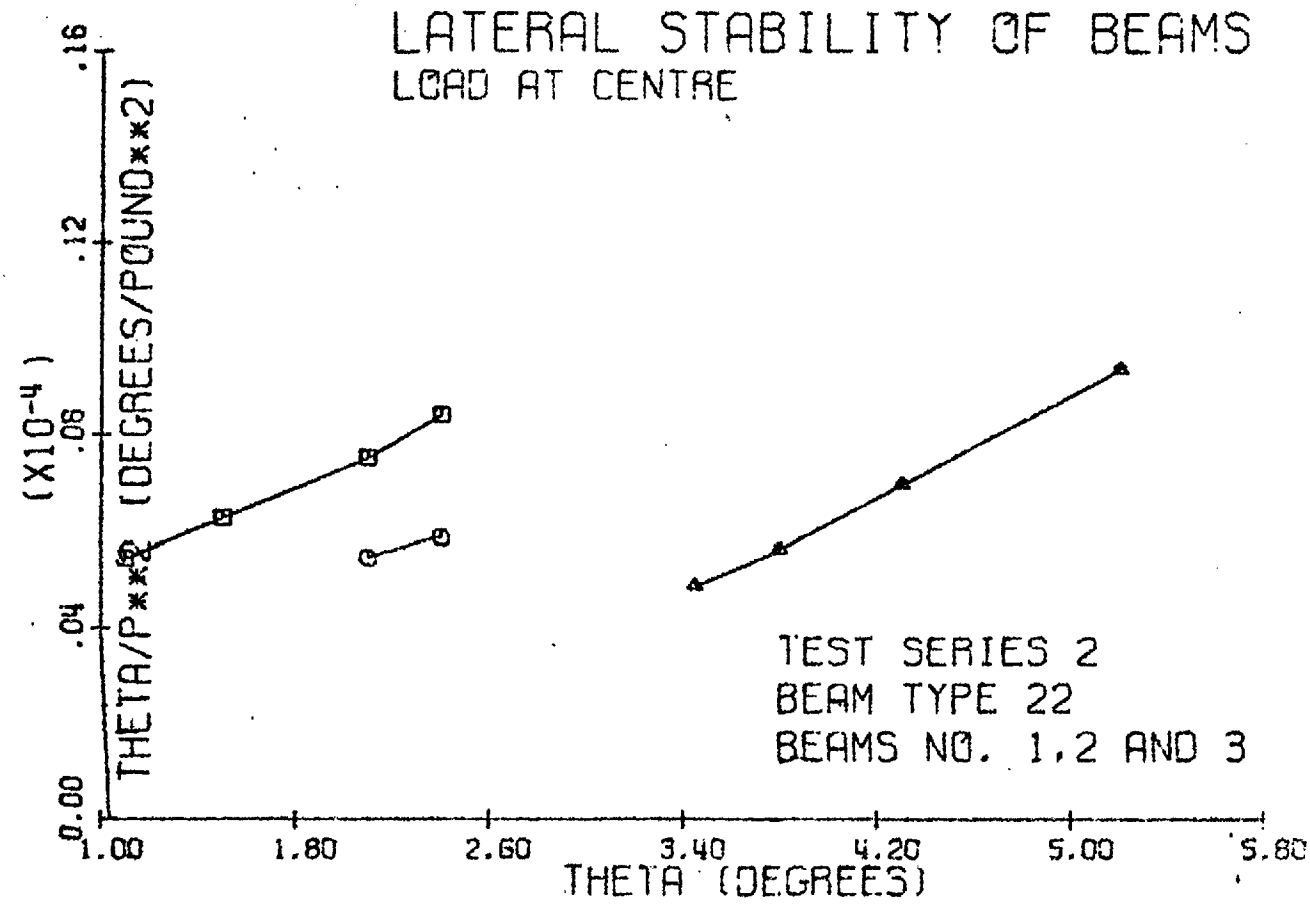


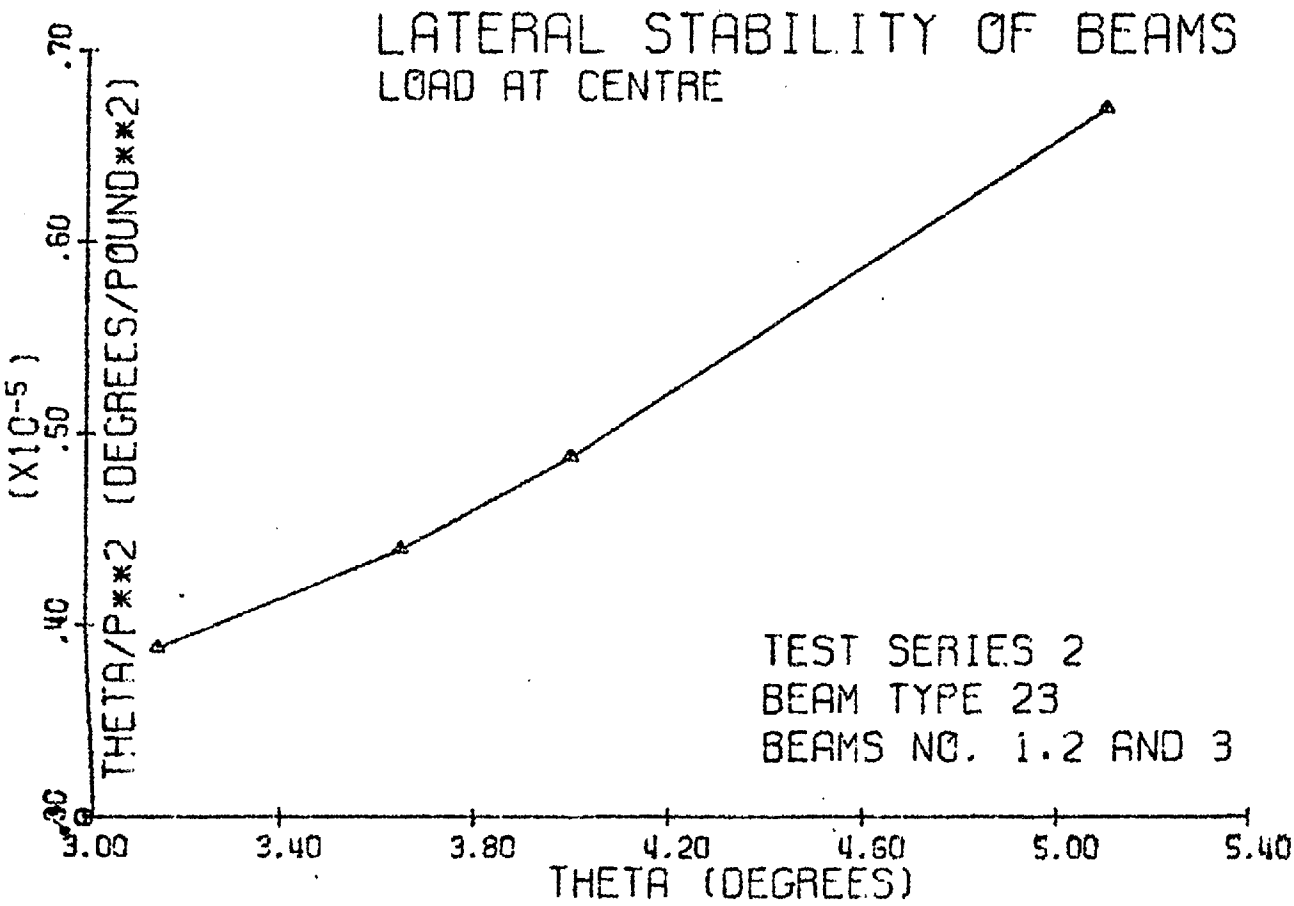


Figure C-1(b) (Continued) Southwell plot, Test Series 2

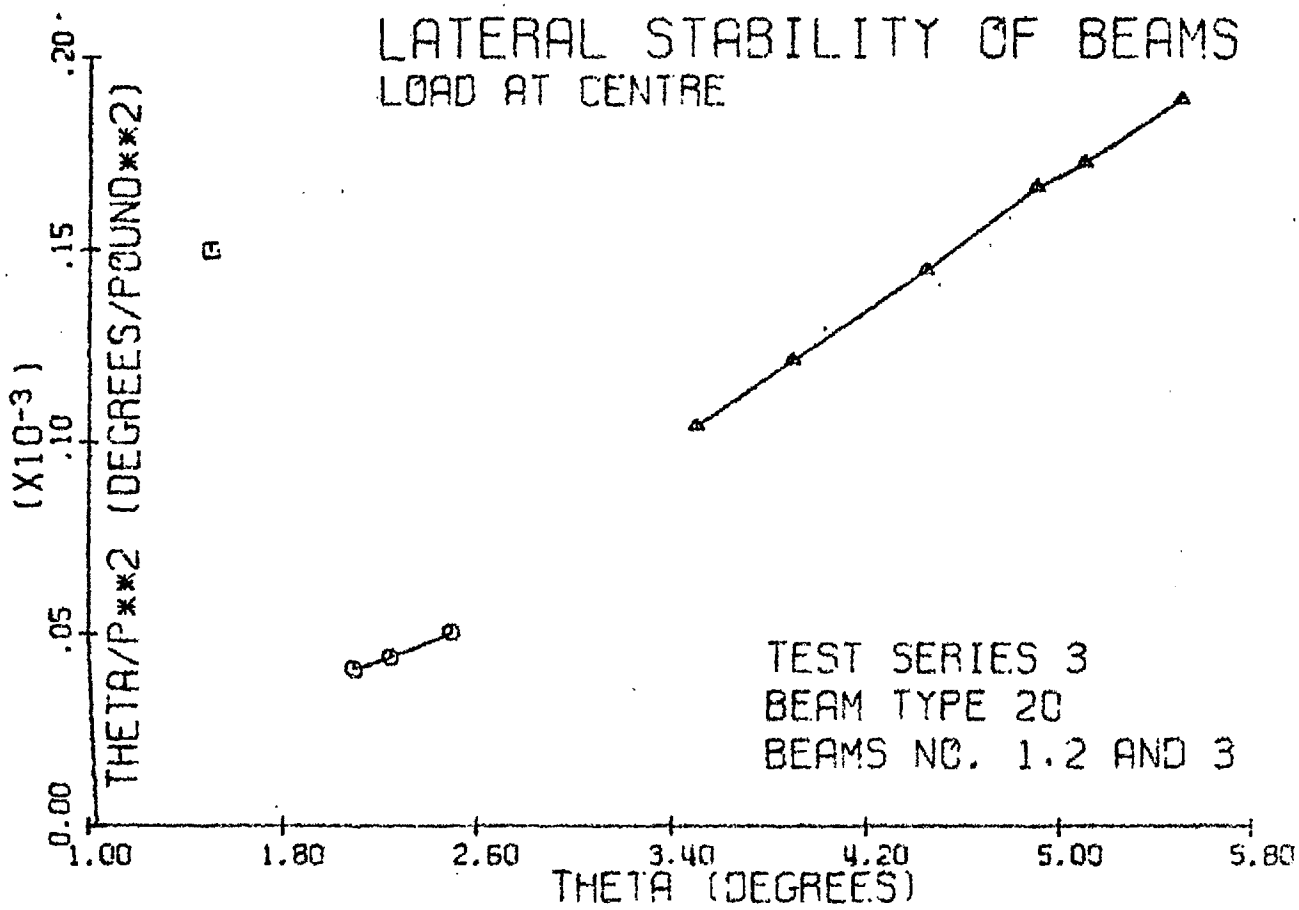


Figure C-1(c) Southwell plot, Test Series 3

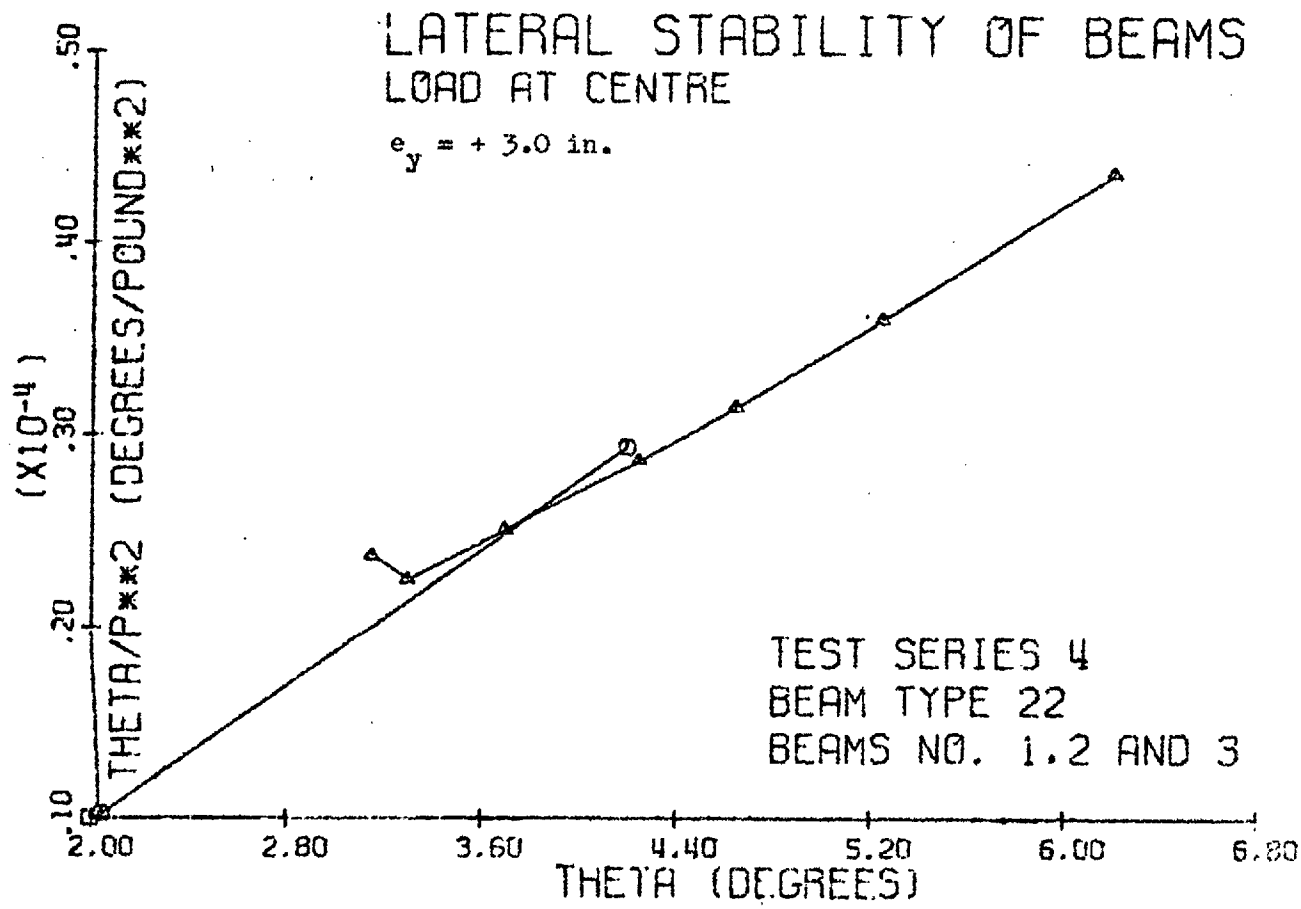


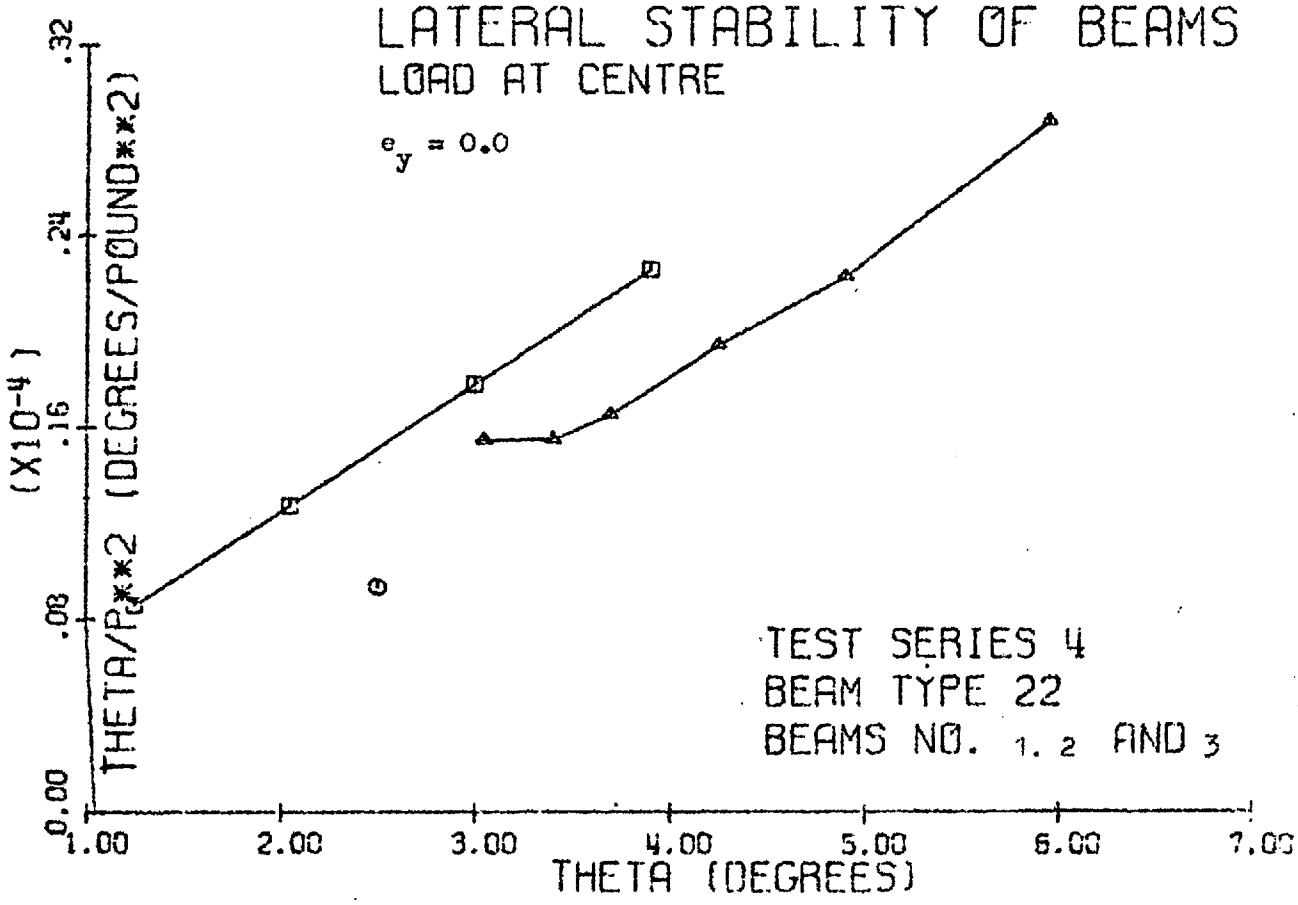


Figure C-1(d) Southwell plot, Test Series 4

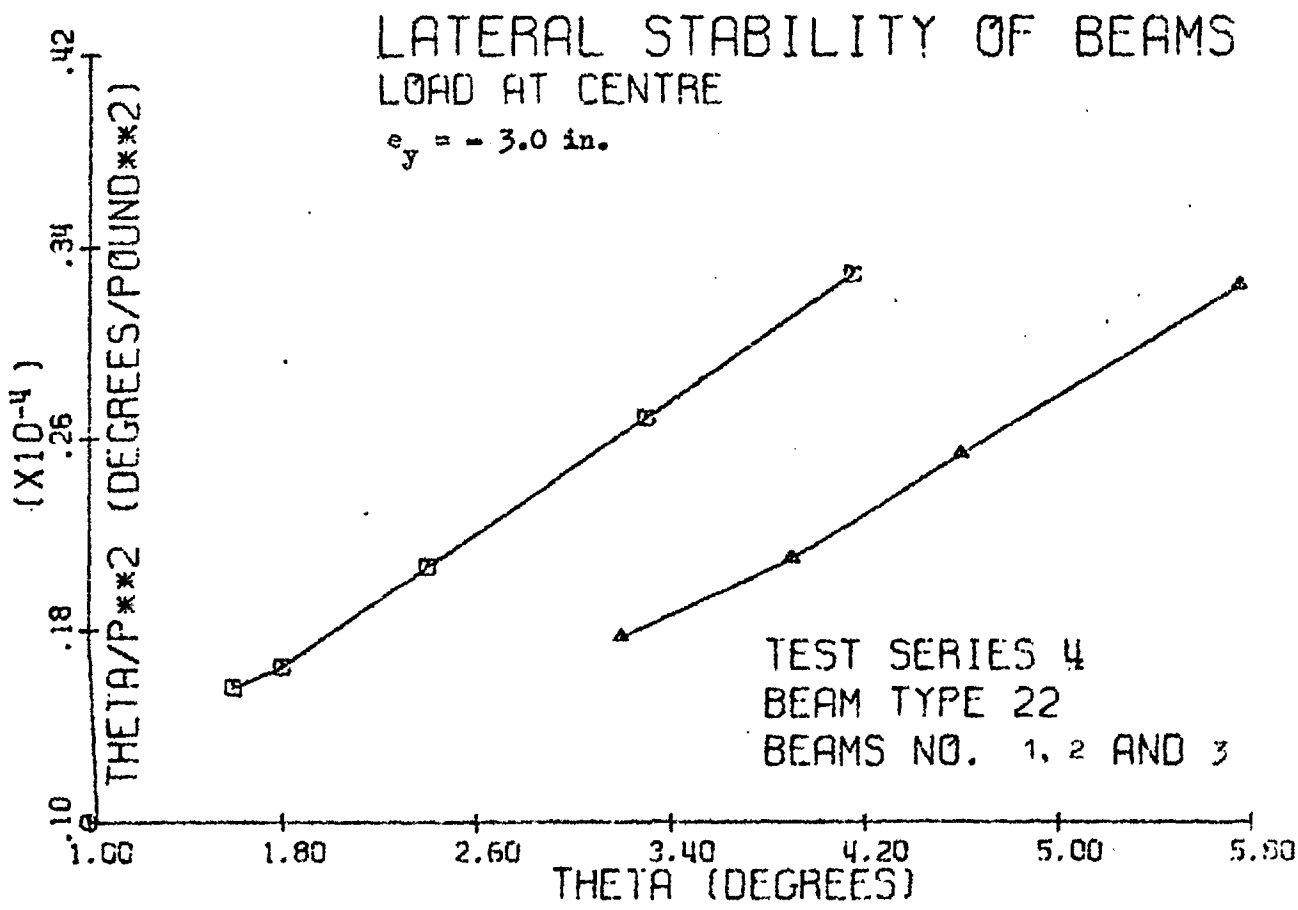


Figure C-1(d)(Continued) Southwell plot, Test Series 4

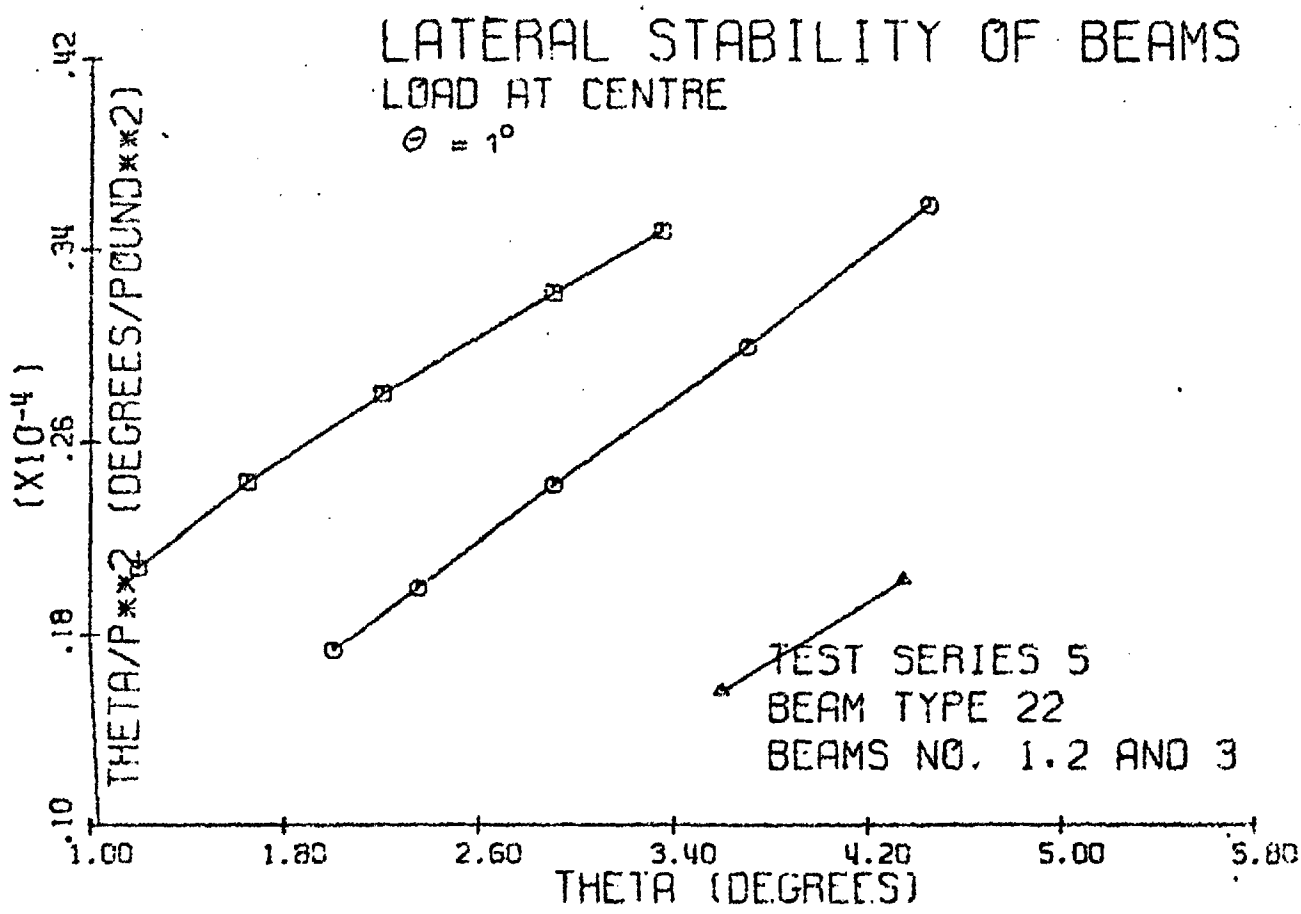


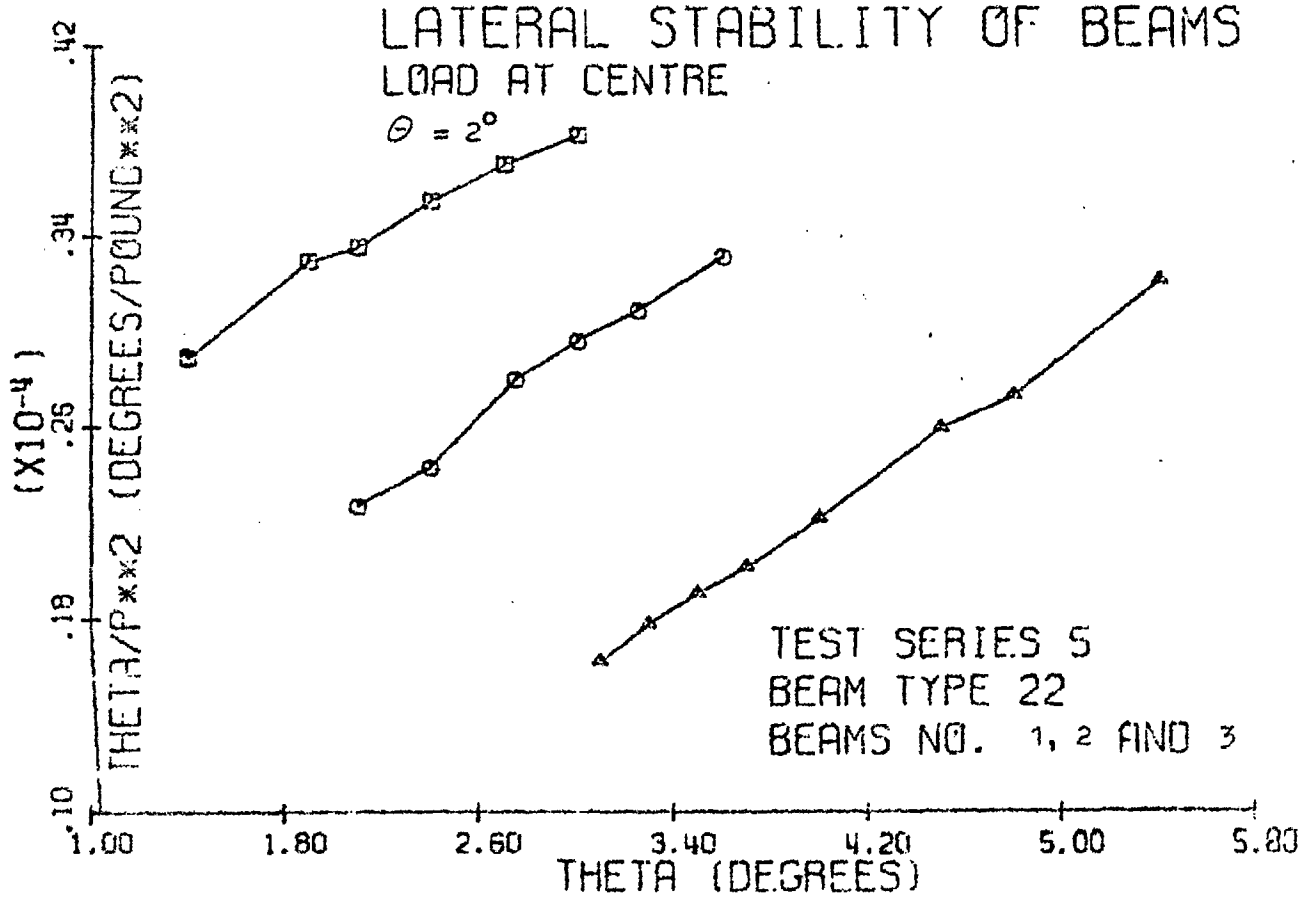


Figure C-1(e) Southwell plot, Test Series 5

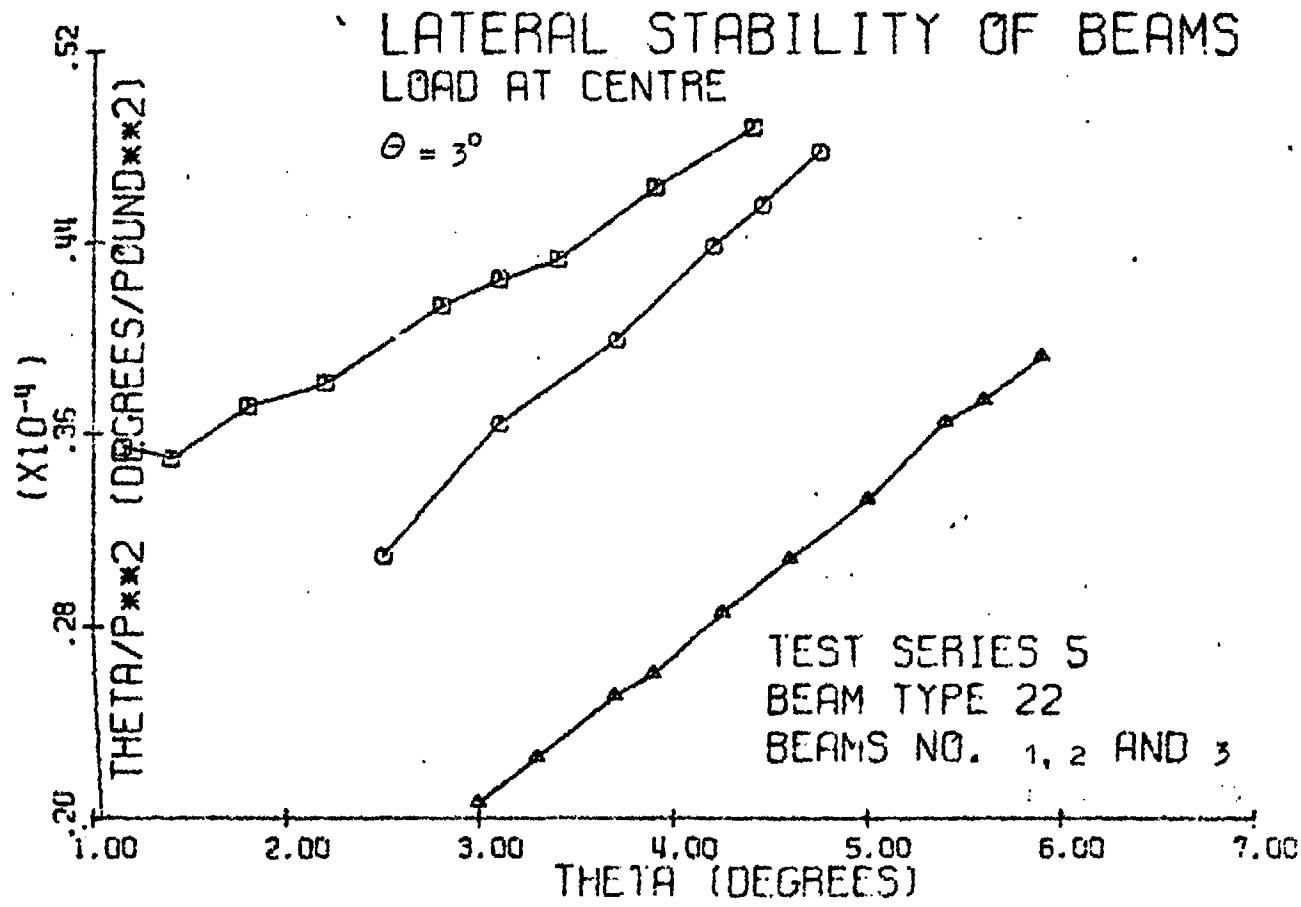


Figure C-1(e) (Continued) Southwell plot, Test Series 5

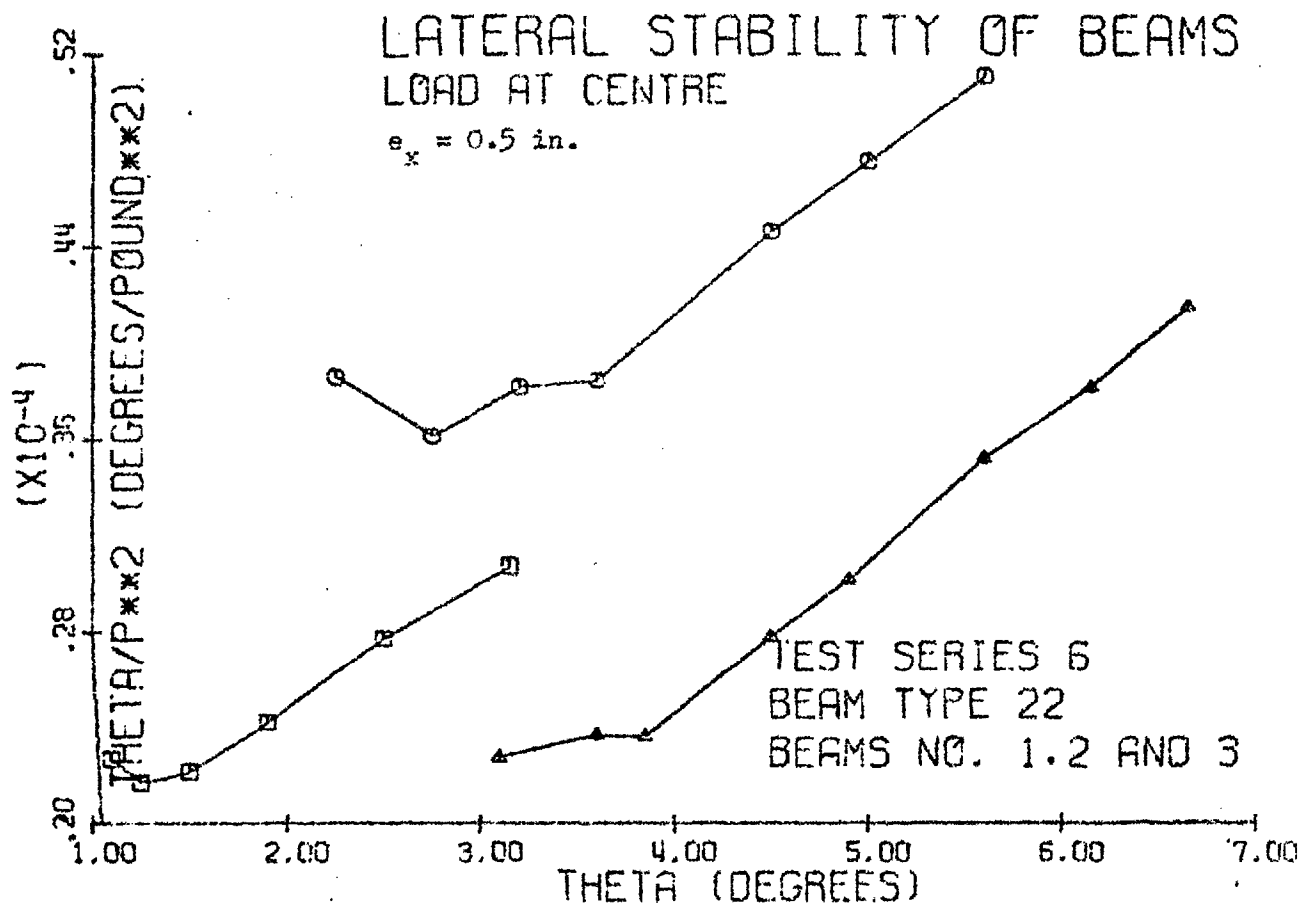


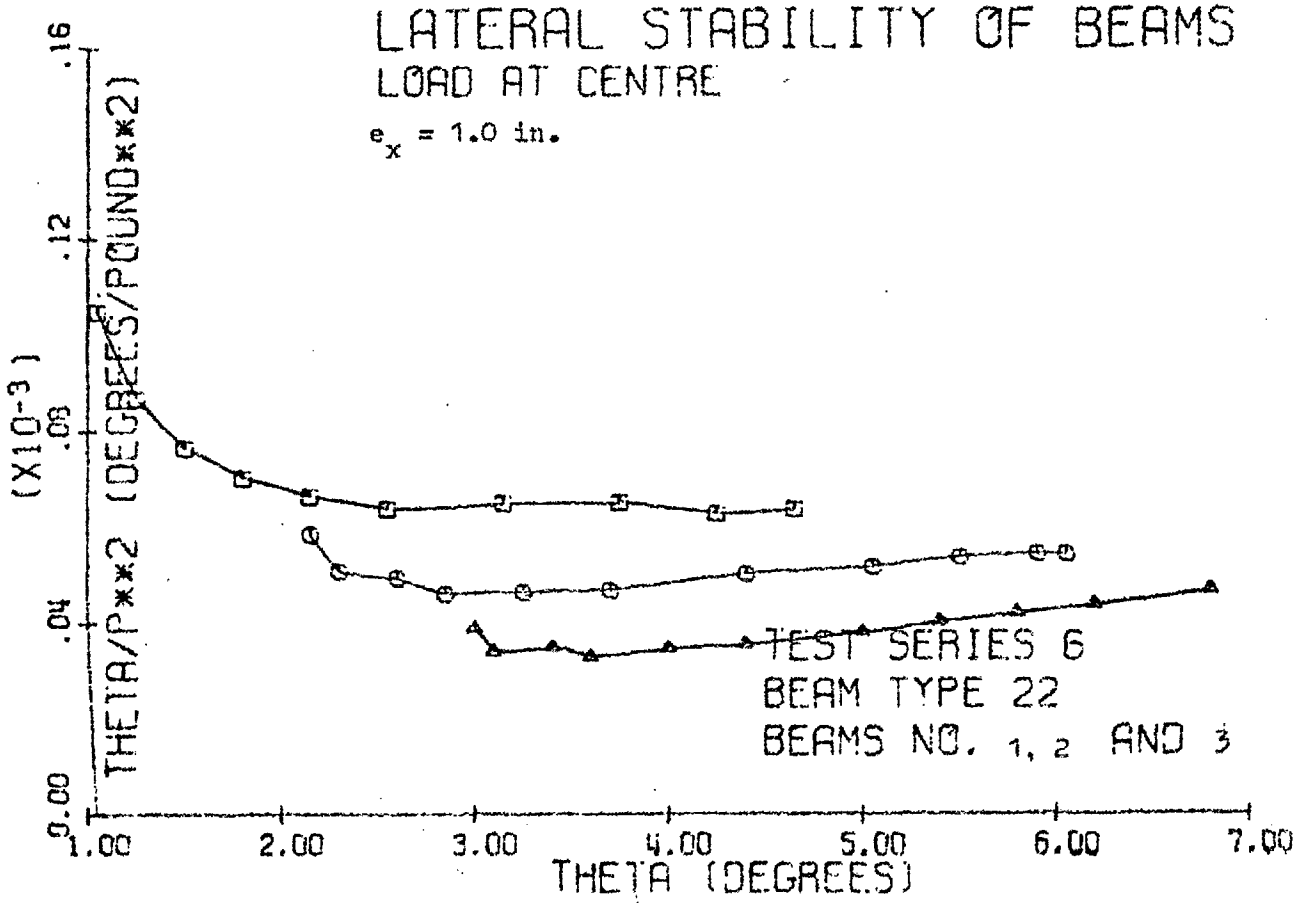


Figure C-1(f) Southwell plot, Test Series 6

# Appendix D

## Shear Deflections of Composite Beams

# SHEAR DEFLECTIONS OF COMPOSITE BEAMS

by

C. K. A. STIEDA

## INTRODUCTION

When computing the deflections of beams, usually only those which result from the deformations caused by bending stresses are considered. Deformations, however, also occur as a consequence of shear stresses and, in certain types of beams, the resultant deflections may be of considerable magnitude and should be considered in addition to the bending deflections.

Shear deflections of beams of isotropic materials, homogeneous throughout the whole section have been considered in detail by Newlin and Trayer (1924), Timoshenko (1955), Hahne (1962) and Cowper (1966). Of particular interest is an approach recently taken by Cziesielski (1965), who has used the strain energy method to calculate shear stiffness factors for beams having box-sections, I sections or cross-sections of unsymmetrical shape. A similar approach has also been taken recently by Mazur (1967), who also considers the shear deflection of beams with I-sections.

The purpose of the present analysis is to apply Cziesielski's approach to composite beams, constructed from plywood and solid timber and to derive an expression for the shear stiffness factor which will take into account the difference in the moduli of elasticity for the web (plywood) and the flanges (solid timber) of such beams. It will be

shown that, for the range of modular ratios usually encountered, the difference in the moduli of elasticity for web and flange has, indeed, little effect on the magnitude of the shear deflection. It is sufficient therefore, to calculate the shear deflection of composite timber beams on the basis that the section is continuously homogeneous throughout web and flanges. A procedure for calculating shear deflections will be given. The effect of differences in the modulus of rigidity on the shear deflection are not included in the present analysis.

## SHEAR DEFLECTION

As shown by Cziesielski (1965), the shear deflection of box- or I-beams can be derived from the condition that the work done by the shear forces V acting on a beam element of length dx must be equal to the integrated work of the shearing stresses, v (y), (Fig. 1) over the whole area A of the cross-section.

$$\tfrac{1}{2}\, V\, \bar{e}_s = \tfrac{1}{2}\, G \int_A v^2(y)\, dA \qquad (1)$$

where $G$ = modulus of rigidity

$\bar{e}_s$ = effective shear deformation of the section

It is assumed here that the modulus of rigidity of web and flange are the same. If the grain of the plywood is oriented either parallel or perpendicular to the grain of the timber, the modulus of rigidity of plywood will indeed be approximately the same as that of timber of the same species (Curry, 1964). If the grain of the plywood is oriented at 45 degrees to the span of the beam, the effective modulus of rigidity of the plywood is about three times that for parallel

orientation (CP 112:1967). This effect has not been considered as yet. However, since the largest contribution to the shear deflection is provided by the web, as will be shown below, it is not anticipated that a difference in the moduli of rigidity between web and flange will affect the shear deflection to any large extent.

When the shearing stress distribution over the cross-section is known, it is possible to evaluate the integral in Equation 1. The expression for the effective shear deformation $\bar{e}_s$ can then be written in the form

$$\bar{e}_s = \frac{V}{GbhF} \qquad (2)$$

where b and h, respectively, are the overall width and height of the section.

The quantity F is called the shear stiffness factor and will be derived below. From Equations 1 and 2, it follows that the shear stiffness factor is defined by

$$F = \frac{V^2}{bh \int_A v^2(y)dA} \qquad (3)$$

The additional deflection due to shear stress will be called $w_s$. From Figure 1, it will be seen that the shape of the shear deflection curve is given by

$$\bar{e}_s = \frac{dw_s}{dx}$$

The increment dx here is in the direction of the span, x being measured from one of the supports. Substitution of $\bar{e}_s$ in Equation 2 yields

$$\frac{dw_s}{dx} - \frac{V}{GbhF} = 0$$

Integration of this equation along the length of the beam up to x gives the shear deflection at the point x

$$w_s = \int_o^x \frac{Vdx}{GbhF} \qquad (4)$$

For beams of constant section the shear deflection becomes

$$w_s = \frac{1}{GbhF} \int_o^x Vdx \qquad (5)$$

And for simply supported beams, where $\int Vdx = M(x)$, the shear deflection at a point x is given by

$$w_s = \frac{M(x)}{GbhF} \qquad (6)$$

For a cantilever beam the shear deflection at the tip of the beam can also be calculated with Equation 6, provided the moment used in the calculation is the fixed end moment of the cantilever.

To obtain an explicit expression for the shear stiffness factor F, an expression for the shear stresses, v(y), must be derived and the integral in Equation 3 must be evaluated. Calculation of shear stresses in composite beams involves the bending stresses F(y), which will be given first.

## BENDING STRESS IN COMPOSITE BEAMS

It will be assumed that the engineer's theory of bending also applies to composite sections, i.e. sections that were

plane prior to bending will be assumed to remain plane during bending. As a consequence the stiffness of the composite section, - the product of the second moment of area, I, and the effective modulus of elasticity of the section, E - can be obtained by adding the stiffnesses of the individual components of the section

$$EI = E_1 I_1 + E_2 I_2 \qquad (7)$$

where $E_1$ ($E_2$) = modulus of elasticity of flanges (web)
$I_1$ ($I_2$) = second moment of area of flanges (web)

All second moments of area are calculated with respect to the centroid of the composite section. The total second moment of area is

$$I = I_1 + I_2 \qquad (8)$$

The stiffness of the composite section, given by Equation 7, should be used for calculating the bending deflections in the normal manner (Hahne, 1962, Timoshenko, 1955).

The flexural stresses in the flange at a distance y from the centroid of the section (Fig. 2) due to a bending moment M (x), are given by

$$f_1(y) = \frac{M(x)}{I} \frac{E_1}{E} y \qquad (9)$$

Similarly, the flexural stresses in the web are

$$f_2(y) = \frac{M(x)}{I} \frac{E_2}{E} y \qquad (10)$$

Introducing the modular ratio $n = E_2/E_1$ and taking account of Equation 7, the flange stresses can also be written as

$$f_1(y) = \frac{M(x)\, y}{I_1 + nI_2} \qquad (11)$$

Correspondingly, the flexural stresses in the web are

$$f_2(y) = \frac{M(x)\, n\, y}{I_1 + nI_2} \qquad (12)$$

It should be noted here that Equation 11 gives the stresses in the material having a modulus of elastcity $E_1$, i.e. in Fig. 2 this is the area (b - t)d called here the "flange". Similarly, "web" refers to all material having a modulus of elasticity $E_2$.

If plywood is considered as a material that can effectively carry loads only with those veneers that are stressed in the direction of the wood fibres - a design method generally adopted in North America (CSA-086, 1959) - then the modular ratio n usually can be replaced by the veneer ratio $t_v$, i.e. the ratio of the sum of all veneer thicknesses oriented parallel to the span to the total plywood thickness (Stieda, 1967). Furthermore, Equation 12, which in its present form is calculated for the total plywood thickness, then reduces to the form given by Equation 11, i.e. stresses for web and flange can be calculated with the same equation in the "parallel plies only" approach.

On the other hand, if plywood box- or I-beams are designed according to the "full cross-sectional" method (Curry, 1964, Booth and Reece, 1967), Equations 11 and 12 should be used to calculate the stresses in the flange and web separately.

Both methods of analysis lead to the same expression for the shear stiffness factor F. In the present analysis the "full cross-section" approach recommended by the British Standard Code of Practice is being used (Booth and Reece, 1967). Accordingly, shear stresses will be derived on the basis of Equations 11 and 12.

SHEAR STRESSES IN COMPOSITE BEAMS

In the engineers' theory of bending shear stresses are calculated by considering the equilibrium of forces acting on an element such as shown in Fig. 3. This element is an isolated part of a beam. On the two faces a distance dx apart normal f and shear stresses v are acting. On the lower face, parallel to the x-direction, only shear stresses are present. The equilibrium of forces in the x-direction requires that the total shear force on the lower surface is equal to the difference between the forces on the element due to normal stresses on flange ($F_1$) and web ($F_2$).

$$v(y).b(y).dx = (F_1 + F_2)_{x=x+dx} - (F_1 + F_2)_{x=x}$$
$$= dF_1 + dF_2 \qquad (13)$$

where $b(y)$ = width of shear area at a distance y from the centroid of the beam cross-section.

The contribution of one flange to the total force on the element dx is

$$F_1 = \int_I^c f_1(y)\,(b - t)\,dy \qquad (14)$$

where the lower limit I of the integral is equal to either y - if y is larger than (c - d) - or (c - d) - if y is less than (c - d) -.

In view of Equation 11 the force on the flange can be written

$$F_1 = \frac{M(x)}{(I_1+nI_2)} \int_I^c (b - t)\,y\,dy \qquad (15)$$

The integral in Equation 15 represents the static moment of the area $A(y) = (b - t)(c - y)$ about the centroid of the

section. This static moment is frequently called Q(y). The difference in the forces acting on the flange (Equation 13) therefore becomes

$$dF_1 = \frac{dM(x)}{I_1 + nI_2} \; Q_1(y) \tag{16}$$

where $dM(x) = M(x + dx) - M(x)$

and $Q_1(y) = \int_c^I (b - t)\, y\, dy \tag{17}$

For the web the difference between the forces on either side of the element is

$$dF_2 = \frac{dM(x)}{I_1 + nI_2} \; n\, Q_2(y) \tag{18}$$

where $Q_2(y)$ is the static moment of the partial web area $A(y) = t.(c - y)$ about the centroid of the whole cross-section

$$Q_2(y) = \int_c^1 tydy \tag{19}$$

With these two expressions for the difference in the direct forces on the element $(c - y)\, dx$ the shear stress can be calculated from Equation 13:

$$v(y) = \frac{dM(x)}{dx\, b(y)} \; \frac{(Q_1(y) + n\, Q_2(y))}{(I_1 + nI_2)} \tag{20}$$

Or, since the shear force $V = dM(x)/dx$,

$$v(y) = \frac{V}{b(y)} \; \frac{Q_1(y) + nQ_2(y)}{I_1 + nI_2} \tag{21}$$

In beams with box- or I-sections the width of the web (b(y) = t) will be only a fraction of the total width of the beam (b(y) = b). It is apparent therefore from Equation 21 that the shear stresses in the web will be several times those in the flange. In addition, the decreasing value of Q(y) as y increases (Equations 17 and 19) will bring a further reduction in the shear stresses of the flange as compared with those in the web.

The shear stiffness factor F can now be obtained by combining Equations 3 and 21

$$F = \frac{(I_1 + nI_2)^2}{bh \int_A \left[Q_1(y) + nQ_2(y)\right]^2 / b^2(y)\, dA} \qquad (22)$$

For any particular cross-section, the integral in Equation 22 can be readily evaluated. As an example symmetrical box- and I sections will be considered. The dimensions of the box-section are given in Fig. 2. The depth $d_1$ and $d_2$ of the compression and tension flanges shall be equal, $d_1 = d_2 = d$. If t is taken to be equal to the summation of all individual web thicknesses, then the expressions given below will also apply to an I-section with a single web of thickness t.

For the whole cross-section the second moments of area in Equation 22 are

$$I_1 = \tfrac{1}{2}(b - t)d(h - d)^2 + \frac{1}{6}(b - t)d^3$$

$$I_2 = \frac{1}{12}\, th^3$$

The numerator in Equation 22 can therefore be written

$$(I_1 + nI_2)^2 = (bh^3)^2 \, C_1^2 \qquad (23)$$

where $C_1 = \frac{1}{6} \alpha (1 - \beta)(3 - 6\alpha + 4\alpha^2) + \frac{1}{12} n \beta$ (24)

and $\alpha = d/h$
$\beta = t/b$

To calculate the denominator of Equation 22, the integral has to be calculated in two parts, for $b(y) = t$ and $b(y) = b$. Considering first the region between $y = 0$ and $y = \frac{1}{2}h - d$, i.e. $b(y) = t$, it is apparent that the contribution of one flange area to the static moment is constant

$$Q_1 = \tfrac{1}{2} bh^2 \, \alpha (1 - \alpha)(1 - \beta) \qquad (25)$$

The contribution of the web area for one half of the section is found from Equation 19 as

$$Q_2(y) = \tfrac{1}{8} bh^2 \, \beta \left[1 - (2y/h)^2\right] \qquad (26)$$

With these two expressions for the static moments $Q_1$ and $Q_2$ the denominator in Equation 22 for the region, where $b(y) = t$, becomes

$$2\,bh \int_0^t \int_0^{0.5h(1-2\alpha)} \left[Q_1(y) + nQ_2(y)\right]^2 / b^2(y) \, dy \, dx = b^2 h^6 C_2 \qquad (27)$$

where $C_2 = \frac{1}{4}\alpha^2(1 - 2\alpha)(1 - \alpha)^2(1 - \beta)^2/\beta$
$+ \frac{1}{12} n \alpha (1 - \alpha)(1 - 2\alpha)(1 + 2\alpha - 2\alpha^2)(1 - \beta$
$+ \frac{1}{120} n^2 (1 - 2\alpha)(1 + 2\alpha + 4\alpha^2 - 12\alpha^3 + 6\alpha^4)\beta$

.....(28)

Similarly for the wider part of the box section, i.e. $b(y) = b$ and $y$ larger than $\frac{1}{2}h - d$, the static moments are

$$Q_1(y) = \tfrac{1}{8} bh^2(1 - \beta)\left[1 - (2y/h)^2\right] \qquad (29)$$

$$Q_2(y) = \tfrac{1}{8} bh^2 \beta \left[1 - (2y/h)^2\right] \qquad (30)$$

The second part of the denominator in Equation 22 therefore becomes

$$2bh \int_0^b \int_{0.5h(1-2\alpha)}^{0.5h} \left[Q_1(y) + nQ_2(y)\right]^2/b^2 \, dy \, dx:$$

$$= b^2h^6C_3 \qquad (31)$$

where $C_3 = \frac{1}{60} (1 - \beta + n\beta)^2(10\alpha^3 - 15\alpha^4 + 6\alpha^5)$ (32)

Finally with these two expressions, Equations 27 and 31, for the double integral in Equation 22 together with Equation 23 the shear stiffness factor F can now be written in a dimensionlar form as

$$F = \frac{C_1^2}{C_2 + C_3} \qquad (33)$$

where $C_1$, $C_2$ and $C_3$ are given by Equations 24, 28 and 32.

## CALCULATIONS

The shear stiffness factor F, Equation 33, has been calculated for a number of flange-depth to beam-height ratios , web-thickness to beam-width ratios , and modular ratios n. Ratios of n for plywood composite timber sections usually range from 0.5 to 0.7. For a homogeneous section

with the same material for flange and web n = 1.0. For a modular ratio of n = 1.0 the values of the shear stiffness factor F become identical to those given by Cziesielski. Shear stiffness factors for modular ratios of n = 0.5 and n = 1.0 are given in Tables 1 and 2.

## EXPERIMENTAL WORK

To check the validity of Equation 5, several simply supported plywood box beams were loaded and the resulting deflections were observed. The bending stiffness, EI, of these beams was calculated from the deflections at the centre relative to the load points, when beams were loaded at the third points.

This bending stiffness was used to compute the overall deflection due to bending alone. An experimental shear deflection, $w_s$, was then calculated by subtracting from the observed overall deflection, w, the calculated bending deflection, $w_b$.

$$w_s = w - w_b \qquad (34)$$

These experimental shear deflections were obtained for sixteen-foot long beams loaded first at the centre and then at the third points as well as for eight-foot long beams loaded at the centre only. Experimental shear deflections were then compared with deflections computed with Equation5 . The modulus of rigidity for these calculations was determined experimentally from small shear plate specimens cut from a number of the test beams after the main tests had been completed.

The cross-sectional dimensions of the test beams are given in Table 3. All beams were a nominal sixteen inches deep. Three different flange depths and two flange widths are represented by the six beam types. Flanges were Douglas

fir lumber, while the webs consisted of 5/16 in Douglas fir plywood. The plywood was nail-glued to the flanges.

The results of these tests are given in Tables 4 to 6. Both the experimental and the computed deflections show that shear deflections in box beams can contribute considerable to the overall deflections. For the sixteen-foot long beams, with a span to depth ratio of 11.6, the computed shear deflections range from about $\frac{1}{4}$ to $\frac{1}{2}$ of the bending deflection, the range for the experimental values is somewhat higher. For the short eight-foot long beams, however, the shear deflection equals or even exceeds the deflection due to normal stresses.

## DISCUSSION

A comparison of the shear stiffness factors given in Tables 1 and 2 shows that for the ratios of moduli of elasticity usually encountered in plywood box- and I-beams shear deflections are not greatly affected by any difference in the moduli of elasticity of flange and web. For example, a plywood box-beam with a flange-depth to beam-height ratio of $\alpha = 0.2$ and a web-thickness to beam-width ratio of $\beta = 0.1$, having a modular ratio of $n = 0.5$, has a shear stiffness factor of 0.107. A beam of the same dimensions, but with the same material in flange and web, i.e. $n = 1.0$, shows an identical shear stiffness factor. Only if the web thickness of the same beam is increased to 0.15 times the beam width, does the shear stiffness factor show any difference at all between the homogeneous section and the plywood beam. Even for a rather unrealistic ratio of $\beta = 0.4$, the value of the shear stiffness factor for the plywood box beam is only two per centlarger than that for the beam with a modular ratio of 1.0.

In engineering calculations, differences of this order of magnitude are insignificant, particularly so when one considers the low accuracy of the value for modulus of rigidity which

must be used to calculate shear deflections. It is suggested, therefore, that the shear stiffness factors for a modular ratio of 1.0 be used also for the calculation of shear deflections of plywood box-beams.

Comparing calculated and measured deflections, it is found that for short beams, shear deflections can be over twice the value of the corresponding bending deflections. Considering the variability of G and the resulting errors in the calculated shear deflections, the observed shear deflections agree reasonably well with those calculated with Equation 5. The use of this equation together with the appropriate shear stiffness factor from Table 2 is, therefore, suggested as an acceptable alternative to the method presently recommended in the Canadian Standard for "Engineering Design in Timber". (Canadian Standards Association, 1959).

## SUMMARY

An analytical expression for the shear deflection of composite box- or I-beams has been derived. A dimensionless factor, the shear stiffness factor, F, has been calculated for various values of the ratio n for the moduli of elasticity for web and flange. The results show that this factor differs little from that computed for similar beams with the same material in flange and web. To find the total deflection of the beam the shear deflections calculated in this manner should be added to the bending deflections computed in the usual way. Equation 33 for the calculation of the shear stiffness factor is identical to that given previously by the author in a report, where the load-carrying capacity of the plywood was considered in terms of veneers oriented parallel to the span of the beam,(Stieda, 1967). Finally, experimental data are presented which indicate that this method gives a reasonable estimate of the shear deflections.

REFERENCES

Booth, L. G. and Reece, P. O. (1967) The Structural Use of Timber. A Commentary on the British Standard Code of Practice, CP.112. Spon, London.

Canadian Standards Assoication (1959) CSA-Code 086-1959, Engineering Design in Timber. Ottawa.

Cowper, G. R. (1966) The Shear Coefficient in Timoshenko's Beam Theory. Journal of Applied Mechanics, Vol. 33, Series E, No. 2, pp. 335-340.

Curry, W. T. (1964) The Derivation of Design Stresses for Plywood. Wood, May, 1964.

Cziesielski, E. (1965) Ermittlung des Schubwiderstandes $F_y^Q$ symmetrischer I-und Hohlkastenquerschnitte sowie symmetrischer und unsymmetrischer Winkelquerschnitte. Bautechnik, Vol. 42, No. 7, pp. 232-237.

Hahne, H. V. (1962) Bending of Beams. Chapter 35 in Handbook of Engineering Mechanics, edited by W. Flügge. McGraw-Hill, London.

Mazur, S. J. (1967) Shear strain energy and shear deflection constants. Studies in Structural Engineering, No. 1. Nova Scotia Technical College, Halifax, N.S.

Newlin, J. A. and Trayer, G. W. (1924) Deflections of Beams with Special Reference to Shear Deformations. U.S. Forest Products Laboratory Report No. 1309. Reaffirmed March, 1956.

Stieda, C. K. A. (1967) A Shear Stiffness Factor for Plywood Box Beams. Forest Products Laboratory, Vancouver. Information Report VP-X-31.

Timoshenko, S. (1955) Strength of Materials, Part 1, Third Edition, Van Nostrand, London.

ACKNOWLEDGEMENT

The experimental work reported in this paper was done at the Vancouver Forest Products Laboratory of the Department of Forestry and Rural Development, Government of Canada.

TABLE I - SHEAR STIFFNESS FACTOR F FOR PLYWOOD BOX- AND I-BEAMS

$n = 0.50$

| ALPHA = d/h | 0. | 0.050 | 0.100 | 0.150 | 0.200 | 0.250 | 0.300 | 0.350 | 0.400 | 0.450 | 0.500 |
|---|---|---|---|---|---|---|---|---|---|---|---|
| BETA = t/b | | | | | | | | | | | |
| 0.05 | 0.042 | 0.050 | 0.050 | 0.052 | 0.055 | 0.059 | 0.067 | 0.080 | 0.109 | 0.185 | 0.833 |
| 0.10 | 0.083 | 0.098 | 0.100 | 0.103 | 0.107 | 0.116 | 0.129 | 0.153 | 0.200 | 0.314 | 0.833 |
| 0.15 | 0.125 | 0.146 | 0.148 | 0.152 | 0.158 | 0.170 | 0.188 | 0.220 | 0.278 | 0.408 | 0.833 |
| 0.20 | 0.167 | 0.193 | 0.196 | 0.200 | 0.208 | 0.221 | 0.243 | 0.280 | 0.346 | 0.480 | 0.833 |
| 0.25 | 0.208 | 0.238 | 0.242 | 0.247 | 0.256 | 0.271 | 0.295 | 0.336 | 0.405 | 0.537 | 0.833 |
| 0.30 | 0.250 | 0.283 | 0.287 | 0.293 | 0.302 | 0.318 | 0.345 | 0.387 | 0.457 | 0.583 | 0.833 |
| 0.35 | 0.292 | 0.327 | 0.332 | 0.337 | 0.347 | 0.364 | 0.391 | 0.434 | 0.504 | 0.621 | 0.833 |
| 0.40 | 0.333 | 0.370 | 0.375 | 0.381 | 0.391 | 0.408 | 0.435 | 0.478 | 0.545 | 0.653 | 0.833 |
| 0.45 | 0.375 | 0.412 | 0.418 | 0.424 | 0.434 | 0.451 | 0.477 | 0.519 | 0.582 | 0.680 | 0.833 |
| 0.50 | 0.417 | 0.453 | 0.460 | 0.466 | 0.475 | 0.491 | 0.517 | 0.557 | 0.616 | 0.704 | 0.833 |

TABLE 2 - SHEAR STIFFNESS FACTOR F FOR PLYWOOD BOX- AND I-BEAMS

$n = 1.00$

| ALPHA = d/h | 0. | 0.050 | 0.100 | 0.150 | 0.200 | 0.250 | 0.300 | 0.350 | 0.400 | 0.450 | 0.500 |
|---|---|---|---|---|---|---|---|---|---|---|---|
| BETA = t/b | | | | | | | | | | | |
| 0.05 | 0.042 | 0.049 | 0.050 | 0.052 | 0.054 | 0.059 | 0.067 | 0.080 | 0.108 | 0.185 | 0.833 |
| 0.10 | 0.083 | 0.097 | 0.099 | 0.102 | 0.107 | 0.115 | 0.129 | 0.153 | 0.200 | 0.313 | 0.833 |
| 0.15 | 0.125 | 0.143 | 0.146 | 0.150 | 0.157 | 0.168 | 0.187 | 0.219 | 0.278 | 0.408 | 0.833 |
| 0.20 | 0.167 | 0.188 | 0.192 | 0.197 | 0.205 | 0.219 | 0.241 | 0.279 | 0.345 | 0.480 | 0.833 |
| 0.25 | 0.208 | 0.231 | 0.236 | 0.242 | 0.252 | 0.267 | 0.293 | 0.334 | 0.404 | 0.536 | 0.833 |
| 0.30 | 0.250 | 0.274 | 0.280 | 0.287 | 0.297 | 0.314 | 0.341 | 0.385 | 0.456 | 0.582 | 0.833 |
| 0.35 | 0.292 | 0.316 | 0.323 | 0.330 | 0.341 | 0.359 | 0.387 | 0.432 | 0.502 | 0.620 | 0.833 |
| 0.40 | 0.333 | 0.358 | 0.365 | 0.372 | 0.384 | 0.402 | 0.431 | 0.475 | 0.544 | 0.652 | 0.833 |
| 0.45 | 0.375 | 0.399 | 0.407 | 0.414 | 0.426 | 0.444 | 0.473 | 0.516 | 0.581 | 0.680 | 0.333 |
| 0.50 | 0.417 | 0.440 | 0.448 | 0.455 | 0.466 | 0.484 | 0.512 | 0.554 | 0.614 | 0.703 | 0.833 |

TABLE 3

SECTION PROPERTIES OF BEAMS

| Beam Type | Total Depth h,in. | Flange | | $\alpha$ =d/h | $\beta$ =t/b | Moment of Inertia I,$in^4$ | Static Moments $Q_1$,$in^3$ | $Q_2$,$in^3$ |
|---|---|---|---|---|---|---|---|---|
| | | Depth d,in. | Width (b-t),in. | | | | | |
| 21 | 15.9 | 5.60 | 1.40 | 0.35 | 0.28 | 580 | 52 | 40 |
| 22 | 15.9 | 3.20 | 1.40 | 0.20 | 0.28 | 500 | 41 | 28 |
| 23 | 15.9 | 1.40 | 1.40 | 0.09 | 0.28 | 333 | 26 | 14 |
| 24 | 15.9 | 5.65 | 2.94 | 0.36 | 0.16 | 1084 | 97 | 85 |
| 25 | 15.9 | 2.80 | 3.20 | 0.18 | 0.15 | 909 | 71 | 59 |
| 26 | 15.9 | 1.40 | 3.20 | 0.09 | 0.15 | 603 | 45 | 33 |

Total plywood thickness t = 2 x 0.29 = 0.58 in.

TABLE 4

AVERAGE DEFLECTIONS OF SIXTEEN-FOOT LONG

PLYWOOD BOX BEAMS LOADED AT THE THIRD POINTS

TOTAL LOAD P = 2000 lb

| Beam Type | Deflections, inches (average from three beams) | | | |
|---|---|---|---|---|
| | Bending | | Shear | |
| | Test | Calculated | Test | Calculated |
| 21 | 0.212 | 0.205 | 0.037 | 0.054 |
| 22 | 0.219 | 0.224 | 0.044 | 0.060 |
| 23 | 0.318 | 0.331 | 0.059 | 0.076 |
| 24 | 0.116 | 0.114 | 0.037 | 0.048 |
| 25 | 0.121 | 0.123 | 0.044 | 0.057 |
| 26 | 0.165 | 0.186 | 0.078 | 0.069 |

TABLE 5

AVERAGE DEFLECTIONS OF SIXTEEN-FOOT LONG

PLYWOOD BOX BEAMS LOADED AT THE CENTRE

TOTAL LOAD P = 2000 lb

| Beam Type | Deflections, inches (average from three beams) | | | |
|---|---|---|---|---|
| | Bending | | Shear | |
| | Test | Calculated | Test | Calculated |
| 21 | 0.251 | 0.241 | 0.068 | 0.082 |
| 22 | 0.263 | 0.268 | 0.074 | 0.093 |
| 23 | 0.374 | 0.409 | 0.120 | 0.118 |
| 24 | 0.138 | 0.133 | 0.049 | 0.073 |
| 25 | 0.145 | 0.147 | 0.075 | 0.088 |
| 26 | 0.195 | 0.220 | 0.117 | 0.104 |

TABLE 6

AVERAGE DEFLECTIONS OF EIGHT-FOOT LONG PLYWOOD BOX BEAMS LOADED AT THE CENTRE

TOTAL LOAD P = 2000 lb

| Beam Type | No. of Beams | Deflections, inches | | | |
|---|---|---|---|---|---|
| | | Bending | | Shear | |
| | | Test | Calculated | Test | Calculated |
| 21 | 4 | 0.028 | 0.029 | 0.030 | 0.038 |
| 22 | 3 | 0.032 | 0.031 | 0.032 | 0.046 |
| 23 | 3 | 0.036 | 0.050 | 0.042 | 0.059 |
| 24 | 4 | 0.017 | 0.015 | 0.024 | 0.035 |
| 25 | 3 | 0.018 | 0.016 | 0.033 | 0.044 |
| 26 | 2 | 0.022 | 0.026 | 0.055 | 0.056 |

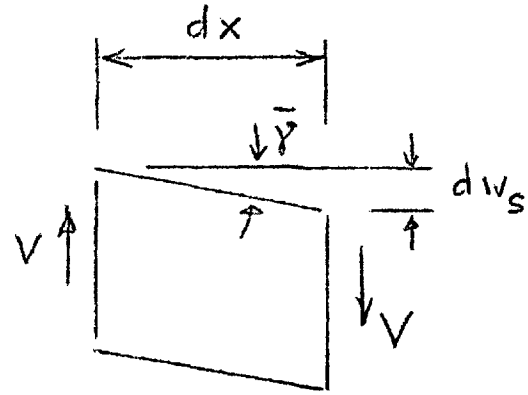


Fig. 1 Effective shear deformation of beam element dx.

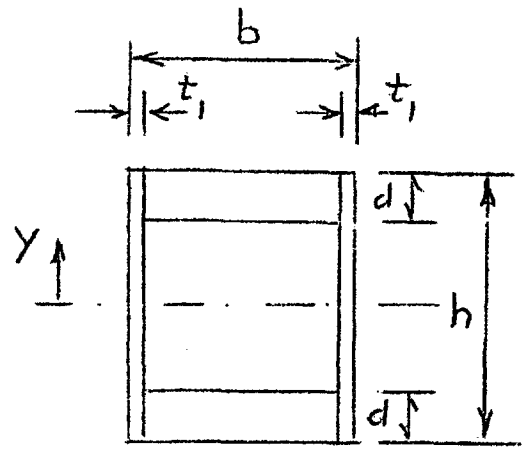


$t = \Sigma t_1$

$t_{||} = \Sigma$ of all plies in web with grain parallel to beam axis

$\alpha = d/h$

$\beta = t/b$

$t_v = t_{||}/t$

Fig. 2 Beam cross-section

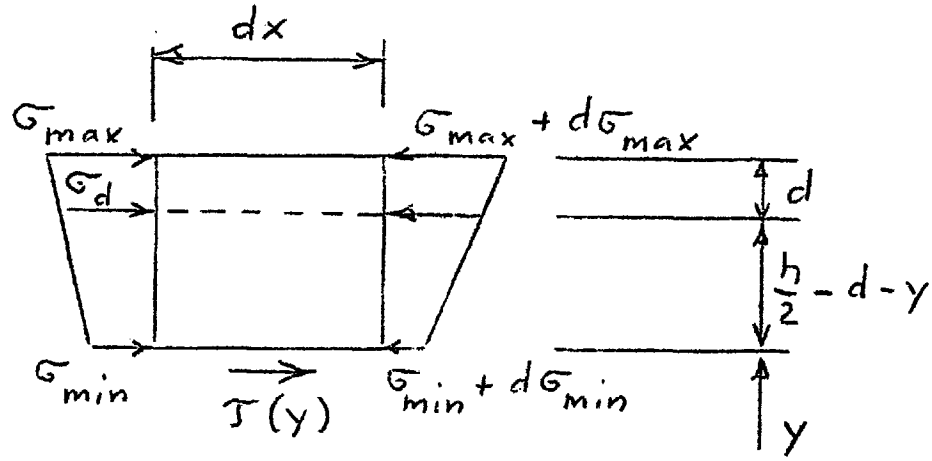


$$\sigma_{min} = \sigma_{max}\, 2y/h$$

$$\sigma_d = \sigma_{max}\,(1 - 2d/h)$$

Fig. 3 Stresses on beam element dx